

NATIONAL LIBRARY  
OTTAWA



BIBLIOTHÈQUE NATIONALE  
OTTAWA

8117

NAME OF AUTHOR... BRIAN W. ROBINSON.....  
TITLE OF THESIS... STUDIES OF THE ECHO  
BAY SILVER DEPOSIT,  
NORTH WEST TERRITORIES, CANADA  
UNIVERSITY... OF ALBERTA.....  
DEGREE FOR WHICH THESIS WAS PRESENTED... Ph. D......  
YEAR THIS DEGREE GRANTED... 1971.....

Permission is hereby granted to THE NATIONAL LIBRARY  
OF CANADA to microfilm this thesis and to lend or sell copies  
of the film.

The author reserves other publication rights, and  
neither the thesis nor extensive extracts from it may be  
printed or otherwise reproduced without the author's  
written permission.

(Signed)... B. Robinson.....

PERMANENT ADDRESS:

..... Sociology Dept.,  
U of A,  
Edmonton.....

DATED... 5th March.....1971

THE UNIVERSITY OF ALBERTA

STUDIES ON THE ECHO BAY SILVER DEPOSIT,  
NORTHWEST TERRITORIES, CANADA.

BY



BRIAN WILLIAM ROBINSON, B. Sc. (Hons.) M. Sc.

A THESIS

SUBMITTED TO THE FACULTY OF GRADUATE STUDIES  
IN PARTIAL FULFILMENT OF THE REQUIREMENTS FOR THE DEGREE OF  
DOCTOR OF PHILOSOPHY


DEPARTMENT OF GEOLOGY

EDMONTON, ALBERTA

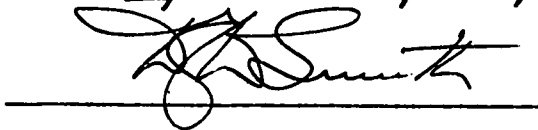
Spring, 1971

THE UNIVERSITY OF ALBERTA  
FACULTY OF GRADUATE STUDIES

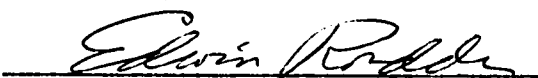
The undersigned certify that they have read and recommend to the Faculty of Graduate Studies for acceptance, a thesis entitled 'Studies on the Echo Bay Silver Deposit, Northwest Territories, Canada' submitted by Brian William Robinson B.Sc. (Hons.) M.Sc. in partial fulfilment for the degree of Doctor of Philosophy.

  
\_\_\_\_\_  
Supervisor

*H. Roy House (Physics Dept.)*  
\_\_\_\_\_

  
\_\_\_\_\_

*H. Boedgaard*  
\_\_\_\_\_

  
\_\_\_\_\_  
External Examiner

## ABSTRACT

The Echo Bay vein type U-Co-Ni-Ag deposit (U-Pb age of 1450 m.y.) occurs within fracture zones in the western part of the Great Bear Province. Proterozoic granites, granodiorites and the Echo Bay Group of sediments and volcanics occur in this area but the mineralised veins are normally confined to the Echo Bay Group which is thought to have been affected by the zeolite facies of regional metamorphism.

Rb-Sr dating on the volcanics of the Echo Bay Group gave an age of  $1770 \pm 30$  m.y. using  $\lambda = 1.39 \times 10^{-11} \text{ yr}^{-1}$ . K-Ar dating on hornblendes and biotites from the granite, granodiorite and volcanics of the Echo Bay area all gave apparent ages of around 1650 m.y., probably owing to prolonged burial-metamorphic conditions.

The mineralisation stages within the lens-shaped veins are, from oldest to youngest: quartz-hematite stage, pitchblende stage, Co-Ni-arsenide stage with native silver and early, intermediate and late sulphide stages. Carbonates occur mainly in the sulphide stages where acanthite, marcasite, chalcopyrite, bornite, galena and mckinstryite are found in up to three periods of deposition. Many of the ore-textures, such as the dendritic vein-structures commonly associated with native silver and the Co-Ni arsenide minerals, are thought to represent replacement.

Sulphur isotope measurements on co-existing sphalerite and galena (2 pairs) for the early and intermediate-sulphide stage gave temperatures of  $230^\circ$  and  $200^\circ$  C. respectively. Primary fluid inclusions

in intermediate sulphide stage dolomites (21 measurements) and late quartz (10 measurements) represent a saturated brine, wherein vapour/liquid homogenisation took place at 150° and 130° C. respectively.

The mineral parageneses and the Fe-contents of sphalerites have provided estimates for the  $fS_2$ - $fO_2$ -pH regimes of the ore fluids.  $\delta S^{34}$  values for the sulphides change from -21 per mil in the early-stage phases to +27 per mil in the late stage phases. This change can be explained by an increase in pH and a decrease in  $fO_2$  values of a solution which initially contained sulphur of +23 per mil and moved from a  $SO_4^{=}$  species-enriched state to a  $HS^-$  enriched state. The sulphur is probably of non-juvenile origin.

$\delta O^{18}$  values of the dolomites are +22 per mil (SMOW) for 2 samples of the pre-sulphide stage and  $+13 \pm 2$  per mil for 5 samples of the intermediate-sulphide stage.  $\delta C^{13}$  values are uniform at  $-3 \pm 1$  per mil for all 7 samples. The change in  $\delta O^{18}$  values possibly represents a lower temperature for the pre-sulphide stage or a decreasing  $\delta O^{18}$  value of the ore fluid. The calcites are mainly isotopically lighter than the dolomites, probably owing to the formation of late calcite during an influx of meteoric water and the preferential recrystallisation of earlier calcites.

The ore fluid was a brine, possibly derived from the alteration of trapped sea water and active enough to become enriched in certain elements. The host rocks are considered as a probable source for the metals which were complexed and transported into the vein fractures where they were deposited due to pH- and other chemical-changes of the ore fluid induced when a new environment was encountered.

## ACKNOWLEDGEMENTS

The author wishes to extend his thanks to Dr. R.D.Morton for initially suggesting the Echo Bay Mine as a thesis area and his guidance during the course of the work. Echo Bay Mines Ltd. and J. Foster Irwin Engineering Ltd. gave permission to work in this area and gave assistance in the collecting and shipment of samples. Mr. R.J. Beckett has been of help with the mine and local geology and by providing samples.

The techniques involved in the isotopic studies of carbonates were introduced to the author by Dr. P. Fritz who has also been of great help in discussing stable isotope results and other data. Gas-source mass spectrometric facilities were provided in the Physics Dept. by Dr. H.R. Krouse who has also contributed in the interpretation of the stable isotope data. Assistance in preparing the sulphur samples and mass spectrometric analysis was provided by Mr. R. Shaw.

Dr. H.Baadsgaard and Dr. R.K. O'Nions assisted the author in the K-Ar and Rb-Sr dating techniques and the solid-source mass spectrometric facilities were maintained in the Physics Dept. through Dr. G. Cumming. Dr. R.K. O'Nions contributed greatly in discussions of the geochronological and other data.

Dr. R.W. Boyle provided the G.S.C. facilities for the host-rock analyses and secondary alteration mineral analyses and also contributed to this study through various discussions.

Assistance with the techniques of electron microprobe analysis was provided by Dr. D.G.W. Smith and Mr. D. Tomlinson.

Dr. H. Ohmoto was of great help with the fluid inclusion and solution geochemistry studies.

Other members of the Department have contributed to this study partly through the P.G.I.M. seminars.

Mr. A. Stelmach provided assistance in the chemical laboratory and the thin sections and some of the polished sections were produced by Mrs. E. Vincze. The author is also grateful to Mr. F. Dimitrov for draughting and photographic services and Mr. V. Warren for draughting services.

I would like to thank my wife for typing the initial draught of this thesis and Mrs. D. Haugan for typing the final draught.

Financial assistance was provided by Graduate Teaching Assistantships, Graduate Research Assistantships and National Research Council and Geological Survey of Canada grants.

## TABLE OF CONTENTS

	Page
ABSTRACT .....	i
ACKNOWLEDGEMENTS .....	iii
CHAPTER 1. INTRODUCTION .....	1
CHAPTER 2. REGIONAL GEOLOGICAL SETTING .....	5
Echo Bay Group .....	5
Cameron Bay Group .....	7
Hornby Bay Group .....	8
Intrusives .....	8
Giant Quartz Veins .....	9
Metamorphism .....	10
Structure .....	11
Mineralised Vein Zones .....	11
CHAPTER 3. LOCAL GEOLOGY .....	13
The Lower Echo Bay Sub-Group .....	13
The Cliff Series .....	15
The Hornblende Feldspar Porphyry Series .....	16
The Tuff Series .....	17
The Mine Series .....	17
The Eldorado Vent Deposit .....	18
The Upper Echo Bay Sub-Group .....	18
The Gossan Zone .....	20
The Granite .....	20
The Granodiorite .....	21



The Diabase Dykes .....	22
The Diabase Sill and Actinolite-Magnetite Veins .....	22
Metamorphism .....	23
1. Contact Metamorphism .....	23
2. Regional Metamorphism .....	29
Structure .....	32
Veins and Mineralisation .....	35
CHAPTER 4. GEOCHRONOLOGY .....	40
Previous Work .....	40
Rubidium-Strontium Dating .....	45
Potassium-Argon Dating .....	53
Hudsonian-age Paleoenvironment of The Bear Province .....	61
CHAPTER 5. THE GEOCHEMISTRY OF THE HOST ROCKS .....	65
CHAPTER 6. MINERALOGY OF THE DEPOSIT .....	77
Non-metallic Minerals .....	77
a. Quartz .....	77
b. Carbonates .....	79
c. Fluorite .....	81
d. Chrysotile .....	81
Metallic Minerals .....	82
a. Pitchblende .....	82
b. Co-Ni-Arsenide Minerals .....	84
b(i). Niccolite .....	85
b(ii). Rammelsbergite .....	85
b(iii). Skutterudite .....	87
c. Iron Minerals .....	87

c(i). Hematite .....	88
c(ii). Marcasite .....	88
d. Copper Minerals .....	89
d(i). Chalcopyrite .....	89
d(ii). Bornite .....	90
d(iii). Chalcocite .....	91
e. Sphalerite .....	91
f. Galena .....	92
g. Silver Minerals .....	93
g(i). Acanthite .....	94
g(ii). Mckinstryite .....	94
g(iii). Native Silver .....	94
h. Native Bismuth .....	99
Dendritic Vein Structures .....	100
The Paragenetic Sequence of the Echo Bay Ores .....	104
Comparison With The Mineralogy of Other Similar Vein Deposits .....	107
Wall Rock Alteration .....	110
Secondary Minerals at Echo Bay .....	112
CHAPTER 7. STABLE ISOTOPES OF THE DEPOSIT .....	118
S-Isotopes .....	118
O and C Isotopes .....	124
CHAPTER 8. GEOTHERMOMETRY AND FLUID INCLUSION STUDIES .....	131
General Considerations .....	131
Temperatures Derived From Stable Isotope Data .....	134
Fluid Inclusions .....	138

Geobarometry .....	141
CO <sub>2</sub> Content of the Fluid Phase .....	143
K/Na Ratios .....	144
Summary .....	149
CHAPTER 9. MINERAL ASSEMBLAGES AND SOLUTION GEOCHEMISTRY ...	150
CHAPTER 10. INTERPRETATION OF THE STABLE ISOTOPE DATA .....	176
Sulphur Isotopes of the Sulphides .....	176
Oxygen Isotopes of the Carbonates .....	185
Carbon Isotopes of the Carbonates .....	189
Electron Microprobe Analyses of the Carbonates .....	191
CHAPTER 11. TRANSPORT OF METALS IN SOLUTION .....	196
CHAPTER 12. GENESIS OF THE DEPOSIT .....	200
CONCLUSIONS .....	207
REFERENCES .....	211
APPENDIX A. DESCRIPTION OF ANALYSED SPECIMENS .....	A 1
APPENDIX B. CHEMICAL PROCEDURES FOR K, RB AND SR .....	A 8
Potassium .....	A 8
Rubidium .....	A 9
Strontium .....	A10
APPENDIX C. COMPUTATIONS FOR K-AR AND RB-SR AGE CALCULATIONS .	A12
1. Potassium-Argon .....	A12
2. Rubidium-Strontium .....	A13
APPENDIX D. STABLE ISOTOPES : ANALYTICAL PROCEDURES AND	
DATA CORRECTION .....	A14
1. Sulphur Isotopes .....	A14
a) Preparation of SO <sub>2</sub> .....	A14

b) Mass Spectrometry .....	A15
c) Correction Factors .....	A16
2. Oxygen and Carbon Isotopes .....	A18
a) Preparation of CO <sub>2</sub> .....	A18
b) Mass Spectrometry .....	A19
c) Correction Factors .....	A20
APPENDIX E. SOLUTION CHEMISTRY COMPUTATIONS .....	A22
1. Sample Calculation for a Carbonate Buffer System ....	A22
2. Sample Calculation of the Molality of Sulphur Species in the Fluid .....	A24
APPENDIX F. CORRECTIONS OF THE MICROPROBE DATA AND MICROPROBE STANDARDS .....	A28
APPENDIX G. Mckinstryite from the Echo Bay Mine, Northwest Territories, Canada. B.W. Robinson & R.D. Morton, Economic Geology (in press) .....	A30

## LIST OF FIGURES

	Page
FIGURE 1:	Location Map of Great Bear Lake and Port Radium, N.W.T. .... 3
FIGURE 2:	Geology and Sample Locations of the Echo Bay Mine Area, N.W.T. .... 14
FIGURE 3:	a) ACF Diagram for the Hornblende-Hornfels Facies ..... 26
	b) ACF Diagram for the Albite-Epidote-Hornfels Facies ..... 26
FIGURE 4:	Equal Area Projection and Contours of the Poles to the Faults and Fracture Planes in the Echo Bay Area ..... 33
FIGURE 5:	Isotopic Age Map of the Western Canadian Shield ..... 41
FIGURE 6:	Whole Rock Rb-Sr Isochron for the Echo Bay Volcanics ..... 50
FIGURE 7:	Plot of $Ar^{40}$ Versus $K^{40}$ for Biotites and Hornblendes from the Echo Bay Granite, Granodiorite and Volcanics ..... 58
FIGURE 8:	Regional Facies Belts of the Bear, Slave and Churchill Provinces (HOFFMAN, 1969) ..... 63
FIGURE 9:	Underground Plan of the Three Adit Levels of Echo Bay Mine Showing the Main Sampling Areas .. 78
FIGURE 10:	Paragenetic Sequence for the Echo Bay Veins ... 106
FIGURE 11:	Paragenetic Sequence for the Port Radium Veins ..... 107
FIGURE 12:	Sulphur Isotope Values of the Echo Bay Sulphides and the Vein Sulphide Paragenetic Sequence ..... 122
FIGURE 13:	$\delta O^{18}$ Versus $\delta C^{13}$ Plot for the Echo Bay Carbonates ..... 128

FIGURE 14:	$\delta O^{18}$ Versus $\delta C^{13}$ Plot for the El Bonanza Mine Carbonates .....	129
FIGURE 15:	$\delta O^{18}$ Versus $\delta C^{13}$ Plot for the Terra Mine Carbonates .....	130
FIGURE 16:	Graph Showing the Results of Calculations and Experiments to Determine the Variation with Temperature of Sulphur Isotope Fractionation Between Galena and Sphalerite .....	136
FIGURE 17:	Temperature Versus K/Na Atomic Ratio Plot for the Echo Bay Fluid Inclusions .....	147
FIGURE 18:	Log $fO_2$ -log $fS_2$ Diagram for the Fe-O-S and other Systems at 150° C. ....	153
FIGURE 19:	Log $fO_2$ -log $fS_2$ for the Fe-O-S and other Systems at 200° C. ....	159
FIGURE 20:	Graph Showing the Interrelationship of Temperature, pH and $fCO_2$ for a Carbonate Buffer System .....	160
FIGURE 21:	pH-log $fO_2$ Diagram for Equilibrium Relations in the Fe-O-S System and Aqueous Sulphur Species at $\Sigma S 10^{-4}$ m and 150° C. ....	164
FIGURE 22:	pH-log $fO_2$ Diagram for Equilibrium Relations in the Fe-O-S System and Aqueous Sulphur Species at $\Sigma S 10^{-3}$ m and 150° C. ....	165
FIGURE 23:	pH-log $fO_2$ Diagram for the Equilibrium Relations in the Fe-O-S System and Aqueous Sulphur Species at $\Sigma S 10^{-4}$ m and 200° C. ....	167
FIGURE 24.	pH-log $fO_2$ Diagram for Equilibrium Relations in the Fe-O-S System and Aqueous Sulphur Species at $\Sigma S 10^{-3}$ m and 200° C. ....	168
FIGURE 25.	Log $fO_2$ -log $fS_2$ -temperature Diagram Representing the Hypothetical movement of an Ore Fluid Producing a Similar Mineralogy to the Echo Bay Deposit .....	170

FIGURE 26:	pH-log $fO_2$ -temperature Diagram Representing the Hypothetical Movement of an Ore Fluid Producing a Similar Mineralogy to the Echo Bay Deposit .....	171
FIGURE 27:	Activity Diagram for the System HCl-H <sub>2</sub> O-CaO-CO <sub>2</sub> -MgO-SiO <sub>2</sub> at 200° C. (HELGESON, et al., 1969) .....	174
FIGURE 28:	Graph to Demonstrate the Theoretical Fractionation of Sulphur Species as a Function of Temperature, Data from SAKAI (1968) .....	179

## LIST OF TABLES

	Page
TABLE 1:	The Sequence of Geological Events, East Arm of Great Bear Lake ..... 6
TABLE 2:	Rb-Sr Analytical Data for Whole Rock Isochron, Echo Bay Volcanics ..... 49
TABLE 3:	K-Ar Data for Echo Bay, Volcanics, Granodiorite, Granite and Hornblende/ Actinolite Veins ..... 57
TABLE 4:	Echo Bay Host Rock Analyses ..... 68
TABLE 5:	Correlation Coefficients Between Ten of the Analysed Elements and CO <sub>2</sub> , Echo Bay Tuffs and Volcanics ..... 70
TABLE 6:	Ni/Co, U/Pb and Rb/Sr Ratios of the Echo Bay Host Rocks ..... 73
TABLE 7:	Electron Microprobe Analyses of Native Silver .. 98
TABLE 8:	Echo Bay, El Bonanza and Terra Mine S-isotope Samples and Analyses ..... 120 & 121
TABLE 9:	Echo Bay, El Bonanza and Terra Mines O and C Isotope Samples and Analyses ..... 126 & 127
TABLE 10:	Electron Microprobe Sphalerite Analyses ..... 133
TABLE 11:	K/Na Analyses of the Fluid Inclusions ..... 146
TABLE 12:	Thermodynamic Data Used in the Construction of fS <sub>2</sub> -fO <sub>2</sub> Diagrams ..... 152
TABLE 13:	Equilibrium Constants Used for the Construction of fO <sub>2</sub> -pH Diagrams ..... 162
TABLE 14:	Electron Microprobe Analyses of Carbonates .... 193



LIST OF PLATES

PLATE I.	Opposite page 37
PLATE II.	Opposite page 38
PLATE III.	Opposite page 39
PLATE IV.	Opposite page 114
PLATE V.	Opposite page 115
PLATE VI.	Opposite page 116
PLATE VII.	Opposite page 117

## CHAPTER I - INTRODUCTION

The shores of Great Bear Lake were first investigated geologically during the expedition of J. McIntosh Bell and Charles Camsell in the summer of 1900. After travelling toward the Coppermine River the party returned down the east shore of the lake and were forced to shelter in a small bay that was immediately named Echo Bay. Here, Bell made geological observations which were published by the Geological Survey in 1903 and which can be summarised by his sentence: 'In the greenstones east of McTavish Bay occur numerous interrupted stringers of calcspar containing chalcopryrite and the steep rocky shores which here present themselves to the lake are often stained with cobalt bloom and copper green.'

Not until 1929 was this record spotted by Gilbert LaBine who, accompanied by E.G. St. Paul, visited the area in the same year. Returning in 1930, LaBine staked claims in the mineralised area at the entrance to Echo Bay (the area to become the Port Radium Mine of Eldorado Mining and Refining Ltd.).

The Eldorado Mine was brought into production in 1934 producing silver and radium ores until 1940 when it closed down. World War II caused the mine to reopen in 1942 as a uranium producer and for political reasons the company became a Crown Corporation. Ore reserves were finally exhausted in 1960 when operations ceased.

The adjacent Echo Bay property was staked for Cominco in 1930 and mining development proceeded until 1941. G.S.C. parties mapped the area from 1944 to 1946 and Cominco carried out further explorations in 1948. The current mining operation of Echo Bay Mines Ltd. commenced in

1964 as an extension to Cominco's Nos. 1 and 2 adits. In 1967 a third adit was opened and very high grade silver and uranium ore were produced. Sinking of a three compartmental shaft was completed in 1968 and mining has proceeded on six new levels to date. The company utilises the former Eldorado camp and mill facilities. During 1969 the mine produced 2.4 millions ozs. of silver, thus making it one of the principal silver producers of the country. 682,000 lbs. of copper were also produced.

Joining the revival at Great Bear Lake, Terra Mining and Exploration Ltd., Caesar Silver Mines Ltd. and Silver Bay Mines Ltd. are all operating and producing silver about 30 miles south of Echo Bay on the Camsell River.

The location of the area is given in Fig. 1. Port Radium is the site of the old Eldorado Mine and the camp now used by Echo Bay Mines. It is situated on Labine Point about half way up the east side of McTavish Arm, Great Bear Lake. It is 30 miles south of the Arctic Circle at longitude 118°02'W and latitude 66°05'N. Access to the area is by float-equipped planes in the summer and by ski-equipped planes in the winter. A winter road from Rae serves the mine and barges connect with Hay River in the summer. Port Radium is 275 miles northwest of Yellowknife.

The climate in the area is sub-Arctic. Annual rainfall is usually less than 10 inches and Great Bear Lake is usually ice-free from mid July to mid October. The topography along the east shore of McTavish Arm is quite rugged, cliffs often rise out from the lake to over 500 feet above lake level. Great Bear Lake is 511 feet above sea level and the maximum relief in the vicinity of Port Radium is around 1000 feet. Outcrop is

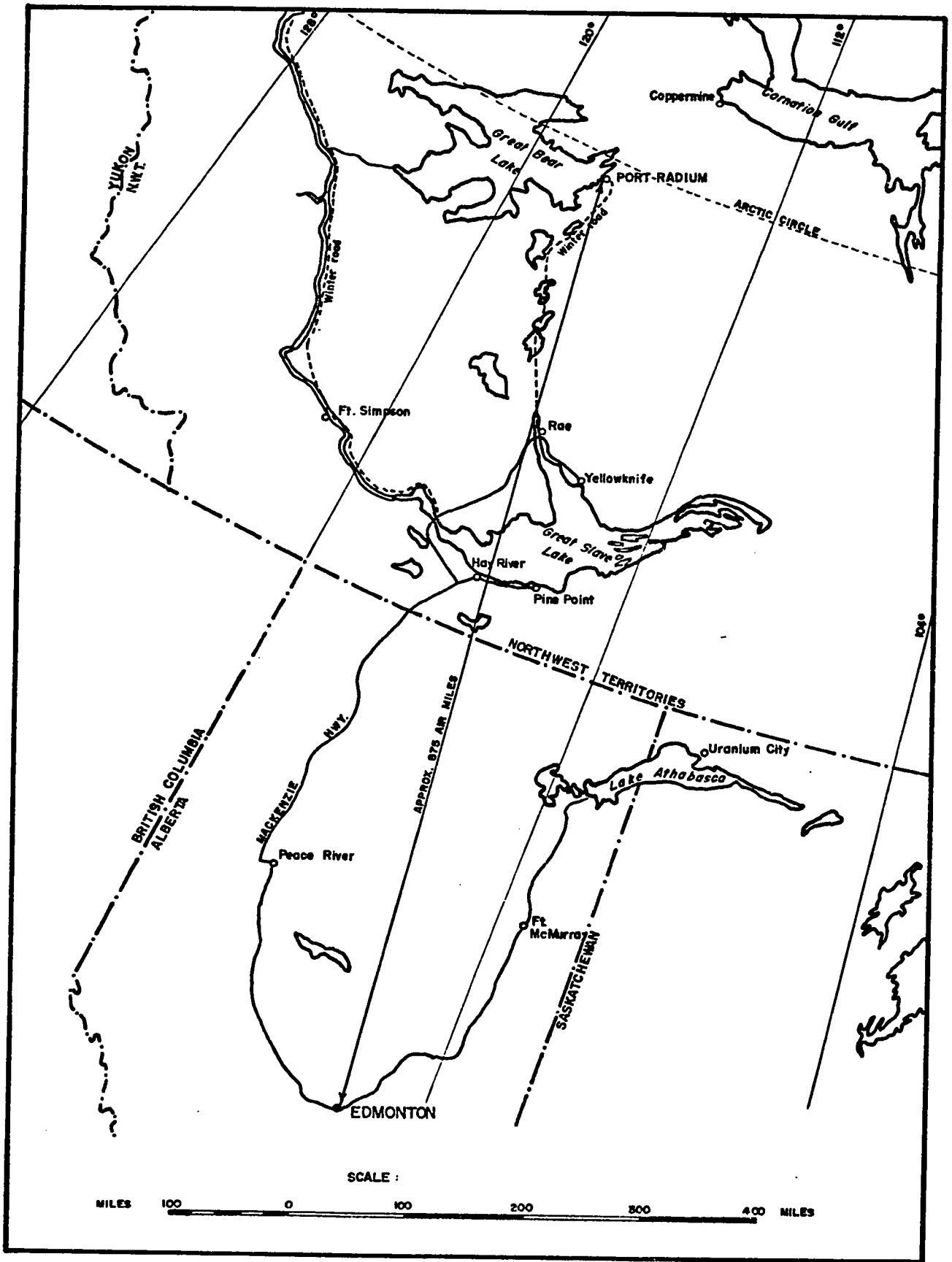


Fig. 1. Location map of Great Bear Lake and Port Radium, N.W.T.

about 70 per cent in the Port Radium area commonly with glacially polished surfaces. Most depressions are filled with glacial drift and muskeg.

This study of the Echo Bay deposit was initiated in the summer of 1968 by a program of mapping and collecting. The mine area was mapped on a scale of 1 inch to 100 feet for Echo Bay Mines Ltd. Various traverses were made over the general area to check the geology and collect different rock types for dating and analytical purposes. Collecting was undertaken underground in the Echo Bay Mine mainly at the areas being worked in 1968, i.e. the 302 stope, the 206A East Drive and the 209A West Sub-drive.

To elucidate the more nebulous features of the field relationships studied, a geochronological study was completed. The mineralogy and paragenetic sequence of the deposit were studied by polished section work and X-ray powder diffractometry. A special study of the mineral mackinstryite was undertaken.

Stable-isotope studies were conducted on the vein material. Fluid inclusions were examined and a geochemical model for the origin of this deposit has been obtained.

## CHAPTER 2 - REGIONAL GEOLOGICAL SETTING

The east shore of Great Bear Lake is part of the Bear Province as defined by JOLLIFFE (1948). It is characterised by NE-SW trending faults and mineralisation of the uranium - native silver - bismuth - cobalt-nickel arsenide - copper sulphide type which defines this metallogenic province. The Bear Province is younger and geologically distinct from the adjoining Slave Province. Fig. 5 shows the provinces of the western part of the Canadian Shield together with the K-Ar ages which characterise them.

The regional geological setting is considered to be within the east, or McTavish, Arm of Great Bear Lake. A sequence of geological events for this area is given in Table 1. Three sedimentary-volcanic stratigraphical groups, the Echo Bay, Cameron Bay and Hornby Bay Groups have been distinguished in the field. The former two Groups crop out primarily along the east shore of McTavish Arm and the latter in the north part of the area. Intrusive granites, granodiorites and some feldspar porphyries are the predominant rock types of the area. In a study of the Hunter Bay area, north of Port Radium, MURSKY (1963) distinguished a series of regionally metamorphosed sedimentary and volcanic rocks as belonging to the Yellowknife Group. This observation has not been substantiated by any other study.

### Echo Bay Group

Probably the oldest rocks in the area belong to the Echo Bay Group which has been correlated by many workers with the Snare Group (CAMPBELL, 1955). The Snare Group consists of sedimentary and volcanic

TABLE 1

The sequence of geological events, East Arm of Great Bear Lake

ERA	SERIES	EVENT
P R O T O E R O Z O I C		Intrusion of Diabase sill
		U/Ag Mineralisation
		Intrusion of Diabase dykes
		Faulting
	HORNBY BAY GROUP	Deposition of sandstone and conglomerate
		Faulting?
		Erosional unconformity
	CAMERON BAY GROUP	Deposition of sandstone and conglomerate
		Folding and Tilting
		Intrusion of Granite
		Intrusion of Granodiorites
		Intrusion of some feldspar porphyries
	UPPER ECHO BAY GROUP	Extrusion of andesite flows with some tuff and breccia
	LOWER	Deposition of bedded tuffs with some lavas and basal sediments

rocks which crop out in elongated basins between Great Bear and Great Slave Lakes. Lithologically the rocks are most similar to those of the lower part of the Great Slave Group. The Echo Bay Group can be subdivided into a lower, dominantly sedimentary, sub-Group having a known thickness of 4,300 feet, lying above an intrusive granite contact and an upper, dominantly volcanic sub-Group at least 5,000 feet thick (FENIAK, 1947).

The lower Echo Bay sub-Group is composed of argillites with minor limestones, cherts, lavas and pyroclastic rocks. This Group is of limited occurrence in the area. More widely occurring is the upper Echo Bay sub-Group which consists of porphyritic- and amygdaloidal-andesite flows intercalated with occasional pyroclastics. The flows are massive and usually devoid of any primary structures except for orientated phenocrysts and amygdules near the tops. Fresh-looking purple, green, brown and grey lavas with phenocrysts of feldspar and hornblende contrast with the more altered and recrystallised tuffs of the lower Echo Bay sub-Group.

#### Cameron Bay Group

The Cameron Bay Group, which crops out in large expanses in the north of the present area, unconformably overlies the Echo Bay Group (ROBINSON, 1933). It has a minimum thickness of 1,000 feet and has as its basal member, a crumbly weathering, highly ferruginous conglomerate. The basal conglomerate contains clasts representing members of all the rock types of the Echo Bay Group plus granite pebbles. Thus a significant time interval between the accumulation of each Group is suggested, although



there is a concordance of bedding. The rocks are also loosely consolidated. However intercalations of andesite similar to those of the Echo Bay sub-Group have been observed in the Cameron Bay Group (ROBINSON, 1933). MURSKY (1962) considered the Cameron Bay Group to be more related to the Hornby Bay Group; thus it is placed before this Group in the stratigraphic column. Granitic rocks intrude the Cameron Bay Group and might, on first sight appear to present a problem of sequence. However, if a spread for the age of the granites is postulated, then the granite pebbles in the basal conglomerate can be explained. Overlying the basal conglomerate is a series of greywackes, coarse grits, arkoses and sandstones, all poorly cemented.

#### Hornby Bay Group

The Hornby Bay Group crops out at the north end of McTavish Arm where it unconformably overlies the Cameron Bay Group. It is itself overlain unconformably by Palaeozoic and Mesozoic strata. The Group consists of multicoloured sandstone and quartzite which are medium- to coarse-grained and contain interbeds of quartz pebble conglomerate. These strata are little disturbed and seldom dip at more than 10 degrees. A minimum thickness of 1,000 feet has been assigned to this group (KIDD, 1931).

#### Intrusives

The oldest of the intrusives in the district are probably the group of porphyry bodies which have been termed 'feldspar porphyry'. They occur as irregular sills, stocks and dykes cutting rocks of both

the Echo Bay and Cameron Bay Groups (KIDD, 1933). These intrusives make up a large proportion of the area and vary greatly in composition. It is felt that certain volcanic rocks occurring within the Echo Bay Group may have erroneously been classified as 'intrusive feldspar porphyries', in this area.

Cutting all pre-Hornby Bay Group rocks are bodies of granitic affinity reaching batholithic proportions. They range in composition from granodiorite to granite, with diorite phases occurring locally. FENIAK (1947) recognised three groups of granites based upon field relationships. These are from oldest to youngest: a quartz monzonite-aplite complex, a granodiorite-diorite complex and granite. It is considered that these phases could have been intruded over a relatively short span of geological time.

Basic dykes cut all the previously mentioned rocks of the area and are of widespread occurrence. The most common type is steeply dipping, up to 100 feet in width and can be classified as dolerite or diabase. The trend of the dykes is roughly east-west. A sill-like body, (or perhaps more than one), of quartz diabase outcrops at many places between Echo Bay and the head of Hornby Bay. It is found as a series of isolated occurrences that may have been one continuous body. Its thickness is from 50 to 150 feet and it often exhibits columnar jointing.

#### Giant Quartz Veins

Veins often referred to as 'giant quartz veins' and quartz stockworks are common in this area. They may be up to 1,000 feet wide and traceable for considerable distances. Dipping steeply, they parallel

the northeast trending faults and fracture zones of the area. They trend in the same direction and are probably related to the mineralised veins of the Port Radium area. Most of the large veins show at least two phases of quartz deposition and at times carry hematite and copper minerals. At least the later generation of quartz is considered to post-date the Hornby Bay Group (KIDD, 1933).

### Metamorphism

Regional metamorphism and alteration in this area have been reported by many workers as being negligible. Contact metamorphic effects around the granite bodies have also been reported as negligible. However a contact metamorphic aureole does exist around the granite at Port Radium and this therefore casts doubt upon the accuracy of previous reports. The granodiorite bodies are locally fringed by haloes of recrystallisation and granitisation. Extensive haloes of recrystallisation and metasomatism have been genetically connected with the feldspar porphyries (CAMPBELL, 1957).

It is considered that, at least locally, burial metamorphic effects are exhibited by the middle portion of the Echo Bay Group. These effects may also be developed in the lower Echo Bay sub-Group but as yet have not been recognised.

Many blebs, impregnations and lenticular bodies of magnetite, apatite and actinolite have been reported within the Echo Bay area and farther north (FENIAK, 1947). From the geochronological work done in the Echo Bay area it is considered that these small intrusive magnetite bodies are associated with the diabase intrusive activity of the area.

### Structure

The sedimentary and volcanic rocks of the Echo Bay- and Cameron Bay-Groups occur as northerly-elongated, roof pendants within the intrusive rocks. The strata strike from northwest to northeast and usually dip at less than 45 degrees. Folding is not common and is usually of an open nature where it does occur. The general features of folding and tilting are probably merely a result of the major intrusive activity.

Four main fault and fracture systems are recognisable in the area striking N30° - 60°E, east, northwest and north respectively. The first set comprise the main structural features and contain the principal mineralised veins. All the systems are steeply dipping and along the fault zones fault breccias are more characteristic than intensely sheared rock. The maximum displacement noted on any of these faults is 10 miles in a horizontal sense. The Cameron Bay fault, four miles south of Port Radium has 2 1/2 miles of horizontal displacement. Usually the displacements are relatively minor in extent.

### Mineralised Vein Zones

The mineralised vein zones in the area lie within the northeast trending structures. Oreshoots are usually located in favourable horizons such as tuffaceous horizons which were less competent during fracturing and thus in general provided larger dilatant zones. The mineralised veins can all be classified as vein-type uranium deposits (a group which has been sub-divided, on a world wide basis, into three types (MCKELVEY, et al., 1955)). In this area the veins belong to the so-called Ni-Co-native Ag-U type which usually has metasediments and volcanics as host

rocks, a complex mineralogy of uranium minerals, sulphides, Co-Ni arsenides and precious metals present within a carbonate and quartz gangue.

### CHAPTER 3 - LOCAL GEOLOGY

The area considered herein consists of the region around the Eldorado Mine and the Echo Bay Mine as shown in Fig. 2. The detailed geology of the Eldorado Mine area has been obtained from CAMPBELL (1955), JORY (1964) and from personal observations in 1968. Also in 1968 the area above the Echo Bay Mine was mapped in detail by the author. This area is underlain by rocks of the middle portion of the Echo Bay Group. A description of all the rock units encountered is given below. Petrographic descriptions of a representative set of samples is presented in Appendix A.

#### The Lower Echo Bay Sub-Group

CAMPBELL (loc. cit.) divided this sub-Group into four units which outcropped on Cobalt Island and Labine Point. Above these, two new units have been added by the author to cover the Echo Bay Mine area. The units are as follows:

#### IV. Cliff Series (youngest)

Approximately 1,000 feet of banded well bedded tuffs.

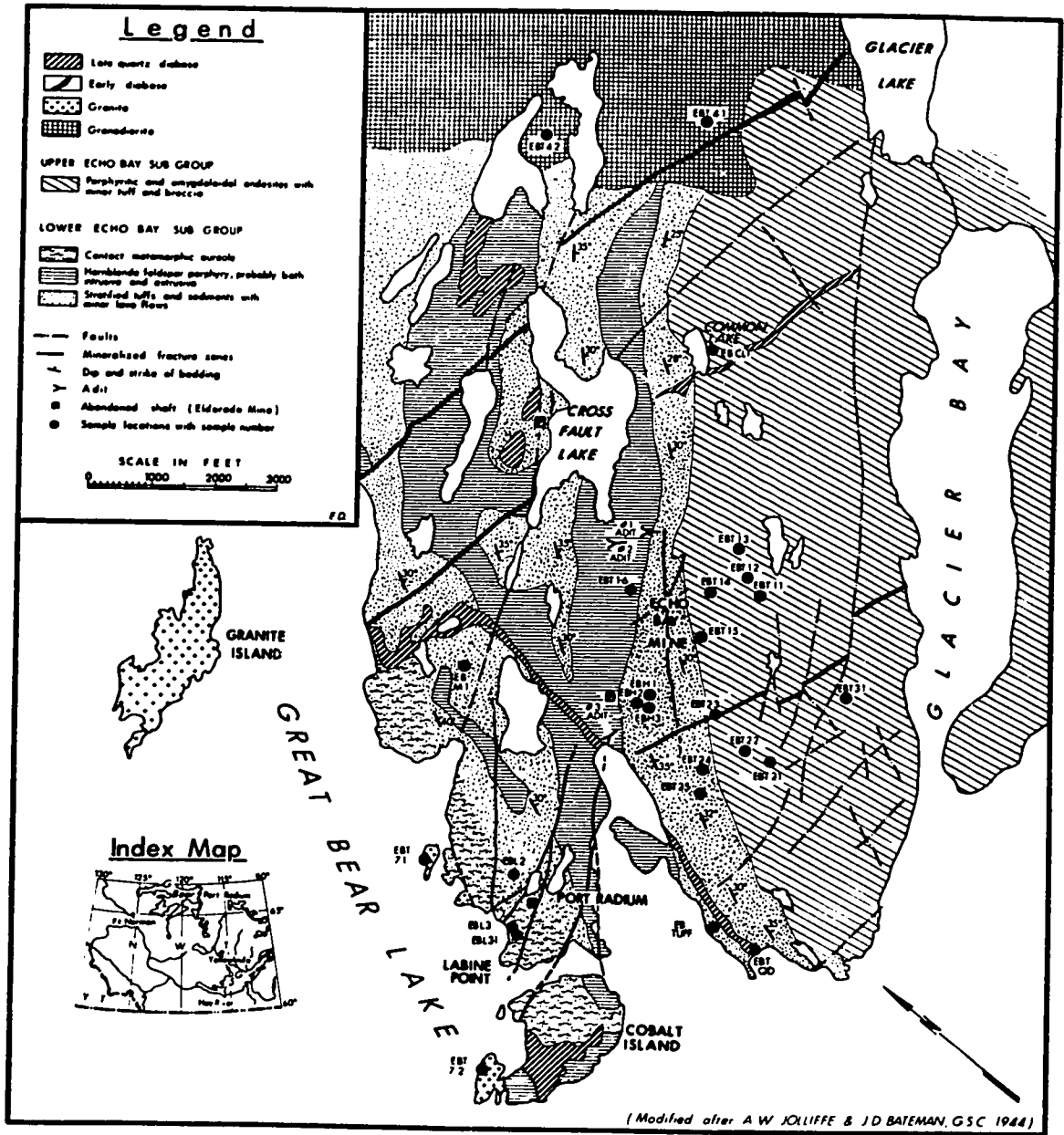
#### III. Hornblende feldspar porphyry Series

Approximately 600 feet of (probably) extrusive porphyry.

#### II. Tuff Series

(ii) Upper beds: (800 feet) - brown cherty and silty bedded tuff.

(i) Transition Formation: (500 feet) - buff fragmentals and cherty tuffs. Some cherts and flows.



GEOLOGY OF THE ECHO BAY MINE AREA, N.W.T.

Fig. 2. Geology and sample locations of the Echo Bay Mine area, N.W.T.

I. Mine Series (oldest)

(ii) Mine Formation: (800 feet) - thin bedded ferruginous and massive cherts.

(i) Cobalt Island Formation: (700 feet) - thin bedded quartzites and cherts, generally calcareous.

Thick bedded cryptocrystalline cherts.

Campbell concluded that the "cherty argillites" were initially almost pure cherts which had attained their characteristic pink and dark green thin laminations through a metasomatic introduction of ferromagnesian minerals. However JORY (loc. cit.) showed that the "cherts" of the Mine Formation are actually microcrystalline, sodium-rich plagioclase tuffs.

The Cliff Series

In the original studies of this area, the bedded tuffs which crop out in the Echo Bay Mine area were either not recognised or included with the upper Echo Bay sub-Group. Their affinities obviously place them within the lower Echo Bay sub-Group and in this study they have been termed the Cliff Series. This 1000 ft. thick series acts as host for the veins of the Echo Bay deposit and strikes northeast across the area. In hand specimen, the tuffs are typically medium grained, well banded with 1 inch thick alternating green and red bands. In some areas they are more massive and grey in colour. On the east shore of Labine Bay, the tuffs show sedimentary structures such as graded bedding, cross bedding, washout channels and convolute bedding as shown in Plate I, Fig. 1. These structures indicate that the tuffs are water



deposited and are the right way up. In some parts as in Plate III, Fig. 2, original feldspar fragments can be discerned although they are usually extensively corroded.

The tuffs are normally recrystallised and contain fibrous laths of actinolite and hornblende up to 4 mm. in length. The mafic minerals are usually concentrated in the darker bands whereas red hematitised feldspar is concentrated in the lighter coloured bands. Minor minerals include magnetite, quartz, pistachite, sphene, apatite, zoisite, chabazite and calcite. In certain horizons, the tuffs contain up to 10% pyrite which is concentrated into blebs and bands in the rock. Excellent examples of these are seen in the third adit level of the mine (Plate I, Fig. 2). A porphyritic, andesite lava flow of lensoid form occurs within the Cliff Series near its top, but the top of the Series is taken as the last uninterrupted deposit of tuff.

#### The Hornblende Feldspar Porphyry Series

A body of this rock type, 500 to 700 feet in thickness, strikes north easterly through Labine Bay. In previous works, it has been regarded as an intrusive (mainly because small dykes and irregular bodies of related "feldspar porphyry" occur within the Mine Series). They have been reported to produce contact metamorphic aureoles, but it is felt that such metamorphism can be explained by contact metamorphism induced by the granite or in some places by late solutions emanating from the diabase.

In the area mapped, no evidence was found to indicate that this body is intrusive and, because of its concordant nature, it is considered

to represent a hornblende feldspar porphyritic lava. The rock has a maroon- to brick-red-coloured ground mass due to the presence of disseminated hematite. Phenocrysts of euhedral feldspar and hornblende are common. Thin sections show the rock to be extensively altered; the feldspar is highly sericitised and has inclusions of hematite and calcite, see Plate III, Fig. 3. Very thin veins and blebs of calcite are scattered throughout the rock. Chlorite almost totally replaces the hornblende and original igneous textures are almost indistinguishable. No variations in grain size or chilled margins were detected in the field and the contacts between the porphyry and the tuffs are generally rather diffuse.

#### The Tuff Series

The tuffs of the Upper Beds are pink to brown in colour and fine to medium in grain size. Recrystallisation has taken place but the uneven thin-bedded structures are still well preserved. Near the top of the Series a 100 foot thick bed of conglomerate occurs.

The Transition Formation is gradational below into the Mine formation and above into the rest of the Tuff Series. It is characterised by the presence of beds of poorly defined fragmentals and occasional lava flows which exhibit trachytic textures as shown in Plate III, Fig. 4.

#### The Mine Series

Cropping out on the central and western part of Labine Point, the Mine Formation is a sequence of pink and dark-green to black, fine grained, thin bedded tuffs rich in plagioclase (Plate I, Fig. 3). The Cobalt Island Formation crops out on the island and on the western tip

of Labine Point. It consists of tuffs with 10-35% carbonate in rhombs and patches, interbedded grey quartzite and two thin lenticular limestone beds near the base. FENIAK (1947) noted that there are two similar limestone beds near the base of a 'cherty' argillite sequence of lower Echo Bay strata on Dowdell Point, six miles south-west of Port Radium. Underlying that sequence on Dowdell Point is an undesignated thickness of maroon and green 'argillites'. The presence of argillites, limestone beds, calcareous tuffs and quartzite beds might suggest that the lower beds of the Cobalt Island Formation accumulated under normal marine conditions.

#### The Eldorado Vent Deposit

Cropping out on the northern part of Labine Point is a homogeneous unstratified body of massive crystalline tuff measuring more than a mile in length. CAMPBELL (1955) interpreted this as a remnant of a caldera and named it the Eldorado Vent Deposit. It is felt that this body could simply represent a normal tuff which has undergone contact metamorphism due to the granitic intrusion to the west.

#### The Upper Echo Bay Sub-Group

This sub-Group represents a considerable thickness of dominantly porphyritic and amygdaloidal andesites. Beds and lenses of volcanic agglomerate and massive tuff are quite common in the sequence, especially in the lower part.

The porphyritic andesite occurs as lava flows of varying thickness now exposed in the southern part of the area. Generally the rocks appear

of Labine Point. It consists of tuffs with 10-35% carbonate in rhombs and patches, interbedded grey quartzite and two thin lenticular limestone beds near the base. FENIAK (1947) noted that there are two similar limestone beds near the base of a 'cherty' argillite sequence of lower Echo Bay strata on Dowdell Point, six miles south-west of Port Radium. Underlying that sequence on Dowdell Point is an undesignated thickness of maroon and green 'argillites'. The presence of argillites, limestone beds, calcareous tuffs and quartzite beds might suggest that the lower beds of the Cobalt Island Formation accumulated under normal marine conditions.

#### The Eldorado Vent Deposit

Cropping out on the northern part of Labine Point is a homogeneous unstratified body of massive crystalline tuff measuring more than a mile in length. CAMPBELL (1955) interpreted this as a remnant of a caldera and named it the Eldorado Vent Deposit. It is felt that this body could simply represent a normal tuff which has undergone contact metamorphism due to the granitic intrusion to the west.

#### The Upper Echo Bay Sub-Group

This sub-Group represents a considerable thickness of dominantly porphyritic and amygdaloidal andesites. Beds and lenses of volcanic agglomerate and massive tuff are quite common in the sequence, especially in the lower part.

The porphyritic andesite occurs as lava flows of varying thickness now exposed in the southern part of the area. Generally the rocks appear

fresh in hand specimen although heavily hematitised bands about 10 feet thick do occur and are interpreted as being the weathered tops of individual lava flows. Andesine phenocrysts up to 5 or 6 mm. in length occur in a very fine-grained ground mass. The hornblende appears fresh in hand specimen but in thin section it is found to be extensively pseudomorphed by chlorite and actinolite. The feldspar phenocrysts exhibit sericitic alteration which picks out the zoning (see Plate III, Fig. 5). Chabazite and thompsonite are present in the ground mass of many of these lavas as shown in Plate III, Fig. 5.

Erratic in distribution, the amygdaloidal andesite is thought to represent the upper parts of the andesite flows. It contains large quartz filled amygdales which constitute up to 30% of the rock; otherwise, it is similar to the porphyritic lavas (see Plate III, Fig. 6). Both lava types often have disseminated magnetite in the ground mass and phenocrysts.

Bands of volcanic agglomerate crop out in this sub-group and above the Echo Bay Mine a band, 10 feet thick, is continuous for 1,000 feet. Elsewhere, the agglomerate is more lensoid in configuration. Characteristically, it contains angular to subangular fragments of lava up to 3 cm. in size, set in a matrix of tuff. The agglomerates are often rich in pyrite and east of Cross Fault Lake, almandine garnets are found in the matrix. Massive tuff bands occur up to 100 feet in thickness in this sequence but are normally much thinner. They are distinguished in the field by their medium-grained recrystallised texture, grey-black colour and lack of bedding or banding (see Plate III, Fig. 2). Mineralogically, they consist mainly of hornblende and andesine.

### The Gossan Zone

A large outcrop of gossan exists just south of the Number 1 adit to Echo Bay Mine, within the middle portion of the Echo Bay Group. It is considered that although this gossaning is above the mine it is no indication of the vein mineralisation below but simply a reflection of a high concentration of pyrite and pyrrhotite in the tuffs of the Cliff Series and the agglomerates of the upper Echo Bay sub-Group (the rock types present in this area). Also, this local area appears to have been a focus for fracturing and faulting which has facilitated weathering of the sulphides. White encrustations of gypsum, malachite and other weathering products are also present. Gossan Hill, the area just discussed, is depicted in Plate I, Fig. 4.

### The Granite

The granite batholith lying under Great Bear Lake crops out on Cobalt Island, on the east shore of Labine Point and on Granite Island. Its eastern contact dips steeply to the east into the old Eldorado Mine workings. A very sharp contact between the granite and massive tuffs is observed on the east shore of Labine Point (see Plate I, Fig. 5). This probably indicates a shallow depth of emplacement, emphasised where the rocks have been converted to structureless hornfelses (TURNER and VERHOOGEN, 1960). Xenoliths of massive tuff are common in the granite. They are only a few inches in width near the contact but are found to be two feet or larger about ten feet from the contact and by about twenty-five feet from the contact, no xenoliths are seen. At the contact the granite exhibits a highly leucocratic selvage averaging

one inch in width and composed of feldspar and quartz. It seems improbable that such a complete transfer of mafic material should occur on the contact and therefore this phenomenon is related to an aplitic stage. Late, fine-grained, pink to buff coloured aplite dykes and stringers cut the granite and the tuffs and extend up to 500 feet into the latter on Labine Point. The aplite dykes are illustrated in Plate I, Fig. 6.

The granite is a mottled pink and dark green colour. It is coarse grained and contains feldspar laths up to 8 mm. in length. The principal minerals in their approximate modal percentages are: quartz 45%, orthoclase 20%, hornblende 8%, biotite 8% and sericite 3%. Accessory minerals include calcite, pyrite, apatite, chlorite, zircon, sphene and hematite. The plagioclase shows little zoning and only minor sericitisation of the feldspars has taken place. Chloritisation of the hornblende is minor and the biotite is essentially unaltered.

#### The Granodiorite

Cropping out in the north of the area is a large body of granodiorite which intrudes the Echo Bay Group. The rock is coarse-grained and a mottled pink and dark green to black in colour. It contains plagioclase and less quartz and orthoclase than the granite. The biotite and hornblende are about twice as abundant as in the granite. Much of the feldspar has been sericitised, but the hornblende and biotite are relatively fresh. The contact with the Echo Bay Group is diffuse and a certain amount of assimilation of the tuffaceous rocks has taken place.

### The Diabase Dykes

The diabase dykes of this area strike about 100° east of north and cut all the rock types except the veins and the diabase sill. From observations in the Eldorado Mine (JORY, 1964) it appears that the dykes are younger than the initial development of the vein structures but older than most of the vein minerals. Texturally the rock consists of an intergranular to a sub-ophitic intergrowth of plagioclase and augite. The main minerals are oligoclase and augite with minor orthoclase, sericite, calcite and chlorite. Ilmenite and magnetite total about 10% of the rock. The alteration consists of some sericitisation of the feldspars and chloritisation of the pyroxene.

### The Diabase Sill and Actinolite-Magnetite Veins

In this area the diabase sill strikes northeasterly and dips to the east, cropping out in a steep cliff on the east shore of Labine Bay. Here its columnar jointing makes it a very distinctive feature conformably intruding the Cliff Series (see Plate I, Fig. 7). The sill averages about 100 feet in thickness. A similar body crops out on Cobalt Island off Labine Point. The two probably belong to the same sheet which once curved over the top of Labine Point. Dipping through the present working of Echo Bay Mine, the sill apparently cuts the mineralised vein. In the Eldorado Mine, it was found that the sill cut all but the latest stages of vein mineralisation.

The texture of the rock is granular to sub-ophitic and the main minerals are labradorite and augite. Quartz, orthoclase, ilmenite and magnetite are present as well as minor amounts of biotite, sphene, apatite



and sericite. The rock is therefore classified as a quartz dolerite.

Above the number 3 adit of the Echo Bay Mine, the local area is completely disrupted in that the tuffs of the Cliff Series have been brecciated on a large scale. Blocks of rock up to several feet in size have been turned through angles of up to 90°. Infilling between these blocks are large veins of actinolite-hornblende and magnetite with minor scapolite, pyrite and rhodochrosite. This phenomenon is illustrated in Plate I, Fig. 8. It was also found to occur at depth in the number 3 adit. In the field, this was mapped as an area of autobrecciation and was thought to be associated with the volcanic activity. However, dating of the actinolite showed this material to be possibly more or less contemporaneous with the diabase sill. It might, therefore, be a late stage phenomenon related to the intrusion of the sill; the veins possibly representing a late mobile-fraction of the magma. It is also felt that other areas of actinolite and magnetite at the contact of the hornblende feldspar porphyritic lava and the tuffs are actually related to the diabase intrusive, rather than to metamorphic effects of the once termed 'feldspar porphyry'.

### Metamorphism

#### 1. Contact Metamorphism

On Cobalt Island and on the western part of Labine Point the contact metamorphic aureole of the granite body which underlies this portion of Great Bear Lake can be observed. The aureole was studied in the field and in thin sections from samples taken from three traverses across the aureole on Labine Point. In past reports the metamorphic

effects have been described as 'negligible' (JORY, 1964) and of a 'weak nature' (FENIAK, 1947). Patches of diopside garnet skarn were noted on Cobalt Island but were not considered to be related to the granite. It is now thought that these skarns are certainly related to the granite. In many sectors on Labine Point the volcanics are apparently contorted by the intrusion of the granite. Small folds are abundant and in places a type of flow- or ptygmatic-folding was observed. This contortion is illustrated in Plate II, Figures 1 and 3.

All the rocks studied in the south and west part of Labine Point exhibit contact metamorphic characteristics in that they are recrystallised to a greater or lesser extent and have lost their original textures. These effects gradually die out eastwards. The actual metamorphic assemblages produced in the rocks very much depend upon the original chemistry and it is obvious that the diopside garnet skarn reported from Cobalt Island merely reflects the original calcareous nature of the rocks at that location.

The banded tuffs of the Mine formation, as well as being contorted, are completely recrystallised. About 800 feet from the contact, the recrystallised tuff contains hornblende and plagioclase with minor calcite and zoisite. 500 feet from the contact, diopside starts to appear, apparently having formed at the expense of the hornblende and 300 feet from the contact, andradite (?) is present. This progression probably represents increasing temperature and also the increasing calcium content of the rocks. Many rocks of the Mine formation exhibit beautiful trachytic textures which become obscured in the contact aureole. The plagioclase is recrystallised to a granular mosaic and pyroxene

replaces the original mafics of the rock.

Idocrase was found in the tuffaceous members within approximately 400 feet of the contact. It occurs with recrystallised hornblende, feldspar and small amounts of pyroxene exhibiting a sub-granoblastic texture (see Plate III, Fig. 7). Epidote is common in these rocks replacing hornblende but it is possible that all or some of this mineral are retrograde in character. A more siliceous lava about 300 feet from the contact contains granoblastic quartz and radiating fibrous masses of cummingtonite with epidote and idocrase (see Plate III, Fig. 8). The intergranular texture of all these rocks is very characteristic of contact metamorphism.

The diagnostic minerals of the aureole are recrystallised plagioclase and hornblende, andradite, idocrase and diopside. In most of the rocks, minor amounts of quartz and calcite are present. This assemblage therefore places the rocks within the hornblende-hornfels facies of contact metamorphism as defined by TURNER (1968). The lack of hypersthene or tremolite/actinolite negates the possibility of their being in either the epidote- or pyroxene-hornfels facies. Figure 3a is the ACF diagram for the hornblende-hornfels facies for rocks with an excess of  $\text{SiO}_2$  and  $\text{K}_2\text{O}$ . The assemblage plagioclase + hornblende, 1, and plagioclase + hornblende + diopside, 2, are obtained from the more basic rocks such as andesite. The more calcareous rocks produce the assemblage diopside + andradite + plagioclase, 3. Idocrase appears with a calcium-rich assemblage of calcite, andradite and diopside, 4, and the mineral will represent the approximate composition of the rock. Idocrase was once considered to be a product of high grade metamorphism

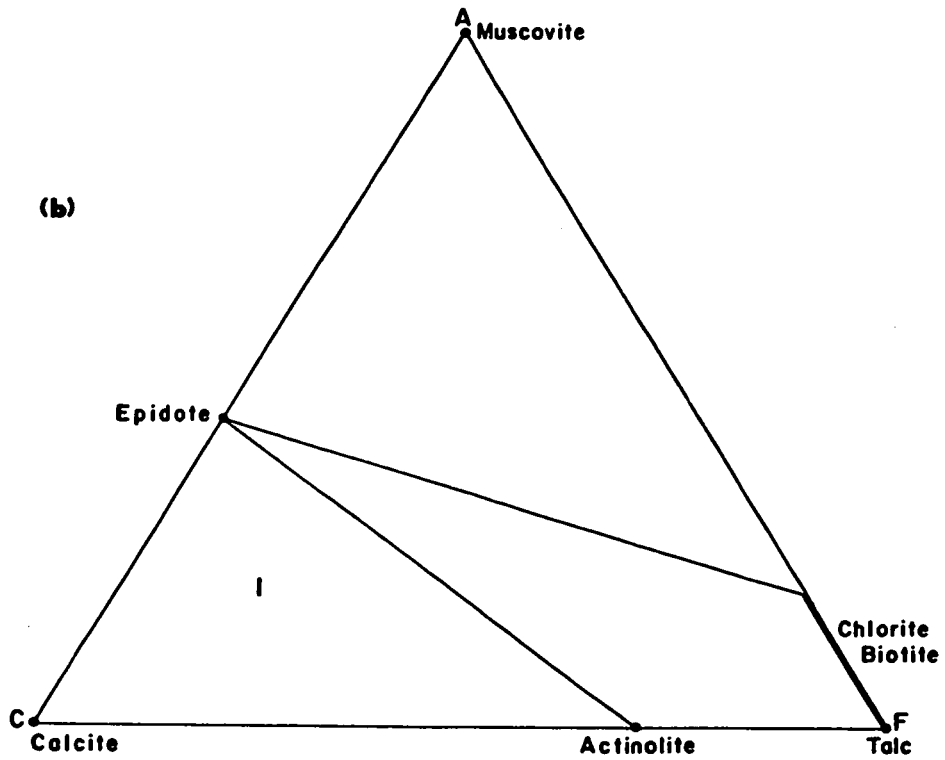
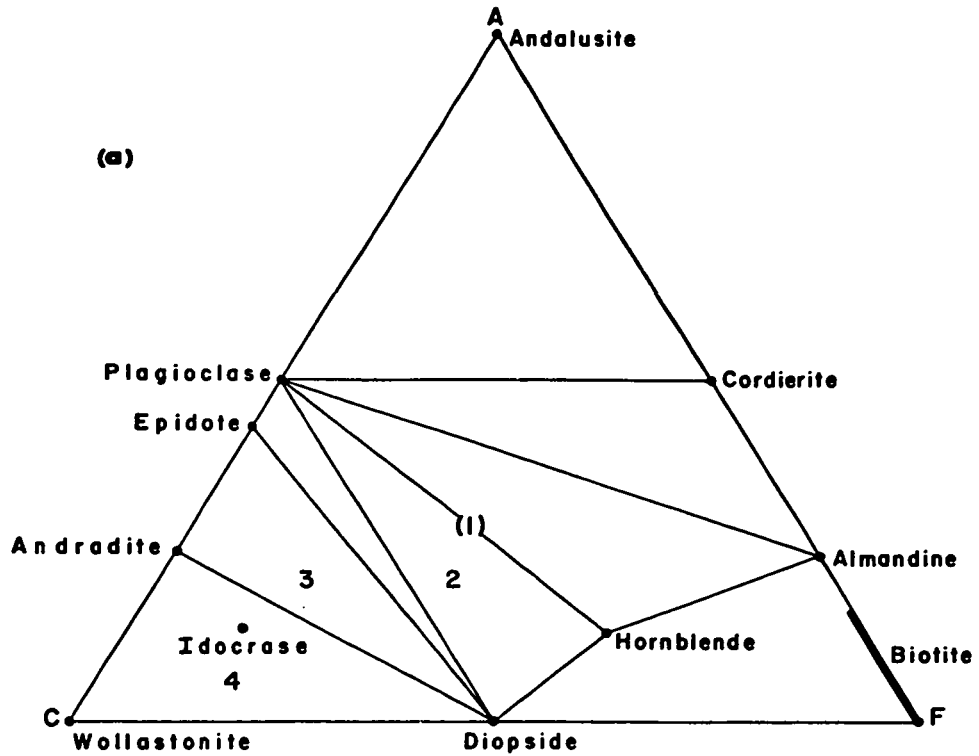


Fig. 3. (a) ACF diagram for the hornblende-hornfels facies with quartz and plagioclase as possible additional phases. (b) ACF diagram for the albite-epidote-hornfels facies for rocks with excess  $\text{SiO}_2$  and  $\text{K}_2\text{O}$ . Quartz, albite and microcline are possible additional phases.

only but it has now been demonstrated to be of much wider occurrence (CHATTERJEE, 1962).

The third traverse of this study was conducted in the northern part of Labine Point within a body of massive tuff. This tuff was sampled from 400 feet away from to within 6 inches of the granite contact. The samples are all fine-grained and exhibit a recrystallised granular texture. They are fairly consistent in mineral content with dominant plagioclase and hornblende. Sericitisation of the feldspars and chloritisation of the hornblende has occurred. At the contact the tuff is completely recrystallised and possesses a granoblastic texture. The texture very soon becomes sub-granoblastic and at 400 feet from the contact is granular. A constant dominance of plagioclase and hornblende, together with the metamorphic textures, suggest that these rocks also belong to the hornblende-hornfels facies of contact metamorphism. Their composition must be between the plagioclase and hornblende line 1, (Fig. 3a).

A contact metamorphic aureole belonging to the granodiorite body was studied in the northern part of the area. Since this aureole is not too well exposed and is of a much smaller extent than the one just described, only thin sections from one traverse were studied. The traverse was made in the most easterly part of the area where the granodiorite intrudes rocks of the middle portion of the Echo Bay Group (i.e. of around andesite in composition). About 200 feet from the contact the rock is a recrystallised tuff containing minor epidote. The feldspars are heavily sericitised and calcite is common. Most of the hornblende appears to have been altered to chlorite. Progressing

to about 100 feet from the contact, the same rock type contains plagioclase, minor hornblende and epidote. The rock is recrystallised and most of the hornblende has been altered to actinolite. Minor calcite is present, but chlorite and biotite are absent. This mineralogy of epidote, actinolite and calcite is characteristic of the albite-epidote hornfels facies of metamorphism for rocks with an excess of  $\text{SiO}_2$  and  $\text{K}_2\text{O}$  (TURNER, 1968). On the ACF diagram for this facies, shown in Fig. 3b, the rock composition would lie somewhere within the epidote + actinolite + calcite field, 1. Assuming an andesitic composition, then this would be probably close to the epidote-actinolite join. At about 50 feet from the contact, again the rock has a granular texture and contains plagioclase, hornblende and pyroxene with minor amounts of quartz, sericite and hematite. Original hornblende does exist but most of it has been altered to diopside which occurs as large crystals up to 5 mm. in length. The rock appears to have been hematitised and sericitised after metamorphism.

This assemblage of plagioclase + hornblende + diopside would place the rock within the hornblende-hornfels facies of contact metamorphism, with the rock composition lying within the area 2 in Fig. 3a.

It would appear then that the contact metamorphic effects are less widespread in this area, possibly due to a difference in intrusion temperature of the granodiorite, compared with that of the granite. However, the granodiorite would presumably intrude at a higher temperature than the granite, so it is possible that its size and shape are modifying factors. It should also be noted that the rocks there are poorer in calcium than those at Labine Point. With the granodiorite body, a facies gradation is encountered in the aureole. This is not present

within the granite aureole where the hornblende-hornfels facies shows a diffuse boundary with non-metamorphosed rocks.

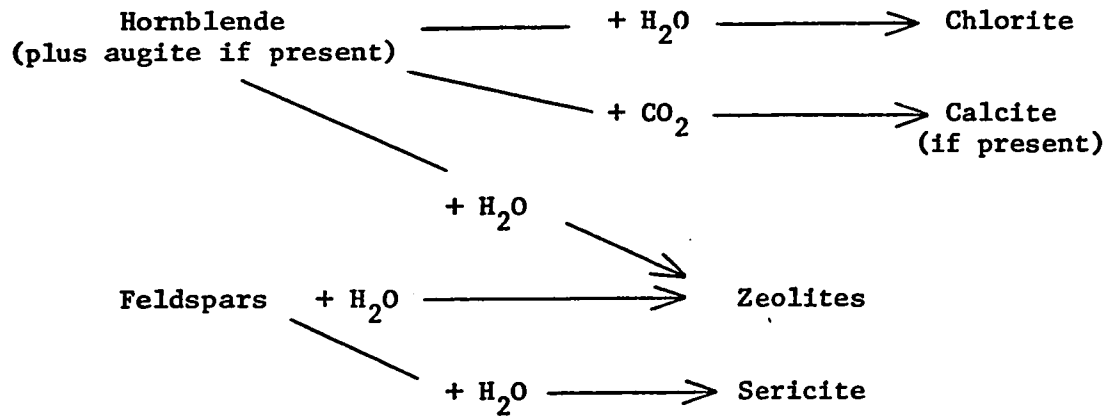
## 2. Regional Metamorphism

The volcanic and sedimentary sequence studied in detail in the area includes the Cliff Formation and the upper Echo Bay sub-Group. Within the tuffs and lavas of this group similar alteration patterns were noticed. Often the tuffs and lavas were difficult to distinguish but the tuffs are probably more altered than the lavas.

The feldspar phenocrysts are usually sericitised and often have dusty hematite inclusions. Any original pyroxene and most of the hornblende have been altered to chlorite. The chlorites are free from inclusions of any other minerals, particularly magnetite. Often the phenocrysts of hornblende are not completely replaced, but have a rim of chlorite around them. Original magnetite occurs in the hornblende and feldspar as tiny inclusions; it is sometimes found in the alteration products. The ground-mass of these rocks appears to be where a large part of the total alteration has taken place. It would be feasible to assume that the ground-mass would consist essentially of fine grained hornblende and andesine with or without magnetite. The fine-grained nature would promote more rapid and complete chemical reactions during any subsequent metamorphism.

It is in the ground-mass of two of these lavas and in the matrix of two of the tuffs examined that the zeolites, chabazite and thomsonite were observed. These minerals are thought to have been formed from the breakdown products of andesine and hornblende with the possible addition

of water and carbon dioxide. It is difficult to trace exact reactions for these changes but a generalised scheme of alteration is postulated below:



Connate water would be available for these reactions. The temperature and pressure for the reactions can only be estimated from the depth of burial. For a depth of burial of 6,000 to 8,000 feet (a reasonable estimation), a lithostatic pressure of 0.6 to 0.8 Kb would be operative. If this depth of burial is correct, then a high geothermal gradient would have to be postulated to obtain a temperature of only 100°C. This may not be all that unreasonable in a volcanically active area. Together with connate waters mineralising agents such as F, Cl, Na and K might be released during mineral breakdown to form a rather potent solution. Also the mineral assemblage present is metastable with a tendency towards a retrograde situation.

The lowest grade of regional metamorphism usually recognised is the zeolite facies as defined by COOMBS (1961). The type-locality for this facies is the New Zealand metagreywackes where heulandite + analcite + quartz are taken to be the characteristic assemblage of the lowest



grade of zeolite facies. However, WINKLER (1967) considers the start of the zeolite facies to be upon the first formation of laumontite hence naming it the laumontite-prehnite-quartz facies. Considering this definition, then zeolites such as heulandite, analcite, chabazite and thomsonite are not metamorphic minerals, since they are stable under sedimentary conditions. Their formation may thus be considered as part of diagenesis. A temperature of 200° C. and pressure of around 2 Kb must be attained for the onset of the laumontite-prehnite-quartz facies.

In a study of the Tertiary basalts of eastern Iceland WALKER (1960) described the zonation of zeolites in amygdale minerals. The deepest zone is rich in mesolite and scolecite; this is succeeded by an analcite zone whose top is thought to be about 2,000 feet below the original top of the lava pile. A restricted assemblage of chabazite and thomsonite lies above the analcite zone and the top zone in the lavas is thought to be zeolite free. It was concluded that the zeolite zones are approximately parallel to the original top of the Tertiary basalt lava pile. This type of regional zonation, occurring mainly in amygdale minerals, has been noted in many localities and the zones are thought to reflect the temperature attained in the lavas during zeolitisation. Experimental work has not yet been done to enable the use of geotherms. Many problems undoubtedly would be involved, the largest being the attainment of equilibrium in experimental work at such low temperatures.

By analogy, it would seem that the Echo Bay area lies within the chabazite-thomsonite zone of zeolitisation of the andesite pile.

The actual temperature of zeolitisation is not known, but would probably be less than 200° C. Using the example of Iceland, the pressure could be as low as 0.1 to 0.2 Kb.

### Structure

The rocks in the area mapped form part of a roof pendant within the granitic rocks of the Echo Bay area. They strike N 30° east and dip from 25° to 45° S, the average dip being 30° S. This tilting of the area is attributed to movement during, or just after, the intrusion of the granite. Anomalous strikes found on the 1944 map of this area by A.W. Joliffe and J.D. Bateman are now considered to be due to concentrations of magnetite in the areas concerned. All recorded dips and strikes were taken within the tuffaceous horizons, especially the banded tuffs. The lavas as part of the same sequence have the same general dip and strike.

As mentioned previously, there are four major directions of faulting or fracturing in the area. During the field season of 1968, the dips and strikes of all faults and fracture planes were recorded at each locality. These, plus data on major faults and veins in the area, gave a total of 159 readings which were used as data for a Fortran IV program (STPLOT) supplied by Dr. H.A.K. Charlesworth. This program converts the strikes and dips into a percentage pole diagram which in this case gave the percentage of points per 2% area of the stereo net. A contoured plot is shown in Fig. 4 (i.e. this is a contoured stereographic plot of the poles to the fracture planes).

The main pole maximum lies on the perimeter in the SE and NW quadrants of the net. This represents a plane whose mean strike is

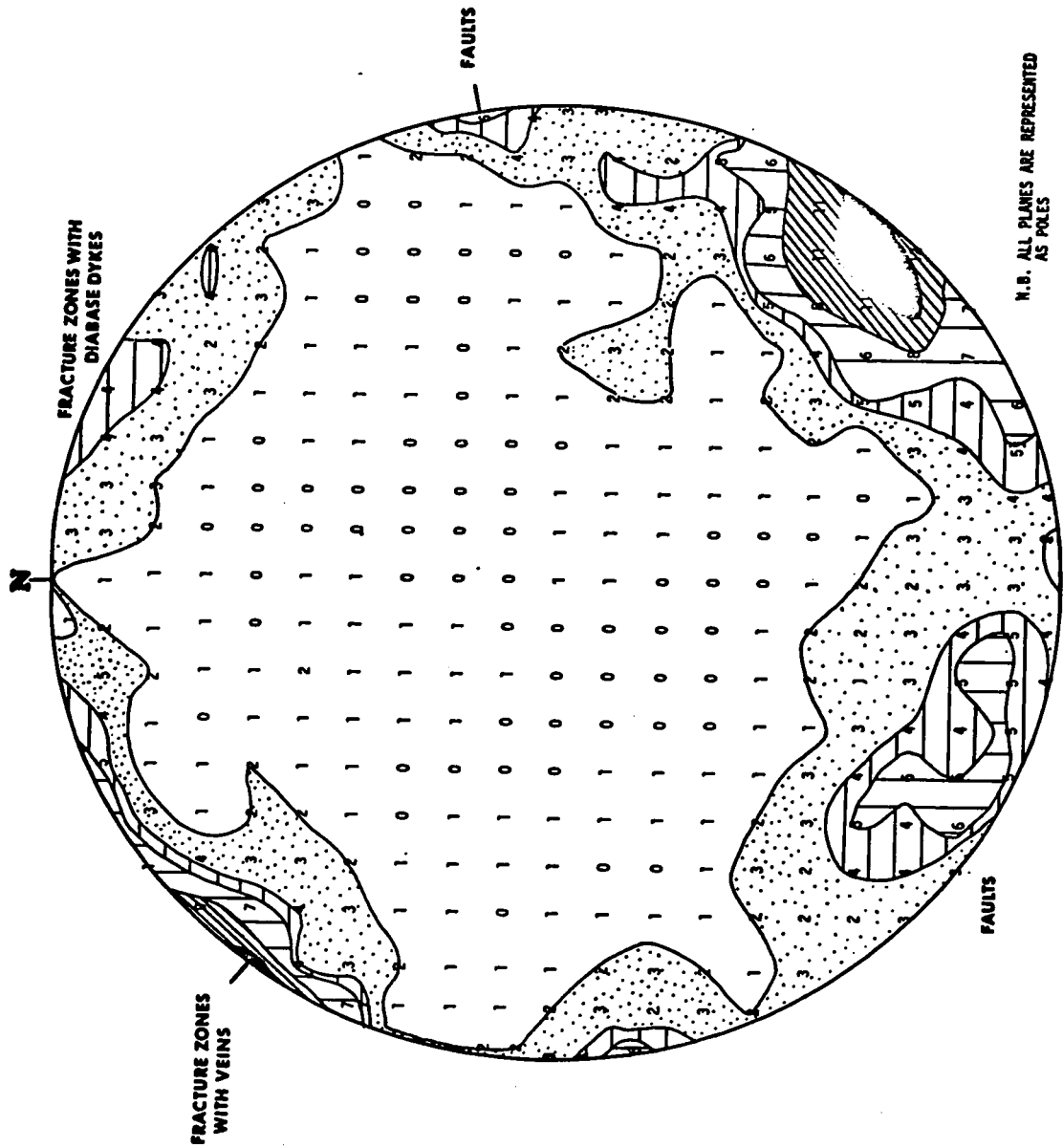


Fig. 4. Equal area projection and contours of the poles to the faults and fracture planes in the Echo Bay area.

N 35° E which corresponds with the trend of the main mineralised veins in the area and large faults such as the Cameron Bay fault, a major dextral shear. Complementary to this is a pole orientation at S 10° W plunging steeply north. This represents a complementary fault with a mean trend of E 10° S. Considering the area in general, it seems feasible that these could represent complementary structures with their P Max trending about N 70° E. The structures trending E 10° S appear to have acted as channelways for the diabase dykes in the area. These are usually older than the mineralised veins. Movement along the N 35° E trending structures has produced local offsets in the diabase dykes usually of no more than 100 feet. Both structures are usually vertical or very steeply-dipping and normally show very little displacement. The term 'fracture zone' has been applied to the major structure and hence to its complementary set. These fracture zones are often up to several feet in width, their characteristics depending on the competency of the rocks involved. A fracture zone in the Cliff Series on the east shore of Labine Bay is shown in Plate II, Fig. 2. The rocks here are not as competent as the lavas and mineralised veining has occurred. The same fracture zone is shown in Plate II, Fig. 5 where it occurs in the hornblende feldspar porphyritic lavas. The rock is more competent and thus no veining is observed.

A third fault system is evidenced from the stereo plot for a plane striking from E 80° S. Also a maximum at S 30° W plunging steeply north indicates a complementary fault system trending E 30° S. These two systems appear to be complementary but it is not known if they are contemporaneous. These two sets of faults do not appear to be channelways

for either mineralisation or diabase dykes. They may have been formed later than the first set of fracture zones, possibly as tensional structures resulting from regional uplift.

Confusing the age relationships of the two fracture systems is a probable spread in the time of formation of the diabase dykes. Often there is a close association between the dykes and the vein material. In general the dykes are cut by the vein structures; occasionally the dykes will cut early quartz in the veins but not the later mineralisation. The E 10° S trending fracture zones probably developed first and allowed diabase emplacement. They were followed by formation of the N 35° E trending fracture zones which offset many of the dykes. The shape of the veins and brecciation of vein material suggests that there has been more than one phase of movement in these structures.

#### Veins and Mineralisation

The Eldorado vein zones trend northeast across Labine Point. They are flanked by alteration zones of microcline, hematite, chlorite, white mica and carbonate. Most of the ore was confined to a zone lying between the hornblende feldspar porphyritic lavas in the east and the granite on the west. Ore shoots occur mainly where Echo Bay sedimentary rocks form one or both walls of the veins (JORY, 1964). Descriptions of the Eldorado veins can be found in CAMPBELL (1955) and JORY (loc.cit.).

The main mineralised zone of the Echo Bay Mine strikes northeast and occurs mainly within the tuffs of the Cliff Formation. Mineralisation appears to be most common in the sedimentary rocks rather than the lavas. The lensiform nature of many of the veins has probably resulted from secondary movement along the initial slightly sinuous fracture zone

R.J. Beckett, pers. comm.). Vertical movement of one side relative to the other would thus produce lens shaped areas of greater dilatancy within the fracture zone. Most of the mineralised zones outcrop under muskeg filled depressions at surface. The main Echo Bay #2 zone occurs as a wide muskeg filled depression above the mine continuing down towards Labine Bay. On the east shore of Labine Bay, the presumed continuation of this zone bifurcates near the contact with the hornblende feldspar porphyritic lavas as shown in Plate II, Fig. 2.

Some quartz veins are found in the upper Echo Bay sub-Group lavas. They are up to two feet in width, occur in relatively tight fractures and contain no mineralisation (see Plate II, Fig. 4). A typical vein in the Echo Bay Mine is shown in Plate II, Fig. 6. The area in the left of the picture contains hematitised wall rock and pitchblende. The carbonate vein contains sulphide mineralisation as specks and vug infillings. A detailed description of the mineralogy and paragenetic sequence are given later.

PLATE I

Figure

1. Convolute bedding in banded tuffs of the Cliff Series.
2. Pyrite rich tuffs of the Cliff Series, #3 adit level, Echo Bay Mine.
3. Fine grained, thinly bedded, plagioclase tuffs of the Mine Series.
4. Gossan Hill, south of #1 adit, Echo Bay Mine.
5. Contact between granite and massive tuffs, east shore of Labine Point.
6. Aplite dikes, associated with the granite, cutting the tuffs of Labine Point.
7. Diabase sill exhibiting columnar jointing and intruding the Cliff Series.
8. Actinolite-magnetite veins and disrupted tuffs of the Cliff Series.

# PLATE I

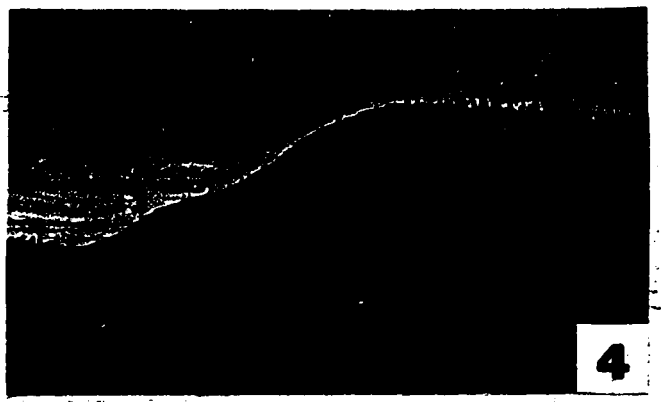
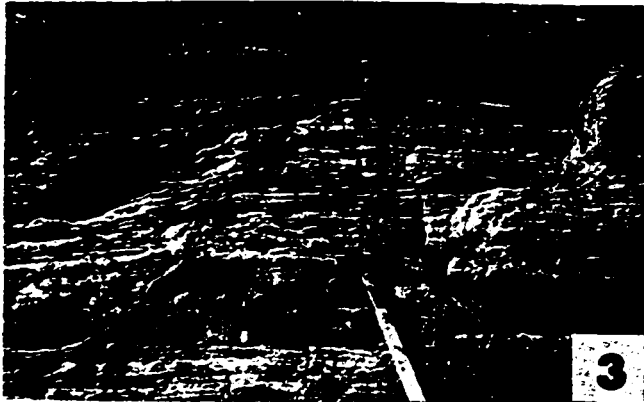
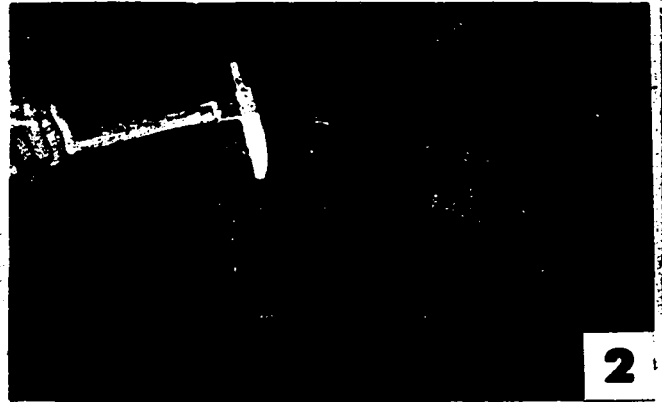




PLATE I

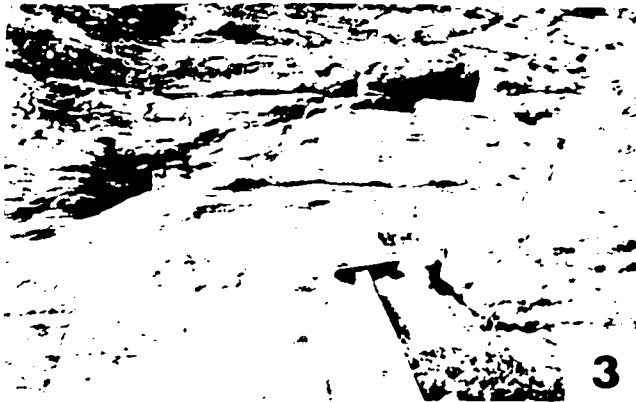
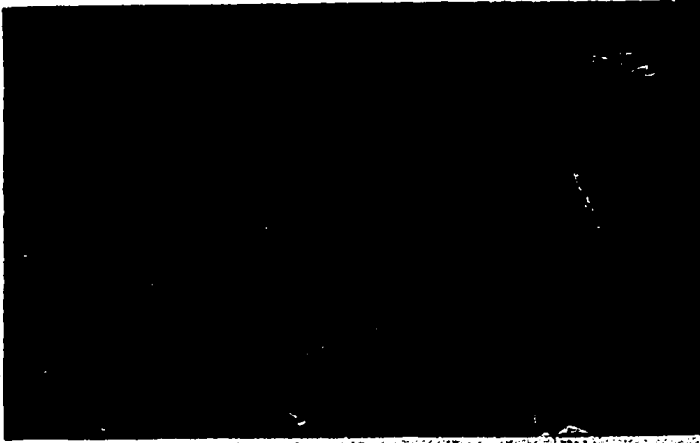


PLATE II

**Figure**

1. **Folding in the tuffs of the Mine Formation.**
2. **Fracture zone in the Cliff Series carrying the southern extension of the Echo Bay Mine main #2 vein.**
3. **Contortion of the tuffs of the Mine Formation.**
4. **Barren quartz vein in the Upper Echo Bay sub-Group.**
5. **Fracture zone in the hornblende-feldspar porphyry.**
6. **#2 vein, #3 adit level, Echo Bay Mine.**

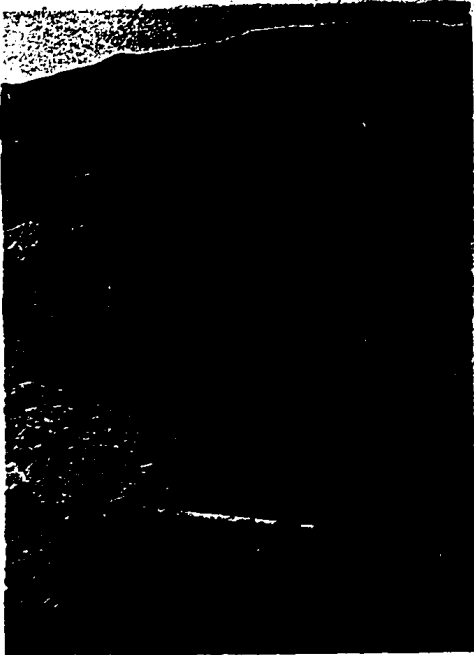
**PLATE II**



**1**



**2**



**3**



**4**



**5**



**6**

# PLATE II



1



2



3



4



5



6

PLATE II



1



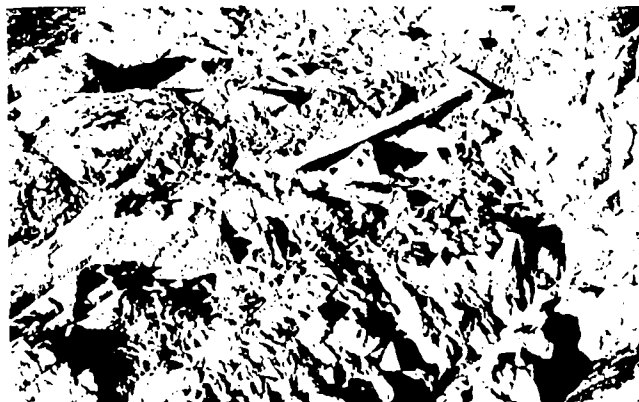
2



3



4



5



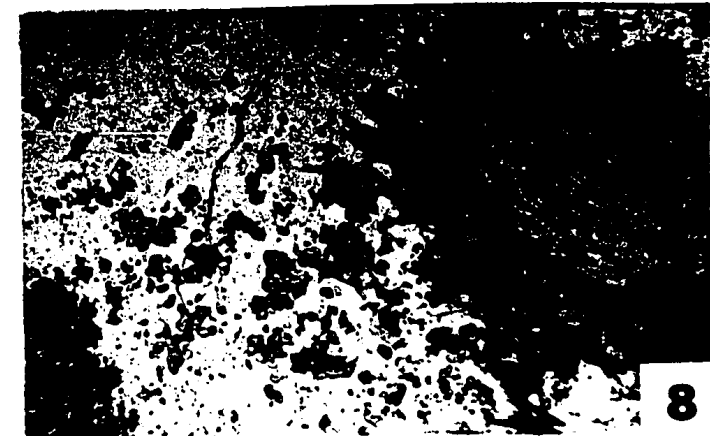
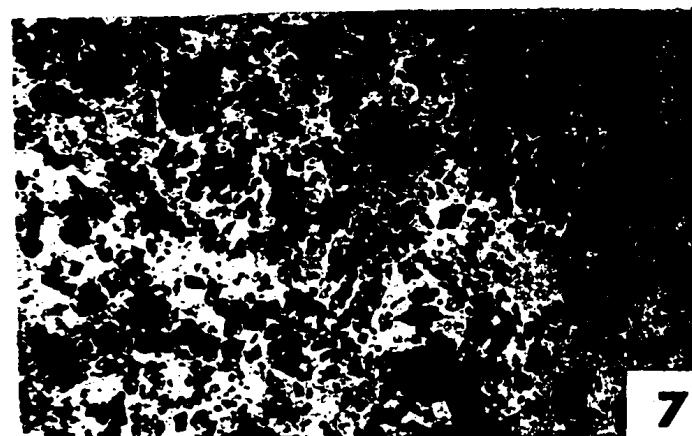
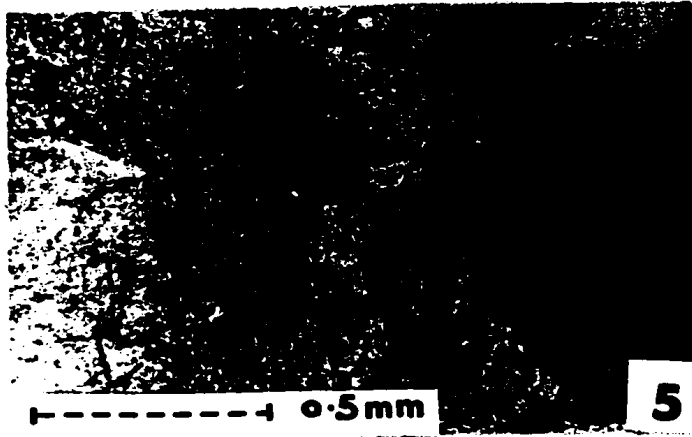
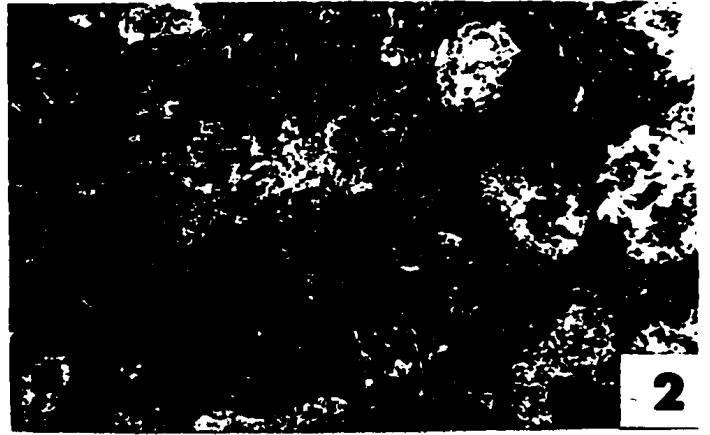
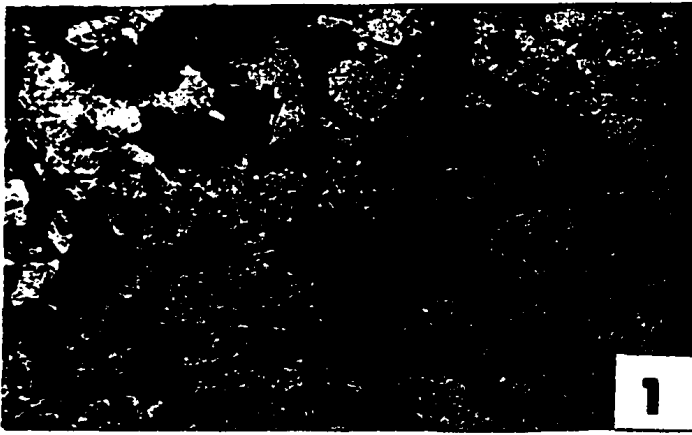
6

PLATE III

Figure

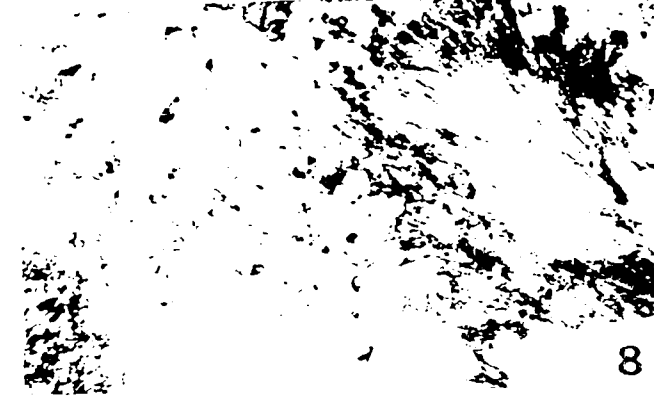
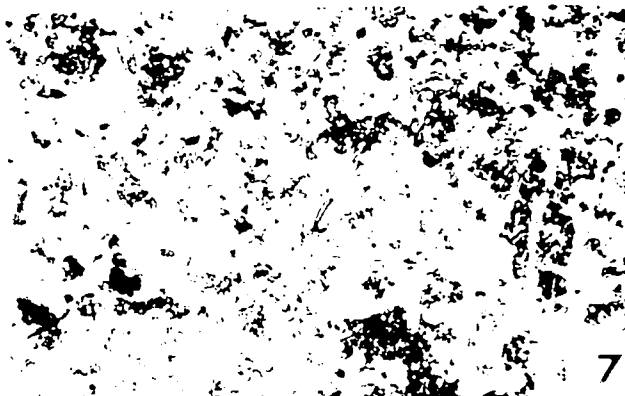
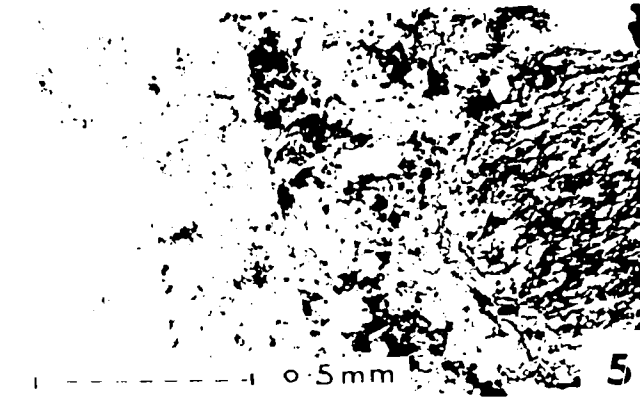
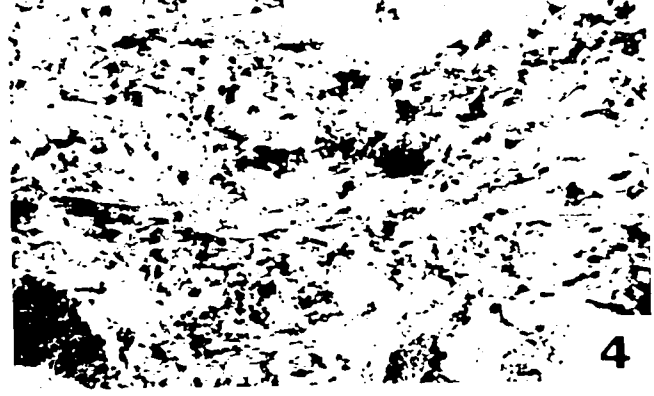
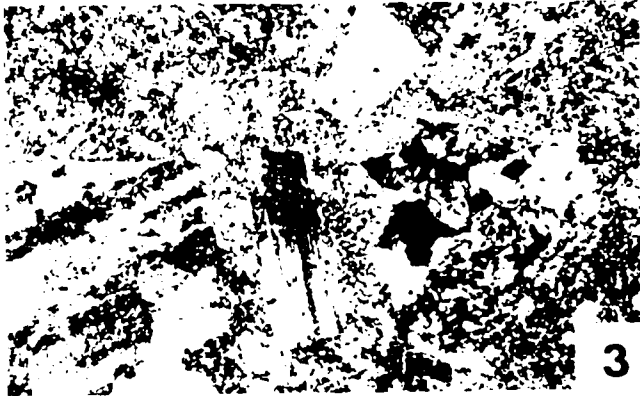
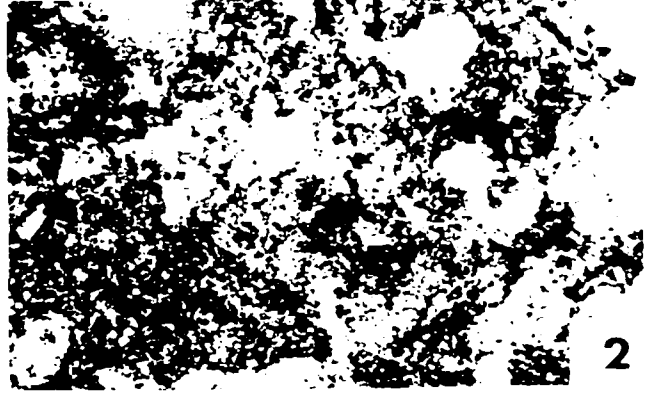
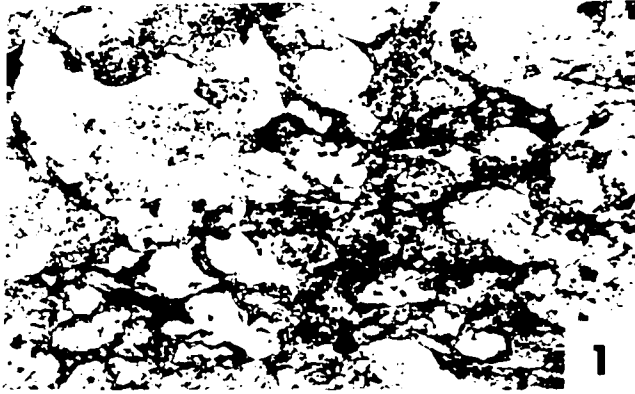
1. EBT 1.1: Volcanic tuff consisting mainly of corroded quartz and feldspar fragments. Most of the ground mass is chlorite.
2. EBT 1.3: Recrystallised massive tuff composed mainly of hornblende and feldspar.
3. EBT 1.6: Hornblende feldspar porphyritic lava (crossed nicols). The rock is extensively altered to chlorite, sericite and carbonate.
4. EBL 2: Trachytic texture in the lavas of the Mine formation, (crossed nicols).
5. EBT 1.2: Porphyritic andesite. Sericite picks out the zoning of the feldspar. Zeolites are amongst the alteration products in the matrix.
6. EBT 1.4: Amygdaloidal andesite showing part of a quartz amygdale on the right hand side of the frame. The feldspar phenocrysts and fine grained ground mass are similar to those found in the porphyritic andesite.
7. EBL 3: Granular metamorphic rock from the granite's contact metamorphic aureole. Intergranular textures are present and diopside, idocrase and epidote can be seen.
8. EBL 3.1: Metamorphosed siliceous volcanic rock. Although the rock is composed dominantly of quartz, cummingtonite can be seen in the right hand side of the frame. Some idocrase and epidote are also present in this rock.

# PLATE III



1mm

PLATE III



0.5mm



## CHAPTER 4 - GEOCHRONOLOGY

### Previous Work

Geochronological studies of the Bear Province as a whole are confined to the work done by the Geological Survey of Canada in their age determination program of Canada (LOWDON, 1960, 1961; LOWDON et al., 1963; LEECH et al., 1963; WANLESS et al., 1965, 1966, 1967 & 1968). Some interpretation of the ages obtained is given in these papers. Fig. 5 is a reproduction of part of the G.S.C. Isotopic Age map of Canada (WANLESS et al., 1968). It depicts the Bear Province and the K-Ar ages obtained from this Province, compared with those from the adjacent Slave Province. A total of about 25 K-Ar age determinations has now been published by the G.S.C. for the Bear Province, but they are almost exclusively representative of the eastern sector.

K-Ar ages on a biotite from a granite unconformably overlain by the Hornby Bay Group give 1765 m.y. (GSC 60-39) and a biotite associated with the Muskox intrusion which intrudes the Hornby Bay group gives 1155 m.y. (GSC 60-38). Unpublished data of L.T. Silver, obtained from JORY (1964), would suggest that the Muskox Complex is older than 1155 m.y. On an apatite separate from a granophyric differentiate of this Complex, Silver obtained a  $Pb^{207}/Pb^{206}$  age of  $1500 \pm 100$  m.y. This is a geologically more reasonable age. The Hornby Bay Group is thus bracketed between about 1500 and 1765 m.y.

A granodiorite which cuts the Snare and Cameron Bay Groups has given a K-Ar biotite age of 1815 m.y. (GSC 64-45) and a K-Ar muscovite age of 1855 m.y. (GSC 64-46). Thus the Cameron Bay Group is older than about 1855 m.y. 1765 was the K-Ar biotite age (GSC 61-85) obtained for

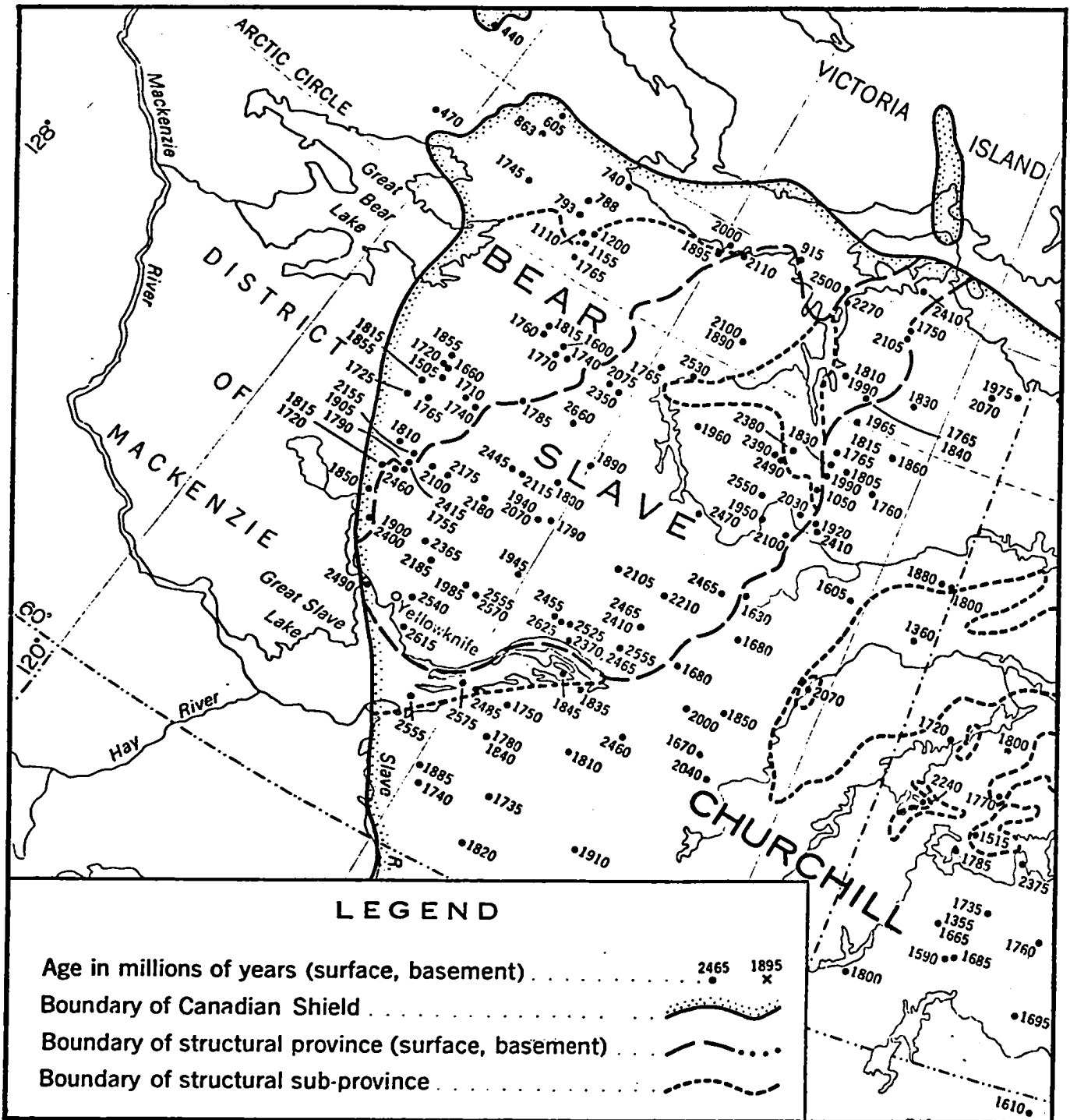


Fig. 5. Isotopic age map of the Western Canadian Shield from (WANLESS et al., 1968).

an intrusive porphyry which cuts the Echo Bay and Cameron Bay Groups, thus suggesting them both to be older than about 1765 m.y.

A K-Ar muscovite age of 1905 m.y. (GSC 61-60) and an associated K-Ar biotite age of 1755 m.y. (GSC 61-63) for a granodiorite older than the Snare Group thus gives an approximate minimum age for this Group. A biotite from the Big Spruce Lake nepheline complex gave a K-Ar age of 1785 m.y. (GSC 62-92). This complex intrudes a basal limestone of what is thought to be the Snare Group. Thus an approximate minimum age is established for this Group. Biotites from schists and gneisses of the Snare Group have given ages of 1760 m.y. (GSC 64-59), 1720 m.y. (GSC 60-64 and 41), 1740 m.y. (GSC 60-44) and 1725 m.y. (GSC 60-42). These apparent ages probably give the age of metamorphism of the Snare Group. A biotite K-Ar age from a granodiorite in the Camsell River area gave 1785 m.y. (GSC 61-55), an age which is typical for the igneous rocks of this area. In a study of the Eldorado mine KIELLER (1962) obtained a K-Ar age on a biotite from the granite body off Labine Point. The sample was obtained from the western part of the Eldorado mine and the age given was 1930 m.y., with no assigned error. This age is older than the lead-uranium age obtained for the same body (JORY, loc.cit.) and also the rubidium-strontium age obtained by the author for the volcanics which are intruded by this granite body. An error in the potassium determination is possibly the cause of this discrepancy.

K-Ar whole rock dating has yielded 1600 m.y. (GSC 65-67) for a porphyritic andesite from the Epworth Group, 1660 m.y. (GSC 64-42) and 1550 m.y. (GSC 64-43) for basic volcanic rocks overlying the Snare Group. These whole rock apparent ages will probably be younger than

the true ages, owing to loss of radiogenic argon from feldspar.

No Rb-Sr dating has been done in this area by the G.S.C. and most of the K-Ar dates in the area merely reflect the effect of the Hudsonian orogeny on the Bear Province either by metamorphism or by intrusion (STOCKWELL, 1964). The K-Ar ages produced on the intrusive bodies of this Province are probably meaningful. However the K-Ar dating method is not useful in obtaining the true age of the sedimentary - volcanic groups, either owing to the lack of suitable potassium-bearing minerals or to the effect of subsequent metamorphism. However, the evidence so far would suggest that the Snare Group is no older than about 1900 m.y. and that inliers of Yellowknife rocks do not exist in this Province.

Dates for the diabase dykes and sills in this area do not appear in the G.S.C. reports quoted. In a study of the diabase dyke swarms of the Canadian Shield FAHRIG and WANLESS (1963) show a dyke swarm in the Bear Province which trends approximately N 70° E. This is in fairly good agreement with aforementioned approximate east-west trend for the dykes of this Province. The age assigned to this dyke swarm is 875 m.y. (FAHRIG and WANLESS, op. cit.). This age however is based only upon two whole-rock samples and thus could be rather suspect. Also this age would not be in good agreement with the estimated 1450-1500 m.y. for the dykes in the Echo Bay area. It is considered that many more samples would have to be taken to characterise the dykes of this Province. Also whole-rock K-Ar dating is not the most powerful method which could be applied. The study by LEECH (1965) on the basic intrusive rocks of the Canadian shield was of no value in obtaining a characteristic age for the dykes of the Bear Province.

JORY (loc. cit.) in his study of the Eldorado mine, Port Radium, obtained lead- and uranium-isotopic data on zircons from the granite body off Labine Point. Five zircon fractions were derived from a sample on Granite Island and two fractions were taken from a sample from the western underground workings of the Eldorado mine. Different size fractions of the zircons were taken, since it is usually found that the degree of discordance increases with decreasing size. A chord was drawn through the points representing the various zircon fractions, and it intersects the concordia curve on a  $Pb^{206}/U^{238}$  versus  $Pb^{207}/U^{235}$  plot at 1820 m.y. and 50 m.y. One size fraction was omitted from the data since it gave unusual isotopic data, possibly due to laboratory contamination of a small sample. Thus, from the data obtained, the age of the granite was considered to be  $1820 \pm 30$  m.y. The straight line fit of the points was within analytical error. However, analytical error would allow the lower concordia curve-intersection to vary between zero and 100 m.y. It was felt by Jory that neither laboratory loss of lead nor recent leaching were plausible explanations. Also the chord is much steeper than the continuous diffusion curves for lead. It was therefore concluded that the discordance was caused predominantly by a relatively recent, episodic lead loss, although continuous diffusion may have contributed to the overall discordant pattern. No known geological event occurs within this area that might explain this episodic lead loss.

Many attempts to date the Port Radium pitchblende by chemical means were made in the early 1930's. This early work and later dates derived from mass spectrometry were summarised by CUMMING et al. (1955). JORY (op. cit.) isotopically analysed microscopic and macroscopic samples of three pitchblende specimens from the Eldorado mine for lead

and uranium. On two microscopic samples in carbonate gangue, concordant lead-uranium ages were obtained. This age of  $1445 \pm 20$  m.y. is the only concordant age to be measured on the Port Radium ores. For a specimen of pitchblende in siliceous gangue two analyses define a chord which intersects the concordia curve at 1450 and 300 m.y. A continuous diffusion of lead is used to explain the lower intersection. However, GREEN (1968) explained a similar lower intersection of about 300 m.y. for lead-uranium work on zircons from the western Granodiorite, Yellowknife as being possibly due to a mid-Paleozoic event. Evidence for this event is found in the northern Yukon (BAADSGAARD et al., 1961). The different degree of discordance noted for some samples was explained by a greater lead loss near permeable fractures. Also plotting along the chord which intersects at 1450 m.y. and 300 m.y., are samples from other studies (CUMMING, loc. cit., ECKELMAN and KULP, 1957) on Port Radium samples and other samples from Contact Lake about 10 miles south of Port Radium, and a sample from the Hottah Lake area. This suggests that pitchblende mineralisation occurred at the same time in these other areas.

#### Rubidium - Strontium Dating

This method of dating is probably the most powerful one available. Hand-sized specimens of rocks may remain closed systems with respect to rubidium and strontium even when subjected to high-grade metamorphism. Rubidium, although forming no minerals of its own, is readily admitted into the lattice of potassium-bearing minerals. It consists of two isotopes of mass 85 and 87.  $\text{Rb}^{85}$  is stable but  $\text{Rb}^{87}$

decays by  $\beta$ -particle emission to  $\text{Sr}^{87}$  at a rate which renders the  $\text{Rb}^{87} - \text{Sr}^{87}$  decay scheme amenable to the radiometric dating of older geological material.

FLYNN and GLENDENIN (1959) counted the specific activity of natural rubidium by dissolving an organic rubidium salt in a liquid scintillator and determined a decay constant of  $\lambda = 1.47 \times 10^{-11}/\text{yr}$ . ALDRICH et al. (1956) determined a value of  $\lambda = 1.39 \times 10^{-11}/\text{yr}$ . by comparison of  $\text{Rb}^{87}/\text{Sr}^{87}$  ratios of pegmatitic minerals with concordant U-Pb ages on cogenetic uraninites. CUMMING (1969) has revised existing Pb, Rb-Sr and K-Ar data for meteorites and suggests a decay constant of  $\lambda = 1.436 \times 10^{-11}/\text{yr}$ . is optimum. The University of Alberta is currently using the decay constant of  $\lambda = 1.39 \times 10^{-11}/\text{yr}$ . which appears to give more consistent results with U-Pb and K-Ar values. The half-life then of about 5 b.y. thus limits the application of the Rb-Sr method to being most useful in Precambrian terrains.

A whole-rock Rb-Sr study was undertaken on the Echo Bay volcanics and sediments to determine their age of formation. Analyses of a series of cogenetic whole-rock samples with differing Rb-Sr ratios is also a test for 'closed system' behaviour. For the selection of rocks most suitable for Rb-Sr dating, preliminary analyses for rubidium and strontium were made on finely ground whole-rock samples. Samples were selected to give the largest range and best spacing of Rb-Sr ratios. All samples showing signs of weathering were discarded.

For the isotope dilution analysis of strontium and rubidium, optimum amounts of sample were decomposed to give  $\text{Sr}^{86}/\text{Sr}^{84}$  ratios of approximately 1.0 and  $\text{Rb}^{87}/\text{Rb}^{85}$  ratios of approximately 2.0. The analytical techniques employed for the determination of rubidium and

strontium are given in Appendix B. The single tantalum filaments used in the mass spectrometer are degassed before use. Strontium is loaded as the chloride onto oxidised filaments where it is glowed in air and then pretreated to remove potassium and rubidium. The rubidium is loaded as the sulphate onto an outgassed tantalum filament.

The mass spectrometer employed was a 6 inch radius, solid source, single filament machine with a 60°-sector magnetic deflection designed and built by Dr. G. Cumming, Dept. of Physics, University of Alberta. Surface ionisation from the tantalum filament produces an ion beam which is amplified directly using a Cary 31 vibrating reed amplifier with a  $10^{11}$  ohm resistor. The mass ratios 88/86, 87/86 and 84/86 were measured for strontium using a rapid peak switching procedure facilitated by preset magnet current settings. The signals were recorded through an integrating digital voltmeter with a digital printer. A slow scan of the whole strontium spectrum was taken after every set of mass ratios and used for making baseline and tailing corrections. Rubidium was isotopically analysed by switching between masses 87 and 85 and measuring the isotopic mass ratio from chart output. The 87/85 ratios were measured from the first obtained data so as to have the least fractionation. The measurement precision of the strontium mass ratios is usually 0.1% and the rubidium ratios is usually within 0.5%, but due to fractionation the latter may be as high as 1 or 2%.

Considering a whole-rock phase which contained common strontium at the time of its formation and accumulated radiogenic strontium for a time,  $t$ , where  $t$  is the age of the system, then:



$$\text{Sr}_p^{87} = \text{Sr}_o^{87} + \text{Rb}^{87} (e^{\lambda t} - 1)$$

where the subscript p and o refer to the present and the original concentrations respectively.

Dividing by  $\text{Sr}^{86}$  we have:

$$\frac{\text{Sr}^{87}}{\text{Sr}^{86}} = \frac{\text{Sr}^{87}}{\text{Sr}^{86}} + \frac{\text{Rb}^{87}}{\text{Sr}^{86}} (e^{\lambda t} - 1)$$

which is the equation of a straight line of the form  $y = c + mx$ , where  $y = (\text{Sr}^{87}/\text{Sr}^{86})_p$ ;  $c = (\text{Sr}^{87}/\text{Sr}^{86})_o$ ;  $x = (\text{Rb}^{87}/\text{Sr}^{86})_p$  and  $m = (e^{\lambda t} - 1)$

which is approximately  $\lambda t$ .

A plot of  $(\text{Sr}^{87}/\text{Sr}^{86})_p$  versus  $(\text{Rb}^{87}/\text{Sr}^{86})$  on related whole rock samples will yield a straight line whose slope is approximately  $\lambda t$ .

This straight line is termed an isochron (NICOLAYSEN, 1961).

Since the rocks of the Echo Bay area have not been subjected to high grade metamorphism of a regional type, then a closed system behaviour of the whole rock Rb-Sr system is assumed. Table 2 shows the analytical data on which the Rb-Sr isochron is based. The results are plotted as a standard Nicolaysen diagram in Fig. 6. The isochron was fitted to the data points by an APL program RBSRISOCHRON written by Dr. H. Baadsgaard. This program uses a least squares fitting of the straight line, but allows for non-uniform variance in the  $\text{Rb}^{87}/\text{Sr}^{86}$  ratios and incorporates prior estimates of the precision for both co-ordinates. The estimates of variance used were: for  $\text{Sr}^{87}/\text{Sr}^{86} = 3.0 \times 10^{-5}$  and for  $\text{Sr}^{87}/\text{Sr}^{86} = 2.5 \times 10^{-6}$ . The ratios for individual samples were also calculated by an APL program (RBSRCOM) written by Dr. H. Baadsgaard. The age given by the isochron is 1770 m.y. with a

TABLE 2

Rb-Sr analytical data for whole rock isochron, Echo Bay volcanics

Sample Number	Description	Rb (p.p.m.)	Sr (p.p.m.)	Rb <sup>87</sup> /Sr <sup>87</sup> atomic ratio	Sr <sup>87</sup> /Sr <sup>86</sup> atomic ratio
EBT 1.1	Banded tuff	147.2	38.2	11.476	0.9871
EBT 1.3	Massive tuff	192.5	166.3	3.377	0.7905
EBT 1.5	Banded tuff	130.9	130.4	2.924	0.7717
EBT 3.1	Porphyritic andesite	174.8	198.0	2.570	0.7650
EBT 1.2	Porphyritic andesite	176.9	286.9	1.792	0.7473
EBM 1	Banded tuff	28.5	97.2	0.849	0.7277
EBT 2.4	Massive tuff	14.2	80.4	0.511	0.7101

All runs recorded on integrating digital voltmeter

Rb<sup>87</sup>/Sr<sup>86</sup> values  $\pm$  1%

Sr<sup>87</sup>/Sr<sup>86</sup> values  $\pm$  .001

(Rb<sup>87</sup>)  $\lambda = 1.39 \times 10^{-11} \text{ yr}^{-1}$

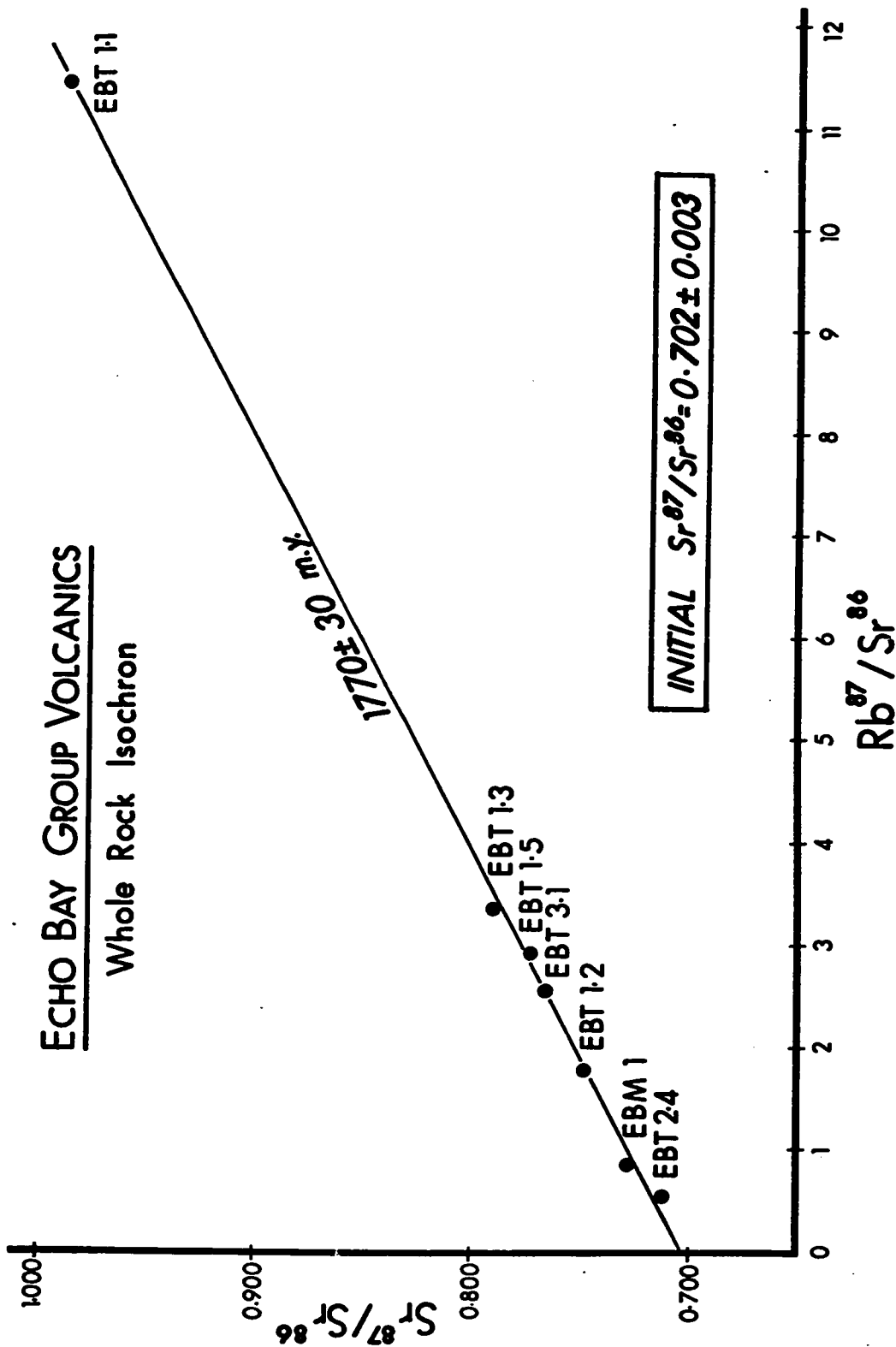


Fig. 6. Whole rock Rb-Sr isochron for the Echo Bay group volcanics.

standard deviation of 30 m.y., i.e. a date of  $1770 \pm 30$  m.y.

The whole-rock isochron represents a reasonable fit to the analytical data. Only one sample, EBT 1.1, displays a favourable Rb/Sr ratio and thus the isochron is very much influenced by this point. However if this point is ignored, the isochron for the other 6 data points with the more unfavourable ratios is  $1810 \pm 90$  m.y. A much larger error is attached to this age, but statistically these two isochrons are indistinguishable.

The three points which show the least deviation from the isochron are EBT 1.1, EBT 1.2 and EBT 3.1. EBT 1.1 essentially determines the isochron, but the other two points can be distinguished since they are samples of lava, compared with the other points which represent samples of tuffaceous material. This would possibly suggest that the less permeable and more competent lavas exhibit closed system characteristics. The samples of tuff deviate slightly from the isochron and possibly represent a tendency towards a small degree of open system behaviour. It appears that some are slightly enriched and some slightly depleted in radiogenic strontium. These small deviations are outside experimental error, and probably correlate with the larger degree of alteration in the form of chloritisation and hematization that has taken place within the tuffs as compared with the lavas. It should also be mentioned that although the samples are fairly closely related spatially, they could display slight variations in initial ratios. This would mean that a number of parallel isochrons with slightly different initial ratios would be required to define the system. However, it seems quite feasible that the tuffs may have exchanged a small amount of radiogenic strontium

amongst themselves. It is thus possible that EBT 1.1 may contain a slight excess or deficiency of radiogenic strontium, but its agreement with the other data points suggests that if this is so, then it is within the error of the isochron. A good check on this fact is the agreement of the 6 point and 7 point isochrons.

The age obtained for the granite body which intrudes the Echo Bay volcanics was 1820 m.y. (JORY, op. cit.). Although this is an apparent reversal of ages i.e. considering the ages without the assigned errors the granite appears to be older than the volcanics which is not the case. The granite body is assigned an age of  $1820 \pm 30$  m.y. on Pb-U dating of zircons and the volcanics are assigned an age of  $1770 \pm 30$  m.y. on whole-rock Rb-Sr dating. Thus it can be seen that these two ages cannot be distinguished from one another within the error limits. Therefore the two geological events, i.e. the extrusion of the andesites and tuffs and the intrusion of the granite cannot be differentiated on the basis of the data available. It would appear then that both the extrusive and intrusive activity occurred at  $1800 \pm 60$  m.y. Obviously there are difficulties in comparing Pb-U dating with Rb-Sr dating, especially when the two dates were obtained in different laboratories. The Rb<sup>87</sup> decay constant of  $1.39 \times 10^{-11}$ /yr. which was used should give good agreement with Pb-U dating. Interlaboratory checks are often difficult to assess for the same method and impossible when comparing dates from different dating methods. However, since the ages given agree within error, then a reasonable check has been established. The initial Sr<sup>87</sup>/Sr<sup>86</sup> ratio of the volcanics as given by the 7 point isochron is 0.702, (a figure which is consistent with a subcrustal origin for

these rocks).

MUKHERJEE (pers. comm.) obtained a Rb-Sr age for the granite to the northwest of Flin Flon (Manitoba) of  $1805 \pm 14$  m.y. The Rb-Sr work on the Amisk volcanics, which this granite intrudes, was not conclusive. However, it does appear that the volcanics are not much older than the granite; both events occurring around 1800 m.y. This area of the Churchill province thus seems very similar to the Echo Bay area in the geological setting and relative timing of events.

#### Potassium-Argon Dating

This method of dating is of widespread applicability because of the abundance of K-bearing minerals. However, only the minerals biotite and amphiboles, which show good argon retentivity, have been used in this study. In a Precambrian K-Ar system, the incorporation of small volumes of contaminant argon upon crystallisation of the mineral are not significant.

Potassium consists of three isotopes:  $K^{39}$ ,  $K^{40}$ ,  $K^{41}$ .  $K^{40}$  decays to  $Ca^{40}$  and  $Ar^{40}$  by a branched decay scheme; 89% of the disintegrating nuclei go to  $Ca^{40}$  by beta emission and 11% to  $Ar^{40}$  by K-electron capture. A potassium-argon age may be calculated from the following equation:

$$\frac{Ar^{40}}{K^{40}} = \frac{\lambda_e}{\lambda_\beta + \lambda_e} \cdot (e^{[\lambda_e + \lambda_\beta]t} - 1)$$

where  $\lambda_e$  is the decay constant for K-electron capture,  $\lambda_\beta$  is the decay constant for decay by beta emission and  $t$  the age of the K-Ar system. The decay constants used are shown in Table 3. A half life

for the system of  $1.36 \times 10^9$  years makes this method very versatile in geochronology. The  $Ar^{40}/K^{40}$  ratio often, however, only yields an apparent age for the system since it will only indicate the time at which a specific mineral became a closed system to the diffusion of radiogenic argon. Biotites probably become closed systems at about  $150^\circ$  to  $200^\circ$  and hornblendes at rather a higher temperature. Thus, K-Ar ages may actually depict 'cooling ages' of a large intrusive body or in a metamorphic area they usually give the time of metamorphism.

All the samples collected for K-Ar dating were fresh rock. Thin sections of the samples were made and many discarded on the basis of alteration. Most of the hornblende in the volcanics is altered to chlorite and thus out of ten original samples, only two were used. Samples for both biotite and hornblende were selected from the granite and granodiorite and for hornblende and actinolite from the hornblende-actinolite veins.

All samples were crushed to specific mesh sizes (usually around -60 to +120 mesh) depending upon the grain-size and mineral separates required. The mafic minerals were initially separated by using the Franz isodynamic separator and heavy liquid techniques (tetrabromoethane). Hornblendes were then separated by the use of methylene iodide and centrifuge tubes. Biotites were separated by 'rolling' the mafic separate on sheets of rough-textured paper. The mineral concentrates used here were usually 97% pure. The impurities normally contained negligible potassium and therefore only acted as dilutants which did not affect the  $Ar^{40}/K^{40}$  ratio. A small amount of hornblende in a biotite separate will not significantly affect the age, however only 5% of biotite in a hornblende separate may contribute 25 - 50% of the total radiogenic

argon. Chlorite in the system is considered as a dilutant. Two G.S.C. dates: 60-40 and 60-41 (LOWDON, loc. cit.) are a good example. Duplicate concentrates were made from the same sample of biotite schist from the Snare Group. One contained mainly fresh biotite and the other mainly altered biotite. Both samples gave the same age of 1720 m.y.

Potassium determinations of both micas and hornblendes were performed by the potassium tetraphenyl boron precipitation method used in the Geology Department, University of Alberta. Duplicate analyses on micas yield a standard deviation of about 1%. The precision of this method for low-K minerals was assessed by O'NIONS (1969). For a hornblende containing 0.52%  $K_2O$ , a standard deviation of 2.8% was obtained. In this study the K values of the hornblendes and actinolites were checked by flame photometry. Good agreement with the tetraphenyl boron method was obtained especially for the very low potassium values. A precision for this method is estimated at 3% (GREEN, loc. cit.). Correction is made for a small amount of coprecipitated rubidium tetraphenyl boron.

Argon was extracted from a portion of the samples by a NaOH flux-infusion technique similar to that described by GOLDRICH et al. (1961). Individual calibrated  $Ar^{38}$  spikes were added to the samples during the fusion and before the final purification process.

Mass spectrometry was carried out with the A.E.I. MS-10 instrument. This is a single focusing, 2 inch radius,  $180^\circ$  deflection instrument with an electron impact ion source. Vacuum requirements are met by a water cooled oil diffusion pump and a Varian Associates VacIon getter pump. Ion currents are amplified by a Carey vibrating



reed amplifier. Scanning is carried out by varying the acceleration voltage. Measurements are made dynamically and mass discrimination effects are monitored before and after each run by measuring purified air argon introduced into the mass spectrometer under the same pressure conditions. The  $\text{Ar}^{40}/\text{Ar}^{36}$  ratios obtained for air argon were usually just over 300 and all analyses were normalised to the standard Nier  $\text{Ar}^{40}/\text{Ar}^{36}$  value of 295.5. Contaminant argon corrections were usually small and always less than 5%. Residual argon was measured before the introduction of each sample. The precision of duplicate argon determinations is about 1% (BAADSGAARD, 1965).

The data for the age calculations is given in Table 3. The decay constants used are those of ALDRICH and WETHERILL (1958). Possible errors in the decay constants are neglected and the precision of the analyses in terms of the analytical errors in the K and Ar determinations are quoted. A standard deviation of 1% for  $\text{Ar}^{40}$  is assumed, 1% for  $\text{K}^{40}$  in the biotites, 3% for hornblendes with more than 0.5%  $\text{K}^{40}$  and 5% for the hornblendes and actinolites, with less than 0.5%  $\text{K}^{40}$ . Errors were calculated using a FORTRAN IV program (KARG) written by R.K. O'Nions. The total uncertainty in the apparent ages takes into consideration errors in the decay constants and varies between approximately 120 and 150 m.y. for the ages given.

Considering the data given for the granite, granodiorite and the volcanics, no significant differences are detected. Neither group is statistically older or younger than the other; neither do the hornblende or biotite separates show any significant differences. Fig. 7 shows the data as a  $\text{Ar}^{40}$  versus  $\text{K}^{40}$  plot and the best fit line through the data is shown as a 1650 m.y. Reference Isochron. As a reference,

TABLE 3

K-Ar data for Echo Bay volcanics, granodiorite, granite  
and hornblende-actinolite veins

Sample No.	Description	Mineral*	K <sup>40</sup> + (p.p.m.)	Ar <sup>40</sup> ‡ (p.p.m.)	Apparent Age (m.y.)
EBT 1.4	Amygdaloidal andesite	H	0.33	0.0482	1580 ± 60
EBT 2.2	Porphyritic andesite	H	1.91	0.2941	1650 ± 40
EBT 4.1	Granodiorite	B	4.76	0.7230	1650 ± 20
EBT 4.2	Granodiorite	B	4.81	0.7767	1700 ± 20
EBT 4.1	Granodiorite	H	0.86	0.1301	1630 ± 40
EBT 4.2	Granodiorite	H	0.81	0.1288	1690 ± 40
EBT 7.1	Granite	B	5.02	0.7840	1620 ± 20
EBT 7.2	Granite	B	2.64	0.3961	1660 ± 20
EBT 7.1	Granite	H	0.98	0.1405	1570 ± 40
EBT 7.2	Granite	H	0.92	0.1384	1620 ± 40
EBH 1	Hornblende vein	H	0.49	0.0609	1435 ± 60
EBH 2	Actinolite vein	A	0.18	0.0213	1370 ± 60
EBH 3	Actinolite vein	A	0.13	0.0165	1415 ± 60

\* H = Hornblende, B = Biotite, A = Actinolite

+K<sup>40</sup> values: 1 σ = ± 1%, ± 3%, and ± 5% for high, intermediate and low  
K contents respectively.

‡Ar<sup>40</sup> values: 1 σ = 1%

NOTE: K<sup>40</sup> : λe = 5.85 × 10<sup>-11</sup> yr<sup>-1</sup>, λβ = 4.72 × 10<sup>-10</sup> yr<sup>-1</sup>

K<sup>40</sup>/K = 0.000119 (atomic ratio)

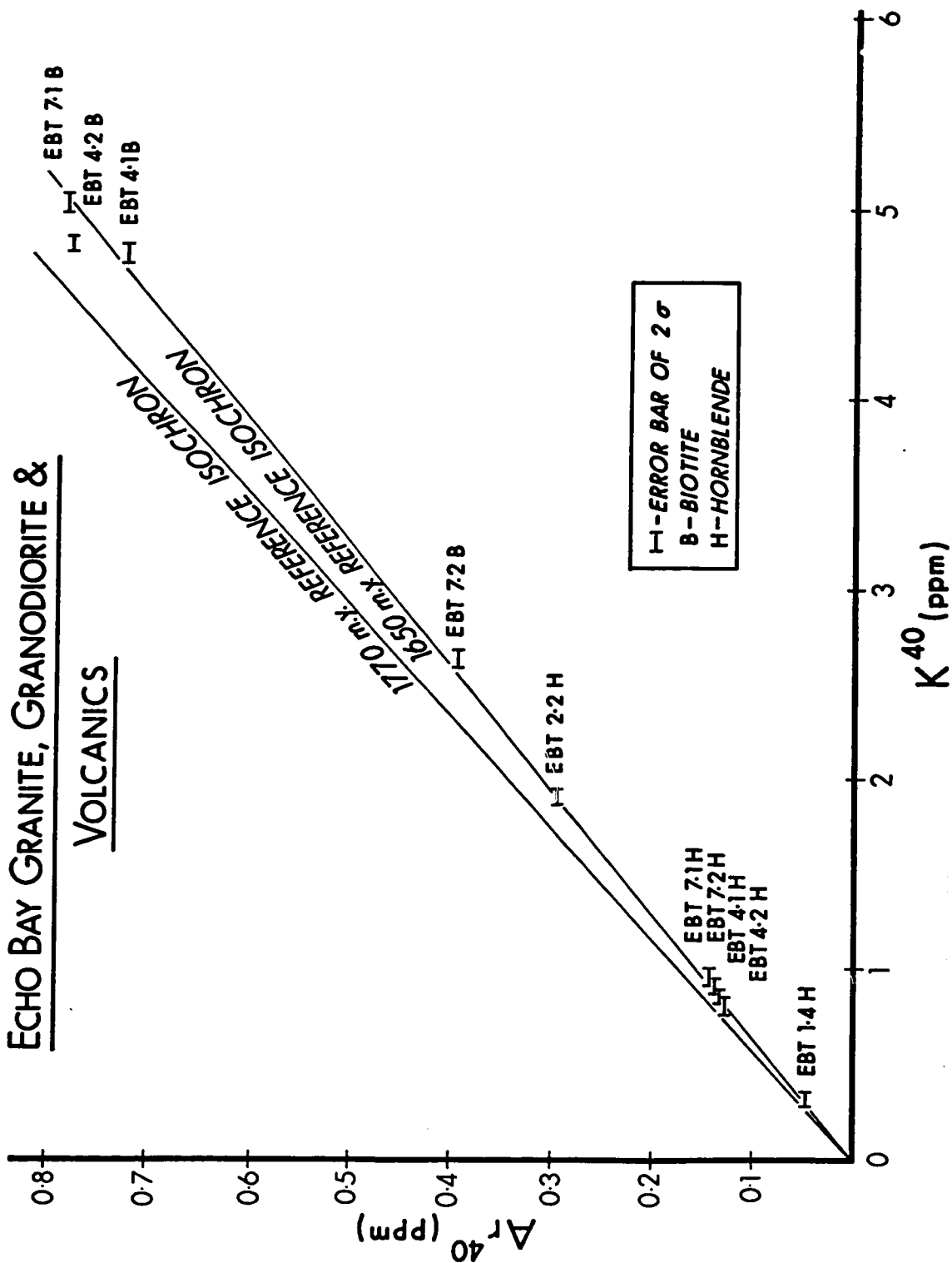


Fig. 7. Plot of  $Ar^{40}$  vs.  $K^{40}$  for biotites and hornblendes from the Echo Bay granite, granodiorite and volcanics.

a 1770 m.y. isochron is drawn, (this being the Rb-Sr date from the volcanics). All the data points except one lie on the 1650 m.y. reference isochron which is statistically distinct from the 1770 m.y. reference isochron. Thus it appears that the K-Ar data on this group of rocks is not yielding the true age of the rocks but is possibly indicating some later event. The lack of any systematic difference between coexisting biotite and hornblende ages suggests that a cooling phenomenon has not been operative. The biotites and hornblendes have become closed systems at approximately the same time. K-Ar ages from different sectors of the Canadian Shield are thought to reflect tectonic processes undergoing the final stages of uplift and cooling (HARPER, 1967). The K-Ar ages published by the G.S.C. for the Bear Province are in closer agreement with the Rb-Sr work than the K-Ar work here. It would therefore appear that this loss of radiogenic argon up to around 1650 m.y. is a parochial effect.

HURLEY et al. (1962) showed that in orogenic belts, losses of radiogenic Ar from biotites vary with the depth of burial and there is almost complete loss at 9,000 feet. Also a single Rb-Sr analysis on one biotite showed an almost equal loss of radiogenic Sr. It is also known that the usual difference in argon retentivity between biotite and hornblende is not always observed. In work on the geochronology of the igneous rocks of Eastern Queensland (WEBB and MCDUGALL, 1968), K-Ar ages were measured on 51 pairs of cogenetic biotite and hornblende. If biotite and hornblende are equally retentive, of argon, the mean ratio of biotite/hornblende age would be 1. It was found that the mean ratios are not significantly different either from each other or from

1.00. The area is thought to have undergone low grade metamorphic conditions - the effect of which is that the argon retentivity of hornblende is not significantly greater than that of biotite. No accompanying loss of radiogenic strontium was detected and it was the Rb-Sr total-rock age that indicated the leakage of argon. The estimated maximum temperature reached in this area was 300° C. for 5 m.y. This could easily account for the argon loss of the biotites, but appears to be a lower temperature than that expected for the outgassing of the hornblende. DAMON (1967) has calculated that diagenesis at less than 100° C. sustained for 50 m.y. would cause less than 10% leakage in biotite and virtually no loss from hornblende; low grade metamorphism (100-150° C) sustained for 50 m.y. would cause losses of from 10 to 90% for biotite and less than 10% for hornblende; high grade metamorphism (500° C.) for 500,000 years would result in complete loss of argon for all minerals used in K-Ar dating.

The Echo Bay biotite/hornblende age ratios are shown below:

EBT 4.1	1.012
EBT 4.2	1.006
EBT 7.1	1.032
EBT 7.2	1.025

The errors on these ratios are about 0.04 and therefore the ratios do not statistically differ from each other or from 1.00. Thus in this area the biotites and hornblendes have shown the same argon retentivity. In the work done on the regional metamorphism of this area it was shown that the temperature was less than 200° C., but possibly greater than

100° C. According to Damon's calculations, these temperatures would be too low to effect a complete loss of Ar from both biotites and hornblendes over a period of 50 m.y. However, it appears that the time interval in this case may have been about 120 m.y. A temperature of approximately 100 - 150° C. for 120 m.y., coupled with the probable effect of active fluids percolating the rocks, may have been factors of sufficient magnitude to completely reduce the argon retentivity of both the hornblendes and the biotites. The ages of around 1650 m.y. thus represent a probable age of uplift in the area.

Considering now the three dates produced from the hornblende-actinolite veins, these consist of two dates on actinolite and one on hornblende. Since the precision of the K measurement on these low-K minerals is considered to be about 5%, then the errors assigned to these ages are large. However, all three dates agree with each other within experimental error. If the data for these samples is considered to be plotted on a  $Ar^{40}$  versus  $K^{40}$  diagram, then the best fit line through these points gives a good average age. The best fit straight line is an isochron of 1420 m.y. The error on this is assumed to be the same as the individual measurements, i.e. 60 m.y. Thus a date of  $1420 \pm 60$  m.y. is obtained for the hornblende-actinolite veins. These are now thought to be related to the diabase sill of the area and therefore give the possible time of intrusion of this sill at 1420 m.y.

#### Hudsonian-age Paleoenvironment of the Bear Province

In a sedimentary analysis of the East Arm fold belt, Great Slave Lake, HOFFMAN (1968) concluded that the sequence of Aphebian rocks exposed there constitute an erosional remnant of an Appalachian-

type geosynclinal complex with an NNW depositional strike. Hoffman describes the Aphebian as a cover of volcanic and sedimentary rocks between 2390 and 1640 m.y. old, occurring in the western part of the Canadian Shield. The analysis has depicted a preorogenic miogeosyncline which received sediment from a distant cratonic source to the ENE and whose sediments became thicker and more eugeosynclinal to the WSW, a regressive syn-orogenic clastic wedge of sediment derived from rapidly-uplifted tectonic lands to the WSW and a continental post-orogenic trench which received sediment locally from block-faulted scarps with the local area.

Using this model, HOFFMAN (op. cit.) has provided the criteria for establishing stratigraphic correlation between the East Arm area and other Aphebian sequences in the western Canadian Shield. After a cursory examination, this correlation appears to be feasible, but it would need much detailed work to be firmly established. The regional facies belts and areas of Aphebian rocks are shown in Fig. 8. The Slave Province has predominantly late Archean ages and is placed within the 'Kenoran orogen'. Characteristic of the Churchill and Bear provinces are late Aphebian ages and these areas are classified as the 'Hudsonian orogen'.

Considering the Echo Bay area, the sequence of andesitic lavas and water-deposited tuffs is not unlike those of the volcanic centres along the orogenic belts of the Circum-Pacific andesite line. Active volcanic arcs are associated with trenches which parallel the arcs. The actual 'andesite line' divides the area of predominantly andesitic lavas and tuffs from that characterized by basaltic volcanism; it also is the boundary between the continental crust with sial and the oceanic

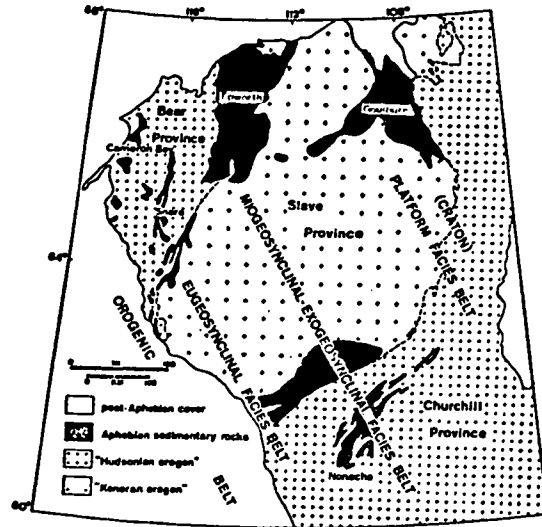


Fig. 8. Predicted regional facies belts of the Bear, Slave and Churchill Provinces, from HOFFMAN (1969).



crust without sial. Fitting this into Hoffman's model is feasible, if the volcanic activity is considered to have occurred within a volcanic-arc type archipelago on the seaward edge of the eugeosynclinal basin. If this area can be correlated with the Flin Flon area of Manitoba, then an island arc approximately parallel to the present day andesite line could be postulated. HOFFMAN (op. cit.) postulated that the Bear province may have been the site of the orogenically active zone of the geosyncline but that part of the Churchill province near the East Arm may be of epirogenic origin. It is considered that the major extrusive and intrusive activity preserved in the Echo Bay area is part of the post-orogenic magmatic episode. Initial andesitic volcanism is followed by granitic and granodioritic plutonism which may have been followed by basaltic volcanism which is only now exposed in the south of the province. By considering the circum-Pacific orogenic region DICKINSON (1969) postulates that batholith belts probably formed beneath volcanic chains and represent the eroded roots of arcs. The andesitic magmas are probably derived from the mantle by partial melting and the granites by anatexis of deep crustal material. Thus the intimate association of the extrusive and intrusive rocks in the Echo Bay area can be explained by this model. The Snare Group of rocks may or may not be equivalent in time to the Echo Bay Group of rocks, but the K-Ar dating demonstrates them to have been metamorphosed at around the same time as the formation of the Echo Bay Group. This may represent a deep burial of the Snare Group in the eugeosyncline while the Echo Bay Group was forming in a shallower and more marginal position of the geosyncline. The K-Ar dates in the Echo Bay area probably represent the age of uplift of the area.

CHAPTER 5 - THE GEOCHEMISTRY OF THE HOST ROCKS  
OF THE Ni-Co-Ag-U VEINS

As mentioned previously, the Ni-Co-native silver vein type uranium deposits characteristically occur within metasediments and volcanics. This generalisation holds for the majority of deposits in the Great Bear Lake area. However, the El Bonanza and the Contact Lake deposits near to Echo Bay occur within intrusive rocks. These deposits are still very close to the Echo Bay Group of sediments and volcanics and their location is considered to be due to a favourable structural anisotropy. From considerations of the dating carried out in this area, it can be seen that the large intrusives have no direct relationships with the mineralisation since they are much older. The only igneous activity which occurred at around the same time as the mineralisation was the intrusion of the diabases. In general the diabase dykes precede the vein deposits and the diabase sill cuts all but the last stage of mineralisation. Field evidence and age relationships do not suggest that there is any genetic relationship between the mineralisation and the diabases. Very minor amounts of mineralisation have been found in the diabases by JORY (1964) and in a drill core into the diabase sill in the Echo Bay Mine. Both cases are attributed to mobilisation of initial vein material by the intrusion. Also spatially the deposits are related more to the sedimentary and tuffaceous horizons of the Echo Bay Group than to the igneous rocks.

In the Terra mine the mineralised veins cross cut a copper rich zone which was probably ultimately of sedimentary origin. At Echo Bay it has been mentioned that many of the tuffs of the Echo Bay

Group contain pyrite which has been segregated into bands, blebs and small stringers in the rock.

Many experiments have been performed to produce conformable monomineralic sulphide bands (e.g. LAMBERT & BUBELA, 1970). It has been found that sulphide ions will diffuse into contact with metals which are in solution or absorbed to minerals. Under conditions of high-grade metamorphism it has been shown that pyrite is mobile and will act as a scavenger for base metals within silicates and carbonates (ROBINSON & STRENS, 1968). It is felt though that these latter effects could be operative under conditions of much lower temperature and pressure, provided that adequately active solutions and sufficient geological time are available. During the diagenesis and metamorphism of a sedimentary-volcanic pile appreciable amounts of water are released (YODER, 1955). The fluids produced can be from connate and meteoric waters together with the breakdown of hydrous minerals during metamorphism. Clay minerals, for example, contain about 14% water and the change to feldspars must release this (GOODSPEED, 1952). Many sediments contain solutions of salt and other chlorides, the concentration of them increasing with depth (WINKLER, 1965). The salt solution between mineral grains is preserved in rocks compacted at depth. It is also possible that the breakdown of hornblende would add potassium and sodium to intergranular solutions. This could be particularly important in the Echo Bay area. It can thus be seen that during the diagenesis and metamorphism of the Echo Bay sedimentary-volcanic pile sulphides were mobilised into bands and fluids could probably be produced potent enough to become enriched in the chalcophylic elements of the host rocks.

BOYLE, (1968) has commented upon the vast number of sulphide-rich black schists and gneisses in the Precambrian greenstone and sedimentary belts of the Canadian Shield. These are comparable to the fahlbands of Norway (GAMMON, 1966). In the Canadian Shield these sulphide-rich rocks are seen in every mineralised belt, BOYLE (loc. cit.), and can be tuffaceous in origin. It would thus appear that sulphide-rich rocks might be important reservoirs of metals and sulphur, from which ore deposits could be concentrated. To test the feasibility of the Echo Bay group sequence being a possible source of the metals in the ore deposit Dr. R.W. Boyle, G.S.C., Ottawa, kindly performed analyses for Zn, Cu, Pb, Ni, Co, As, Sb, Bi, Ag, U, S and CO<sub>2</sub> on five samples of tuff and six samples of andesite from the Echo Bay Group, and one sample each of the dolerite, quartz dolerite, granite and granodiorite. All the samples were taken well away from the veins and their locations are given in Fig. 2. Descriptions of the analysed samples are given in Appendix A. Table 4 gives the final results of all the analyses. These analyses were produced mainly by atomic absorption and colorimetric methods. Duplicate analyses were run on EBT 7.1, EBT 4.1 and EBT QD and average figures are quoted. Also the high values of uranium in EBT 1.5 and EBT 7.1 were checked in duplicate on new samples.

It can be seen that the values are particularly high in EBT 2.4 which is a sulphide-rich tuff. The average tuff shows greater concentrations of these trace metals than the average andesite, but this is mainly due to the high values exhibited by EBT 2.4. The analyses of the intrusive rocks are for comparative purposes only. Although many appear to be enriched over the volcanic rocks, (in particular the dolerite shows mainly higher values than the average tuff),



the lower sulphur values show that the metals in these are not present as a sulphide phase. Thus they are probably in silicate lattices and oxide minerals. In order to test which metals occur together and which occur within the sulphide phase, correlation coefficients were calculated between ten of the analysed elements: Zn, Cu, Pb, Ni, Co, As, Sb, Ag, U, S and CO<sub>2</sub>. This was facilitated by the use of an APL program (COEFF) written by R.K. O'Nions, which gives the slopes of the best fit line through the data points, the intersection on the y axis and r the correlation coefficient which can vary between +1 and -1. Values at which r become significant for 95% confidence limits were calculated for the number of samples considered in each correlation. Significant correlations are underlined in Table 5. All of these are positive.

The S correlates with Cu, Pb, Ni, As and Ag in the rocks, thus suggesting that these metals occur in sulphide phases such as pyrite. Some of the Pb may also be in a carbonate phase. Surprisingly the Ni and Co values do not correlate with each other. Neither does cobalt correlate with S or any other of the metals in the sulphide phase; it does however correlate with U and CO<sub>2</sub>. This would suggest that the Ni was preferentially taken into the sulphide phase with possibly some in the carbonate phase and the Co may be in the carbonates or with uranium in an oxide phase. If the oxidation potential was sufficiently high, CoO(OH), an oxide of trivalent Co may have been formed.

Sb does not correlate with any of the other elements, probably because its concentrations are so low that they do not show sufficiently accurate variations to permit correlations with the other metals. Zn

TABLE 5

Correlation coefficients between ten of the analysed elements  
and CO<sub>2</sub>, Echo Bay tuffs and volcanics

	Zn	Cu	Pb	Ni	Co	As	Sb	Ag	U	S	CO <sub>2</sub>
Zn	1.000	0.097	<u>0.620</u>	0.145	0.260	0.628	0.053	0.473	0.242	0.694	0.125
Cu		1.000	0.328	0.666	0.263	<u>0.795</u>	0.444	<u>0.800</u>	0.247	<u>0.867</u>	0.397
Pb			1.000	0.371	0.362	<u>0.943</u>	0.369	<u>0.677</u>	0.088	<u>0.935</u>	<u>0.628</u>
Ni				1.000	0.391	<u>0.876</u>	0.026	<u>0.645</u>	0.059	<u>0.869</u>	<u>0.551</u>
Co					1.000	0.574	0.375	0.090	<u>0.634</u>	0.592	<u>0.760</u>
As						1.000	0.343	<u>0.886</u>	0.055	<u>0.983</u>	0.677
Sb							1.000	0.232	0.037	0.114	0.522
Ag								1.000	0.160	<u>0.908</u>	0.272
U									1.000	0.135	0.277
S										1.000	<u>0.625</u>
CO <sub>2</sub>											1.000

r values calculated for individual populations at 95% confidence limit.

Significant correlations are underlined.

does not correlate with S but it does correlate with Pb. It would seem then that not all of the Zn is in the sulphide phase, the rest of it possibly being in the oxide phase of the rocks. If any movement of metals takes place in these rocks then it would appear that they would move as a group: U (which is often very mobile) plus Co and Zn, Cu, Pb, Ni, As, possibly Sb, Ag and S which are all related. It is also feasible that these metals may form complexes amongst themselves. From the work done on many ore deposits in Canada, BOYLE (pers. comm.) believes that the metals may travel as As and Sb complexes.

The average content of Co and Ni in intermediate rocks is given as a maximum of 31 ppm and 80 ppm respectively (GOLDSCHMIDT, 1958). TAYLOR, (1969) quotes average values of 24 ppm and 18 ppm for Co and Ni respectively in circum-Pacific andesites. The lavas and tuffs are thus significantly enriched in Ni and Co. The dolerites exhibit normal values whilst the granite and granodiorite are slightly enriched above 'normal' values. TAYLOR (loc. cit.) quotes averages of 54 ppm and 0.13 ppm for Cu and Ag respectively in circum-Pacific andesites. From these figures, which agree with those found in GOLDSCHMIDT (loc. cit.), it would appear that the lavas and tuffs are significantly enriched in Ag and often display high Cu values. The igneous rocks in the area also display high Cu and Ag values.

Zn analyses of igneous rocks are not very comprehensive but the average value is probably around 50 ppm. All these Echo Bay rocks display higher values than this, especially the dolerite. TAYLOR (loc. cit.) gives a figure of 6.7 ppm Pb for the average circum-Pacific andesite and GOLDSCHMIDT (loc. cit.) gives an average of 24 ppm for Pb in granites; this higher value demonstrates the concentration of Pb in the potassic



rocks. The volcanics and sediments are significantly enriched in Pb. Data on the As, Sb and Bi content of andesites is scanty. TAYLOR (loc. cit.) did not detect Bi in the average circum-Pacific andesite, but obtained a value of 0.22 ppm for Sb, with no data for As. The higher values of As in the volcanics and tuffs represent a substantial enrichment and Sb and Bi could be enriched to some extent. The U values for all the rocks are about average, except for an enrichment in a tuff sample EBT 1.5. In the tuffs and volcanics the amount of S reflects the content of Cu, Pb, Ni and to some extent Zn.

It would seem that with respect to the majority of the analysed elements, the host rocks in the Echo Bay area are enriched above 'normal' values. The results of the analyses are similar to those done from the tuffs of the Yellowknife district (BOYLE, 1961) where it is thought that the general wide distribution of the minor elements in all rock types points to a syngenetic origin for the elements. It has been found that the pyrite in the country rocks of the silver-rich areas seems to have higher than average amounts of silver (BOYLE, 1968). This would appear to be the case in the Echo Bay area. Relatively large amounts of silver (10-12 ppm) have been detected in the recent volcanic ash of two volcanoes in Ecuador (MALLET, 1887, 1890); the silver occurring in the form of the chloride. This is significant in that the silver deposits of the Great Bear Lake area are often associated with volcanic tuffs.

Table 6 gives various elemental ratios for the rocks analysed. The U-Pb and Rb-Sr ratios are very variable but the Ni-Co ratios are much more consistent. Most of the tuffs and lavas display a Ni/Co ratio of less than 1, whilst the intrusive rocks show higher ratios usually

TABLE 6

Ni/Co, U/Pb and Rb/Sr ratios of the Echo Bay host rocks

	Ni/Co Ratio	U/Pb Ratio	Rb/Sr Ratio
EB-TUFF Tuff	0.72	0.11	-
EBT 1.1 Tuff	0.45	<0.01	3.85
EBT 1.3 Tuff	0.20	0.02	1.16
EBT 1.5 Tuff	0.45	0.37	1.00
EBT 2.4 Tuff	1.56	0.01	0.18
EBT 1.2 Andesite	0.74	0.03	0.62
EBT 1.4 Andesite	0.87	0.06	-
EBT 2.1 Andesite	0.62	0.05	-
EBT 2.2 Andesite	0.78	<0.01	-
EBT 2.5 Andesite	1.30	0.03	-
EBT 3.1 Andesite	0.48	0.003	-
EBT 2.3 Dolerite	0.91	<0.001	-
EBT-QD Qz. Dol.	1.63	0.13	-
EBT 7.1 Granite	1.34	0.17	-
EBT 4.1 Granodiorite	1.79	0.12	-

greater than 1. The nickel content of a typical andesite is frequently about 20 ppm and the Ni-Co ratio is usually less than 1. TAYLOR et al. (1969) explains these and other phenomena by a two stage process of mantle derivation. However the andesites at Echo Bay display much higher Ni values and some slight variations in the Ni/Co ratios but it is not mandatory to invoke a two stage model for the evolution of this rock type (D.B. Clark, pers. comm.). It should be possible to produce a suite of intermediate rocks with a wide range of Ni and Co contents, depending on the extent of partial melting of mantle peridotite under wet conditions, and upon the pre-eruptive history of the magma. It would seem then that the metallogenic province of the Great Bear Lake area could be connected to sub-crustal differences in magma production. The andesites of the Echo Bay group appear to have had a history which produced enrichment in trace metals. If this is correct, then the distribution of ore deposits is probably directly related to a petrographic province.

Until any quantitative work can be done, the origin of the metals in these deposits is still speculative. Obviously the only metal which can be used as a tracer is lead, since its isotopic ratios should yield information pertaining to its history. Up until 1964 only four galenas from the Eldorado mine at Port Radium had been isotopically analysed. JORY (1964) isotopically analysed eight samples of galena and one of chalcopyrite from the Eldorado mine. Three of the galenas were a fine disseminated kind, which had isotopically ordinary lead. Four galenas were much more coarsely crystalline, more abundant and contained J-type anomalous lead which gives negative ages. One galena and the chalcopyrite

sample are considered by Jory to have mixtures of ordinary lead and lead from the decay of pitchblende. The ordinary lead is considered to have been introduced shortly after the pitchblende mineralisation, but all the anomalous lead is considered to be much later. The anomalous leads are quite distinct and exhibit no mixing with the ordinary leads. JORY (op. cit.) estimates that the lead was introduced less than 300 million years ago in an event which supposedly disturbed the lead-uranium system in the pitchblende and the granite zircons analysed by Jory. No local field evidence is available to support this postulated event. The mineralogical division applied to the galenas in the Port Radium deposit could be applied to the Echo Bay ores, but no large difference in age could be reconciled, as postulated for the Eldorado deposit.

The previous work done on the Eldorado galenas is in agreement with Jory's data, allowing for a slight shift along 204 error lines. Also preliminary data produced by the G.S.C., has depicted anomalous and ordinary galena groups at Echo Bay and Terra Mine (R. Thorpe, pers. comm.). However, it is the author's present opinion that these two distinct groups may have actually been produced by sampling biases within the vein mineralisation. If more samples, in particular of minerals other than galena, were analysed then a possible spread might be obtained between the two groups. If this were the case, then a two stage anomalous lead line which intersects the single stage growth curve at the age of the source rocks could be established. Using a  $\mu$  value ( $U^{238}/Pb^{204}$ ) of 8.7 for the source an anomalous lead line through Jory's data gives an intersection on the single stage growth curve of approximately 1800 m.y. which is the age of the host rocks. To explain this model, initial lead in the volcanics must have remained in a very different U-Th environment before it

moved into the veins approximately 350 m.y. later.

Obviously considering the data available, mere speculations concerning the source of the lead can be made. A complete set of samples from the paragenetic sequence of Echo Bay needs to be analysed, together with samples from the host rocks. No further lead isotope work is incorporated here, but work in this field is being planned by the author in conjunction with R.K. O'Nions.

## CHAPTER 6 - MINERALOGY OF THE DEPOSITS

The sequence of vein mineralisation at Echo Bay has been divided in this study into six stages which are as follows:

1. Quartz-hematite stage
2. Pitchblende stage
3. Co-Ni-arsenide stage with native silver
4. Early sulphide stage
5. Intermediate sulphide stage
6. Late sulphide stage including native silver

These stages agree very well with those proposed for the Eldorado Port Radium deposit (JORY, 1964). The differences which have been encountered will be mentioned in the text. In this chapter a description is given of the metallic and non-metallic constituents of the veins and their inter-relationship in the paragenetic sequence. The large majority of the samples used in the mineralogical study were collected underground from the areas marked in Fig. 9.

### Non-metallic minerals

The non-metallic vein minerals consist of mainly quartz and carbonates of variable composition and very minor fluorite.

#### a. Quartz

Two generations of quartz can be recognised in the veins; the main criterion of classification being on crystallinity, variety of quartz and mineral associations. The early chalcedonic quartz encountered in the Eldorado deposit is not recognised at Echo Bay. Initial quartz formation at Echo Bay occurs as a milky quartz which is finely crystalline

ECHO BAY MINES LTD. COMPOSITE PLAN 1969

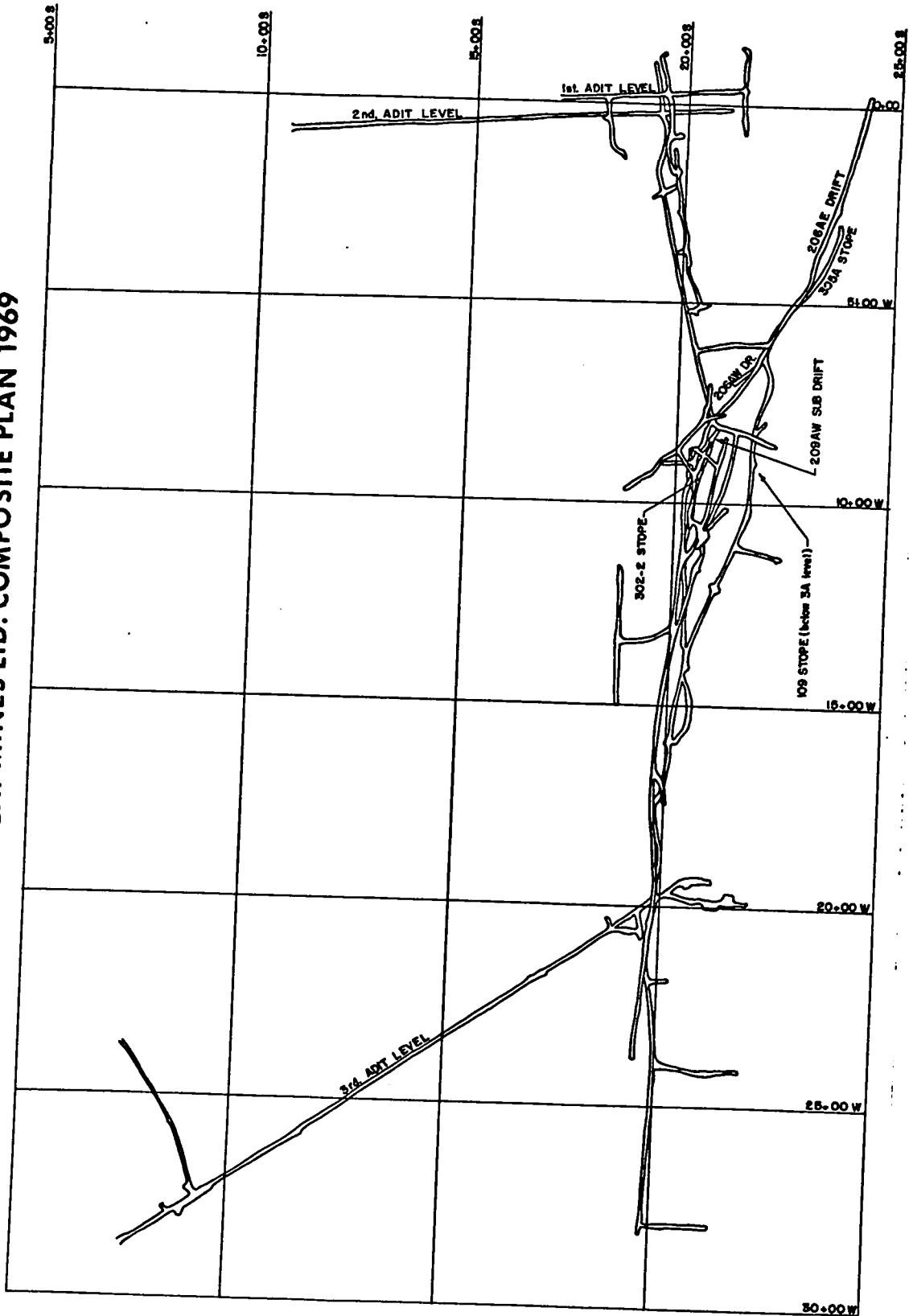


Fig. 9. Composite underground plan of the Echo Bay Mine (1969) showing the main sampling areas.

and is usually found with hematite as bands, rosettes and patches. The latter two minerals thus constitute stage 1 of deposition. Banded hematite and quartz are often characteristic of the giant quartz veins which have been mentioned previously. A quartz vein with banded hematite occurs on the third level of the mine and is shown in Plate IV, Fig. 1. These veins appear to have been emplaced at an early stage in relatively 'tight' fractures in the host rock and brecciated xenoliths of the latter are very common in the vein material. Vugs in these veins are relatively scarce, but when they occur they are mostly filled by well crystallised carbonate.

Although in the Port Radium deposit quartz was found to accompany both the deposition of the pitchblende and the Co-Ni-arsenides, this was not observed at Echo Bay. Polished section work shows that many of the later minerals replace an earlier quartz, which is considered to be the one just described. No quartz was seen to accompany the sulphides and carbonates of the first two sulphide stages.

However, a very clear, crystalline, but coarse granular quartz was found accompanying the deposition of late silver at the end of the late sulphide stage. This quartz appears to be co-genetic with the wire silver and occurs mainly as infillings within the other vein material. Large primary fluid inclusions are abundant in this quartz. Filling temperatures are discussed later but it is noteworthy that the temperature of deposition was found to be about 200° C.

#### b. Carbonates

X-ray diffraction analysis was used to distinguish between calcite and dolomite which occur in the veins.



Carbonate deposition started in the Co-Ni-arsenide stage and continued through to the beginning of the late sulphide stage. Dolomite and calcite are about equally abundant but the dolomite tends to occur more with the vein sulphides and the calcite as later vug fillings and stringers.

The earliest carbonates are dirty cream-coloured granular dolomites. No carbonate was deposited before niccolite but rammelsbergite is found to replace a granular dolomite. Dolomite is most abundant in the intermediate sulphide stage of deposition and is commonly found with chalcopyrite in the #2 vein on the #3 adit level. Here the dolomite appears cleaner looking and, although massive in form, it is well crystallised and breaks into large cleavage blocks. Both primary and secondary fluid inclusions are found in these later dolomites and their temperature of formation was found to be about 200° C. The abundance of dolomite decreased with time and very little is found in the late sulphide stage.

A small amount of finely crystalline calcite is found with the early acanthite and was apparently deposited just after the marcasite. Late in the early-sulphide stage, calcite is found with acanthite and other sulphides. Here the calcite is of a larger grain-size and often exhibits rhombs which are not seen in the case of the earlier carbonates. Calcite is also found with the later sulphides in the intermediate- and late-sulphide stages of deposition. However no calcite is found deposited with the native silver or later minerals. The calcite is widely distributed as vug infillings and late veinlets and stringers. Here the mineral is found with a rather flat scalenohedral habit individual crystals being often up to 10 mm. in length. Very few mixtures of

dolomite and calcite are found in the veins.

Although some of the carbonates have a slight pink colouration, analyses have shown that none of them contain more than a few per cent of manganese. No true rhodochrosite was found in Echo Bay. This is in contrast to manganese carbonates found at Port Radium and El Bonanza mines, where the mineral is associated with late silver deposition. Many carbonate samples found on the surface are encrusted with a manganese oxide which attests to the presence of manganese in the carbonates. No siderite was found at Echo Bay.

It is interesting to consider the development of the crystal habit of the carbonates with increasing time. Both the early calcites and dolomites are granular or fine-grained. Later dolomites and calcites exhibit a well crystallised rhombohedral habit and the latest calcites to be deposited occur as flat scalenohedral crystals. It would seem that the evolution of carbonate crystal morphology is from granular to rhombohedral through to scalenohedral crystals. This trend has been observed in other carbonates (P. Fritz, pers. comm.) and could reflect changes in the ore forming solution. Although most of the calcites are clear and well crystallised, no fluid inclusions were found in them.

c. Fluorite

Fluorite was found in very small quantities in one sample from Echo Bay. A #2 adit level drill core passed through a small vein which cut the host rock and contained carbonate with a little purple fluorite.

d. Chrysotile

Chrysotile was identified in a single sample from the 1-11 stope of the Echo Bay mine. It occurs in a vug and is intergrown with

a well-crystallised late calcite. Since this occurrence is remote from all other samples studied at Echo Bay, any significance placed on the occurrence should only be of a parochial nature. This is discussed in the chapter on solution geochemistry.

### Metallic minerals

An abundant variety of metallic minerals occurs in the Echo Bay veins. These minerals will be dealt with singly or in related groups below.

#### a. Pitchblende

The textures and sequential relationships of the pitchblende in the Port Radium deposit have been described in detail by KIDD and HAYCOCK (1935) and CAMPBELL (1955). The following terms have been used to describe the pitchblende textures: botryoidal, colloform, cellular, dendritic, spherulitic, brecciated and vein. From the work of KEILLER (1962) on the #2 zone of Eldorado, it was found that the type of pitchblende varies with the depth, from spherulitic near the surface through botryoidal and mammillary to massive at the greatest depths. Colloform, spherulitic and dendritic forms were detected at Echo Bay but the limited amount of pitchblende occurrence and sampling did not permit correlation to be made between the texture and depth in the vein. The pitchblende at Echo Bay is a hard, black, dense form which probably corresponds to Kidd and Haycock's Type 1 which has a  $UO_2$  to  $UO_3$  ratio of 10 to 2.2. Type 2, the softer, sooty form associated with carbonate at Eldorado was not detected at Echo Bay. As in similar deposits, the pitchblende is one of the earliest metallic minerals

deposited and is older than the arsenides, native silver and the sulphides. At Echo Bay, the pitchblende often tends to occur as disseminated spherulitic and colloform types within Co-Ni arsenides (see Plate IV, Figs. 2 and 3). Plate IV, Fig. 2 shows a relict, radiating colloform mass of pitchblende about 0.5 mm. in diameter which has been replaced by niccolite and skutterudite. Spherules of pitchblende approximately 0.1 mm. in diameter are seen in Plate IV, Fig. 3 surrounded by rammelsbergite. In this particular case, native silver has invaded the syneresis cracks in the pitchblende. Where the pitchblende is found in the more massive form, it is as veins up to a maximum of 10 cm. in width occurring within 'tight' fractures in the host rock. In these areas the host rock is often extensively hematitised so as to obscure its original nature. The veins of pitchblende are sporadic in occurrence. In the 206 A W Drift of the mine, a small occurrence of pitchblende was associated with native silver as seen in Plate IV, Fig. 4. Here, the pitchblende has replaced early quartz to give a dendritic pattern. Quartz forms the cores and the matrix for the dendrites and pitchblende is the enveloping mineral. The silver is clearly later, since it cuts across the aforementioned minerals and has in parts replaced some of the quartz, particularly in the cores of the dendrites. Thus in part the silver assumes a dendritic habit. Parts of the quartz also appear to have been replaced by a granular carbonate.

As in other similar deposits, the pitchblende does not replace or vein any other metallic minerals and is therefore early in the paragenetic sequence. To explain the colloform and spherulitic habit of the pitchblende JORY (1964) postulated deposition from siliceous colloidal solutions. However, there is no requirement that colloform minerals form

from originally colloidal deposition (ROEDDER, 1968). Also colloids are now considered to be unstable in ore forming solutions (BARTON, 1959). However, 'syneresis cracks' are very common and must still be attributed to post-depositional shrinkage.

b. Co-Ni-Arsenide Minerals

Co-Ni-arsenide minerals, especially niccolite, are common at Echo Bay. Niccolite, where it occurs, usually is found in fairly large quantities in the vein, such as in the 209 A W Sub Drift and the 206 A E Drift. Rammelsbergite is much more limited in occurrence and skutterudite was only identified in a few polished sections. In contrast to other similar deposits where up to about fifteen different Co-Ni-arsenide minerals may be present, only the three aforementioned ones were found to be present at Echo Bay. This lack of diversity in this group of minerals could be a function of the position in the vein or the physical and chemical conditions of deposition. The sequence of Co-Ni-arsenide minerals is found to be niccolite, rammelsbergite and skutterudite, which confirms the general progression of deposition from nickel-rich to cobalt-rich arsenides as given by KIDD & HAYCOCK (loc. cit.), CAMPBELL (loc. cit.) and JORY (loc. cit.) for the Port Radium deposit. In a similar manner to the pitchblende, the Co-Ni-arsenides tend to occur in relatively tight fractures in the host rock, where minor amounts of the early granular carbonate are present. A period of brecciation appears to have occurred after the deposition of the niccolite. Plate V, Fig. 1 shows remnant fragments of niccolite which have been annealed by carbonate and skutterudite. The Co-Ni arsenides are more often associated with pitchblende, early quartz, early carbonate and early silver than with later carbonates and sulphides. In the paragenetic sequence, they

are placed after pitchblende but before the sulphide stage. The quartz deposition which accompanies the Co-Ni-arsenides in Port Radium deposit was not detected at Echo Bay.

b(i). Niccolite

Although niccolite is often associated with the other Co-Ni-arsenide minerals, as shown in Plate IV, Fig. 2; Plate V, Fig. 1; Plate VII, Figs. 1 and 2, it can occur without them (Plate IV, Figs. 3 and 8). Most commonly, the niccolite occurs in a massive form as veinlets up to 10 cm. in width, but it also can be found with a dendritic habit. Plate V, Fig. 2 shows the massive niccolite which has often been brecciated. In Plate IV, Fig. 3, niccolite is seen as the enveloping mineral of dendrites with cores of pitchblende and a matrix of granular carbonate. Niccolite also forms the enveloping mineral of dendrites which have carbonate as both the cores and the matrix (see Plate IV, Fig. 8). In this case it is thought that the niccolite has replaced the carbonate which has subsequently been recrystallised to give rhomb-shaped cores containing specks of sphalerite. In samples from the 206 A E Drift, niccolite rosettes were encountered (see Plate VII, Fig. 1). Often these occur in a radiating polycrystalline manner as shown in Plate VII, Fig. 2.

b(ii). Rammelsbergite

Rammelsbergite was identified from two samples, one from the 302-2 stope and the other from the 209 A W Sub-drive. In each case the rammelsbergite exhibited a beautiful dendritic texture with carbonate cores and matrix. In polished sections rammelsbergite occurred as a thin rim around the niccolite rosettes shown in Plate VII, Figs. 1 and

2. In some cases the niccolite contained small inclusions of rammelsbergite towards the margin and these inclusions increased in concentrations until a rim of rammelsbergite was achieved. The rammelsbergite is clearly later than the niccolite but it was not clear if the aforementioned texture represents replacement by the rammelsbergite or coprecipitation of both minerals for a short interval of time.

It is felt that the dendritic rammelsbergite is formed by the replacement of carbonate. Every stage in the development of the dendrites can be seen. In the poorly developed stage the rammelsbergite replaces the carbonate to give a 'fish-bone' like texture in the carbonate as seen in the upper portion of Plate IV, Fig. 5. A slightly larger extent of replacement breaks up this texture to give irregularly-shaped cores in an envelope of rammelsbergite, as shown in the lower right hand portion of Plate IV, Fig. 5. Where discrete cores have been developed, the carbonate often appears to have been recrystallised to give perfect rhombs (Plate IV, Fig. 6). This carbonate is of a later generation than the early granular carbonate which the rammelsbergite replaces and it often contains minor amounts of sphalerite and other sulphides. Where two dendrite structures cross, 'Marienberg crosses' can be formed as shown in Plate IV, Fig. 7. In some places the dendritic texture appears to have developed so far replacing the carbonate that the texture as such is destroyed and a mosaic of rammelsbergite and carbonate is produced.

X-ray powder diffraction studies indicate that rammelsbergite and not pararammelsbergite is the stable  $\text{NiAs}_2$  polymorph at Echo Bay. YUND (1961) has shown that the transition temperature for pararammelsbergite to rammelsbergite is  $590^\circ \text{C}$ . when the  $\text{NiAs}_2$  is in equilibrium

with niccolite; the pararammelsbergite being the high temperature form. This transition is raised a small amount by an increase in pressure. Temperature studies of the deposit would suggest that the rammelsbergite is deposited at around 200° C. or less. The solid solution of Fe, Co and S in the  $NiAs_2$  lowers the inversion temperature by more than 100° C. (YUND, loc. cit. ). Therefore the stability of rammelsbergite at 200° C. might be explained by the presence of Fe, Co or S in the mineral and the fact that it may not be in equilibrium with niccolite.

b(iii). Skutterudite

Skutterudite was identified in polished section mainly by the use of reflectance and micro-hardness equipment. In Plate IV, Fig. 2 it is seen occurring after niccolite. Zoned skutterudite is found around native silver cores in Plate V, Fig. 2. The zonation suggests that the skutterudite has grown around native silver cores. This interpretation is preferred to the one that would suggest that the native silver has replaced calcite cores in the skutterudite. Thus although the texture is dendritic in nature, it presumably has a different mode of origin than the ones discussed previously. All the dendritic textures were examined with the Normarski differential interference device and the only zonation detected was in the sample described.

c. Iron Minerals

The main iron minerals occurring in the veins at Echo Bay are hematite and marcasite. Although pyrite and magnetite have been recorded as vein minerals in the Port Radium deposit, they were not found at Echo Bay. Pyrite, magnetite and hematite are all, however, present in the host rocks at Echo Bay.



c(i). Hematite

Hematite has been mentioned previously as occurring with the early quartz. It is very common in the host rocks but is not abundant in the vein material. It occurs exclusively in the hematitic quartz of the 'giant quartz vein type' and in the red alteration of the wall rocks which appears to be pre- and syn-pitchblende in age.

c(ii). Marcasite

Marcasite is of limited occurrence in Echo Bay and was only found in the 206 A drift. It is, however, of a very distinctive nature since it is found in continuous colloform masses with a smooth, shiny, botryoidal surface. This marcasite is often deposited on a granular dolomite of the Co-Ni arsenide stage and the deposition of marcasite is sometimes followed by a small amount of granular calcite which often appears to have replaced the marcasite (see Plate V, Fig. 5). More often sphalerite is found deposited on the smooth unconformable surface of the marcasite (see Plate V, Fig. 3). In some cases the sphalerite appears to have replaced the marcasite. In Plate V, Fig. 4 the sphalerite-marcasite boundary is rather irregular and there are patches of marcasite in the sphalerite. In one instance (see Plate V, Fig. 6) the marcasite appears to have been almost completely replaced by the carbonate associated with early sphalerite and galena deposition.

d. Copper Minerals

Economically the copper mineralisation is important at Echo Bay and chalcopyrite is the most abundant sulphide mineral in the veins. Bornite is widespread, but not abundant and chalcocite was found in one sample only from the 109 Stope. Two generations of chalcopyrite and

bornite can be recognised, although the chalcopyrite precipitation may have been continuous throughout the latter part of the early-sulphide stage and the whole of the intermediate sulphide stage. This would account for its abundance. The chalcocite is considered to be later than the bornite and the chalcopyrite and is possibly secondary in origin.

d(i). Chalcopyrite

The earliest chalcopyrite is found to occur with the early sphalerite which was deposited later than the marcasite. It occurs as blebs within the sphalerite (see Plate V, Fig. 3) but commonly it is of a more massive nature and occurs with bornite as seen in Plate V, Fig. 8. The later chalcopyrite is also found associated with bornite as seen in Plate V, Fig. 7. The two generations can be distinguished in hand specimen and are usually separated by a period of rhombic carbonate deposition.

However, some of the chalcopyrite, particularly in the 206A drift is found as banded chalcopyrite ore. Here, the chalcopyrite occurs in bands, up to 3 cm. in width, blebs and segregations within the host rocks, very close to the main vein. No other sulphide is found to accompany the chalcopyrite and thus it is difficult to place it in the paragenetic sequence. It is, however, accompanied by some carbonate alteration of the host rock and therefore it is considered to cover the time span of the early and late chalcopyrite or occur in between them. Where the chalcopyrite is banded, it appears that it may have replaced original sulphide rich bands in the host rock. Continued deposition of chalcopyrite through the intermediate sulphide

stage is witnessed by blebs of this mineral found in all the intermediate stage dolomites.

Chalcopyrite is also found to occur in very minor quantities in the vugs of the carbonates which immediately preceded and anteceded the marcasite deposition. The chalcopyrite is clearly later but it is not clear to which chalcopyrite generation it belongs.

d(ii). Bornite

Bornite usually occurs in quite small amounts with the two generations of chalcopyrite mentioned previously. Where it occurs with the early chalcopyrite it appears to be in part replacive as shown in Plate V, Fig. 8 or shows no discrete mutual boundaries as in Plate VI, Fig. 6. Here, only its spatial association with the chalcopyrite and no other minerals suggests that it is not the later generation bornite. The late bornite and chalcopyrite appear to be contemporaneous with each other and are associated with a carbonate which is deposited later than the early bornite and chalcopyrite. The earlier pair of minerals are usually more massive and do not tend to be associated with carbonate. Fine exsolution laths of chalcopyrite in bornite are found (see Plate VI, Fig. 6) usually as two sets approximately at right angles to one another. Heating of bornite samples with exsolved chalcopyrite usually produces homogenisation between 300° C. and 500° C. However, this is not thought to be consistent with the minimum temperature of formation (GAUCHER, 1964). At low temperatures bornite can contain up to 25% chalcopyrite which will exsolve when heated up to about 200° C. It would appear that the exsolution of chalcopyrite in bornite is not a reliable indication of the minimum

temperature of formation.

d(iii). Chalcocite

Chalcocite was only found in one polished section of the ores from Echo Bay. It was found in a sample from the 109 slope occurring with late bornite and chalcopyrite. The mineral appears to occupy fractures in the bornite, chalcopyrite and associated carbonate but does not exhibit replacive textures. It is considered to be later than these minerals, but its exact position in the paragenetic sequence cannot be determined. It is well known that chalcocite is often found as a supergene mineral and although this mineral is found at about 600 ft. below the surface level in the Echo Bay mine, this possibility is not discounted.

e. Sphalerite

Sphalerite is the only zinc bearing mineral to occur in the veins at Echo Bay. It is very limited in its occurrence, but distinctive in its slightly translucent, honey-yellow colour. The most common sphalerite is the first generation which belongs to the early-sulphide stage. Here, it is often associated with marcasite and chalcopyrite, as seen in Plate V, Figs. 3 and 4. Also in this part of the sequence sphalerite can be found coexisting with galena, as is shown in Plate V, Fig. 6. Sphalerite and galena are seen with an early rather granular carbonate in Plate VI, Fig. 1. A later rhombic carbonate can be seen to have grown in the earlier carbonate. Sphalerite and galena are also found to co-exist with a carbonate which is deposited after the first generation of chalcopyrite and bornite but

before the second generation of these minerals. This situation constitutes a second generation of sphalerite which is of very limited occurrence.

Trace amounts of sphalerite were detected occurring along the grain boundaries of the late quartz which contains 'wire' silver. This sphalerite is noted as a third generation in the paragenetic sequence.

f. Galena

Galena is more abundant in the veins than sphalerite, but it is also divisible into three generations. An early galena occurring with sphalerite is not very common, but is often distinctive in that it forms almost perfect cubes up to 5 mm. in size. The outward pointing faces of these cubes have developed a 'hopper' effect presumably due to rapid crystallisation. Galena occurring with the second generation of sphalerite is more abundant and occurs as cubes up to 10 mm. in size. These cubes are not as perfect as the earlier ones; they often overgrow each other and do not exhibit 'hopper' faces. Early chalcopryrite in a 1 mm.-wide vein in granular carbonate is seen to be followed by a later galena in Plate VI, Fig. 3.

A fine-grained, massive type of galena is also found in the veins. It is often associated with what is considered to be a late calcite and it is therefore placed in the late sulphide stage of mineralisation. Since it is not found to occur with any other minerals in this situation, its exact position in the sequence cannot be determined.

JORY (loc. cit.), in his study of the Port Radium galenas, distinguishes two groups: one which is finely crystalline and intimately associated with the other sulphides and the silver minerals and another which is coarsely crystalline and more massive. These two types were separated by their isotopic character: the finely crystalline ones being the ordinary galenas and the coarsely crystalline ones being the anomalous ones. However, since Jory's classification of the galenas was made after the isotopic analyses, it is not considered to be completely valid and Jory states about the coarsely crystalline galenas: 'if this galena was not known to be isotopically anomalous, there would be no obvious reason for giving it special consideration.'

Although the two types of galena appear to agree roughly with those found at Echo Bay, their occurrence and mineral associations do not agree. The galenas at Echo Bay have been classified by hand specimen and polished section work and a suite of galenas have been separated for Pb-Pb work. These will be considered as a future project by the author.

g. Silver Minerals

The most common silver minerals at Echo Bay are native silver and acanthite. Although the  $\text{Ag}_2\text{S}$  may have been formed above  $175^\circ \text{C}$ ., i.e. as  $\alpha \text{Ag}_2\text{S}$ : argentite, it is always found as  $\beta \text{Ag}_2\text{S}$ : acanthite. Silver minerals are usually found in all the veins and are abundant. A limited amount of mckinstryite was found in the 206 A E drift of the mine but the stromeyerite, jalpaite and hessite reported as found at Port Radium were not detected at Echo Bay.

g(i). Acanthite

Most of the acanthite at Echo Bay occurs in the massive form, sometimes exhibiting a botryoidal texture. The early acanthite occurs as pods of massive material in which vugs and cracks are filled by a later carbonate and chalcopyrite. No other minerals appear to have been precipitated together with the acanthite. Small amounts of acanthite are found to occur with a carbonate and chalcopyrite in the late part of the early-sulphide stage of mineralisation. This constitutes the second generation of acanthite. The third generation of acanthite is represented by a massive form occurring in the late-sulphide stage of mineralisation. Here the acanthite occurs with minor amounts of calcite. In Plate VI, Fig. 4 it is seen replacing chalcopyrite.

g(ii). Mckinstryite

Mckinstryite is seen in polished section in Plate VII, Figs. 1 and 2. It is considered to be a late sulphide in the mineral sequence and exhibits a rather anomalous composition. A full description of the occurrence, physical properties, and chemical composition of the mckinstryite at Echo Bay was given by ROBINSON and MORTON (1971).

g(iii). Native Silver

Native silver is the most abundant of all the silver-bearing minerals found at Echo Bay. It is present in most of the veins and occurs in a variety of forms. The native silver is the most difficult mineral to fit into the paragenetic sequence. Most of the textures exhibited by this mineral are replacive or cross-cutting. It does, however, appear to occur in two distinct associations: both with pitchblende and the Co-Ni arsenides and with the sulphides. In each

case it is most often cutting or replacing the minerals with which it occurs. This makes it difficult to establish if there is more than one generation of native silver. In this respect the geochemical model developed for the deposit does allow for two generations of native silver; a major early generation and a minor later generation. Plate V, Fig. 2 shows cores of native silver surrounded by zones of skutterudite. This texture can be interpreted as either an early silver followed by skutterudite or silver replacing cores which were originally another mineral. The cores appear cubic or possibly rhombic in form and the only similar mineral which has been noted to occur in other cases is carbonate. However, the intimate zoning of the skutterudite around the silver cores does not suggest that the cores were originally carbonate which recrystallised to form rhombic cores (as found in some of the dendrites) and then were replaced by native silver. This silver is thus considered to be an early generation, contemporaneous with that which cuts across and fills cracks in the pitchblende and replaces early quartz (see Plate IV, Figs. 3 and 4). The early generation of silver also includes the spectacularly large samples of massive and leaf silver produced from the 302-2 stope. Here, the silver is in fairly tight fractures and is associated with minor amounts of niccolite, early carbonate and brecciated fragments of host rock.

The later generation of silver is typified by the thin veins and replacive patches occurring with the sulphides and the wire silver and granular quartz which formed in the late sulphide stage of deposition. These two types of silver are considered to be contemporaneous. The wire silver occurs as twisting striated growths up to 10 cm. in total



length and 5 mm. in width within the late granular quartz. This association is seen to be deposited later than the late generation of the sulphides. Veins and replacement patches of native silver can be seen in Plate VI, Figs. 5 and 6. In Plate VI, Fig. 5 a thin vein of native silver is seen to cut through and partially replace chalcocopyrite and carbonate on the margins of the vein and in Plate VI, Fig. 6 native silver is seen cutting and replacing chalcocopyrite, bornite and carbonate.

A third variety of silver was found in the 206 A E drift in very minor quantities. This silver occurs as very fine (about 0.2 mm.) hairs, which are often coiled within an ice breccia. The ice breccia consists of brecciated fragments of vein material and host rock which are held together by ice. It probably represents a very late movement within the fracture zone and is of limited occurrence. The fine hairs of native silver appear to have grown in the ice and in places through the fragments of vein material and host rock. When samples of the vein breccia were brought out from underground, they were reduced to a crumbling mass of fragments with scattered hairs and coils of native silver. This occurrence of native silver in the ice at Echo Bay is very similar to native metal occurrences noted in the veins at Yellowknife (BOYLE, 1951) and Keno Hill (BOYLE, 1960).

In a study of the native silver and silver-antimony minerals in the Cobalt-Gowganda ores (PETRUK and HARRIS, 1969), it was found that the early silver contained significant amounts of mercury and large amounts of antimony. The late silver, however, contained much smaller amounts of these elements and the very late silver is 100.0% Ag. It

was thus considered that there might have been a similar change in the composition of the silver with time at Echo Bay. This theory was tested by Mr. G. Nordin in the Geology Department, University of Alberta. Four types of native silver were analysed: early massive silver from the 302-2 stope, early leaf silver from the 302-2 stope, coarse wire silver from the 302-2 stope and fine hair silver from the ice breccia in the 206 A E drift. Analyses were conducted on the electron microprobe for Ni, Co, Cu, Au, Hg, As and Bi and the results are shown in Table 7. The analyses do not compare with one quoted by BOYLE (1968) for the massive silver, #2 vein, Eldorado Mine, Great Bear Lake, where a larger variety and higher concentration of elements were noted. This is probably due to the presence of inclusions in the silver from Port Radium.

From the Echo Bay analyses it can be seen that copper is the only element which occurs in all the silver samples. The massive silver has the highest concentrations and also contains 0.54% mercury and a small amount of arsenic. This is what would be expected for silver deposited at the early stage. The later wire silver contains much less copper and arsenic and no mercury and the hair silver contains only 320 ppm copper. The leaf silver is also fairly pure and only contains 303 ppm copper and 108 ppm gold. The purity of the hair suggests that it formed through the movement of existing silver in the veins. Its presence in the ice can possibly be explained by water vapour transport of the silver (BOYLE, 1965). It is not clear if the leaf silver is an early silver or a mobilisation product of the early silver. The hair silver has not been included in the paragenetic sequence since its

TABLE 7

Electron microprobe analyses of native silver

	EBS1 Massive Silver	EBS2 Leaf Silver	EBS3 Wire Silver	EBS4 Hair Silver
Ni	n.d.	n.d.	n.d.	n.d.
Co	n.d.	n.d.	n.d.	n.d.
Cu	1,143	303	488	320
Au	n.d.	108	n.d.	n.d.
Hg	5,430	n.d.	n.d.	n.d.
As	74	n.d.	34	n.d.
Bi	n.d.	n.d.	n.d.	n.d.

All figures in ppm

n.d. = not detected

The precision of the analyses is  $\pm 10\%$  for 2  $\delta$  variations

time of formation is presumably comparatively recent and its occurrence is rare.

A polished section of one problematical silver specimen from the 305 stope is shown in Plate VI, Fig. 7. The silver is massive but in part exhibits a dendritic form and in hand specimen appears to be replacing chalcopyrite. Its massive form would tend to associate it with the early native silver but if it is replacing chalcopyrite as it appears to be in hand specimen, then it must belong to the later generation of native silver. Polished section work has not solved the dilemma. The dendrites consist of chalcopyrite cores which are often rhomb-shaped and rims of native silver within a matrix of chalcopyrite in which a later rhomb-shaped carbonate has grown. The rhomb-shaped chalcopyrite cores indicate that the chalcopyrite must have replaced a well-crystallised carbonate and it is not clear if this took place after or before the native silver deposition. One feasible explanation is that the silver is early and initially replaced a granular carbonate. As appears to be the case in other dendrites, some of the carbonate recrystallised to give rhomb-shaped cores which were replaced by chalcopyrite. The existing carbonate rhombs are either a later phenomenon or were not replaced by the chalcopyrite. The above explanation allows the silver to be classified as an early generation which it was initially thought to be.

h. Native Bismuth

Native bismuth is the only bismuth-bearing mineral detected at Echo Bay. Only two hand specimens containing native bismuth were seen and unfortunately only one could be retained for polished section

work. This specimen of bismuth is from DDH 2-9-10, 248' where a pink carbonate vein was found to contain native bismuth and skutterudite. The bismuth is associated with, but appears to be a little later than the skutterudite. This is a similar situation to that observed in native bismuth samples from the Eldorado, Port Radium mine. Here, the native bismuth is seen to vein and partly replace niccolite and rammelsbergite as seen in Plate VI, Fig. 8. A generation of bismuth is thus thought to be associated with the Co-Ni arsenide stage of mineralisation. At Echo Bay, one sample of native bismuth was seen where the mineral appeared to be later than a late vein calcite with which it occurred. It is thus felt that there may have been a second generation of native bismuth occurring around about the same time as the late native silver deposition.

#### Dendritic Vein Structures

Dendritic textures in vein minerals are widespread and fairly abundant at Echo Bay. In dendrites there are three mineralogical zones to consider: the core, the enveloping mineral and the matrix. There is quite a variation in the minerals of these zones at Echo Bay and these will be discussed in due course. Initially some aspects of dendrites from other localities will be considered.

The Card Index of Ore Photomicrographs (1960) describes dendrites as Marienberg textures which represent former skeletal silver growths. The sections from Marienberg, Erzgebirge, Saxony consist of dendrites with calcite cores, Co-Ni arsenides constitute the enveloping mineral within a carbonate matrix. Native silver was

presumed to initiate the dendrites by forming the cores which were then encrusted with Co-Ni arsenide minerals.

BASTIN (1950) describes dendrites as being common in the ores of the Co-Ni-native silver type where the core mineral is usually native silver or native bismuth with an envelope of Co-Ni arsenides occurring within a carbonate matrix. Where the skeletal mineral is native silver, it is considered to have determined the isometric form which is common of most of the dendrites and the arsenide minerals form a later replacement or encrustation of the native silver.

In contrast the Co-Ni arsenide minerals of the silver deposits in the Cobalt-Gowganda area in Ontario occur mainly as rosettes sometimes similar to those shown in Plate VII, Figs. 1 and 2. However, the cores of the rosettes are often native silver (PETRUK, 1968) and thus differ from those observed at Echo Bay. The silver in the cores of the rosettes represents an early silver, but two later generations are proposed to explain native silver veinlets and silver with the late sulphides. PETRUK (loc. cit.) suggests that this late silver may have been remobilised and redeposited. From his paragenetic sequence, it would appear that this silver may be stable with pyrite, an association which only occurs within a limited range of fluid chemistry.

KIDD and HAYCOCK (1934), however, describe a 'rhombic control' of the dendrites presumably by a carbonate gangue. They suggest that chalcopyrite and minor sulphides, accompanied by an early carbonate, replaced the early quartz in which the pitchblende and Co-Ni arsenides had formed dendritic growths. A later carbonate and/or native silver replaced both the chalcopyrite and pitchblende dendrites to some extent.

A large part if not all of the dendrites are thus presumed to be pseudomorphous after either safflorite, rammelsbergite or the pitchblende dendrites.

JORY (1964) in his study of the same deposit considers the dendrites to be of cubic control which may have been determined by uraninite or isometric arsenides. He is unable to reconcile an early silver to produce a cubic control and he finds that no single origin for the dendrites, consistent with the known sequence of deposition of the minerals, is tenable.

Although an early silver is proposed in the paragenetic sequence, it is usually not early enough to effect morphologic control over the majority of the dendrites. Some of the dendrites at Echo Bay do appear to have a cubic control but very often this pattern is disrupted and is not consistent. It is considered that the dendrites represent a replacive and recrystallizing texture which is often seen in various stages of development or refinement. To deal with this consideration, the dendrites have been divided into six types depending upon the identity of the mineralogical zones:

Type 1 is seen in Plate IV, Figs. 5, 6 and 7. Here, carbonate forms the cores of the dendrites and the matrix and rammelsbergite is the enveloping mineral. In certain areas the dendrite structure is poorly developed (see Plate IV, Fig. 5) while in others it is very well developed (see Plate IV, Figs. 6 and 7). Where the dendrites are poorly developed, the rammelsbergite appears to be replacing the carbonate in an almost random fashion. Along linear areas of replacement, the rammelsbergite has broken through to leave roughly shaped cores. Many of the cores and some of the matrix then appear to be replaced by a

later carbonate, sphalerite and galena or some of the carbonate is recrystallised at a later date to give the near perfect rhomb-shaped cores.

Type 2 dendrites are classified as those with carbonate cores and matrix with niccolite as the enveloping mineral. They are usually of a well developed nature; this can be seen in Plate IV, Fig. 8. One interesting point about these dendrites is that within the carbonate of the cores, tiny specks of skutterudite are found and these are not found in the matrix. It is possible that the cores of the dendrites were originally skutterudite which would develop in an isometric pattern and was then rimmed with niccolite. Later carbonate and minor sulphides proceeded to replace the cores. However, the normal paragenesis seen is niccolite followed by rammelsbergite and then by skutterudite. It is considered that insufficient evidence is given by the dendrites to alter the paragenetic sequence. It is thus considered that the niccolite may have replaced an early quartz which was then replaced by carbonate. Skutterudite followed by carbonate plus sulphides have subsequently occupied the cores of the dendrites.

Plate V, Fig. 2 shows type 3 dendrites which have cores of native silver rimmed by zoned skutterudite with carbonate as the matrix. As mentioned previously, it is considered that the silver is the original core mineral.

Type 4 dendrites are seen in Plate IV, Fig. 3 where spherules of pitchblende form the cores, niccolite is the enveloping mineral and carbonate is the matrix. Native silver is seen to occupy shrinkage cracks in the pitchblende. Plate IV, Fig. 4 demonstrates type 5 dendrites which are probably the earliest set to form. It is considered



that pitchblende has replaced early quartz to give dendrites with quartz cores and matrix. Much of the quartz was later replaced by carbonate, especially in the cores. The carbonate of the cores has been partially replaced by native silver to give what often appears to be silver dendrites. The type 6 dendrite is seen in Plate VI, Fig. 7 and has been discussed previously. It is thought that early silver replaced carbonate which was recrystallised to give rhomb shaped cores. The carbonate was then almost completely replaced by chalcopyrite.

This summary of the Echo Bay dendrites demonstrates their variety and complexity. Interpretations have been attempted to be consistent with the developed paragenetic sequence and the apparent replacive textures of many of the dendrites. A much more detailed and comprehensive study would be required to attempt to solve all of the problems posed by the dendritic structures.

#### The Paragenetic Sequence of the Echo Bay Ores

The paragenetic sequence for the Echo Bay veins was developed both by hand specimen and polished section work. Most of the criteria used to develop the sequence was obtained from BASTIN (loc. cit.) and PARK and MACDIARMID (1964). Those criteria found most useful at Echo Bay are discussed below. Distinct veining, fracturing and brecciation were considered to be dependable criteria and were often used in hand specimen work. The healing of breccia fragments by later minerals and fracture filling were usually investigated further by polished section work. Layer and growth structures were found to be useful criteria in hand specimen work (especially crustification). This was applicable in

many parts of the vein at Echo Bay where the textures were indicative of deposition in open spaces.

Replacement textures were found much more difficult to establish and they were based exclusively on polished section work. Pseudo-morphic replacement was only rarely observed and replacement in general was only conceded to be valid where replacement veins were located. Corroded boundaries were taken to suggest replacement, but did not have to be used in constructing the paragenetic sequence. The interpretation of the dendrite structures is much more speculative, but the only way it influenced the paragenetic sequence was to place a carbonate stage between the niccolite and rammelsbergite deposition.

The paragenetic sequence as developed is shown in Fig. 10. The difficulties of applying a paragenetic sequence to this type of deposit should be emphasised at this stage. Sampling for this study included the main stoped veins and the 206 A Drift vein. Although these veins are mineralogically very similar, they were obviously developed in a slightly different manner to each other. Also within each vein, numerous 'nests' of mineralisation have developed. The paragenetic sequence as developed applies to these veins as a whole and is a plot of time against the total mineral occurrences. Obviously the sequence differs from area to area, since different generations of different minerals may be omitted. It is often very difficult to correlate from area to area in the veins, unless particular reference minerals or assemblages are present.

Brecciation within the veins is not depicted in the paragenetic sequence and will be described below. The quartz and hematite veins of stage 1 of the mineralisation often contain fragments of brecciated

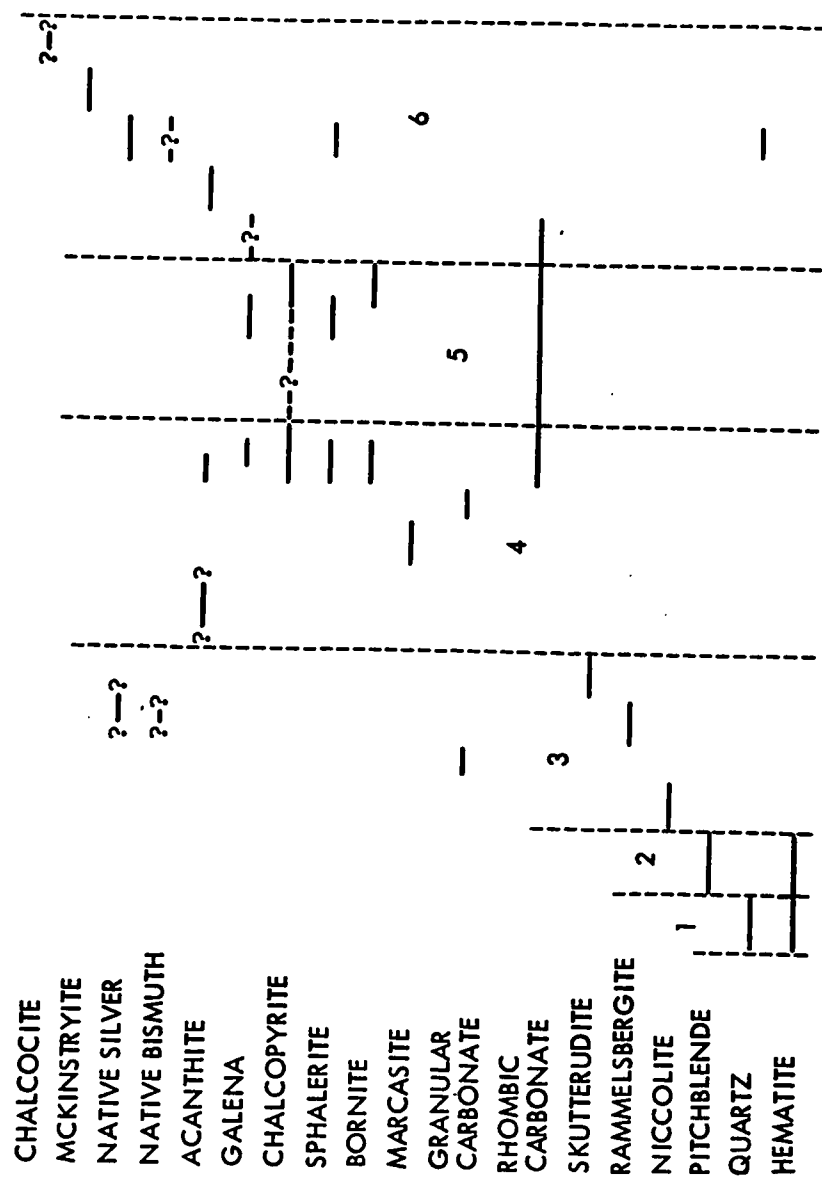


Fig. 10. Paragenetic sequence for the Echo Bay veins.

Fig. 11: Port Radium: Paragenetic sequence (Jory, 1964).

Stage	1	2	3	4	5	6
Apatite	—					
Quartz	—	—	—			
Hematite	—	—			—	
Pitchblende		—				—?
Ni-Co-Arsenides		—	—			
Pyrite				—?		
Chlorite				—		
White Mica				—		
Barite					—	
Siderite					—	
Dolomite			—?			
Sphalerite					—	
Tetrahedrite					—	
Bornite						
Chalcopyrite				—?	—	
Galena				—?	—	
Calcite						—?
Rhodochrosite						—
Silver Minerals						—
Native Bismuth						—?

Stages 1, 2 and 3: predominantly open space  
 Stages 4, 5 and 6: predominantly replacement

host rock as do the native silver veins in stage 2 of deposition. During these periods mineralisation took place along relatively tight fractures. Annealed fragments of niccolite (see Plate V, Fig. 1) depict a period of brecciation which took place just after the niccolite deposition. Mineralisation then appears to have occurred in more open vein structures and carbonate deposition was initiated. The later stages of mineralisation often represent deposition in open spaces and the period of brecciation of niccolite must have marked the beginning of a continuous opening of the veins and much carbonate deposition. Many vein pods are now found to have large cavities and vugs often apparently because this area was sealed off at an early stage. Other pods appear to have become saturated and a series of mineral replacements have taken place. A comparatively recent period of brecciation has occurred as witnessed by the presence of the ice breccia previously described.

#### Comparisons with the Mineralogy of other Similar Vein Deposits

The detailed paragenetic sequences developed for the Port Radium deposit are given in the KIDD and HAYCOCK (loc. cit.) and JORY (loc. cit.). Jory's sequence is shown in Fig. 11 and is in fairly good agreement with that developed for Echo Bay. Some minerals such as pyrite and magnetite are naturally absent from Echo Bay and Jory includes all the silver minerals and native bismuth as late minerals. At Port Radium, there is also a profusion of Co-Ni arsenide minerals which is not the case at Echo Bay.

The deposits of Joachimsthal, Czechoslovakia occur as veins which are similar to those in the Great Bear Province. A summary of

the sequential relationships in the veins can be found in BOYLE (1968) as taken from MRNA (1963) and is as follows:

- Stage 1     Quartz, feldspar, molybdenite, arsenopyrite, wolframite, cassiterite, and tourmaline (veins near granite contact).
- Stage 2     Quartz, galena, sphalerite, bornite and chalcopyrite (NE-SW veins).
- Stage 3     Barren quartz, calcite and ankerite (NE-SE to N-S vein).
- Stage 4     Pitchblende, dolomite and rare fluorite (NW-SE to N-S veins).
- Stage 5     Arsenides, native silver and bismuth and quartz (NW-SE to N-S veins).
- Stage 6     Sulpharsenides, sulphantimonides, arsenic, realgar, argentite, sternbergite, bismuthinite, dolomite etc. (NW-SS to N-S veins).
- Stage 7     Pyrite, sphalerite, galena, arsenopyrite, chalcopyrite, calcite and quartz (NW-SE to N-S veins).

Many of the other veins in this area bear similarities with the Great Bear Province and the native silver and Co-Ni arsenide minerals are similar to those at Cobalt, Ontario both in texture and type. The age relationship between pitchblende and its associated vein minerals is variable. The only consistency is shown in Precambrian deposits in which the pitchblende is an early mineral, preceding almost all the associated metallics. In the other deposits, pitchblende occupies

a variable position and is intermediate to late in age. The position of native silver within the paragenetic sequences is often a question of individual interpretation.

#### Wall Rock Alteration

The pattern of wall rock alteration at Echo Bay was described in MEYER and HEMLEY (1968) as alteration associated with hematite-bearing vein deposits in metamorphic and andesitic rocks. They interpret this type of vein deposit to be sulphur-deficient but with a higher oxygen content. Hematite is a common associate but pyrrhotite is absent. CAMPBELL (1947) describes the alteration at Port Radium as argillic with chloritization, carbonatisation, silicification and hematitisation. The alteration, however, appears to have no influence on the distribution of pitchblende. Reddish albitic feldspathisation is also prominent around the veins at Cobalt, Ontario (THOMSON, 1957). The relatively high oxidation potential apparently precludes strong chloritization, minimizing magnesia metasomatism and will cause the formation of alkali feldspar if the alkali/H<sup>+</sup> ratios are sufficiently high.

JORY (1964) recognised the following alteration minerals in the Port Radium deposit which he divided into three groups:

(Oldest)

Group 1 Apatite, Microcline, Hematite, Quartz

Group 2 Chlorite, Leucoxene, White mica, Sulphides

Group 3 Carbonates

(Youngest)

The wall-rock alteration zones at Echo Bay are erratic in distribution and apparently vary in width from a few inches to a few feet at the maximum. The alteration zones were studied by thin section work to determine diagnostic minerals.

Apatite, quartz, leucoxene, white mica and sulphides were not recognized. Hematite, as mentioned previously, is very common but as in the Port Radium deposit it cannot always be correlated with the occurrence of pitchblende.

It was noted that the alteration minerals did not show persistent uniform zoning, nor did they exhibit consistent spatial distribution relative to ore shoots. The microcline is very fine grained and is hematitised, thus producing a brick-red hard dense rock which resembles jasper. The presence of microcline was inferred by the presence of hematitised rock resembling jasper. Usually the rock was too hematitised to determine the feldspar type. Chlorite is usually developed to a minor extent in the wall rocks, but it could not be determined if this is a wall-rock alteration-product, since chlorite is common in the host rocks in general. Sulphides also are often so abundant in the host rocks that to classify them as wall-rock alteration products near the veins would be very difficult. Carbonates, although present in the host rocks in general, are often more abundant in the wall-rock alteration zones and can thus be classified as wall-rock alteration minerals. As is suggested by JORY (loc. cit.), they probably occur at later stages when the carbonates are more abundant in the veins also.

No characteristic mineral assemblages from the system  $\text{Na}_2\text{O}-\text{Al}_2\text{O}_3-\text{SiO}_2-\text{H}_2\text{O}$  or  $\text{K}_2\text{O}-\text{Al}_2\text{O}_3-\text{SiO}_2-\text{H}_2\text{O}$  are found in the veins at Echo Bay and



it thus does not appear likely that ore forming solutions were buffered by a silicate assemblage as is often the case, (see HEMLEY and JONES, 1964). However, the relatively large amounts of carbonate formed after the initial minerals were deposited, could possibly act as a buffer for the ore forming solution; the pH being controlled by the  $f\text{CO}_2$ .

#### Secondary Minerals at Echo Bay

No secondary enrichment of silver or other elements was observed at Echo Bay, but the surface oxidation of the veins in this area is very distinctive. The main Echo Bay veins are usually represented on the surface by wide muskeg filled depressions, but in some areas the veins actually outcrop. Here, trenching has shown that the surface oxidation zone is very shallow and is usually only a few feet deep. The most common and easily identifiable oxidation minerals at Echo Bay are erythrite, annabergite, malachite, limonite and wad. The gossan zones above the #1 adit at Echo Bay contain limonite, gypsum, and malachite, but as noted earlier, this gossan is not associated with the veins. Malachite and azurite were found in quartz veins which crop out just west of the main Echo Bay vein. Although small amounts of pitchblende were detected on the surface above the Echo Bay mine, no secondary uranium minerals were found to be present. The Great Bear Lake veins as a whole usually exhibit a variety of yellow, yellowish green and orange secondary uranium minerals, azurite, malachite, erythrite, annabergite, secondary carbonates, limonitic material and clinker-like masses of wad (BOYLE, 1968).

As part of a survey by A.S. Dass on the secondary oxidation products of U-Co-Ni-Ag-Bi veins, analyses have been made at the G.S.C. Laboratories, (Ottawa) of material from three trenches above the Echo Bay Mine. The analyses were co-ordinated and the results supplied by Dr. R.W. Boyle. Below is a list of these minerals detected by X-ray methods:

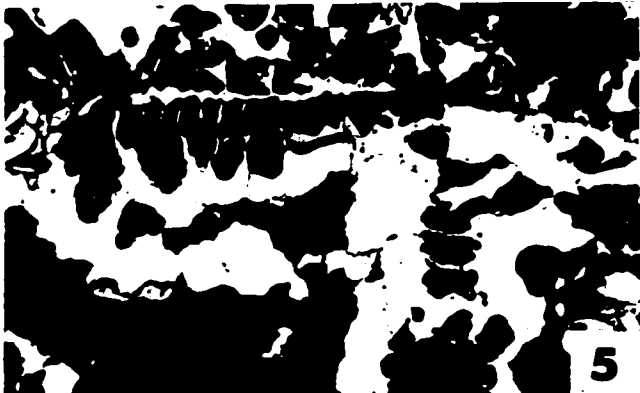
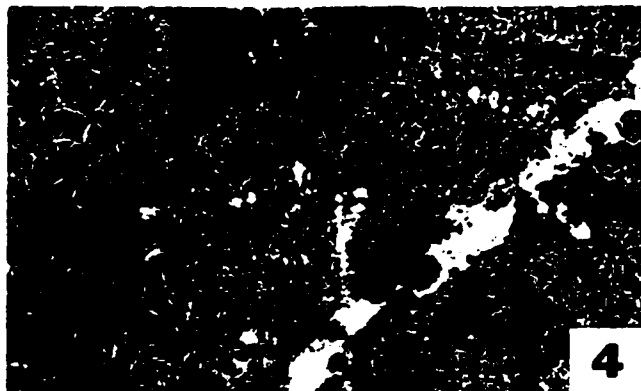
Malachite	$[\text{Cu}_2(\text{OH})_2(\text{CO}_3)]$
Brochantite	$[\text{Cu}_4(\text{SO}_4)(\text{OH})_6]$
Tyrolite	$[\text{Cu}_5\text{Ca}(\text{AsO}_4)_2(\text{CO}_3)(\text{OH})_4 \cdot 6\text{H}_2\text{O}^?]$
Erythrite	$(\text{CoNi})_3(\text{AsO}_4)_2 \cdot 8\text{H}_2\text{O}$
Annabergite	$(\text{NiCO})_3(\text{AsO}_4)_2 \cdot 8\text{H}_2\text{O}$
Hydrozincite	$[\text{Zn}_5(\text{OH})_6(\text{CO}_3)_2]$
Adamite	$[\text{Zn}_2(\text{OH})(\text{AsO}_4)]$
Hemimorphite	$[(\text{ZnOH})_2\text{SiO}_3]$
Limonite	$2\text{Fe}_2\text{O}_3 \cdot 3\text{H}_2\text{O}$
Pharmacosiderite	$[\text{Fe}_3(\text{AsO}_4)_2(\text{OH})_3 \cdot 5\text{H}_2\text{O}]$
Wad	$\text{MnO}_2 \cdot n\text{H}_2\text{O}$

PLATE IV

Figure

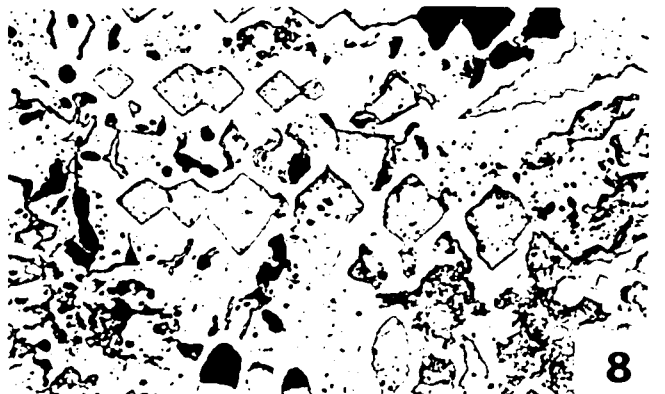
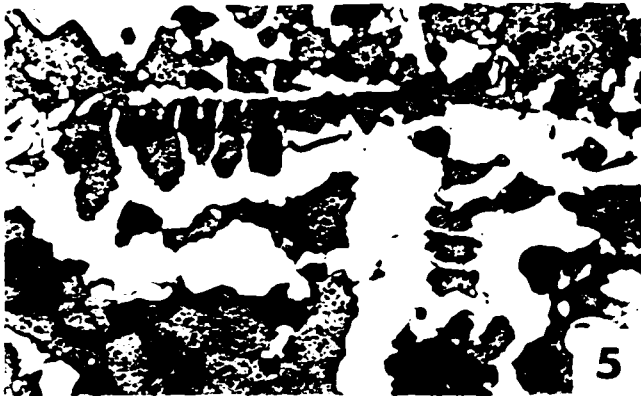
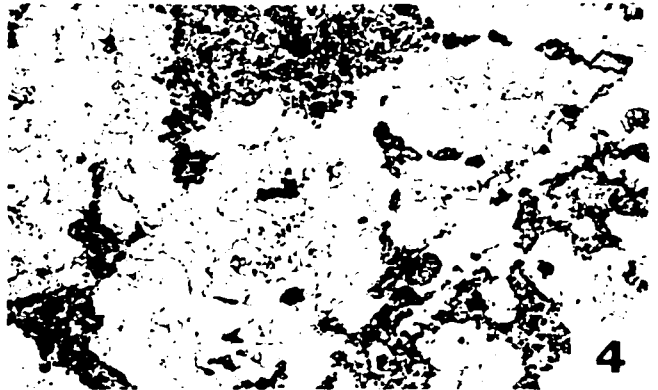
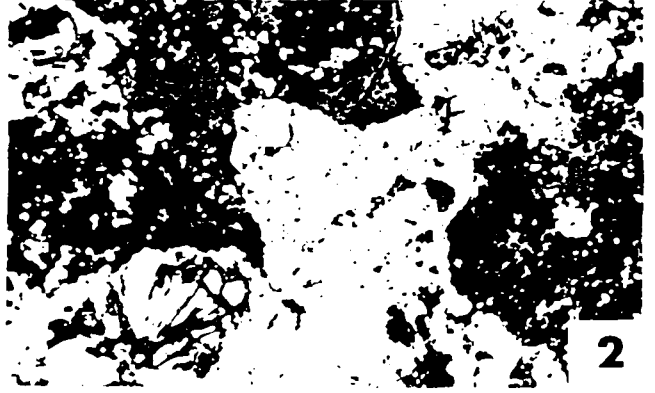
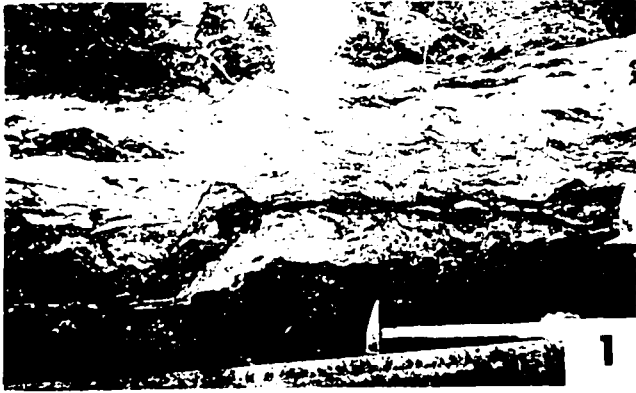
1. Banded quartz-hematite vein with some carbonate in vugs, #3 adit level.
2. Remnant colloform mass of pitchblende (bottom left, light grey) replaced by niccolite (white) and skutterudite (white with dark inclusions) in a matrix of quartz (dark grey). EB 21, Core 2-8-1298'.
3. Spherules of pitchblende (grey) occurring within an envelope of niccolite (greyish-white) which has a thin rim of skutterudite (greyish-white). The matrix is granular carbonate (dark grey) with specks of chalcopyrite. Native silver (white) occurs within cracks in the pitchblende. EB 9, 302 Stope.
4. Native silver (white) cuts originally dendritic pitchblende (light grey) in a matrix of quartz (medium grey) and later granular carbonate (dark grey). EB 10, 206 A W Drift.
5. Rammelsbergite (white) and carbonate (grey) forming a poorly developed dendritic texture. EB 8, 302-2 Stope.
6. A dendrite of rammelsbergite (white) containing recrystallised calcite cores (dark grey) which include small areas of sphalerite (whitish grey) and chalcopyrite (greyish white). EB 7, 302-2 Stope.
7. Carbonate (dark grey) forming 'Marienberg crosses' with rammelsbergite (white). Sphalerite (light grey) occurs in the carbonate. EB 7, 302-2 Stope.
8. Dendritic niccolite (white) replacing carbonate (grey) which has been recrystallised to give rhomb-shaped cores containing specks of sphalerite (light grey). EB 17, 206 A E Drift.

**PLATE IV**



-----| 1mm

PLATE IV



----- 1mm

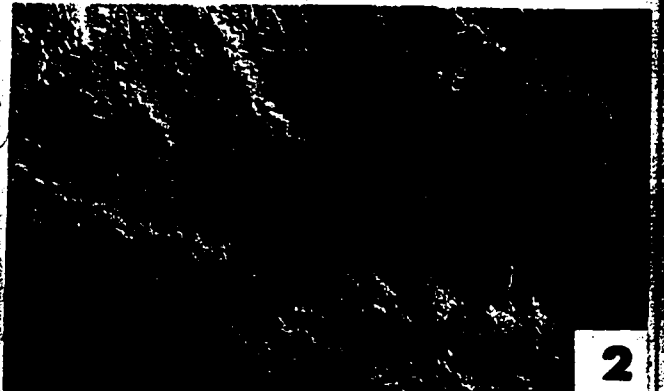
Figure

1. Fragments of niccolite (black speckled greyish white) annealed by carbonate (dark grey) and skutterudite (greyish-white).  
EB 28, 109 Stope.
2. Zoned skutterudite (whitish-grey) occurring around cores of native silver (greyish-white and poor polish) in a matrix of granular carbonate. Photograph taken with the Normarski differential interference device. EB 30, 305 Stope.
3. Sphalerite (grey) and chalcopyrite (whitish grey) are precipitated upon a smooth surface of marcasite (greyish-white) seen in cross section. EB 33, 206 A E Drift.
4. Marcasite (greyish white) partly replaced by sphalerite (grey) which has been followed by deposition of rhombic carbonate (dark grey). Relict patches of marcasite can be seen in the sphalerite.  
EB 25, 305 Raise.
5. Marcasite (greyish-white) post-dated and partly replaced by granular calcite (dark grey), sphalerite (light grey) and galena (greyish-white, poor polish). EB 23, 206 A W Drift.
6. Ghost relicts of marcasite (greyish-white) in carbonate (dark grey). The carbonate is associated with coexisting sphalerite (whitish-grey) and galena (white). This sphalerite and galena were used for the S-isotope temperature measurement of the early sulphide stage. EB 22, Core 2-8-2198'.
7. Carbonate (dark grey) with bornite (light grey) and chalcopyrite (greyish-white) followed by chalcocite (greyish-white and low relief).
8. Early bornite (grey) and chalcopyrite (whitish-grey). The bornite in part appears to be replacing the chalcopyrite and may be a little later.

**PLATE V**



**1**



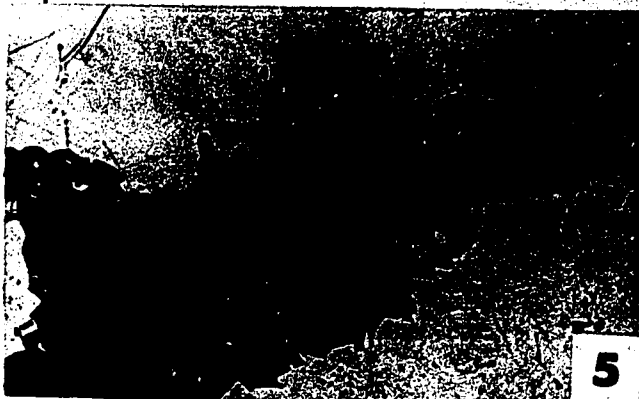
**2**



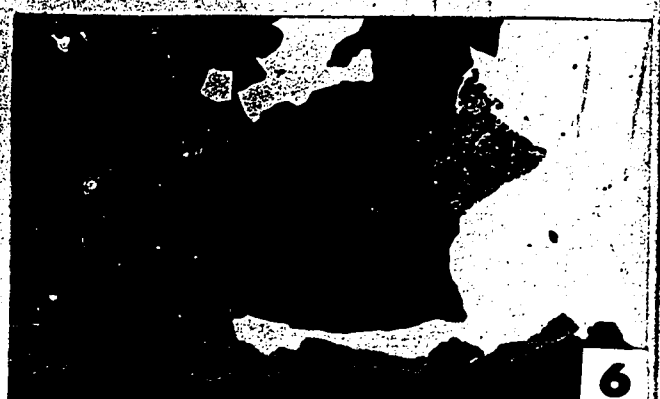
**3**



**4**



**5**



**6**



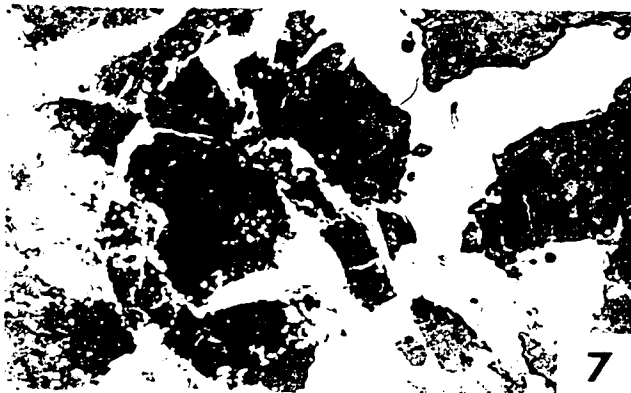
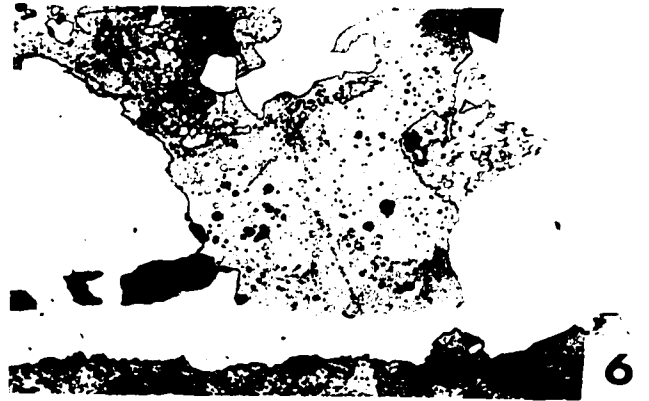
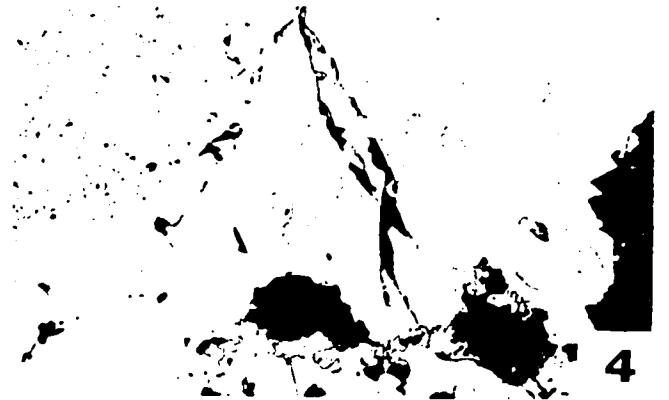
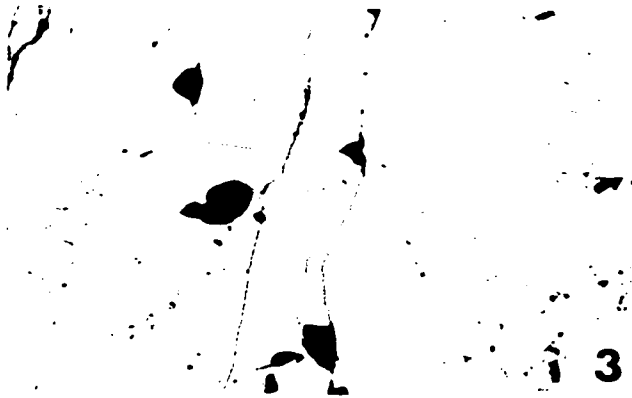
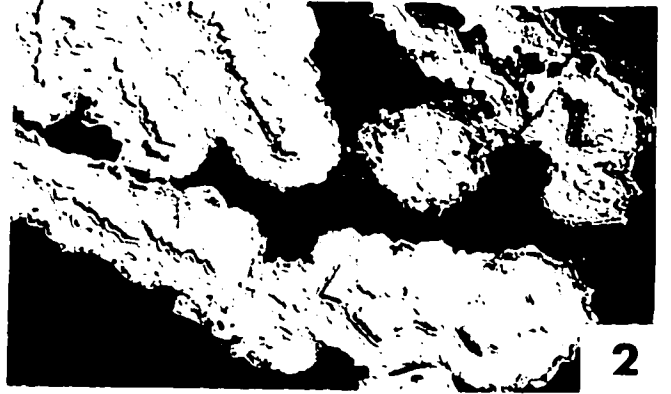
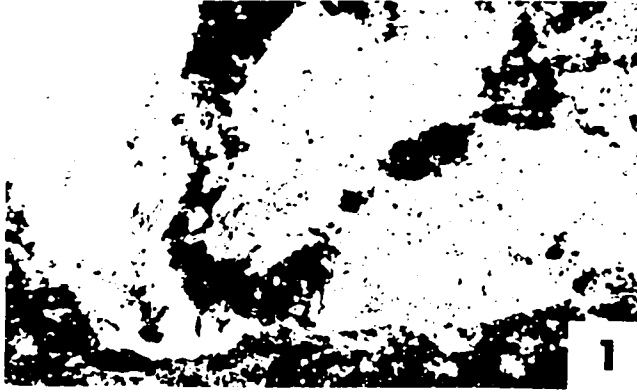
**7**



**8**

-----+----- 1mm

PLATE V



----- 1mm

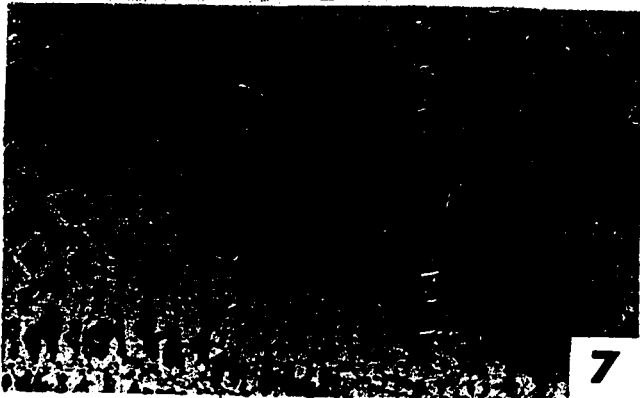
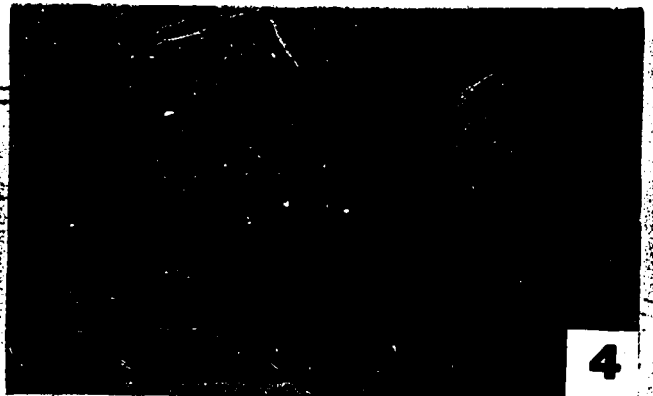
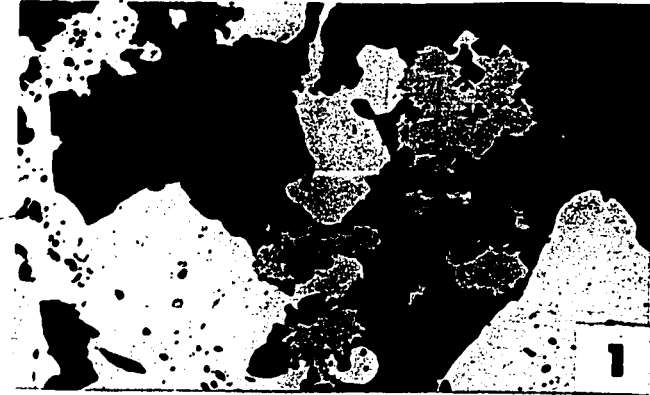


PLATE VI

Figure

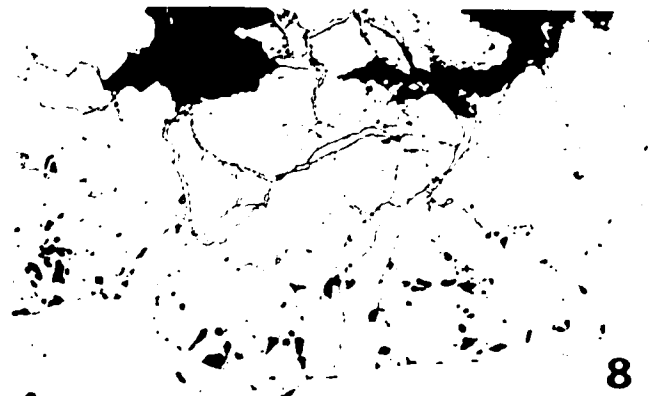
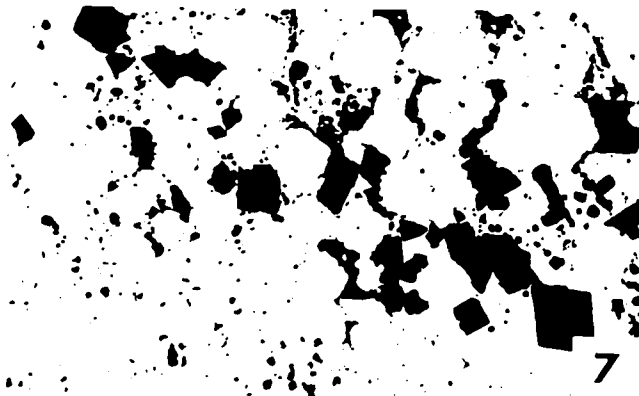
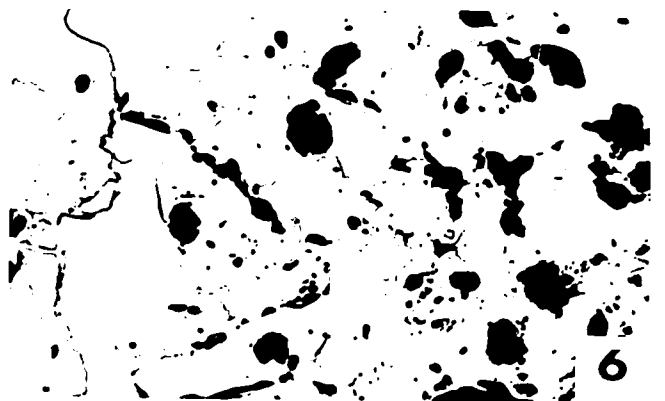
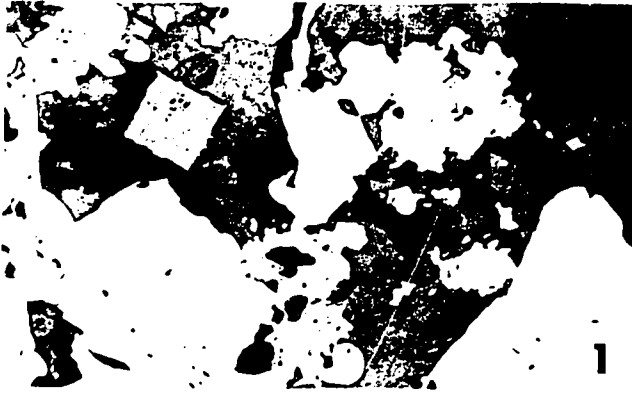
1. Chalcopyrite (greyish-white) and sphalerite (whitish-grey) associated with a granular carbonate (grey). A later rhombic carbonate can be seen growing in the earlier carbonate. EB 24, 209 A W Sub-Drive.
2. Coexisting sphalerite (light-grey) and galena (white) with carbonate (dark grey). This sphalerite and galena were used for S-isotope estimation of the temperature of the intermediate-sulphide stage. EB 16, 206 A E Drift.
3. A vein of galena (center) and chalcopyrite (rims) within an early granular carbonate. EB 15, 302-2 Stope.
4. Acanthite (whitish-grey) with carbonate (dark grey) and replacing chalcopyrite (greyish-white). EB 11, 302-2 Stope.
5. A vein of native silver (greyish-white, poor polish) cutting and partially replacing chalcopyrite (grey) and carbonate (black). EB 13, 302-2 Stope.
6. Native silver (white) veining and replacing bornite (grey), chalcopyrite (whitish-grey) and carbonate (black). Exsolution lamellae of chalcopyrite in bornite can be seen in the extreme left of the frame. EB 2, 302-2 Stope.
7. Dendritic texture with rims of native silver (white) around chalcopyrite cores (light-grey) in a chalcopyrite and carbonate (dark grey) matrix. EB 29, 305 Stope.
8. Native bismuth (white) veining and replacing niccolite (whitish-grey) and rammelsbergite (greyish white) with later carbonate (dark grey). Eldorado Mine, Port Radium.

# PLATE VI



-----| 1mm

PLATE VI



----- | 1 mm

PLATE VII

Figure

1. Rammelsbergite (white) and niccolite (whitish-grey) within mckinstryite (grey) which has partly replaced chalcopyrite (slightly lighter colour and greater relief than mckinstryite). EB 19, 206 A E Drift.
2. Rosettes of polycrystalline niccolite (white) with a rim of rammelsbergite (greyish-white) occurring within a granular carbonate matrix (dark-grey) which is in part replaced by mckinstryite (grey). EB 19', 206 A E Drift.
3. Small primary inclusions in a double polished plate of an intermediate sulphide stage dolomite, in transmitted light. The vapour bubbles can be seen, but the salt crystals are obscure. EB FI1, #3 adit level.
4. General view of primary fluid inclusions in a double polished section of granular quartz and native silver. The inclusions can be seen to parallel growth planes. EB FI3, 302 Stope. Transmitted light.
5. Large fluid inclusions in EB FI3, showing bubbles, salt crystal and daughter material (in the center of the large inclusion). Transmitted light. Late stage quartz.
6. Three-dimensional array of large, primary inclusions as seen above. These larger inclusions may have been affected by secondary fractures. The vapour bubbles and salt crystals can be readily distinguished. Transmitted light. Late stage quartz.
7. A primary composite fluid inclusion in EB FI1; transmitted light. The vapour bubble, salt crystal and other solid material are easily recognisable. This and other smaller primary inclusions do not appear to have been affected by secondary fractures. The ring seen around the vapour bubble is an optical illusion.
8. Secondary fluid inclusion showing a vapour bubble and salt crystal. A trail of much smaller inclusions mark a curved healed fracture demonstrating the inclusions to be of a secondary origin.

# PLATE VII

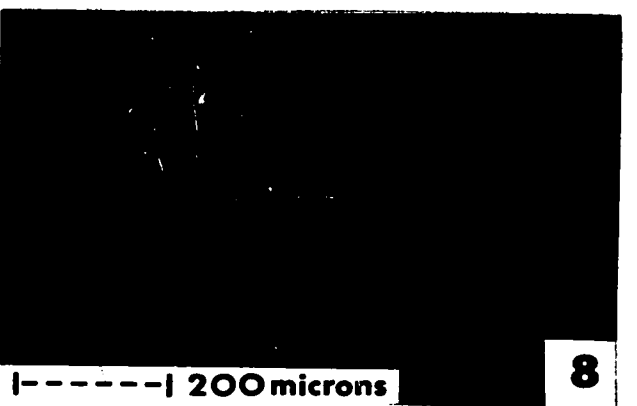
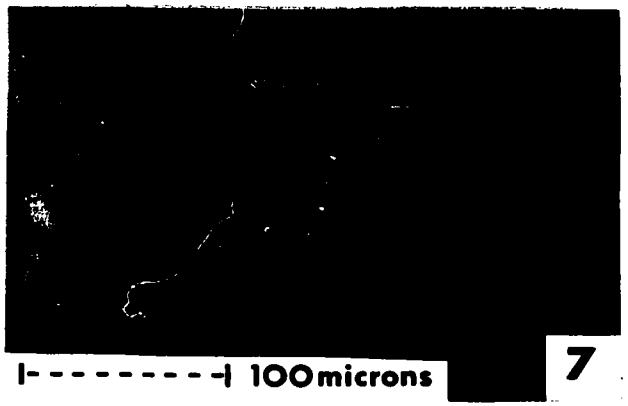
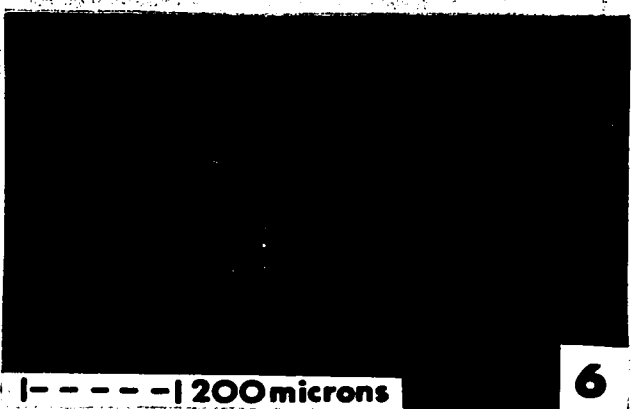
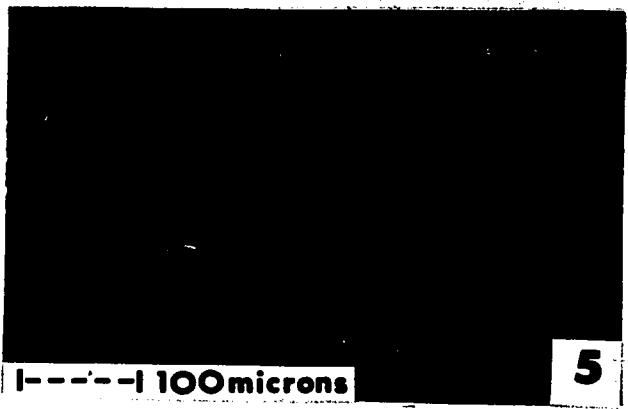
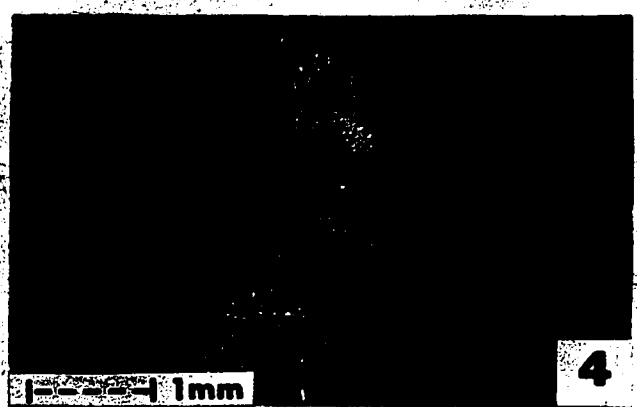
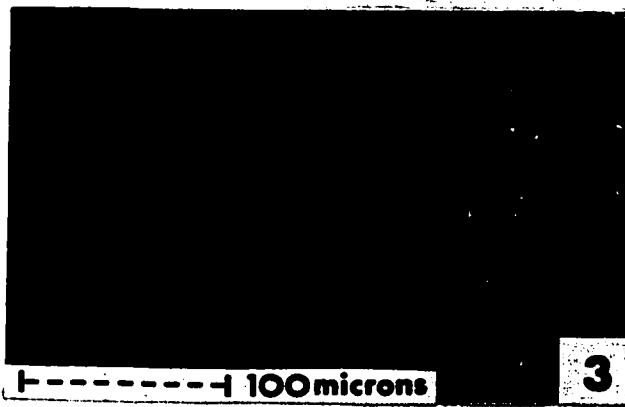
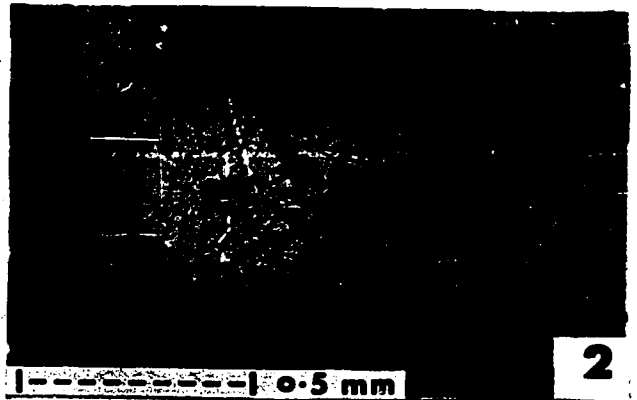
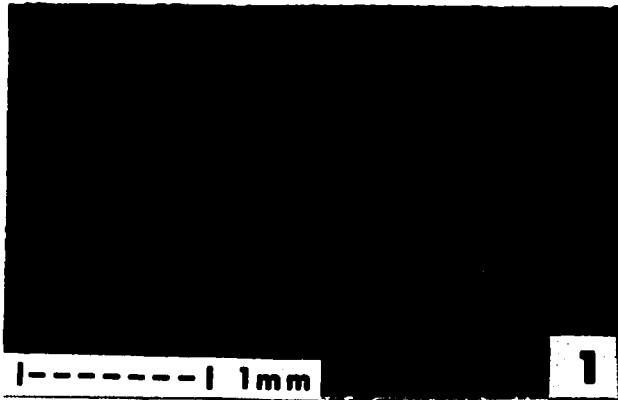
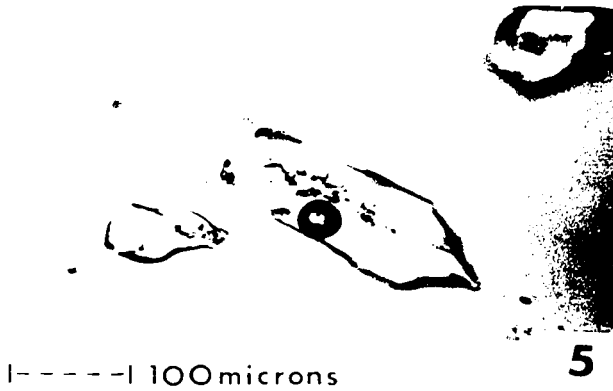
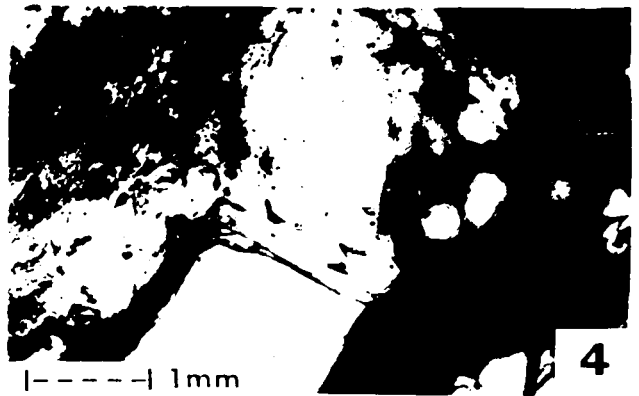
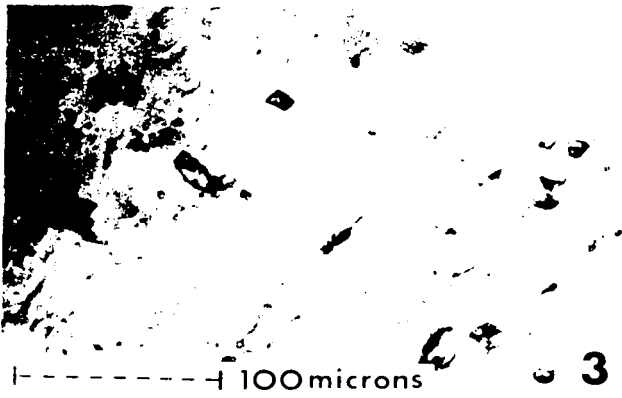
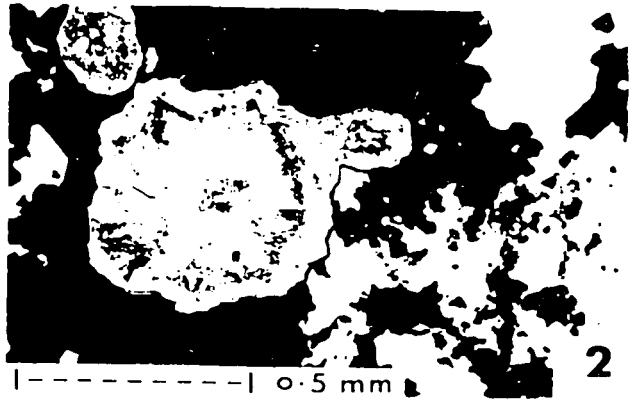
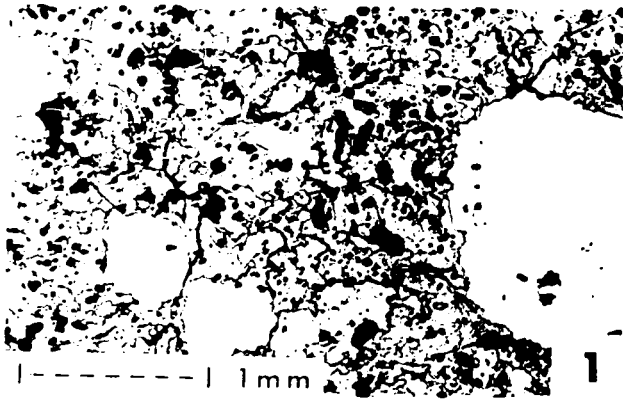


PLATE VII



## CHAPTER 7 - STABLE ISOTOPES IN THE DEPOSIT

After the preliminary mineralogical investigations of the vein material, it was decided that the application of stable isotope analyses to the vein sulphides and carbonates could be of use in the investigation of the thermal and physicochemical history of the deposit. At the time of initiation of this study, the application of sulphur isotopes to ore deposits was of a quantitative nature, see for example JENSEN (1968). The first theoretical work on sulphur isotope fractionation between coexisting sulphides was published by SAKAI (1968). Data was also available on the fractionation of oxygen and carbon isotopes between coexisting dolomite and calcite (O'NIEL & EPSTEIN, 1966 and NORTHROP & CLAYTON, 1966). It thus appeared that it might be possible to make temperature estimations and obtain some information as to the origin of the deposit from this type of work.

### Sulphur Isotopes

Samples for sulphur isotope analysis were chosen from the vein sulphides and those host rocks containing pyrite. A few additional samples of vein sulphides were picked from material collected at the El Bonanza and Terra mine. Nine different host rocks from the Echo Bay group and three samples from the hornblende-magnetite veins were chosen for the extraction of pyrite. All the samples were crushed and fed directly onto a Wilfley table, where pyrite separates were obtained. Magnetite was removed by a hand magnet and a pure pyrite separate obtained by the use of warm Clerici solution. The samples from vein

material were separated by the use of a small drill and a binocular microscope. Where necessary, polished sections were used to check for possible inclusions and exsolution lamellae which might affect sample purity. About five samples of each of all the vein sulphides, some arsenides and native bismuth were obtained for analysis. The treatment of the samples and the mass spectrometric work is described in Appendix D. The correction factors which were applied to the raw data are also documented in the appendix.

The corrected data is represented in  $\delta S^{34}$  values where

$$\delta S^{34} \text{ per mil} = \left[ \frac{S^{34}/S^{32} \text{ sample}}{S^{34}/S^{32} \text{ standard (Cañon Diablo)}} - 1 \right] \cdot 10^3$$

The Cañon Diablo meteorite standard represents the sulphur isotope value for the troilite phase of the Cañon Diablo meteorite, which by definition has a  $\delta S^{34}$  value of 0 per mil. A precision of  $\pm 0.1$  per mil was obtained for the mass spectrometric analyses. The overall error is about  $\pm 0.2$  per mil.

The samples investigated from the Echo Bay, El Bonanza and Terra mines are briefly described in Table 8 where the corresponding  $\delta S^{34}$  values are also given. Insufficient gas yield was obtained from the niccolite and native bismuth samples treated. It can be seen from the data that the host rocks and the hornblende-magnetite veins possess pyrite, which is fairly constant in its  $\delta S^{34}$  values. In contrast, the vein sulphides show a large variation in  $\delta S^{34}$  values. This variation can be correlated with the paragenetic sequence of the sulphides. Fig. 12 shows a plot of the  $\delta S^{34}$  values and demonstrates how they vary within the sulphide paragenetic sequence. It is evident that the  $\delta S^{34}$



TABLE 8

Echo Bay, El Bonanza and Terra Mines S isotope  
samples and analyses

Sample #	Sample description	S <sup>34</sup> value (per mil)
S1	Pyrite from tuff EBT 2.4	+ 4.8
S2	Pyrite from feldspar porphyry EBT 1.6	+ 3.0
S3	Pyrite from pyritic banded tuffs E.B.M. #3 adit level	+ 2.4
S4	Pyrite from pyritic banded tuffs E.B.M. #3 adit level	+ 4.2
S5	Pyrite from E.B. Tuff	N.A.
S6	Lost gas	
S7	Pyrite from breccia EBT 1.5	+ 4.2
S8	Pyrite from garnet agglomerate, Common Lake, EBCL 1	+ 6.2
S9	Pyrite from massive tuff EBT 1.3	+ 5.1
S10	Lost gas	
S11	Pyrite from hornblende-magnetite veins	+ 2.1
S12	Pyrite from hornblende-magnetite veins	+ 2.2
S13	Chalcopyrite with inter. sulphide stage carbonate, E.B.M. #2 adit	+ 7.9
S14	Chalcopyrite, banded ore with bornite, #2 adit level	+ 4.6
S15	Chalcopyrite, massive, #2 adit level	+ 3.7
S16	Chalcopyrite, massive ore with bornite, #2 adit level	+ 5.2
S17	Chalcopyrite with mckinstryite, 206A E Drift	+13.5
S18	Early galena with sphalerite, 206A E Drift	+ 2.4
S19	Galena with late sphalerite, 206A W Drift	+ 9.5
S20	Repeat of S 18 galena sample	+ 2.6
S21	Galena 302 Stope	+ 6.1
S22	Massive galena with late carbonate, 302 Stope	+19.9
S23	Acanthite very early, massive, 302 Stope	-19.7
S24	Massive acanthite 302 Stope	-21.5
S25	Acanthite assoc. with carb. and cp. #2 adit level	- 4.1
S26	Acanthite assoc. with carb. and cp. #2 adit level, drill core	- 0.5
S27	Acanthite assoc. with late carbonate, 302 Stope	+21.3
S28	Marcasite assoc. with later sulphides, 206A E Drift	+ 0.4
S29	"	- 0.9
S30	"	- 2.0
S31	Duplicate sample of S 30	- 2.0
S32	Marcasite, lost	
S33	Sphalerite, assoc. with galena in S 18	+ 5.3
S34	Sphalerite assoc. with inter. sulphide stage carb., 206A W Drift	+10.3
S35	Sphalerite assoc. with early carbonate 206A E Drift	+ 4.1
S36	Sphalerite assoc. with galena in S 19, 206A E Drift	+12.5
S37	Repeat of S 36	+12.6
S38	Mckinstryite 206A E Drift	+24.0
S39	"	+23.6
S40	"	+23.0
S41	"	+26.9

TABLE 8 (Contd.)

S42	Repeat of S 41	+27.1
S43	Bornite assoc. with late chalcopryrite, 209A W Sub-drive	+14.6
S44	Bornite assoc. with early chalcopryrite, #2 adit level	+ 5.8
S45	Bornite assoc. with early chalcopryrite, #2 adit level	+ 6.1
S46	Bornite, lost	
S47	Bornite assoc. with early chalcopryrite, #3 adit level	+ 5.1
S48-S52	Niccolite, insufficient gas yield	
S53-S55	Native bismuth, insufficient gas yield	
S56	Galena, Terra Mine, banded ore	+ 5.2
S57	Chalcopryrite, Terra Mine, banded sulphide ore	+ 5.8
S58	Vein galena, Terra Mine	+16.5
S59	Massive chalcopryrite, Terra Mine	+ 8.4
S60	Pyrite, banded sulphide ore, Terra Mine	+ 5.1
S61	Chalcopryrite, banded sulphide ore, Terra Mine	+ 5.2
S62	Chalcopryrite from massive sulphide vein, El Bonanza	+ 6.0
S63	Galena assoc. with S 62	+ 3.5
S64	Fine grained, massive chalcopryrite, El Bonanza	+ 5.0
S65	Galena, same sample as S 64	+ 2.8
S66	Chalcopryrite, Echo Bay, #3 adit level	+ 7.1
S67	Chalcopryrite, Echo Bay, #2 adit level	+ 6.0

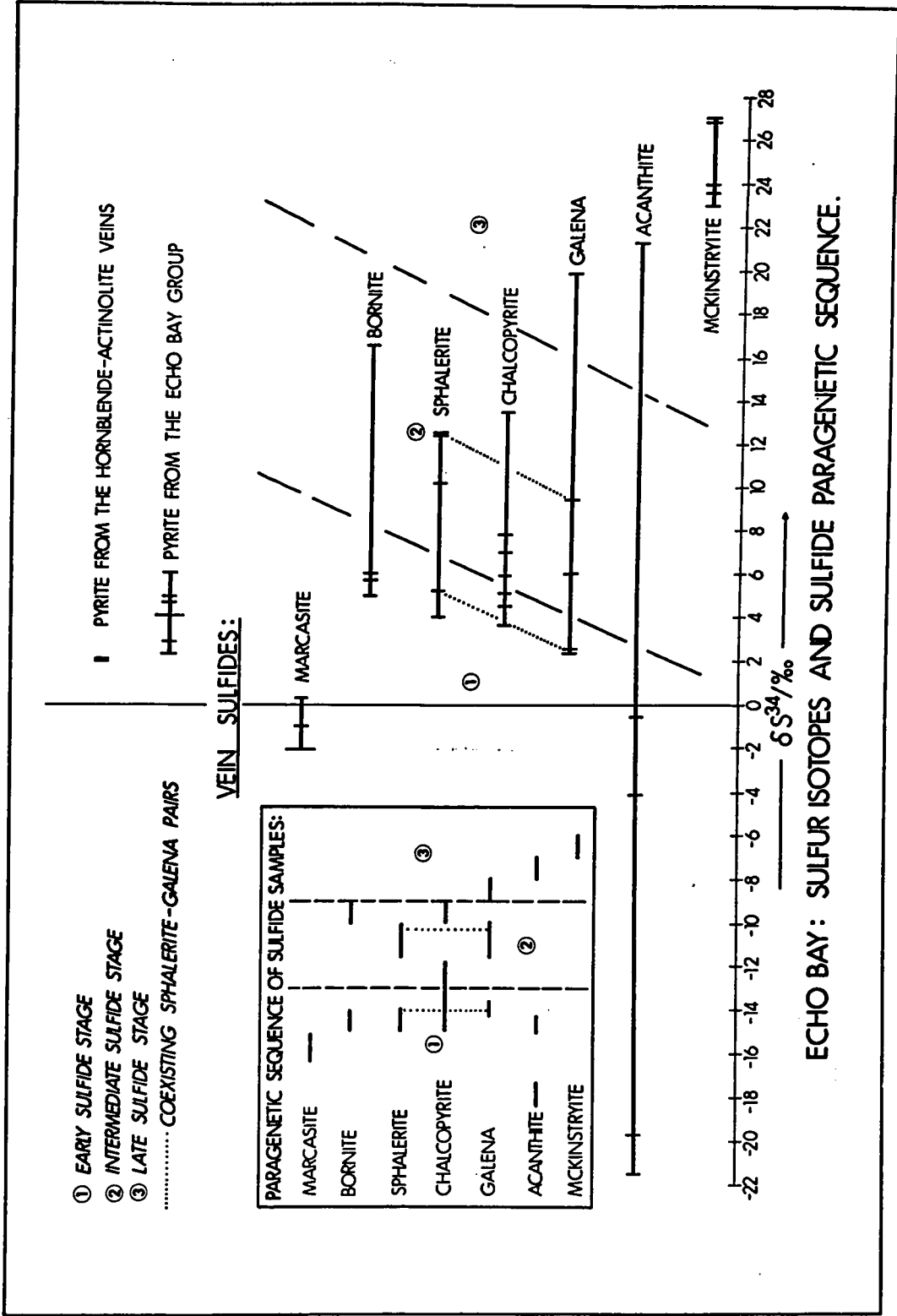


Fig. 12. Sulphur isotope values for the Echo Bay sulphides and the vein sulphide paragenetic sequence.

values increase with time. The minerals sphalerite, bornite, chalcopyrite and galena, which have been shown to be deposited in more than one generation, show a spread of the  $\delta S^{34}$  values. Invariably the later the generation of the mineral, the greater the  $\delta S^{34}$  value. This trend is best demonstrated in the mineral acanthite. The very early acanthite has  $\delta S^{34}$  values of around -20 per mil; the intermediate acanthite gives values of about -2 per mil and the late acanthite has  $\delta S^{34}$  values of +21 per mil. Mckinstryite, which is probably the latest sulphide in the depositional sequence, exhibits  $\delta S^{34}$  values of around +24 per mil.

Another important correlation can be made with the S isotope data. The first generation of sphalerite, bornite, chalcopyrite, galena and acanthite show the normal trend in  $\delta S^{34}$  values, i.e.  $\delta S^{34}$  sphalerite  $> \delta S^{34}$  chalcopyrite  $> \delta S^{34}$  galena. This phenomenon is thought to be due to differences in sulphur-metal bond strengths (BACHINSKI, 1969), where the sulphides are in equilibrium. In an equilibrium assemblage bornite is usually found to be lighter than coexisting chalcopyrite and marcasite is found to be heavier than associated sphalerite. As suggested by the polished section work the marcasite appears not to be in equilibrium with the other early sulphides and is deposited before them. Also the early bornite may not be in equilibrium with the other early sulphides. It does however appear that the early sphalerite, chalcopyrite and galena may be in equilibrium. Nevertheless only two sphalerite-galena coexisting pairs were obtained for this study. One pair was obtained from the early-sulphide stage and the other from the intermediate-sulphide stage. The minerals appeared to be in equilibrium with each other, as shown by the polished section and isotope work. No galena-chalcopyrite pairs were found and although chalcopyrite-

sphalerite pairs appeared to be in equilibrium, from the isotope work, they did not appear to be so in polished section. The chalcopyrite in most cases appeared to be slightly later than the sphalerite. For this reason only, the sphalerite-galena pairs were used to obtain temperature estimates for this study.

Explanations for the variation in  $\delta S^{34}$  values exhibited by the vein sulphides are given in Chapter 10, after the solution geochemistry of the deposit has been discussed.

### O and C Isotopes

Samples for oxygen and carbon isotope study were picked from vein material collected at the Echo Bay, El Bonanza and Terra mines. The samples were separated by a hand drill and usually no purification was required. Appendix D gives the analytical procedures for the production and isotopic measurement of  $CO_2$  from the carbonate samples as well as the corrections applied to the raw data. A similar precision for the mass spectrometric analyses as with the sulphur isotope measurements was obtained. Again the overall error is about  $\pm 0.2$  per mil.

The corrected isotope data are expressed in  $\delta O^{18}$  values and  $\delta C^{13}$  values where

$$\delta C^{13} \text{ (per mil)} = \left[ \frac{C^{13}/C^{12} \text{ sample}}{C^{13}/C^{12} \text{ standard}} - 1 \right] \cdot 10^3$$

$$\text{and } \delta O^{18} \text{ (per mil)} = \left[ \frac{O^{18}/O^{16} \text{ sample}}{O^{18}/O^{16} \text{ standard}} - 1 \right] \cdot 10^3$$

The results are reported against the PDB standard for  $\delta C^{13}$  analyses and the SMOW standard for  $\delta O^{18}$  analyses. Table 9 gives the  $\delta O^{18}$  and the  $\delta C^{13}$  values for all the samples analysed, as well as a brief description of the samples. Figs. 13, 14 and 15 give  $\delta O^{18}$  versus  $\delta C^{13}$  plots for the samples from Echo Bay, El Bonanza and Terra respectively. In all of these plots it can be seen that the calcites normally exhibit lighter isotopic values than the dolomites. Only one coexisting calcite-dolomite pair (023C and D) was obtained for isotopic measurement. All the calcite and dolomites do not however appear to be in equilibrium. An interpretation of the oxygen and carbon isotopic data is given in Chapter 10, after the temperature and solution geochemistry of the deposit have been discussed.

TABLE 9  
Echo Bay, El Bonanza and Terra Mines O and C isotope samples and analyses

Sample #	Carbonate	Location	Description	$\delta^{18}\text{O}$ (SMOW)	$\delta^{13}\text{C}$ (PDB)
01	C	EBM #2 adit level	Flat scalenohedron as vug infillings	+ 8.3	-10.6
02	C	EBM 302 Stope	Well crystalline after marcasite	+ 7.3	- 7.9
03	C	EBM 206A E Drift	Late fissure infilling. Rhombohedral	+ 8.6	-12.7
04	C	EBM 206A E Drift	Finely xtalline, assoc. with cp. after mc.	+ 9.7	-19.0
05	C	EBM 302 Stope	Well xtalline vug, after early acanthite	+12.6	- 4.5
06	C	EBM 302 Stope	Early, finely xtalline, with acanthite	+20.3	-18.8
07	C	EBM 206A E Drift	Vug infilling assoc. with cp.	+ 5.4	-31.2
08	C	EBM 206A E Drift	Well xtalline assoc. with galena and cp.	+14.6	- 8.5
09	C	EBM 302 Stope	Well xtalline with inter. stage acanthite	+15.4	-11.5
010	D	EBM #2 adit level	Very coarse vein with cp.	+13.1	- 2.2
011	C	EBM Common Lake	Very coarse vein	+ 9.5	- 7.2
012	C	EBM Common Lake	Coarse vein carbonate	+10.5	- 5.8
013	D	EBM #2 vein	Coarse vein carbonate with cp.	+15.1	- 1.4
014	C	EBM #2 adit level	Massive vug infilling	+20.1	-12.1
015	D	EBM Shore plat.	Dolomite vein with cp. and hematite	+15.7	- 4.5
016	D	EBM	Late?, with massive cp.	+12.3	- 1.5
017	D	EBM Old Shaft	Mn encrusted carbonate	+15.3	- 2.4
018	C	EBM 206A E Drift	Late vein carbonate	+ 7.8	-12.3
019	D	EBM	Inter. sulphide stage dolomite	+11.8	- 3.0
020	D	EBM	Coarse carb. after hem. and qtz.	+12.1	- 2.3
021	C	EBM #2 adit level	Flat scalenohedron, late vug infilling	+ 8.6	-12.2
022	C	EBM #2 adit level	"	+14.0	-10.8
023	C	EBM #2 adit level	Vug filling in 023D	+17.6	- 8.0
023	D	EBM #2 adit level	Massive gangue with Co-Ni-arsenides	+21.9	- 3.3
024	D	EBM	Massive gangue with niccolite	+22.5	- 2.8

TABLE 9 (Contd.)

025	C	El Bonanza	Late? vein assoc. with native silver	+11.9	- 6.2
026	C+R	El Bonanza	Maroon carb. with silver and fluorite	+11.3	- 4.3
027	S+R+D	El Bonanza	Banded carbonate vein	+16.0	- 3.0
028	D+R+S	El Bonanza	"	+16.4	- 2.8
029	R+S+C	El Bonanza	"	+17.0	- 2.8
030	R	El Bonanza	"	+16.0	- 3.1
031	C	El Bonanza	Early? carbonate	+10.4	- 8.1
032	C	El Bonanza	Later than 031	+11.7	- 6.0
033	C	El Bonanza	Late? carbonate with native silver	+12.4	- 5.1
034	C	Terra Mine	Coarse carb. with coarse galena	+19.6	-11.4
035	S+D	Terra Mine	Vein assoc. with fluorite and native Bi	+13.3	- 4.0
036	C	Terra Mine	Vein with galena	+12.0	- 8.7
037	C	Terra Mine	Very coarse vug filling, clear	+ 6.3	- 7.2
038	C	Terra Mine	Vein calcite, yellow	+15.0	-10.1
039	C	Terra Mine	Limestone	+10.5	- 0.3
040	D	Terra Mine	Carbonate stringer in syenite	+15.5	- 6.1
041	D	EBM	Early- inter. dolomite with cp.		
042	C	EBM	Band between 041 and 043		
043	C	EBM	Band between 042 and 044		
044	C	EBM	Late well xtallised calcite		

C = Calcite, D = Dolomite, R = Rhodochrosite and S = Siderite

EBM = Echo Bay Mine



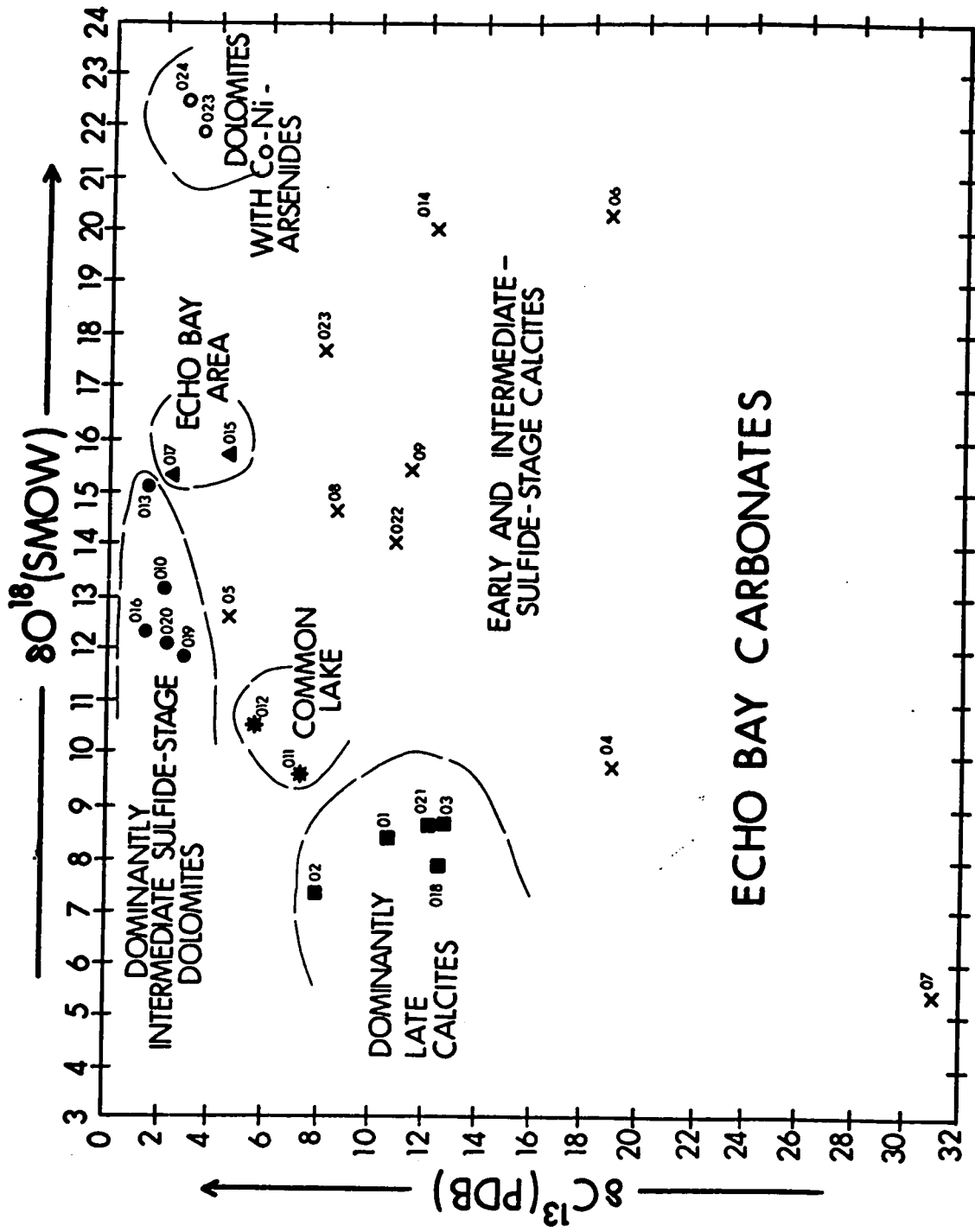


Fig. 13.  $\delta^{18}\text{O}$  vs.  $\delta^{13}\text{C}$  plot for the Echo Bay carbonates.

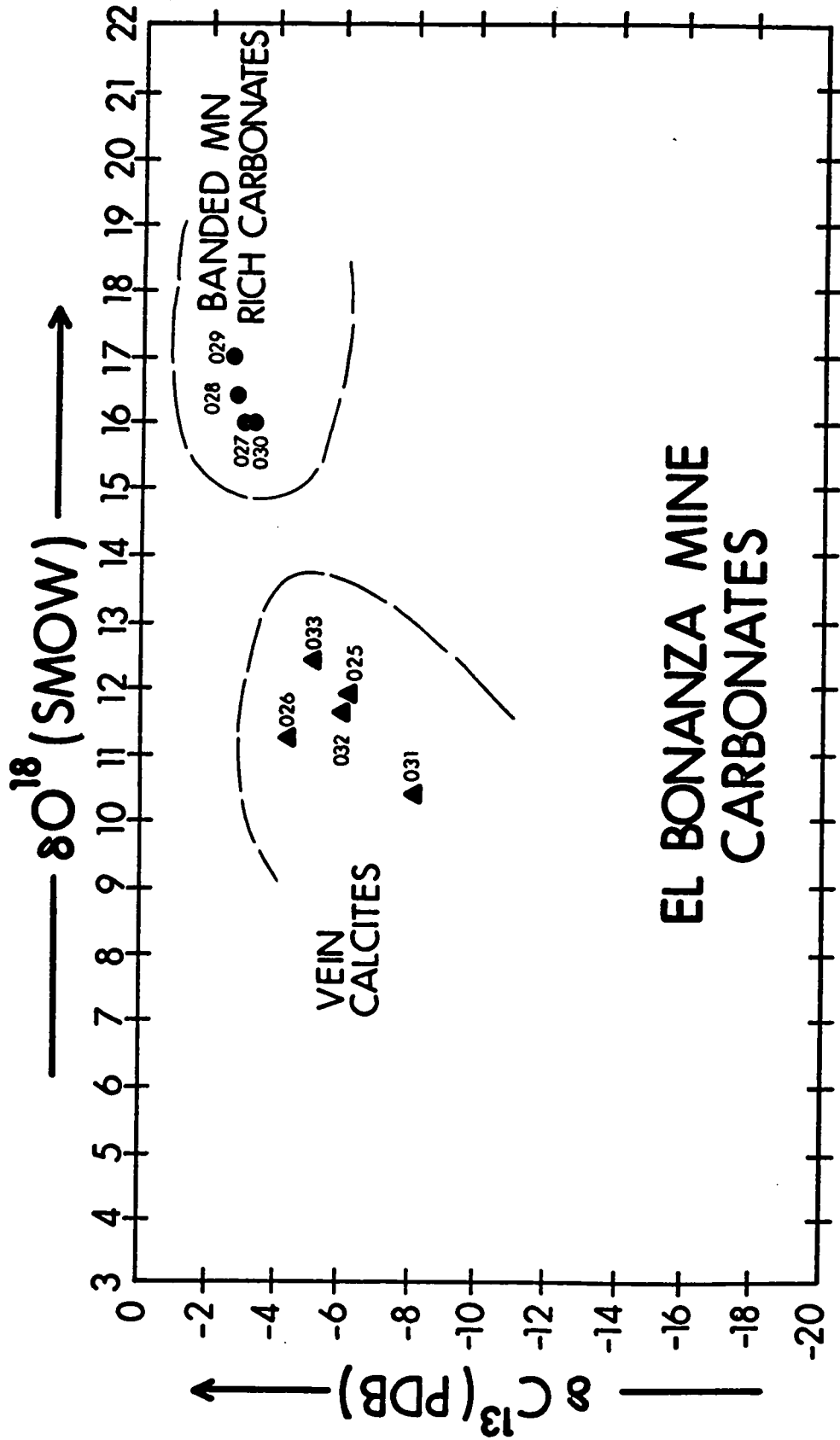


Fig. 14.  $\delta O^{18}$  vs.  $\delta C^{13}$  plot for the El Bonanza Mine carbonates.

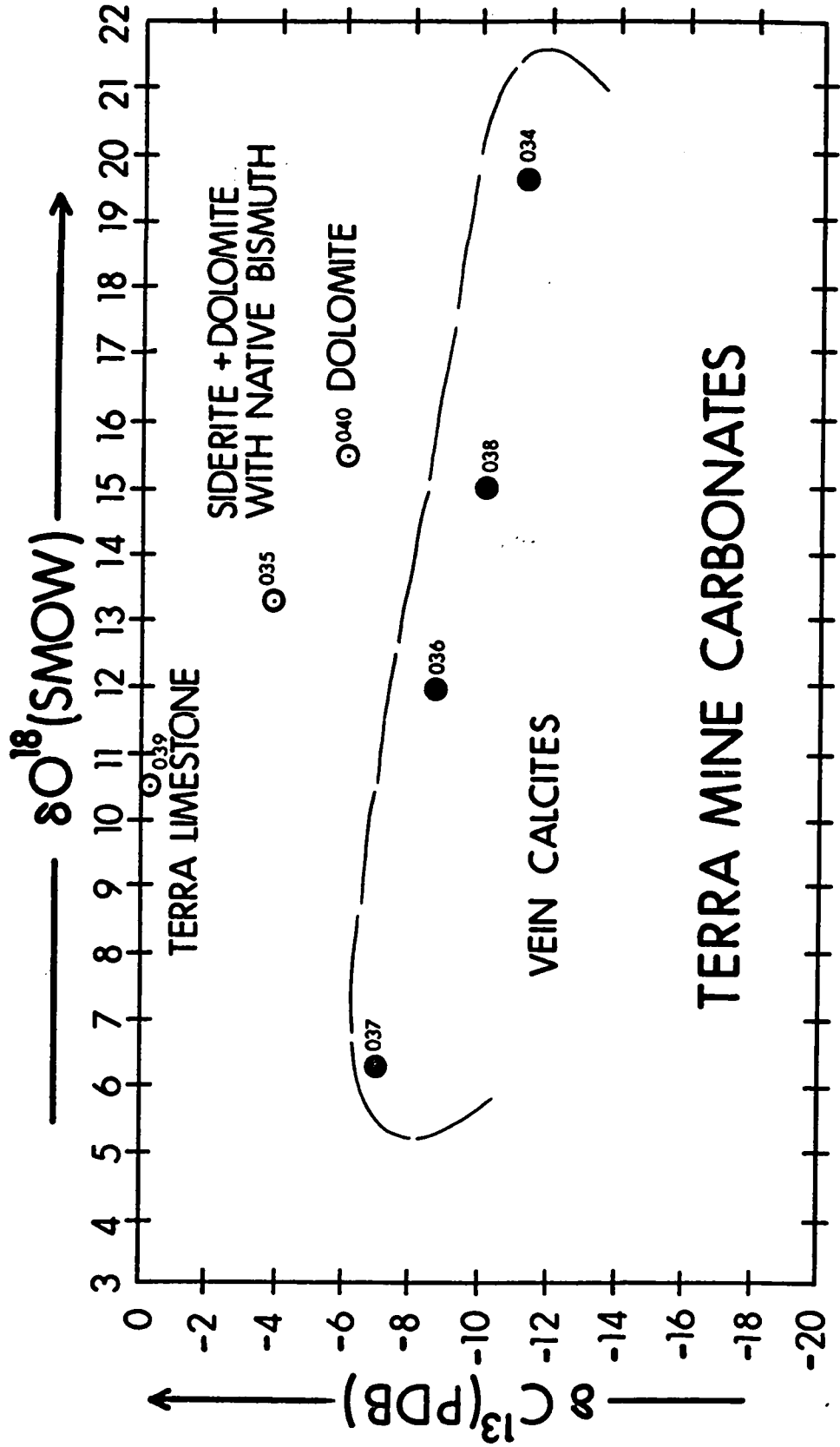


Fig. 15.  $\delta O^{18}$  vs.  $\delta C^{13}$  plot for the Terra Mine carbonates.

## CHAPTER 8 - GEOTHERMOMETRY AND FLUID INCLUSION STUDIES

During the past decade there has been intensive research and some progress in the development of geological thermometers, especially those of use in ore and gangue materials. Only recently, however, have any comparative studies of different methods on the same materials been completed (see for e.g. GROVES et al., 1970 and KELLY and TURNEAURE, 1970). Thus, in general, it has been found that more information (and probably more accurate information) is available from fluid inclusion studies. In one instance, the results obtained with the various sulphide geothermometers were dissappointing and hardly justified the time invested (KELLY and TURNEAURE, loc. cit.).

### General Considerations

The very minor distribution of exsolution textures at Echo Bay were not thought to be diagnostic of any particular temperature of formation as discussed in Chapter 6. However, the occurrence of three minerals: marcasite, native bismuth and mckinstryite is worthy of comment. Marcasite is most often found in sediments and veins of low temperature origin. It is thought to be formed under low temperatures and from acid solutions; pyrite being deposited at higher temperatures and low acidity (ALLEN et al., 1914). In fact the presence of marcasite probably indicates a temperature of formation of less than 300° C. (BARTON and SKINNER, 1967).

The melting point of native bismuth is 271.5° C. (KLEMENT et al., 1963) and this is generally regarded as placing an upper limit on the temperature of formation of the mineral. The melting point is, however, lowered by 7.6° C. per kilobar total pressure (KLEMENTS et al., loc. cit.).

The main assumption in the use of this geothermometer is that the native bismuth is not associated with any other mineral assemblage which may put other limits on the temperature of formation.

The textures displayed by the native bismuth are not usually found to be particularly diagnostic. The mineral most often occurs as veinlets and intergranular fillings. In the Eldorado deposit, rhombohedral bismuth dendrites, rimmed by later minerals supports the argument of the deposition of the mineral as a solid. Drop-like, spherical or other forms which might be diagnostic in establishing initial precipitation as a liquid were not observed. It thus would seem unjustified to place much reliance on the melting-point of bismuth as a geothermometer, since there is some uncertainty as to whether the mineral formed as a solid or as a liquid. However, it is felt that in this deposit the bismuth was deposited in the solid state. In the tin and tungsten deposits of the Eastern Andes, similar occurrences of native bismuth were found to be deposited between 242 and 300° C. by checking with other geothermometers (KELLY and TURNEAURE, loc. cit.).

The presence of mckinstryite in the late-sulphide stage of deposition supposedly places a maximum temperature of 94.4° C. upon the end of this stage. Above this temperature, the mckinstryite breaks down to a two phase assemblage of jalpaite and a cation-disordered hexagonal compound of composition  $(\text{Cu}_{0.96} \text{Ag}_{1.0})\text{S}$ . The absence of twinning also suggests that the mckinstryite did not grow as a mixture of other phases which cooled to give the mckinstryite composition (SKINNER et al., 1966). However, since no thermodynamic data is available for mckinstryite, then the effect of low  $f\text{S}_2$  conditions on its formation temperature cannot be calculated.

Mineral compositions are often a function of temperature and sulphur fugacity. The two cases which appeared to be of use at Echo Bay are the gold content of the native silver and the iron content of the sphalerites. However, the composition of the native silver using the electrum tarnish method of BARTON and TOULMIN (1964) is not applicable, since the native silver is not found to coexist with acanthite. However, the sphalerites in polished sections EB16 and EB18 were found to be coexisting with the iron-bearing mineral chalcocopyrite. Thus a measurement of the FeS content of these sphalerites will reflect the temperature and fugacity of sulphur conditions at the time of formation. Both the sphalerites in EB16 and EB18 are placed in the intermediate-sulphide stage of mineralisation, but that in EB16 is later than the sphalerite in EB18 using the criterion of sequential deposition. The iron content of each of these sphalerites was determined using an A.R.L. 'EMX' microprobe. Peaks and backgrounds were counted for 50 second periods while randomly traversing the sphalerite. The samples were counted versus a marcasite standard which was measured at the beginning and end of this set of samples. Traversing in the sphalerites did not reveal any inhomogeneities in the iron content as found by BARNES and SCOTT (1969). The analyses were corrected and totalled to 100% by the addition of S and Zn. Stoichiometry of the sphalerite was assumed. The corrected analyses are shown below in Table 10.

TABLE 10

Electron microprobe sphalerite analyses

Sample	Wt % Fe	Wt % S	Wt % Zn	Mole % FeS
EB16	0.79	66.26	32.95	2.9
EB18	0.55	66.51	32.94	2.0

The precision of the analyses is  $\pm 1\%$  for 2  $\delta$  variations

Using the data given by BARTON and TOULMIN (1966) for sphalerite in equilibrium with pyrite or pyrrhotite, it can be seen that the differences in the mole percentages of FeS in the sphalerites reflects either a change in temperature, a change in sulphur fugacity or both. From additional data to be presented for temperature estimates and also for the geochemical model derived for the evolution of the deposit, it is more feasible that the temperature remained relatively constant and the sulphur fugacity dropped. Although pyrite and pyrrhotite are absent, comparative results can be obtained for the samples. Taking a temperature of 200° C., the sample EB18 represents a  $\log fS_2$  of -14.7 and the sample EB16 a  $\log fS_2$  of -14.5. These values are plotted in Fig. 19.

#### Temperatures derived from stable isotope data

The use of O and C isotope data on the vein carbonate has been of little value in the temperature determinations. The large fractionation of carbon isotopes and possibly of oxygen isotopes between the dolomites and calcites in the veins suggests a more complicated time, chemical or alteration history than straightforward equilibrium within a common or simple evolving fluid. The  $\delta O^{18}$  values of the dolomites from the Echo Bay Co-Ni-arsenide stage and the intermediate-sulphide stage could, however, represent equilibrium within a fluid whose temperature increased over 50° C. This was in fact the approximate temperature difference between these stages as will be shown later. It should be noted here that a quartz, hematite calcite sample from Port Radium was used for an oxygen isotopic temperature study by CLAYTON and EPSTEIN (1958). The quartz-calcite temperature was 140° C. and the quartz-hematite temperature was 150° C. This is useful in that it is

the only estimate so far available on the early stage of mineralisation of the Echo Bay and similar veins. Due to the possibilities of the alteration of calcite after formation, the quartz-hematite temperature is considered to be probably more reliable. This temperature of 150° C. is assumed for the initial stages of vein deposition at Echo Bay.

However, it was found possible to use coexisting sulphides at Echo Bay and El Bonanza Mines to obtain estimates of the temperature of sulphide formation. Although many sulphide samples from Echo Bay contained several sulphides, polished section work showed that of all the samples only two contained sulphides which appeared to have been formed at the same time. All the other sulphides exhibited replacement or sequential-hiatus textures. The two pairs picked were sphalerite-galena pairs shown in polished section in Plate V, Fig. 6 and Plate VI, Fig. 2. Thus estimates for the early and intermediate sulphide stage temperatures can be made. The early sulphide stage pair comprised of S33: sphalerite, S18: galena and S20: galena whose  $\delta S^{34}$  values are +5.3, +2.6, and +2.4 respectively. The values for S18 and S20 are averaged and subtracted from S33 to give a  $\delta S^{34}\Delta$  for the pair of 2.8 per mil. Similarly, the samples for the intermediate sulphide stage pair are S19, S36 and S37 and the  $\delta S^{34}\Delta$  for this pair is 3.1 per mil.

The various curves presently available for the fractionation of sulphur isotopes between sphalerite and galena pairs as a function of temperature are shown in Fig. 16. Within the temperature range of the Echo Bay deposit, it is evident that these curves give tremendous variations in temperature estimates. It is thus necessary to pick one or possibly two curves to obtain a reasonable temperature range. Placing a limit on the temperature of any one stage as 271° C., then the usable



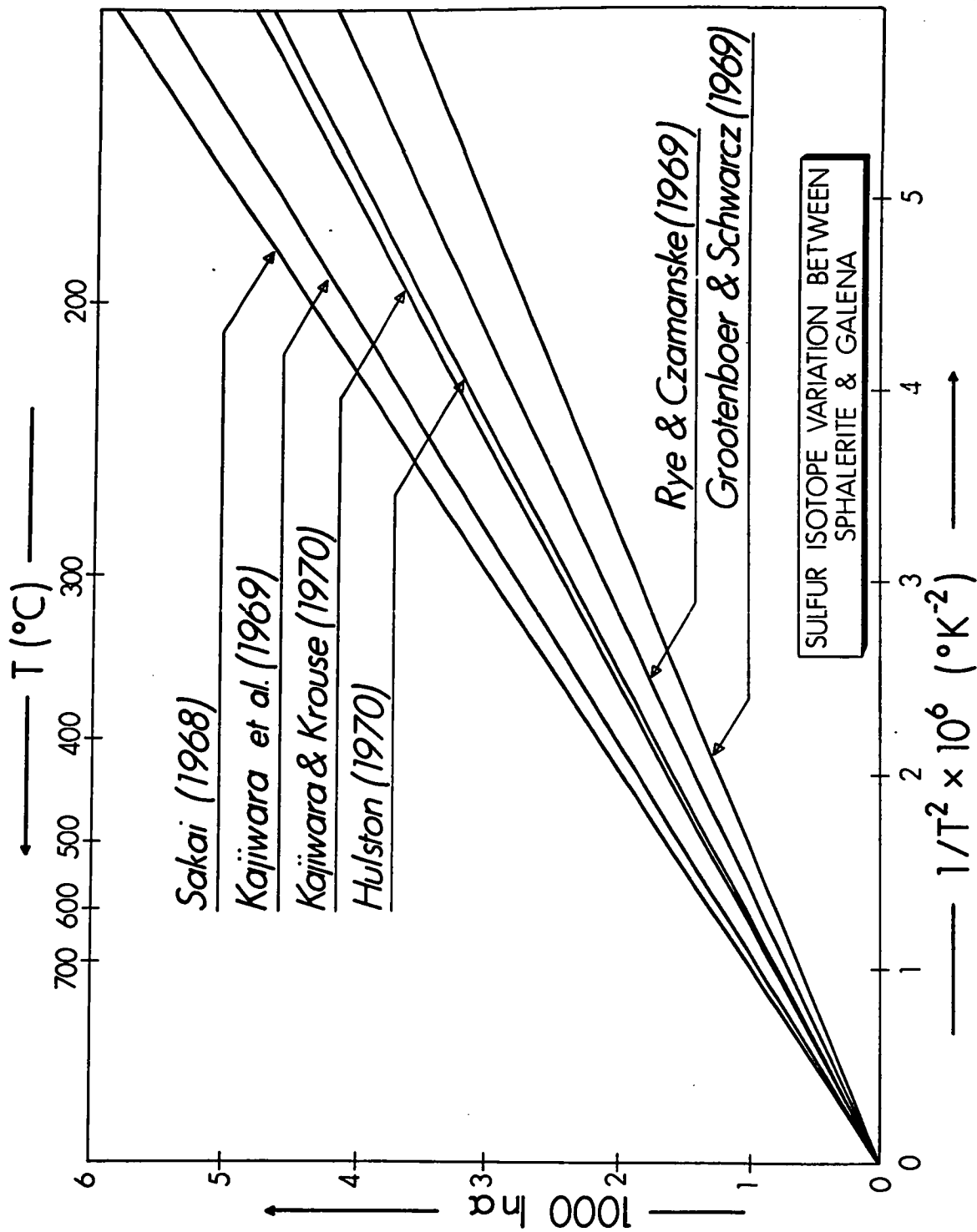


Fig. 16. Graph of  $1000 \ln \alpha$  vs.  $1/T^2 \times 10^6$  showing the results of calculations and experiments to determine the variation of sulphur isotope fractionation between galena and sphalerite.

curves are given below:

	Early Sulphide Stage	Intermediate Sulphide Stage
KAJIWARA and KROUSE (1970)	282°C	252°C
HULSTON (1970)	255°C	229°C
RYE and CZAMANSKE (1969)	227°C	202°C
GROOTENBOER and SCHWARCZ (1969)	194°C	171°C

In the following section, it will be shown that the only feasible pressure corrections for the fluid inclusion filling temperatures are obtained by using the temperatures derived from the curves of RYE and CZAMANSKE (loc. cit.) and GROOTENBOER and SCHWARCZ (loc. cit.). The experimental curve of Grootenboer and Schwarcz was produced by measuring the exchange between metal sulphides and liquid sulphur whereas the curve produced by Rye and Czamanske was obtained from a series of hydrothermal coprecipitation experiments with sphalerite and galena.

In the author's opinion, this latter experiment is more representative of geological conditions and therefore the experimental curve of Rye and Czamanske was used. Thus, the early sulphide stage is placed at about 200° C. and the intermediate sulphide stage at about 230° C. The errors in the S isotope measurements would place an error of about  $\pm 5^\circ$  C. on these temperature estimates but in view of the larger discrepancies between experimental curves then these errors are not significant.

For the El Bonanza deposit sulphur isotope measurements were made on two samples of fine-grained coexisting chalcopyrite and galena.

The samples used were S67 and S63 (first pair) and S64 and S65 (second pair). The  $\delta S^{34}\Delta$  is 2.5 per mil and 2.2 per mil for the first and second pairs respectively. Data from SAKAI (1968) gives very high temperatures for these pairs, but data from KAJIWARA and KROUSE (loc. cit.) on the chalcopyrite-galena pairs gives temperatures of 271° C. and 237° C. respectively. Again in comparison with fluid inclusion data given in the next section, these temperature estimates require large pressure corrections of the fluid inclusion data. These high pressures are not thought to have been operative and in actual fact the temperatures are probably somewhat lower than those estimated above.

#### Fluid Inclusions

In preparation for fluid inclusion studies, representative samples of quartz, dolomite, calcite and sphalerite from all paragenetic stages were chosen. About a half inch square of material was cut and polished on one side. The chip was then cut parallel to the polished side, the thickness depending upon the opacity of the mineral, and the cut side polished. All these chips were examined on a Zeiss Photomicroscope II with magnifications up to X160 normally and with some samples up to X400. Of all the samples examined, fluid inclusions were only detected in the late quartz, the intermediate-sulphide stage dolomite, some sphalerites and a calcite sample from the El Bonanza Mine. Because the highest powered objective which could be used on the heating stage was X32, only the fluid inclusions in the late quartz, dolomite and the El Bonanza calcite were large enough to permit heating experiments. The heating experiments were conducted on a stage specially constructed by H. Ohmoto. A section and description of this stage is given

in OHMOTO and RYE (1970). Essentially, this stage is designed to minimize the temperature gradient within the sample chamber and in fact this is effected by having a cylindrical furnace and a succession of quartz-glass plates and metal and asbestos rings to insulate the sample chamber. The operating temperature is controlled by varying the current flowing in the heating element by means of a voltage regulator. A chrome-alumel thermocouple is placed next to the sample and the temperature is read by a digital thermocouple thermometer. This is calibrated against the melting point of bismuth (271.5° C.) and lead (327° C.) inside the sample chamber. Repeated measurements on the filling temperatures, both on heating and cooling, of specific inclusions usually varied less than 1° C. Including the temperature gradient and uncertainty of the thermometer calibration, the filling temperatures were probably determined with an apparent precision of  $\pm 2^\circ$  C.

Fluid inclusions have now been used with much success in many ore deposits (see for example SAWKINS, 1964, 1966; SAWKINS and RYE, 1970) and have yielded information concerning the origin of deposits, as well as their temperature of formation. The basic techniques for the study of fluid inclusions are given in ROEDDER (1962 and 1963). Reviews of the uses and limitations of fluid inclusions are given by SMITH (1962) and ROEDDER (1967). Most of the early concern with regard to possible leakage of fluid inclusions have been dispelled and the distinction of primary, pseudosecondary and secondary inclusions puts the study on a more meaningful basis. One of the remaining doubts with regard to fluid inclusion work is: are they really representative of the fluids from which their including minerals crystallised? Experiments have been produced whereby, possibly due to absorption effects, fluid inclusions are

enriched in K, Na, Li and similar elements above the mother fluid (R.W. BOYLE, pers. comm.). However, work on fluid inclusions in synthetic sphalerite, grown in NaOH solutions, demonstrated that the salinity of the fluid in the inclusion was less than that of the original solution (H.L. Barnes, pers. comm.). Since this conflicting evidence is only in the initial stages of development, it is assumed for this study that the fluid inclusions are representative of the fluid from which their including mineral crystallised. All the information was obtained from the Echo Bay fluid inclusions by heating experiments; equipment was not available for conducting freezing experiments.

The fluid inclusions observed at Echo Bay are shown in Plate VII, Figs. 3 to 8 inclusive. Relatively small inclusions comprised of liquid, vapour and salt crystals occur in the intermediate sulphide stage dolomite as shown in Plate VII, Fig. 3. Much larger fluid inclusions are found in the late quartz as shown in Plate VII, Figs. 4 to 8 inclusive. Here, a liquid phase, vapour phase, salt crystal and other solid material are normally present. In both the dolomite and the quartz, primary and secondary inclusions can be distinguished. The primary inclusions are relatively large, often lying on mineral growth planes or appearing solitary and remote from healed secondary fractures or cleavage planes.

Some of the large fluid inclusions in the quartz were primary but have been affected by secondary fracture planes thus producing a secondary inclusion on healing.

Upon heating the primary inclusions, the salt crystal was the last phase to disappear and the other solid material observed in the inclusions in quartz does not disappear up to 450° C. or upon prolonged heating at 300° C. This latter phase is thus assumed to be a solid

inclusion of possibly a sulphate. This material occurs as a radiating fibrous mass; it has moderate relief, is birefringent and has straight (?) extinction. The vapour phase in the 21 measurements made on the dolomite disappeared at  $150 \pm 10^\circ$  C. and in the 10 measurements made on the quartz, the vapour phase disappeared at  $130 \pm 10^\circ$  C. In all the Echo Bay fluid inclusion samples measured, the salt crystal finally dissolved at  $165 \pm 10^\circ$  C. Secondary inclusions in the dolomite contained no solid material and on fifteen measurements made, the vapour phase is observed to disappear at  $120 \pm 10^\circ$  C. Heating of the secondary inclusions in the quartz showed them to have similar salinities and homogenisation temperatures as the primary inclusions. Fluid inclusions containing only vapour and liquid phases were observed in a calcite sample from the El Bonanza Mine. Here the vapour phase was found to disappear at  $165 \pm 5^\circ$  C. (5 measurements).

Since the salt crystal was the last phase to disappear in the fluid inclusions at Echo Bay, then the solution was assumed to be saturated with sodium-potassium chloride at this temperature. Since this temperature was fairly constant, then the salinity of the ore-forming fluid was probably constant. Water saturated with sodium chloride at  $165^\circ$  C. contains 30 wt. % NaCl and thus the ore forming solution appears to have contained in the order of 30 wt. % salt, or in other words, it was approximately a 5 m solution.

#### Geobarometry

No evidence for boiling of the ore fluids at Echo Bay, (that is no division of the fluid inclusions into  $\text{CO}_2$ - and vapour-rich types

and liquid types), was observed. Thus the fluid pressure at the time of formation was greater than the vapour pressure of a 5 m NaCl solution at around 200° C. In actual fact this pressure is very low and is in the order of 25 atmospheres.

The actual pressure at the time of ore deposition can be estimated in two ways: either by calculating the overburden and assuming either a lithostatic pressure or a fluid pressure at this depth, or by comparing the fluid inclusion filling temperatures with other temperature estimates from contemporaneous material. Both methods were employed for the Echo Bay materials. The overburden at the time of ore formation in the Echo Bay area was calculated to be between a minimum of 3.4 Km and a maximum of 4.8 Km. The lithostatic pressure at these depths is between 1.0 and 1.4 Kbars. Using a conversion factor of 0.465 for lithostatic to fluid pressure (HOLMES, 1965, p. 1166) the fluid pressure would be from 0.5 to 0.7 Kbars. If an open fracture system is assumed to have been operative, then the water pressure at depth  $h$  is equal to the acceleration due to gravity multiplied by  $h$  and the density of the water. For a first approximation it is assumed that the water density is  $1 \text{ gm./cm.}^2$  and this would give a hydrostatic pressure of from 0.3 Kbars to 0.5Kbars. It is thus evident that, depending upon the degree of openness in the fracture system, the fluid pressure could have been between 0.3 to 0.7 Kbars.

An absolute temperature for the intermediate-sulphide stage was determined by the use of S isotopes on a sphalerite-galena pair. The filling temperatures of fluid inclusions in dolomites of this stage are also known. Thus it can be assumed that the difference between these two temperatures, i.e. 150° C. for the fluid inclusions and 230° C.

for the S isotope temperature, is due to the pressure correction applicable to the fluid inclusion data. This method of correction and temperature-pressure-density relationships of up to 10 wt. % NaCl solution is given by OHMOTO and RYE (1970). However, for higher salt concentrations, the data of LEMMLEIN and KLEVTSOV (1961) is used. Using the temperature estimate from the experimental curve of RYE and CZAMANSKE (loc. cit.), the pressure would be 0.75 Kbars and using the experimental curve of GROOTENBOER and SCHWARCZ (loc. cit.), the pressure would be 0.25 Kbars. Neither of these estimates is really outside the previous ones and accepting all these as limits then, the pressure is taken to be about 0.5 Kbars for the geochemical models developed in later chapters.

#### The CO<sub>2</sub> content of the fluid phase

Crushing experiments were performed on grains of dolomite and quartz known to contain primary fluid inclusions. The grains were crushed in the oil between glass plates on the microscope stage. No gas was observed to escape and the inclusions were assumed to contain no gas under pressure. However, they could still contain a small amount of dissolved CO<sub>2</sub> at room temperature. Work has been done on the solubility of CO<sub>2</sub> in water and sodium chloride solutions at temperatures above 100° C. (ELLIS and GOLDING, 1963 and TAKENOUCI and KENNEDY, 1965). For the Echo Bay inclusions, the data of TAKENOUCI and KENNEDY (op. cit.) are found to be most useful. However, even this data requires extreme extrapolations to be of any use. Data are only given for the solubility of CO<sub>2</sub> in water, 6% NaCl solution and 20% NaCl solution starting at a temperature of 150° C. and pressure of 100 bars. Thus extrapolations of up to 30% NaCl solution and down to low temperatures and pressures have



to be attempted. Because of these extrapolations, no absolute figure could be obtained and this is also only a maximum figure. The estimate is a maximum of  $\log f\text{CO}_2$  -1.5. A further complicating factor was encountered in determining the  $f\text{CO}_2$  from the weight per cent of  $\text{CO}_2$  in solution. The molality can be obtained and the fugacity of  $\text{CO}_2$  can be determined by the use of Henry's Law Constant for  $\text{CO}_2$  in a 5m NaCl solution. However, if the fluid pressure is assumed to be equal to the partial pressure of water plus the partial pressure of  $\text{CO}_2$ , then the  $f\text{CO}_2$  can be calculated knowing the partial pressure and the fugacity coefficient. A lower value for the  $f\text{CO}_2$  is obtained in comparison to the value obtained by the previous method. Thus, depending on whether the ore fluid under the conditions of ore deposition is considered as a homogeneous fluid or as a liquid with a gaseous phase, then different estimates for the  $f\text{CO}_2$  will result. For the geochemical model used later the  $\log f\text{CO}_2$  at early and late stages was assumed to be +1.5 and -1.5. This is within the values of  $\log f\text{CO}_2$  -2 to +2 normally assumed for ore fluids (H. Ohmoto, pers. comm.).

#### K/Na Ratios of Fluids in Inclusions

K/Na ratios of fluid inclusions have sometimes been of value in determining the origin and type of ore forming solution (see for example WHITE, 1968 and RYE and HAFFTY, 1969) and therefore it was decided to effect this study on the Echo Bay fluid inclusions. No sophisticated crushing and extraction line was available and therefore a cruder technique had to be adopted. The material was crushed down to fragments of about 2 mm. diameter and washed several times with water

and several times with warm distilled water. The cleaned material was added to a tungsten carbide swing mill which had previously been cleaned with acid and distilled water and was ground for approximately 3 minutes. The powder was then transferred to a filter paper in a plastic funnel and the salts were leached from the powder with about 15 ml. of distilled water into a polythene bottle. A Perkin-Elmer flame photometer was used for the analyses and known standards of  $K_2O$  and  $Na_2O$  allowed the  $K_2O$  and  $Na_2O$  in the solutions to be read directly. As a check for the blank in this procedure, all the above operations were performed using quartz glass. The blank for  $K_2O$  was 2 ppm and for  $Na_2O$  3 ppm. These values were subtracted from those obtained on the samples and the corrected values together with the K/Na atomic ratios for the samples are shown in Table 11. The values appear to be consistent and reproducible for the minerals studied.

A generalised curve for waters in equilibrium with granitic melts and assemblages is shown on a temperature versus K/Na ratio plot in Fig. 17. Also on this plot are the values for the Echo Bay minerals and for comparative purposes the Red Sea geothermal brine and the Salton Sea geothermal brine. The temperature for both the minerals at Echo Bay has been generalised at 200° C. and it can be seen that at this temperature the fluids were certainly not in equilibrium with a granitic-type mineral assemblage. The data could, however, be interpreted as being due to the fluids being in equilibrium with a granitic-type assemblage at higher temperatures and then being rapidly removed from this environment and cooled. This, however, is probably not a feasible geological situation in this area. On the other hand the K/Na ratio of a fluid which had passed through evaporites would be enriched in potassium over sodium due

TABLE 11

K/Na analyses of the fluid inclusions

SAMPLE	CORRECTED CONCENTRATIONS		K/Na ATOMIC RATIO
	K <sub>2</sub> O (ppm)	Na <sub>2</sub> O (ppm)	
Quartz 1	14	49	0.19
Quartz 2	24	70	0.23
Dolomite 1a	88	150	0.39
Dolomite 1b	41	73	0.37
Dolomite 2a	108	171	0.42
Dolomite 2b	95	165	0.38
Dolomite 3a	48	90	0.35
Dolomite 3b	72	126	0.38

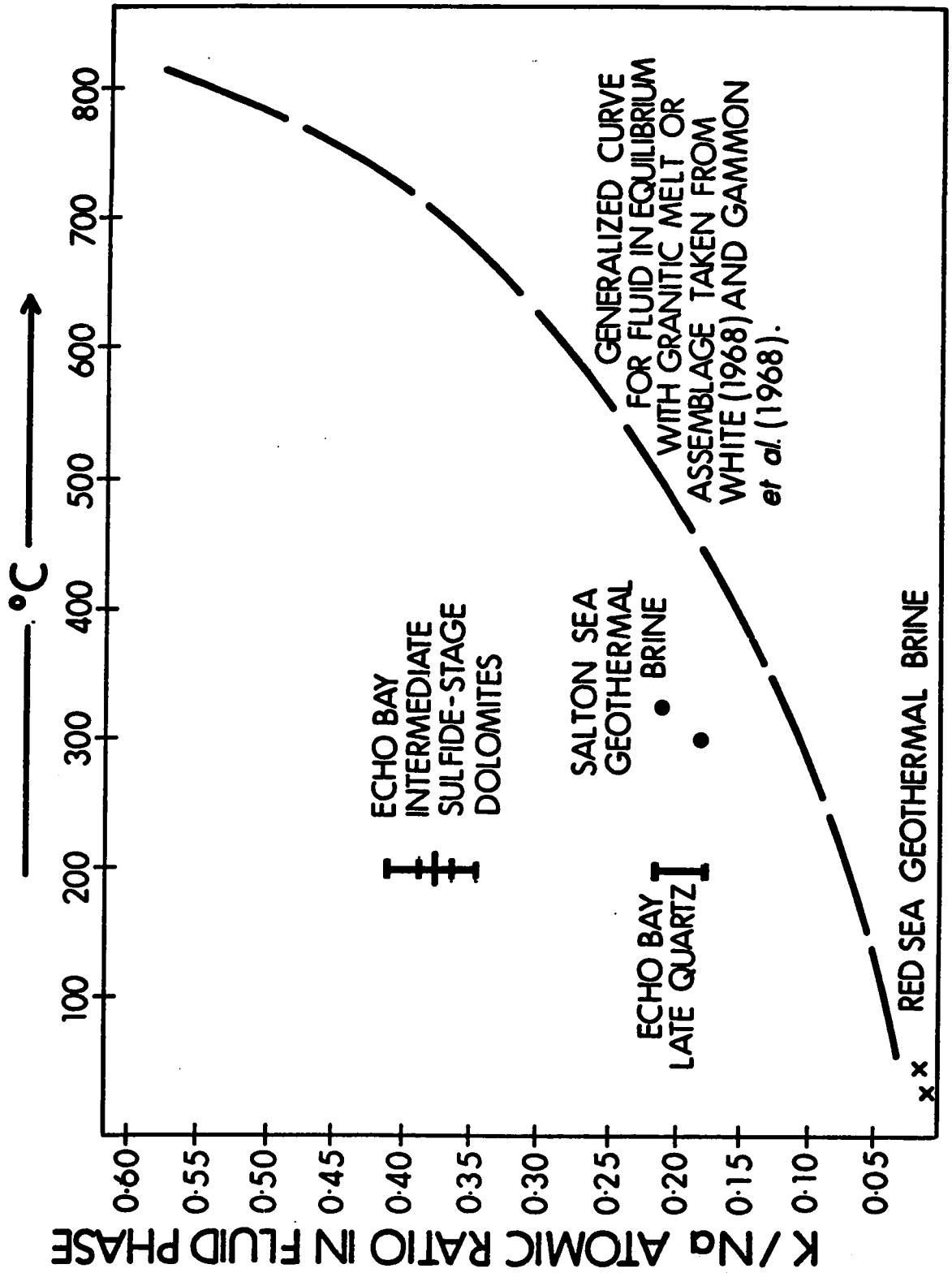


Fig. 17. Temperature vs. K/Na atomic ratio for the Echo Bay fluid inclusions with relation to other data.

to the preferential solubility of potassium salts and would thus exhibit a much higher K/Na atomic ratio (SAWKINS, 1968). The differences in K/Na ratios between the quartz and dolomite is difficult to explain especially when the salinity of the fluid inclusion in these two minerals is similar. Often the K/Na atomic ratios of an ore fluid vary with the salinity (RYE and HAFFTY, loc. cit.) and sometimes these values vary erratically (SAWKINS and RYE, 1970). It thus appears that the K/Na ratios themselves could not be used to postulate such phenomena as the mixing of two fluids at Echo Bay, but they may be used in a negative sense to suggest that the fluid was not in equilibrium with a granitic assemblage. No evaporites are known from the sequence of rocks at Echo Bay and therefore the relatively high K/Na ratios may be explained if the ore fluid is considered to have been circulating within the host rocks at an elevated temperature and losing sodium due to the albitisation of feldspars in certain areas. JORY (1969) recorded that the rocks of the Mine Series and other formations are much richer in sodium than the average andesites and dacites. Also if the fluids were derived from sea water then it should be remembered that the K/Na ratio of Precambrian sea water was probably about 1 (K/Na atomic of about 0.7) (MACINTYRE, 1970).

With the K/Na atomic ratios found at Echo Bay it may have been expected to find two salt crystals in the fluid inclusions: one NaCl and the other KCl. Such a phenomenon is thought to occur in the fluid inclusions of the Casapalca silver-lead-zinc-copper deposit, Peru (SAWKINS and RYE, 1970). On the other hand, at Echo Bay the salt crystal observed is either a mixed crystal or most of the KCl is in the solution.

Summary

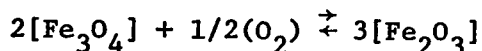
The fluid inclusion data demonstrates that the ore fluid at Echo Bay was a highly saline brine (equivalent to a 5 m NaCl solution) at least during the latter half of ore deposition and the salinity remained constant with time, whilst the K/Na atomic ratio decreased.

If all the temperature determinations are taken as absolute, then the thermal regime of the ore deposition is as follows: early quartz and hematite stage, 150° C; early sulphide stage, 230° C; deposition of late native silver at 180° C. (assuming the same pressure as in the intermediate sulphide stage) and the deposition of mckinstryite was at a temperature of less than 94.4° C. Using this data it appears that the ore deposition started around 150° C., a thermal maximum of 230° C. was reached and then the solution cooled to less than 94.4° C. Due to the uncertainties in all these estimations, a temperature of 200° C. and a pressure of 500 bars has been assumed for the main sulphide stage of mineralisation in some of the calculations found described in the next chapter.

CHAPTER 9 - MINERAL ASSEMBLAGES AND SOLUTION GEOCHEMISTRY

The application of thermodynamic concepts to problems in ore deposits has been discussed by HOLLAND (1959) and BARNES and KULLERUD (1961). Thermochemical data on oxides, sulphides, sulphates and carbonates can be used to outline the stability fields of the major ore and gangue minerals in ore deposits. It is found that these stability fields vary with temperature and in fact the mineralogy of a deposit is largely controlled by the temperature and the fugacity of oxygen, sulphur and carbon dioxide in the ore forming fluids at the time of deposition (HOLLAND, loc. cit.). Thus, for any given temperature, a plot of  $fS_2$  against  $fO_2$  will show the stability fields of oxides, sulphides and sulphates of any particular metal system.

Considering the iron-oxygen system and in particular the reaction:



it can be shown that:

$$A + BT \log T + CT \approx 2.303 RT \log fO_2^{1/2}$$

where A, B and C are related to standard thermodynamic functions of the substances involved. The free energy change for this reaction can be calculated from the entropy and heat of formation of the substances concerned, i.e.:

$$\Delta G = \Delta H - T\Delta S$$

The equilibrium constant K for the reaction is equal to  $1/fO_2^{1/2}$  and thus the free energy is related to the equilibrium constant by the equation:

$$\Delta G_T = -2.303 RT \log K$$

and also:

$$\Delta G_T = A + BT \log T + CT = -2.303 RT \log K$$

T is the temperature in degrees Kelvin; A, B and C are thermodynamic functions and R (the gas constant) is taken as 1.98726 cal/deg/mole (GARRELS and CHRIST, 1965, p. 402).

For the Echo Bay deposit, the minerals of most general use are found within the iron-sulphur-oxygen system and thus  $fO_2$ - $fS_2$  diagrams were constructed for this system at 150° C. and 200° C. The boundaries for the various mineral species were calculated using the above formula and the thermodynamic constants were obtained from various sources which are given in Table 12. Table 12 in fact gives all the reactions used in the construction of these diagrams and also the relevant thermodynamic data and their associated errors. Error margins for the boundary lines on the diagrams are not given since they would make the diagrams unnecessarily complicated and the diagrams are being used only as models and not necessarily as the basis for further calculations.

Figure 18 shows one such diagram calculated for 150° C. In addition to boundaries in the Fe-S-O system, other boundaries pertinent to the mineral assemblage at Echo Bay are also given. The native silver/acanthite boundary and the native bismuth/bismuthinite boundary are drawn across most of the diagram, as is also the covellite/digenite boundary. Boundaries for metal-O-S systems other than the Fe-S-O system are generally displaced toward higher  $fO_2$  values and thus in general do not enter the relevant part of the diagram as shown in Fig. 18.



TABLE 12

Thermodynamic data used in the construction of  $f_{S_2}$ - $f_{O_2}$  diagrams

Reaction	Free Energy Change	Error (Kcal)	Temperature Range	Source
$S_2$ (vapour) = $2S$ (liquid)	- 26,810 + 30.25 T	+1	200 to 800°C.	BARTON & SKINNER, 1967
$4Ag + S_2 = 2Ag_2S$	- 41,980 + 16.52 T	+1	176 to 804°C.	BARTON & SKINNER, 1967
$4/3Bi + S_2 = 2/3Bi_2S_3$	- 52,121 + 36.23 T	+1.5	25 to 271°C.	BARTON & SKINNER, 1967
$1/2[Cu_9S_5] + S_2 = 9/2CuS$	- 44,800 + 53.40 T	+1.5	103 to 350°C.	HOLLAND, 1959
$2Fe + S_2 = 2FeS$	- 71,820 + 25.12 T	+1	138 to 988°C.	BARTON & SKINNER, 1967
$FeS + 1/2S_2 = FeS_2$	log K = -8.48		200°C.	HELGESON, 1969
$3/2Fe + O_2 = 1/2Fe_3O_4$	-133,900 + 41.1 t	+1	25 to 560°C.	HOLLAND, 1959
$4Fe_3O_4 + O_2 = 6Fe_2O_3$	-114,700 + 67.8 T	+5	27 to 927°C.	HOLLAND, 1965
$Fe_2O_3 + S_2 + 5/2O_2 = 2FeSO_4$	-275,000 + 147.1 T	+14	27 to 927°C.	HOLLAND, 1959
$U + O_2 = UO_2$	-258,000 + 40.0 T		25 to 1232°C.	HOLLAND, 1965
$C + O_2 = CO_2$	- 94,200 - 0.2 T	+1	25 to 1727°C.	HOLLAND, 1965
$CaSO_4 + CO_2 = CaCO_3 + 1/2S_2 + 3/2O_2$	+163,500 - 46.3 T	+5	27 to 927°C.	HOLLAND, 1959

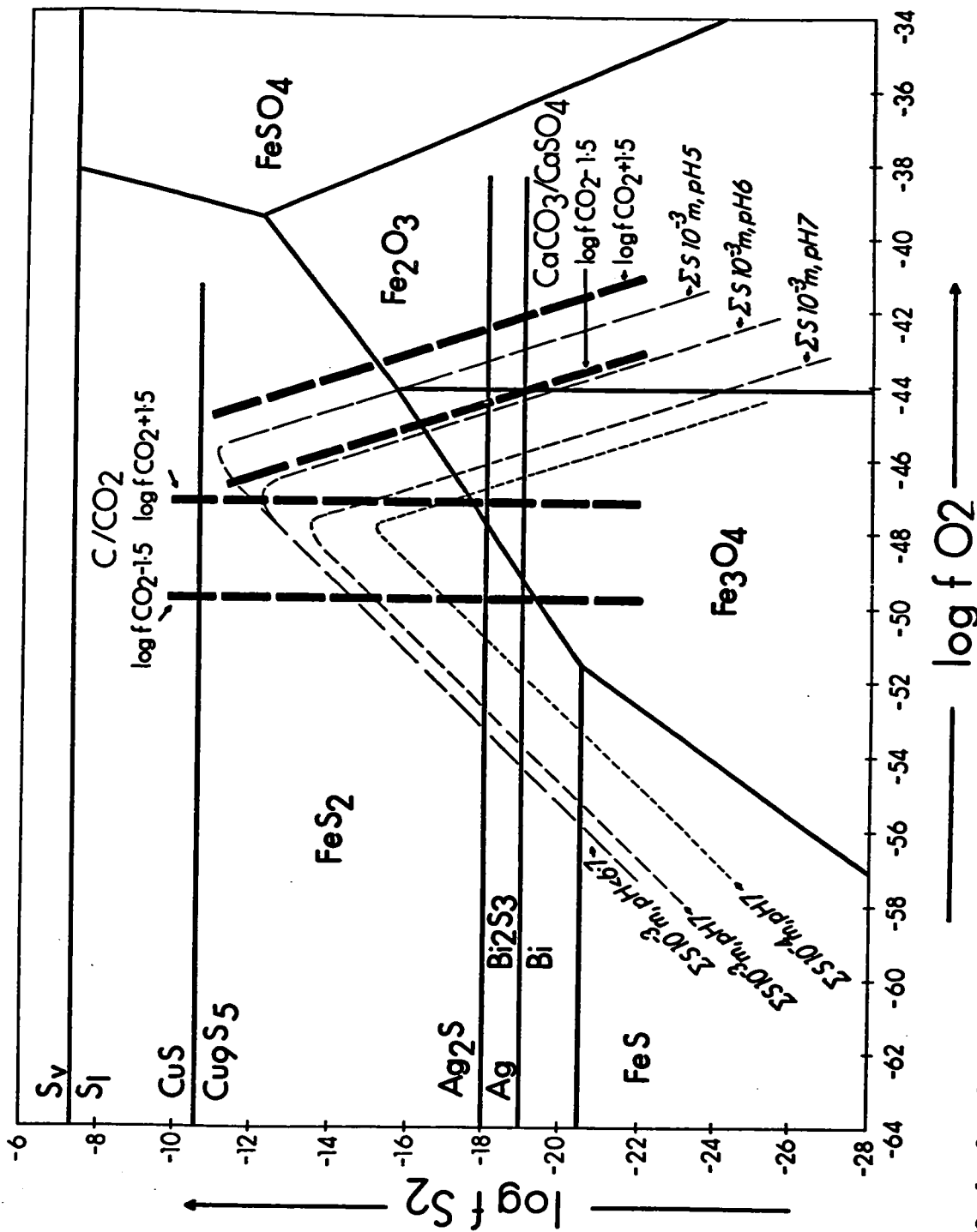


Fig. 18. Log fO<sub>2</sub>-log fS<sub>2</sub> diagram for the Fe-O-S and other systems at 150°C. The solid lines represent boundaries between the mineral stability fields, the heavy dashed lines represent the boundaries between carbon-bearing phases at given values of fCO<sub>2</sub> and the light dashed lines represent total dissolved sulphur at given values of the molality and pH.

The boundaries for calcite/gypsum and carbon/carbon dioxide are given for the limiting values of  $\log f\text{CO}_2$ , +1.5 and -1.5, as determined in the previous chapter. Since 150° C. has been taken as the approximate temperature for the initial stages of mineralisation, Fig. 18 is taken to represent this period.

Because the fractures through and around which the ore forming fluids were moving at this time were relatively tight and little or no carbonate had been deposited, then the chemistry of this solution would be controlled by the host rock chemistry and mineralogy. Since the exact mineralogy of all the rocks with which the fluids had been in contact is not known, then a silicate buffer system as given by HEMLEY and JONES (1964) is not possible to compute exactly. Also, the potassium and sodium contents of the fluid are not known; these control the pH in potassium silicate and sodium silicate buffered systems respectively. Most of the rock types traversed do not contain micas or clay minerals and the fluid would be in equilibrium with K feldspar and albite and would have a relatively high KCl/NaCl content or a relatively high pH. Using rough calculations and assuming a total potassium of 1 m, a total sodium of 2 m and a temperature of 150° C., then a pH in the range of 5 was determined. However, more weight was placed upon other estimates obtained for similar geological conditions. These in fact are in good agreement as values of pH from 2 to 5 have been obtained for fluids in equilibrium with silicate assemblages (HEMLEY and JONES, loc. cit.; HELGESON, 1970). The initial value of 5 is a reasonable one to assume for the system in question (H. Ohmoto and H.D. Holland, pers. comm.).

Now that a pH estimate has been obtained, then feasible estimations, or in fact precise calculations, can be effected to determine the total sulphur in solution. Following the method of RAYMAHASHAY and HOLLAND (1969) and OHMOTO (1970) lines of total sulphur of  $10^{-3}$  m for pH values of 5, 6 and 7 and total sulphur of  $10^{-4}$  for pH of 7 were calculated for  $150^{\circ}$  C. These are plotted on Fig. 18. A sample calculation for the molality of sulphur species in the fluid is given in Appendix E. Here, the sulphur species in the fluid are taken to be  $H_2S$ ,  $HS^-$ ,  $S^{=}$ ,  $HSO_4^-$  and  $SO_4^{=}$ . The molality of each of these species is calculated and the total of all of them gives the molality of the total sulphur in solution. As a simplification the  $KSO_4^-$ ,  $NaSO_4^-$  contents of the fluid calculated by OHMOTO (loc. cit.) were omitted and also the possible  $H_2SO_4$  content as shown by RAFAL'SKIY and ZARUBIN (1969). In each case, these species are formed from the species calculated and thus do not affect the total sulphur calculation. In Appendix E, it is also shown that the species  $SO_2$  and  $SO_3$  can be ignored at the temperatures considered.

In the  $fS_2$ - $fO_2$  diagram, it can be seen that at the lower  $fO_2$  values, essentially all the sulphur is in a reduced form and lines of constant total dissolved sulphur are parallel to lines of constant  $a_{H_2S}$  (or  $a_{HS^-}$ ) at constant pH. At higher values of  $fO_2$ , the most important sulphur species in the hydrothermal solution is  $SO_4^{=}$  for a constant pH. Also at low values of  $fO_2$ , the total sulphur contours are relatively insensitive to the pH of the solution, but at higher values of  $fO_2$ , the total dissolved sulphur is pH dependent and will shift towards lower values of  $fS_2$  and  $fO_2$  with increasing pH of the solution. Various values of the pH for  $\Sigma S = 10^{-3}$  m are shown in Fig. 18 to

demonstrate this point. Also for a pH of 7, lines of constant total sulphur at  $10^{-3}$  m and  $10^{-4}$  m are drawn to demonstrate the shift with changing total sulphur. An imaginary line dissecting the apices of similar total dissolved sulphur contours drawn for different pH values separates areas of dominantly reduced sulphur species on the low  $fO_2$  side from areas of dominantly oxidised sulphur species on the high  $fO_2$  side.

The fluids of the type which deposited the minerals at Echo Bay could be considered to be sulphur-deficient due to the presence of a sulphur-deficient mineralogical association (MEYER and HEMLEY, 1967). The sulphur-poor ore forming fluids of the 'Kuroko'-type mineralisation at Uchinotai, Japan are concluded to contain total sulphur contents of  $10^{-3}$  m and  $10^{-5}$  m at 250° C. (SATO, 1970). Where a more sulphide-rich assemblage is present, such as at the Bluebell Mine, B.C., Canada, the fluids probably had total sulphur of about  $10^{-2}$  m (H. Ohmoto, pers. comm.). If the total dissolved sulphur in the hydrothermal fluids at Echo Bay was  $10^{-3}$  m, then, as will be demonstrated later in this chapter, a geochemical model consistent with other data may be developed. Thus a total dissolved sulphur of  $10^{-3}$  m is assumed for the fluids and this is in good agreement with other estimates made for other deposits.

Although the host-rocks at Echo Bay contain abundant magnetite and pyrite, they also contain hematite and some of this, particularly near to and in the veins was formed in the early stage of ore deposition. The only other metallic mineral to be deposited at this early stage was pitchblende. This mineral would be deposited as  $UO_2$  which is a stable

phase over all of the  $fS_2$ - $fO_2$  diagram, Fig. 18. Thus it is not useful in fixing the  $fO_2$ . However, we now know that the initial fluid after possibly being in equilibrium with pyrite, hematite and magnetite at temperatures probably below 150° C. was probably in equilibrium with hematite in the veins. Its temperature at this point was probably around 150° C. with a total dissolved sulphur of  $10^{-3}$  m and a pH of 5. No estimate of the  $fO_2$  is possible at this stage but the log  $fO_2$  was probably around -40 to -42. After the hematite and pitchblende deposition in the area, the fractures became more open and a period of nickel-cobalt arsenide deposition with native silver, native bismuth and minor carbonate occurred. In the model so far envisaged, the fluid was still within the stability fields of native silver and native bismuth. However, due to the cessation of deposition of hematite and the possible removal of the fluid from hematite bearing areas, then the  $fO_2$  would probably decrease and the fluid would move up the  $\Sigma S 10^{-3}$  m, pH = 5 line to higher values of  $fS_2$ . When the  $Ag_2S$ -native silver boundary was crossed then acanthite was deposited, as witnessed by the early acanthite found in the paragenetic sequence. At this stage the temperature of the fluid may have increased and a critical part of the model is reached. The fluid had to move more or less along the  $\Sigma S 10^{-3}$  m, pH 5 line from the  $Fe_2O_3$  field to the  $FeS_2$  field where marcasite may be precipitated without passing through the magnetite field. Magnetite is not found to be present in the veins at Echo Bay. From Fig. 18, this can be seen to be possible if the temperature did not increase to much above 150° C. and also if the log  $fCO_2$  was greater than about +1, whereby ensuring that carbonate and not gypsum was the stable phase precipitated.

From Fig. 19, which is a similar  $fS_2$ - $fO_2$  diagram constructed for 200° C., it can be seen that this movement could only take place if the  $\log fCO_2$  was greater than +1.5, a figure which is becoming geologically unreasonable. It appears most feasible, then, that the fluid passed into the  $FeS_2$  field at a temperature less than 200° C. and marcasite was precipitated. It is at about this stage that carbonates began to precipitate within the veins in quite large amounts and the veins became much more open. The presence then of  $CO_2$  in the fluid and carbonate in the veins would probably act as a buffer system for the pH. In actual fact, using carbonate equilibria calculations as given in Appendix E, an interrelationship between pH and  $fCO_2$  may be obtained. This relationship is shown in Fig. 20 where pH is plotted against temperature and equilibrium lines are drawn for constant  $\log fCO_2$  values of +1.5, 0 and -1.5. For comparative purposes, the pH neutral line is also drawn. It can be seen that for a system at constant pressure and in equilibrium with carbonate and  $CO_2$ , the  $fCO_2$  is a function of the pH and as the  $fCO_2$  decreases then the pH increases concomitantly. Thus at Echo Bay when the solution was first in contact with carbonate, the  $fCO_2$  was still probably relatively high and the pH would be between 5 and 6. Assuming now a temperature of 200° C., then the position of the fluid can be represented in Fig. 19 on a  $\Sigma S 10^{-3}$  m, pH 6 line in the  $FeS_2$  field. Discussions in the next chapter will show that, although sulphides were then deposited in the sequence, the total sulphur value did not drop appreciably and could still probably be represented as  $10^{-3}$  m.

On the other hand, the deposition of carbonates through the early and intermediate sulphide stages probably resulted in the lowering

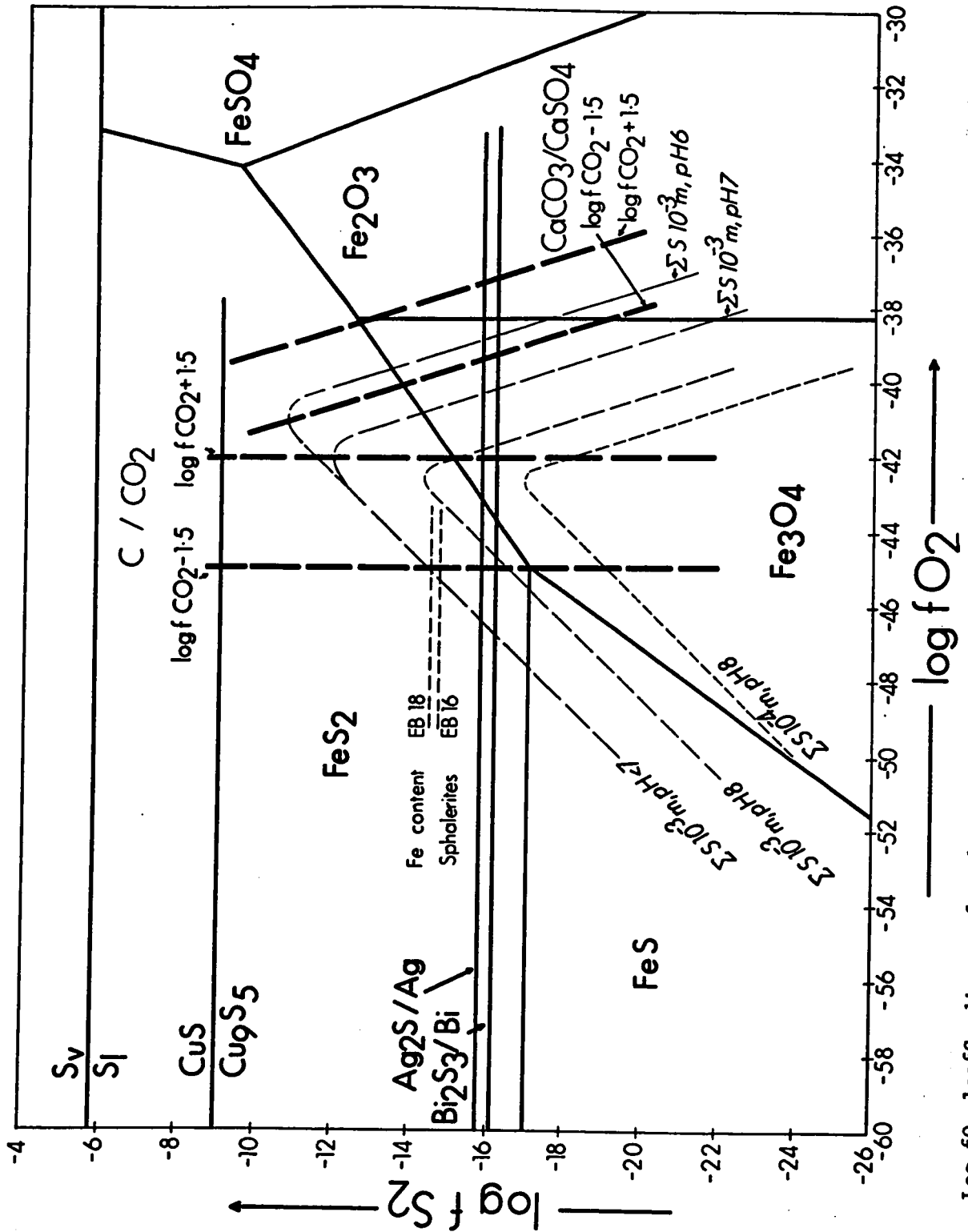


Fig. 19. Log  $f_{O_2}$ -log $f_{S_2}$  diagram for the Fe-O-S and other systems at 200°C. The lines are used with the same meaning as in Fig. 18, except for the horizontal dashed lines which refer to the sulphur fugacities obtained from the Fe contents of sphalerites in samples EB 18 and EB 16, assuming a temperature of 200°C.



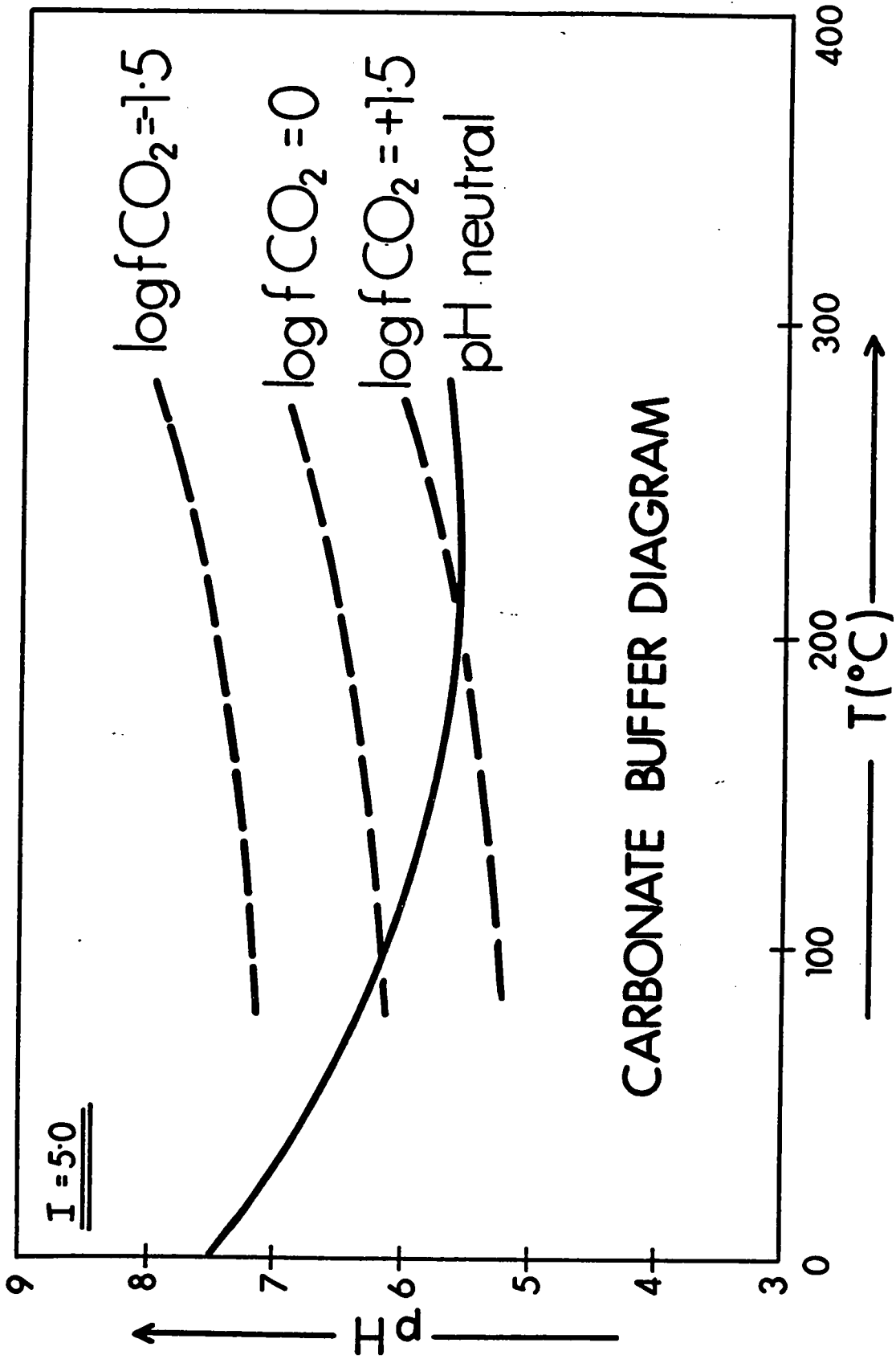


Fig. 20. Graph of temperature vs. pH showing iso-fCO<sub>2</sub> lines in equilibrium with a carbonate buffer system.

of the  $f\text{CO}_2$ . This in turn would cause an increase in pH. A hypothetical representation of the fluid path would move at an oblique angle to the total dissolved sulphur lines in this field due to the increase in pH. This movement would show a decrease in  $f\text{S}_2$  values, as demonstrated by the contents of the analysed sphalerites which are depicted in Fig. 19. If the pH increased to a value of 8, then a fluid with total dissolved sulphur of  $10^{-3}$  m could cross the argentite/native silver boundary. To explain the late native silver in the Echo Bay deposit, this interpretation would be required. It would also be necessary for the  $\log f\text{CO}_2$  to have a value of -1.5 or less in order that  $\text{CO}_2$  and not carbon was stable in the native silver field. No graphite was detected at Echo Bay.

The effect of total pressure on the equilibria discussed in the Fe-S-O system, discussed previously, is of minor importance and thus, as we have seen, the independent variables, temperature, total sulphur as dissolved species, the fugacity of oxygen and the pH are the most important parameters. Temperature and the total sulphur as dissolved species affect the aqueous equilibria in a relatively simple way compared to fugacity of oxygen and the pH. Thus the distribution of species can be delineated on a plot of  $f\text{O}_2$  against pH for given fixed values of total dissolved sulphur and temperature. Four diagrams were constructed: 150° C. for  $\Sigma\text{S} = 10^{-3}$  m and  $10^{-4}$  m; 200° C. for  $\Sigma\text{S} = 10^{-3}$  m and  $10^{-4}$  m using the method of BARNES and KULLERUD (op. cit.) from whence also came the equilibrium constants for the sulphur species reactions shown in Table 13. The boundaries between areas of predominance occur where the activity of one of the predominant species

TABLE 13

Equilibrium constants used for the construction of  $f_{O_2}$ -pH diagrams

Reaction	Log of Equilibrium Constant		
	200°C.	150°C.	
$H_2S = HS^- + H^+$	-6.96	- 6.72	*
$HS^- = S^{2-} + H^+$	-9.57	-10.62	*
$HSO_4^- = SO_4^{2-} + H^+$	-4.49	- 3.74	*
$2H_2S + O_2(g) = S_2(g) + 2H_2O$	36.4	41.2	*
$H_2S + 2O_2(g) = HSO_4^- + H^+$	72.8	84.6	*
$H_2S + 2O_2(g) = SO_4^{2-} + 2H^+$	70.5	81.5	*
$2HS^- + O_2(g) + 2H^+ = S_2(g) + 2H_2O$	44.9	51.7	*
$HS^- + 2O_2(g) = SO_4^{2-} + H^+$	77.0	89.5	*
$S^{2-} + \frac{1}{2}O_2(g) + 2H^+ = \frac{1}{2}S_2(g) + H_2O$	33.2	36.6	*
$S^{2-} + 2O_2(g) = SO_4^{2-}$	83.74	99.0	*
$\frac{1}{2}S_2(g) + \frac{3}{2}O_2(g) + H_2O = HSO_4^- + H^+$	54.2	63.0	*
$\frac{1}{2}S_2(g) + \frac{3}{2}O_2(g) + H_2O = SO_4^{2-} + 2H^+$	54.6	59.8	*
$3Fe + 2O_2(g) = Fe_3O_4$	105.7	120.4	§
$4Fe_3O_4 + O_2(g) = 6Fe_2O_3$	38.2	44.1	§
$Fe + \frac{1}{2}S_2(g) = FeS$	13.9	15.8	§
$FeS + \frac{1}{2}S_2(g) = FeS_2$	8.5	10.2	§
$3FeS_2 + 2O_2(g) = Fe_3O_4 + 3S_2(g)$	38.1	41.0	§
$2FeS_2 + \frac{3}{2}O_2(g) = Fe_2O_3 + 2S_2(g)$	31.7	34.7	§
$3FeS + 2O_2(g) = Fe_3O_4 + \frac{3}{2}S_2(g)$	63.0	71.5	§
$2Ag + \frac{1}{2}S_2(g) = Ag_2S$	7.8	9.0	§

\* Values obtained by extrapolation from BARNES and KULLERUD (1961)

§ Values obtained from HELGESON (1969)

is one half of the total dissolved sulphur. All the reactions are written in terms of  $O_2$ ,  $H^+$  and  $H_2O$ . Thus those reactions only involving a change in oxidation are a function of the  $fO_2$  and the boundaries are horizontal lines on the diagrams. Similarly, reactions involving  $H^+$  have vertical lines on the diagrams and reactions including both oxidation and ionisation have oblique lines. These lines between various sulphur species are shown as broken lines in Figs. 21 to 24 inclusive. The fugacities of the gases coexisting in equilibrium with these solutions can be fixed by the same variables as used for the aqueous phase. From the equilibrium constants given in Table 13, it is thus possible to calculate the fugacity of sulphur and various iso- $fS_2$  lines are plotted on the diagrams in light lines labelled with values of  $\log fS_2$ .

Equilibrium constants available for the Fe-S-O system and the Ag-S system are given in Table 13 as obtained from Helgeson (1969). These equilibrium constants give either  $fO_2$ ,  $fS_2$  or the ratio of these fugacities for the coexistence of each pair of minerals at equilibrium at each temperature. The mineral data is plotted directly on the aqueous diagrams as heavy lines outlining the fields of mineral stabilities as shown in Figs. 21 to 24 inclusive. Again in these diagrams, zones of uncertainty can be placed on all the boundary lines. For the purposes here, these are not desperately important and an estimation of the errors is given in BARNES and KULLERUD (op. cit.).

Two pH- $fO_2$  diagrams are plotted for 150° C; one for total dissolved sulphur  $10^{-4}$  m and the other total dissolved sulphur  $10^{-3}$  m. These correspond to Figs. 21 and 22. It can be seen from these diagrams that a fluid starting at a point with pH 5 and  $\log fO_2 = -4.0$ , could pro-

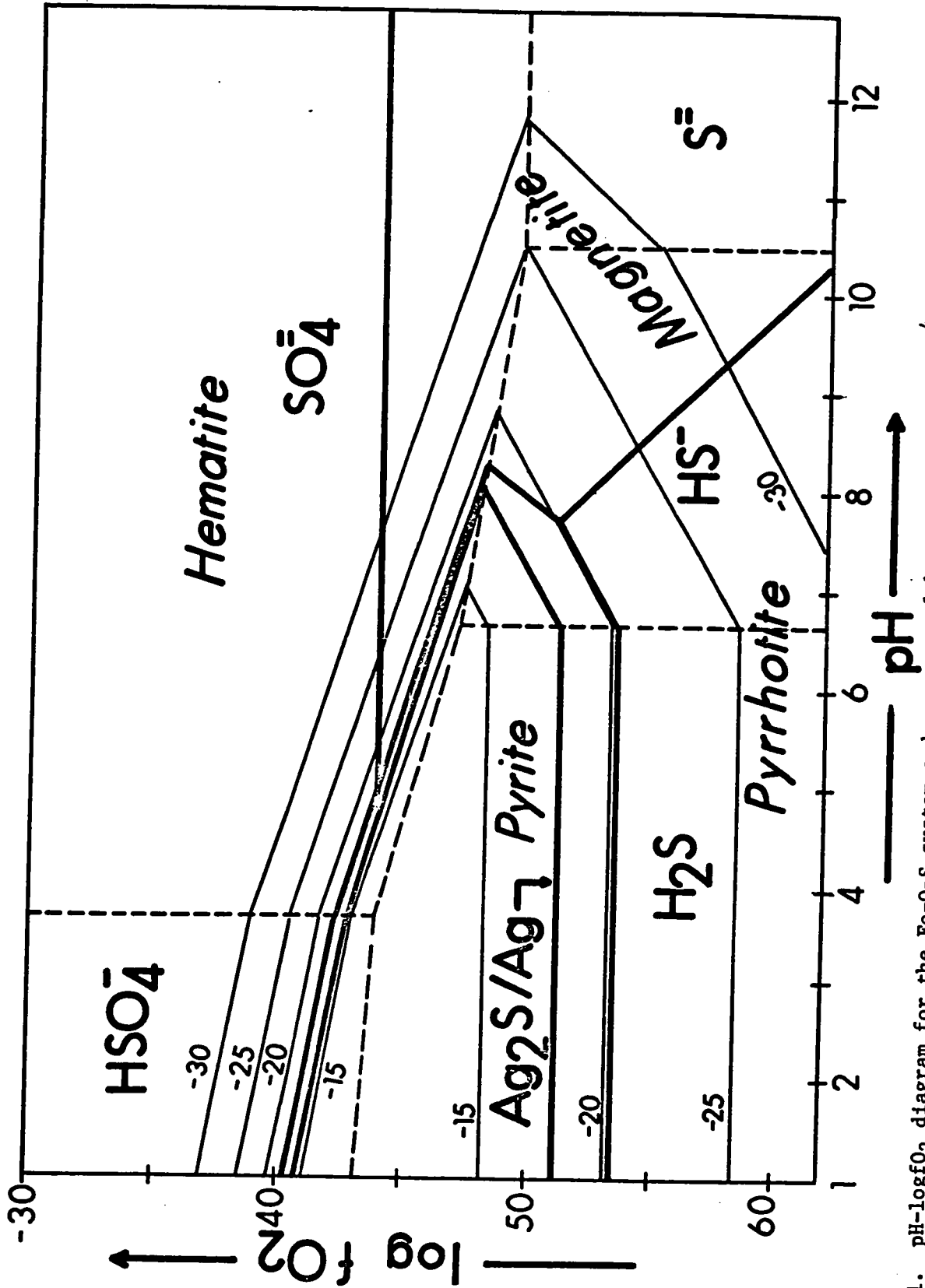


Fig. 21. pH-logfO<sub>2</sub> diagram for the Fe-O-S system and aqueous sulphur species at  $\Sigma S=10^{-4}m$  and 150°C. The heavy solid lines represent the boundaries between the Fe-O-S and Ag<sub>2</sub>S-Ag mineral phases and the dashed lines represent the boundaries between the dominant sulphur species in solution. The light solid lines are iso-logfS<sub>2</sub> lines.

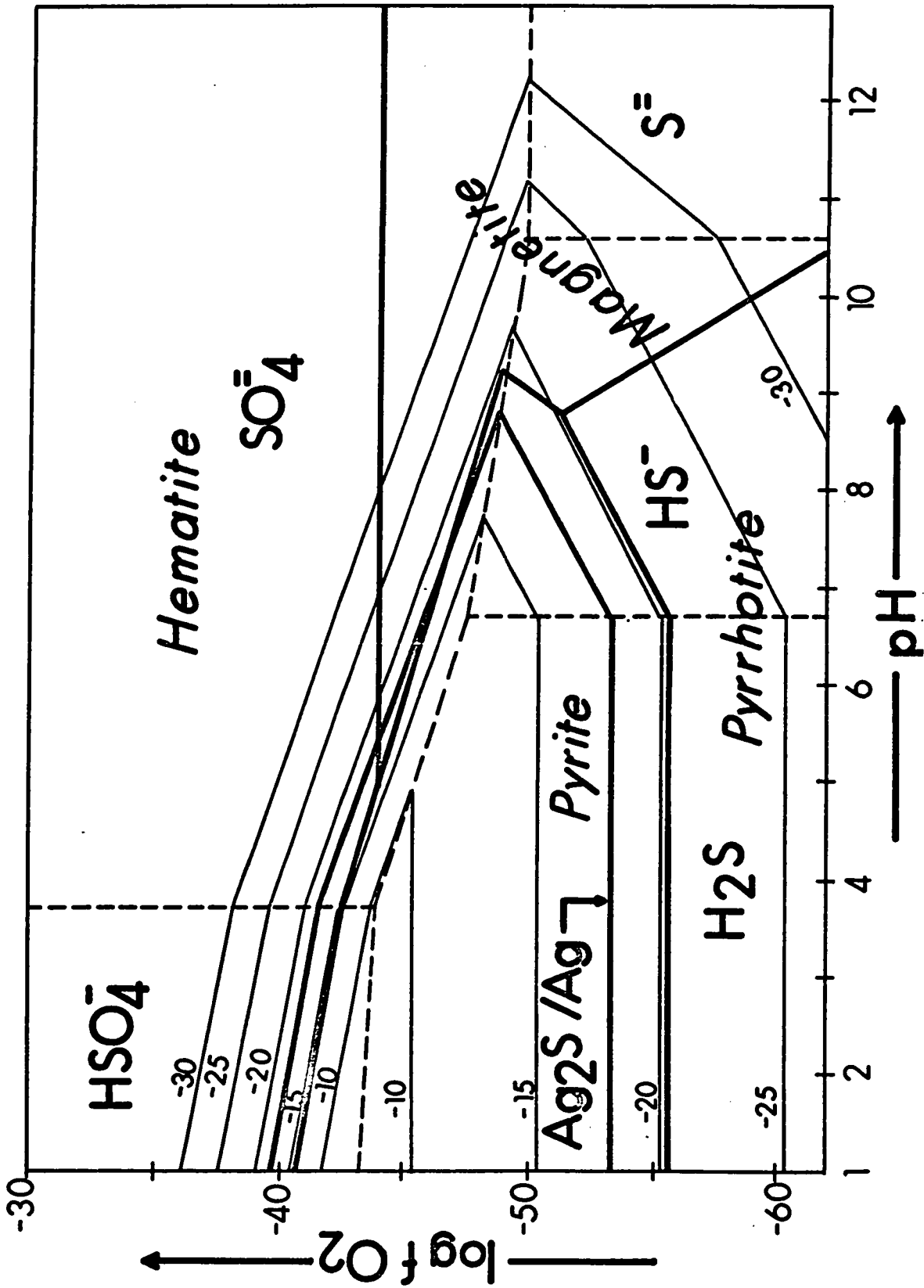


Fig. 22. pH-log $f_{O_2}$  diagram for the Fe-O-S system and aqueous sulphur species at  $\Sigma S=10^{-3}m$  and  $150^\circ C$ . The lines have the same meaning as in Fig. 21.

ceed with increasing pH and decreasing  $fO_2$  into the pyrite field. At this point the  $fS_2$  contours would be crossed as the  $fS_2$  increased. Since the mineral assemblage at Echo Bay suggests that the maximum  $\log fS_2$  was about  $10^{-12}$  atmospheres, then the diagram for  $\Sigma S 10^{-3}$  is quite realistic since in the movement of the fluid mentioned, the  $fS_2$  need not exceed  $10^{-10}$  atmospheres. On the other hand, for the situation with  $\Sigma S 10^{-4}$  m (see Fig. 21) then for a similar movement of the fluid, the  $fS_2$  values would be lower than those expected. It is not impossible to allow the fluid to start with  $10^{-4}$  m total dissolved sulphur and increase to  $10^{-3}$  m but, as discussed previously, a figure kept fairly constant at  $10^{-3}$  m is most compatible with other data. Figs. 21 and 22 show that the fluid starting off with pH 5 is in the hematite and native silver fields, where  $SO_4^{=}$  is the dominant sulphur species in solution. The movement of the fluid proceeds into the  $Ag_2S$  and thence into the pyrite field.  $SO_4^{=}$  is still the dominant sulphur species, but movement in this direction increases the  $a_{H_2S}$  and  $a_{HS^-}$ .

When the fluid was in the pyrite field, the temperature was thought to be around  $200^\circ$  C. and similar pH- $fO_2$  diagrams are plotted for this temperature with  $\Sigma S 10^{-4}$  m: Fig. 23 and  $\Sigma S 10^{-3}$  m: Fig. 24. Again the diagram for  $\Sigma S 10^{-3}$  m is more applicable and the  $\Sigma S 10^{-4}$  m diagram is added for comparative purposes. The fluid now in the pyrite field would continue in the same direction of increasing pH and decreasing  $fO_2$ . The  $fS_2$  values with this direction of movement over the  $fS_2$  contour lines would reach a maximum in the pyrite field and then being to drop again. Ultimately, the fluid would cross the  $Ag_2S$ /native silver boundary and native silver would again be stable. In the latter stages of ore deposition, it should be noted that the dominant aqueous sulphur species would be  $HS^-$ .

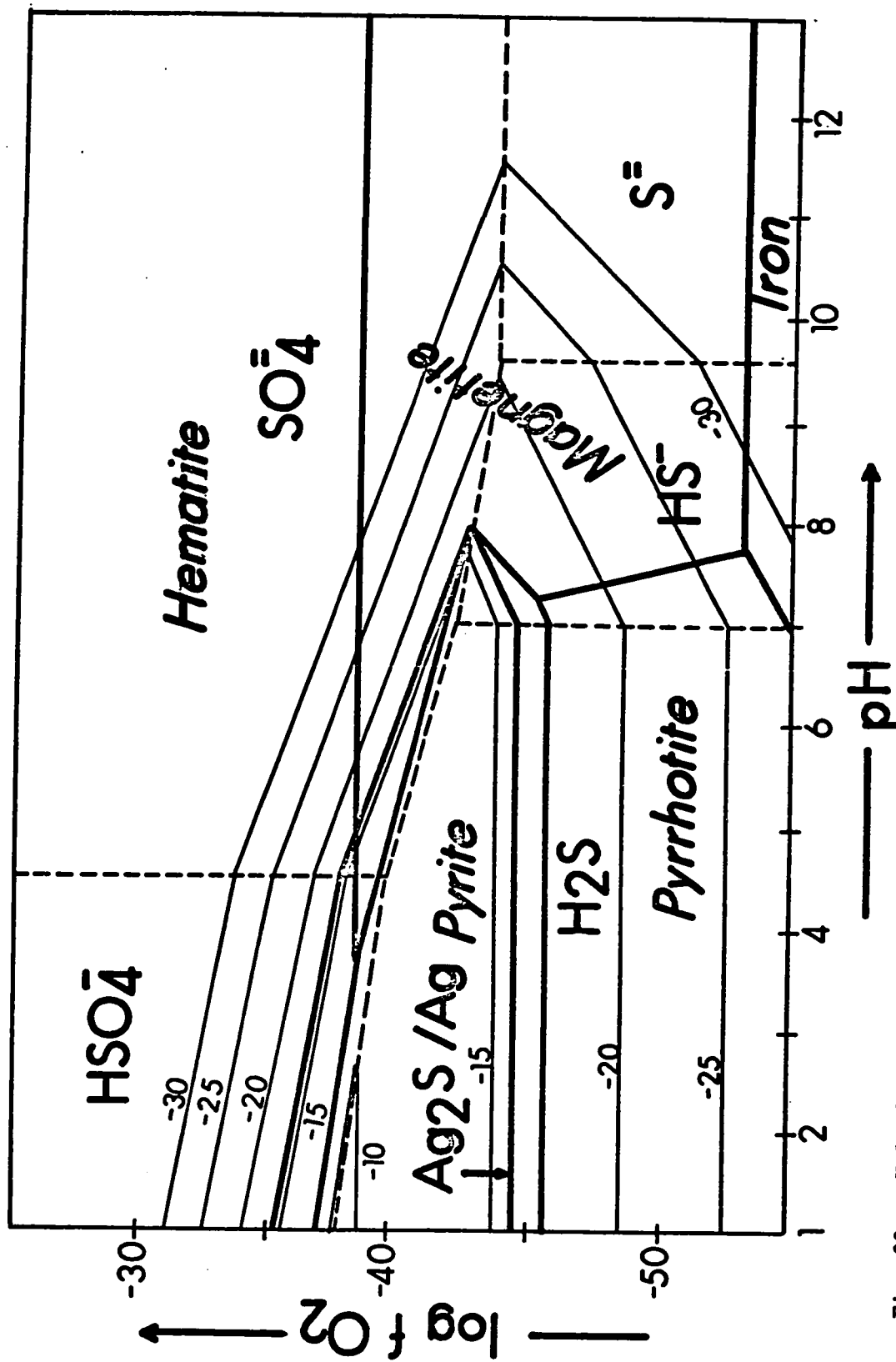


Fig. 23. pH-logfO<sub>2</sub> diagram for the Fe-O-S system and aqueous sulphur species at  $\Sigma S=10^{-4}m$  and 200°C. The lines have the same meaning as in Fig. 21.



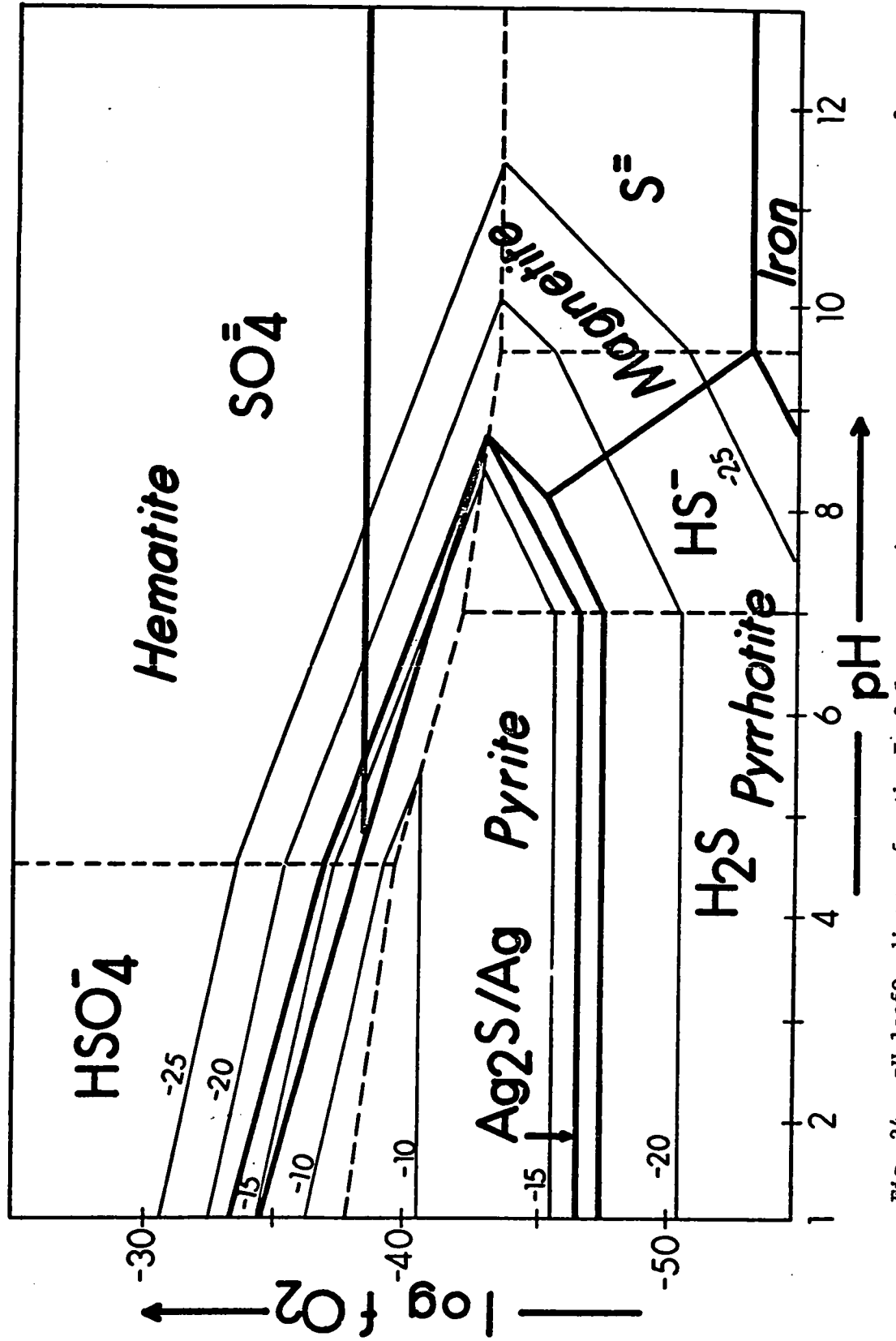


Fig. 24. pH-log $f_{O_2}$  diagram for the Fe-O-S system and aqueous sulphur species at  $\Sigma S$   $10^{-3}m$  and  $200^\circ C$ . The lines have the same meaning as in Fig. 21.

Since at Echo Bay the fluid movement can be followed by studying four variables ( $fO_2$ ,  $fS_2$ , pH and temperature), then the best way of representing this is by the construction of two three-dimensional diagrams: one temperature- $fO_2$ - $fS_2$  and the other temperature- $fO_2$ -pH. Fig. 25 shows the three-dimensional temperature- $fO_2$ - $fS_2$  diagram with temperatures from 150° C. to 200° C. The mineral stability boundaries are now represented as shaded planes. Because the temperature regime at Echo Bay is rather complicated and not completely certain, it was decided to simplify this for ease of representation on the diagram. The tube in the diagram represents the movement of an ore bearing fluid which could produce a similar mineralogy to that of the Echo Bay deposit. The temperature varied gradually from 150°C. to 200°C. The fluid, as represented by the tube, is seen to start in the hematite and native silver field and, after it cuts through the native silver- $Ag_2S$  plane, the decrease in  $fO_2$  takes it around the magnetite field and it is then seen to cut into the pyrite field. After coming into the pyrite field, the  $fS_2$  drops sufficiently to allow the fluid to again cut the  $Ag_2S$ -native silver field where it is seen to end in the diagram.

The second three-dimensional diagram is shown in Fig. 26 where temperature is plotted against pH and  $\log fO_2$ . Mineral stability planes are shaded and a plane for  $\log fS_2 = -10$  is added as a limit for the Echo Bay fluid. The sulphur species boundaries are given at 150° C. and 200° C., but they are not connected as planes as this would unnecessarily complicate the diagram. Again a relatively simple temperature regime of a steady increase from 150° C. to 200° C. is adopted and the hypothetical fluid movement is represented as a tube. The fluid is shown as commencing in the hematite, native silver, sulphate species

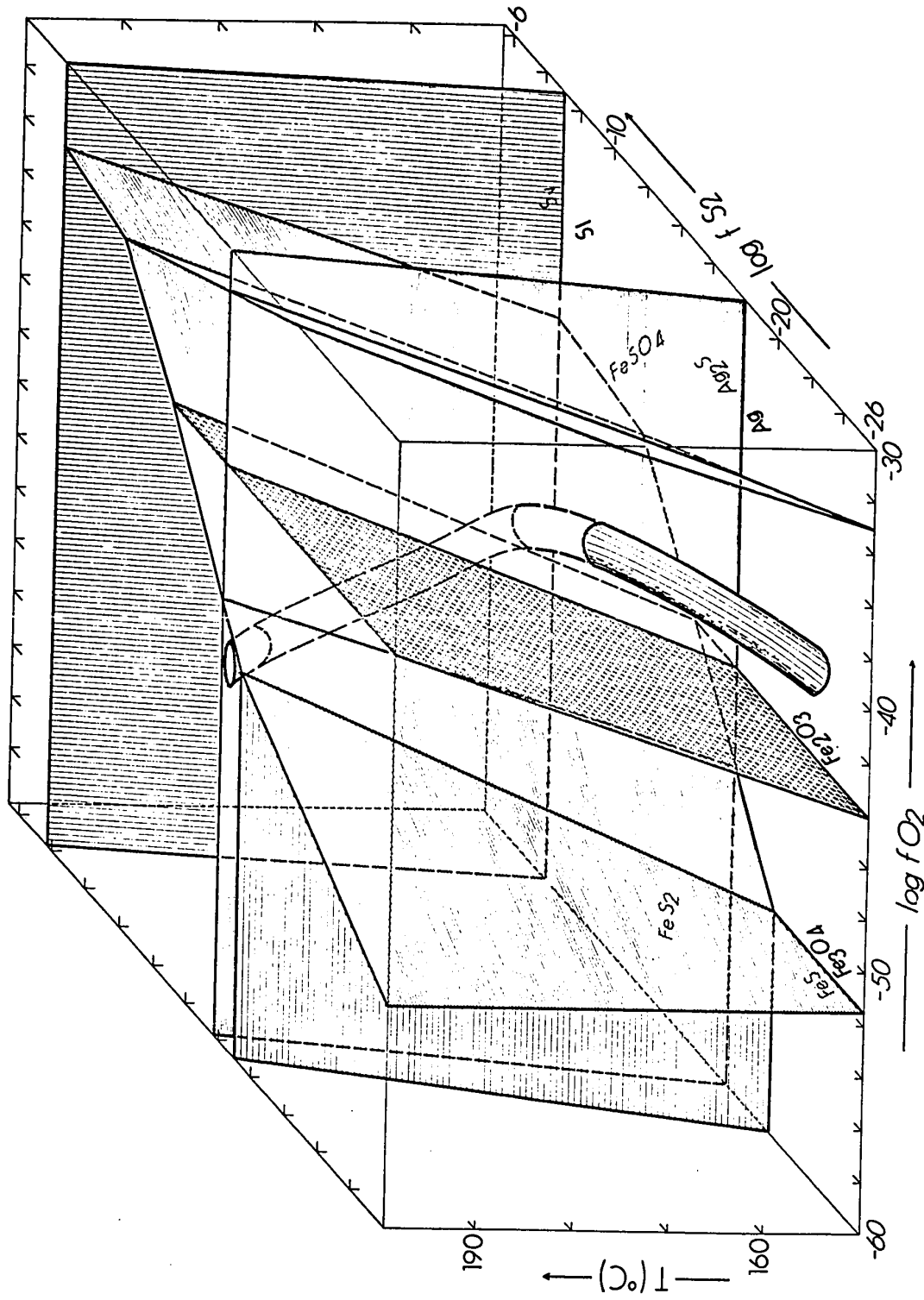


Fig. 25. Three dimensional  $f_{O_2}$ - $f_{S_2}$ -temperature diagram for the Fe-O-S and other systems between 150° and 200°C. The tube represents the hypothetical movement of an ore fluid producing a similar mineralogy to the Echo Bay deposit.

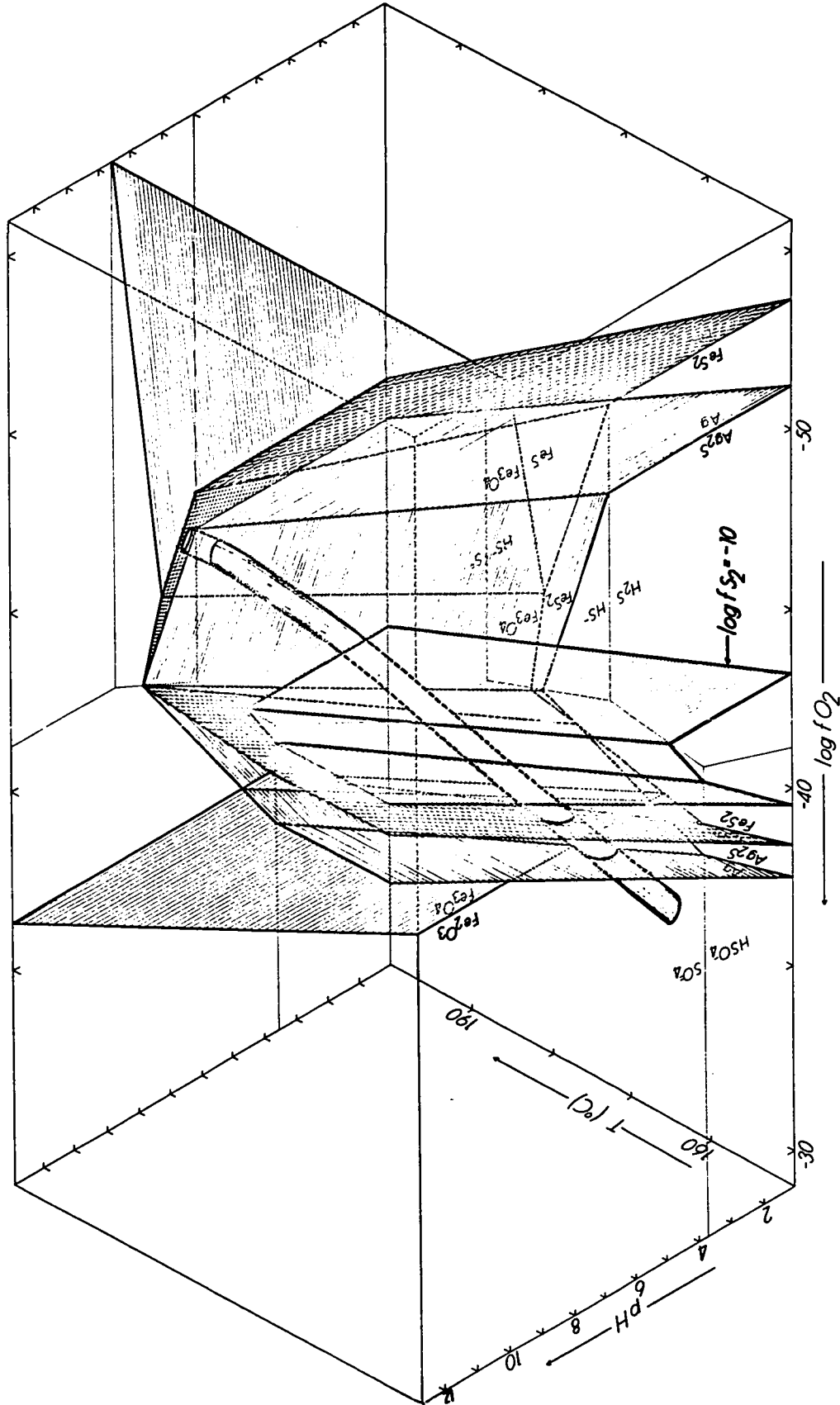


Fig. 26. Three dimensional pH-log $f_{O_2}$ -temperature diagram for the Fe-O-S and Ag<sub>2</sub>S/Ag system and aqueous sulphur species at  $\Sigma S = 10^{-3}m$  from 150° to 200°C. The tube represents the hypothetical movement of an ore fluid producing a similar mineralogy to the Echo Bay deposit. The foremost plane in the diagram represents  $\log f_{S_2} = -10$ .

field; it can be seen cutting the native silver- $\text{Ag}_2\text{S}$  plane and the hematite-pyrite plane but stays behind the  $\log f\text{S}_2 = -10$  plane. It recuts the  $\text{Ag}_2\text{S}$ -native silver plane and can be last seen in the diagram in the native silver and  $\text{HS}^-$  species field.

Although the temperature is generalised for the model, the mineral sequence is as found at Echo Bay. This type of diagram could probably be used for many of the silver deposits in the Great Bear Province. For instance, to more exactly fit the data from Echo Bay, the fluid path would move up a much steeper temperature gradient path from  $150^\circ\text{C}$ . to  $230^\circ\text{C}$ . where the temperature then decreases to about  $180^\circ\text{C}$ . in the late native silver field. After this, the solution cools to less than  $95^\circ\text{C}$ . but the parameters pH,  $f\text{O}_2$  and  $f\text{S}_2$  are not known at this stage.

Activity diagrams are very useful for the representation of various systems in ore deposits. HELGESON (1970) has shown that all equilibria in hydrothermal systems can be represented in terms of the ratios of cations in the aqueous phase to that of the hydrogen ion. The advantages of these diagrams are that the activities of the cations present in the aqueous phase are present in detectable concentrations in fluid inclusions; mineral saturation points can be plotted on the diagrams and silicate, carbonate, oxide sulphate and sulphide equilibria can be represented in terms of the same variables in a single diagram (HELGESON, et al., 1969). Using sixteen thermodynamic components to represent the major compositional characteristics of natural hydrothermal systems, HELGESON (op.cit.) has developed a model of reversible and irreversible chemical reactions which describe the processes in ore deposition and wall rock alteration. These processes

can be represented by a matrix of linear differential equations which describe the movement of components between the different phases as a function of changes in the aqueous phase due to the solution reacting with its environment. A computer evaluation of the matrix equation allows predictions to be made as to the actual chemical environment of wall rock alteration and ore deposition, in particular, with regard to mass ratios, paragenesis and zonation. However, to attempt this type of interpretation the concentrations or activities of sixteen components in the ore bearing fluid have to be known or simply assumed. Insufficient information is as yet available for the Echo Bay deposit. However, continued work in this area would presumably derive sufficient information. For example, the single occurrence of chrysotile in an area of the mine developed after the sampling for this study had taken place gives some reasonable approximation of the  $a_{Mg^{++}}$  in the ore forming fluid if the pH is known or can be assumed. This is demonstrated in the activity diagram for the system HCl-H<sub>2</sub>O-CaO-CO<sub>2</sub>-MgO-SiO<sub>2</sub> at 200° C. taken from HELGESON et al., (1969) and shown in Fig. 27.

Although it has not been possible to adopt this kind of approach at Echo Bay, several useful analogies have arisen between the work of HELGESON (op. cit.) and the geochemical model evolved for the Echo Bay deposit. Helgeson states that the precipitation and replacement of sulphides and oxides in ore proportions may occur at constant temperature and pressure in response to increasing solution pH which has resulted from the reaction of the aqueous phase with silicates and/or carbonates. The fugacities of O<sub>2</sub> and S<sub>2</sub> may increase or decrease in the process. These generalities agree with the geochemical model adopted for the ore

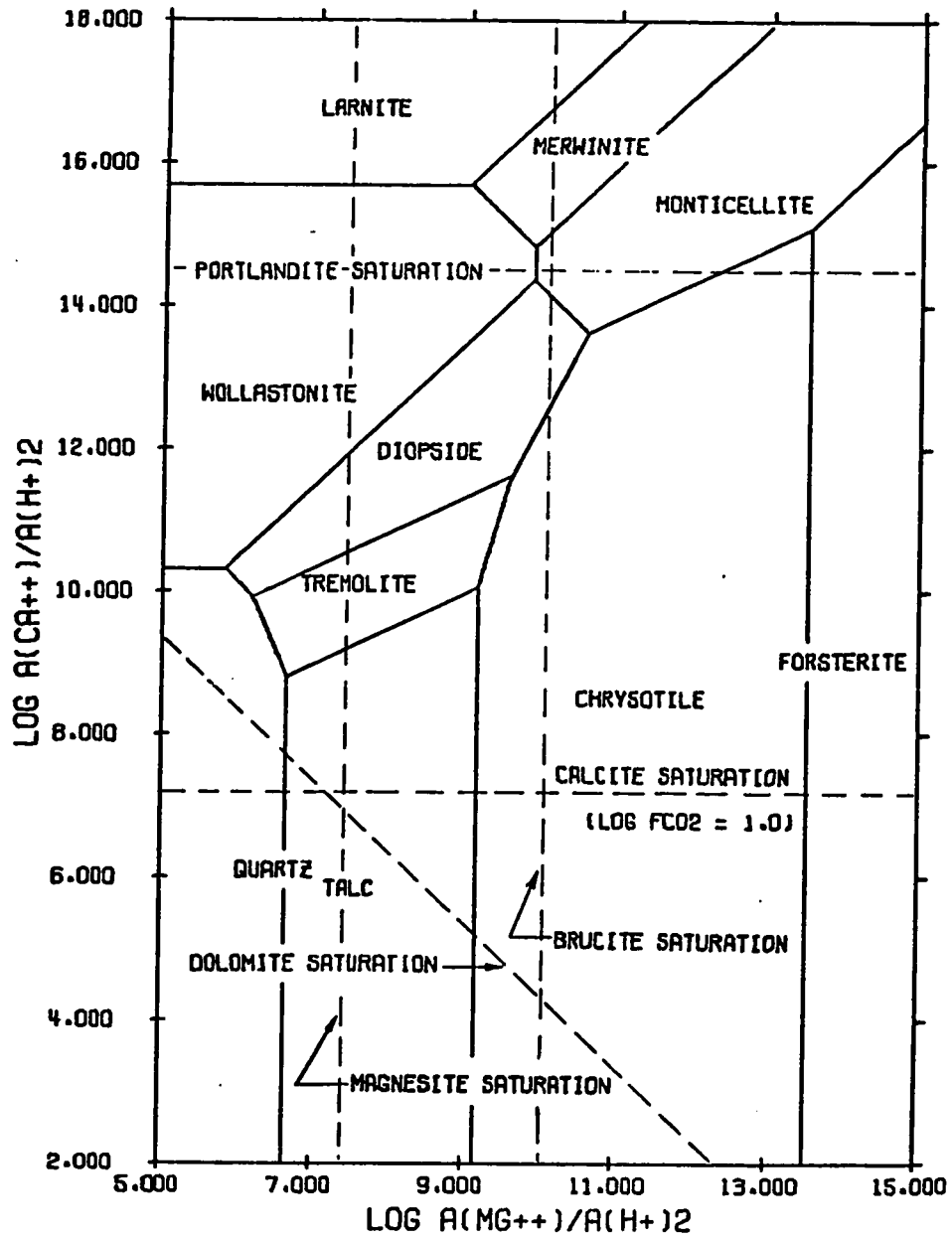


Fig. 27. Activity diagram for the system HCl-H<sub>2</sub>O-CaO-CO<sub>2</sub>-MgO-SiO<sub>2</sub> at 200°C., from HELGESON et al. (1969).

fluids at Echo Bay.

It should be borne in mind that for the construction of the diagrams mentioned in this chapter, and also for the calculations, many estimations, assumptions and generalisations have to be made. In particular, to obtain the values of Henry's Law Constant for  $H_2S$  and  $CO_2$  in a 5 m solution large extrapolations have to be made. Extrapolations have also to be made to obtain many of the equilibrium constants given. This obviously does not mean that all the calculations and diagrams presented so far are invalid; on the contrary, they are probably perfectly valid. They should, however, be kept in perspective by realising their limitations.



CHAPTER 10 - INTERPRETATION OF THE STABLE ISOTOPE DATA

Sulphur Isotopes

The  $\delta S^{34}$  values for the pyrite from the host rocks at Echo Bay are relatively constant, varying between +2.4 and +6.2 per mil. One would expect this sequence of andesites to contain juvenile sulphur with  $\delta S^{34}$  values close to 0 per mil. However, since the formation of the pyrite in its present form was apparently a diagenetic event, a change in the  $\delta S^{34}$  values is feasible. It has also been shown that the oxidation potential of a magma is reflected in the proportions of sulphide and sulphate sulphur (SCHNEIDER, 1970). Due to the high water content and thus the high oxygen fugacity of the alkali rich undersaturated basalts, the  $\delta S^{34}$  values for the total sulphur in these rocks are around +3 per mil. It is thus possible that the values of the pyrite in the host rocks at Echo Bay can be explained as a reflection of the initial magmatic conditions, the diagenetic processes or a combination of both.

Post-depositional metamorphic effects on both the host rock pyrites and the vein sulphides should be considered as a matter of course. The K-Ar studies have shown that no event of greater than about 250° C. occurred in the area as a whole after about 1650 m.y. However, the intrusion of the diabase sills and dykes may have had a very local effect on some sulphides. In particular, it was necessary to check the thermal effect of the diabase sill which cuts through the Echo Bay Mine. The heating of country rock adjacent to an intrusion at a depth of 1-2 Km is demonstrated graphically by WINKLER (1967, p. 63).

Assuming a gabbroic composition with an intrusion temperature in the order of 1200° C., then extrapolation of the data shows that at a distance of twice the thickness of a plate-like intrusion, the temperature is below 100° C. The diabase sill at Echo Bay is of the order of 150 feet thick and thus thermal effects on the sulphides at distances of over 400 feet from the sill can be considered negligible. All the samples used in the sulphur isotope study here were collected from levels about 700 feet above the sill. It would be interesting to study the isotope values of vein sulphides close to the contact with the sill. KAJIWARA and KROUSE (1970) show that although a particular isotopic distribution may be preserved under the conditions of low temperature and low sulphur fugacity, under conditions of higher temperature and high sulphur fugacity, isotope ratios within one mineral phase will tend to homogenise and pairs of minerals will tend towards isotopic equilibrium. Experimental work by PUCHELT and KULLERUD (1969) has also shown that galenas in ore deposits may exchange sulphur isotopes with vapours or gases that contain sulphur and thus lose their initial isotopic composition. This effect would presumably apply to other sulphides. At Echo Bay the correlation of the sulphur isotope values with time is good evidence for these values being the initial ones.

Assuming that any bacterial effects were not operative in the hydrothermal fluids at Echo Bay either due to the age of the deposit or to the temperatures involved, then the variations of the  $\delta S^{34}$  values observed in the vein sulphides could be explained by the chemical changes taking place in the fluid or by a kinetic isotope effect at the source. Both of these and other explanations will be considered here.

In the last chapter it was explained that, for the geochemical model derived, in the initial stages of ore deposition, the solution contains  $\text{SO}_4^{=}$  as the dominant dissolved sulphur species. As a gradual process of evolution, the  $\text{SO}_4^{=}$  species became reduced and towards the end of the ore deposition the dominant dissolved sulphur species was  $\text{HS}^-$ . Data from SAKAI (1968) gives the theoretical equilibrium separation factors of sulphur isotopes between aqueous sulphur species and sulphides. These are seen in Fig. 28 where the per mil differences ( $1000 \ln \alpha$ ) are plotted against temperature and the  $\text{S}^{=}$  (aq) species is the base line, since its  $\delta\text{S}^{34}$  values are assumed to be 0.0 per mil at all temperatures. These theoretical separation factors may not actually occur in nature as postulated for sulphate-sulphide fractionation (STEINER and RAFTER, 1966). However, experimental work on hydrothermal systems indicates that comparatively rapid attainment of equilibrium between sulphide and sulphate in solution takes place and that equilibrium between sulphide precipitates and aqueous sulphate ion is also attained. This and evidence of isotopic exchange between seawater sulphate and some sulphide ores is given by SASAKI and KAJIWARA (1970). Thus, the assumption is made that equilibrium existed between the sulphur species in the hydrothermal fluids at Echo Bay.

Fig. 28 shows that at temperatures between  $150^\circ \text{C}$ . and  $200^\circ \text{C}$ ., the  $\text{SO}_4^{=}$  (aq) has a  $\delta\text{S}^{34}$  value of around +45 per mil and the  $\text{HS}^-$  a  $\delta\text{S}^{34}$  value of around +5 per mil. In qualitative terms, it is thus apparent that in the initial ore-forming stage when  $\text{SO}_4^{=}$  (aq) was the dominant sulphur species,  $\delta\text{S}^{34}$  would be preferentially concentrated in the  $\text{SO}_4^{=}$  (aq) species and the precipitating sulphides will be enriched in  $\text{S}^{32}$ . As the solution evolves and the  $\text{SO}_4^{=}$  was gradually reduced, more  $\text{S}^{34}$  was available to form in the sulphide phase.

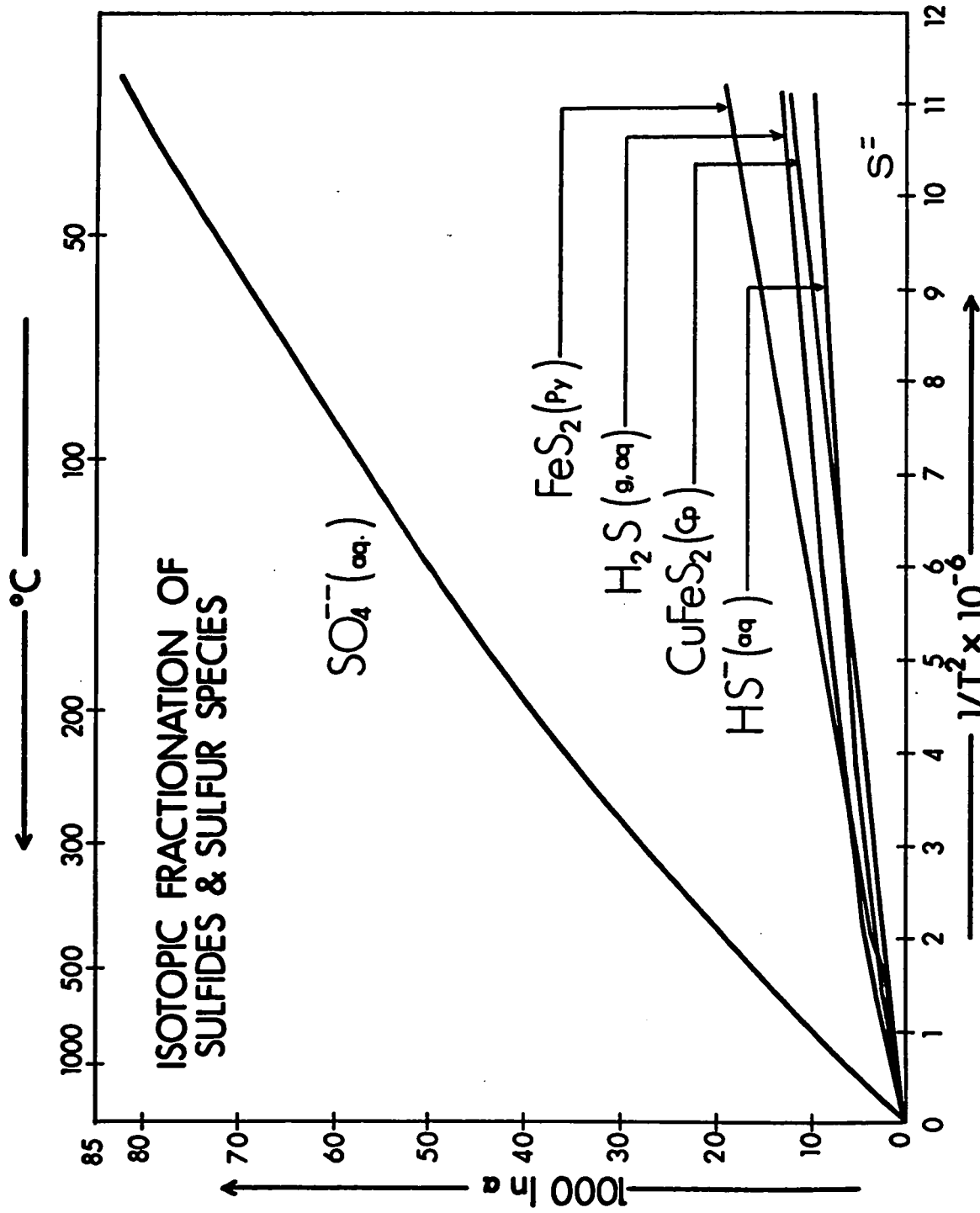


Fig. 28. Graph of  $1000 \ln \alpha$  vs. temperature to demonstrate the theoretical fractionation of sulphur species as a function of temperature, from SAKAI (1968).

Eventually when  $\text{HS}^-$  was the dominant sulphur species in the fluid, then  $\text{S}^{32}$  was preferentially kept in solution and  $\text{S}^{34}$  was enriched in the precipitating sulphides. This explanation is consistent with all the other data at Echo Bay and explains how the vein sulphides show increasing  $\delta\text{S}^{34}$  values with time. This approach has been put on a more quantitative basis by OHMOTO (1970) where iso- $\delta\text{S}^{34}$  lines for precipitating pyrite are plotted on pH-f $\text{O}_2$  diagrams for the required conditions. These contours show that a fluid movement such as that proposed for the Echo Bay deposit would cause the  $\delta\text{S}^{34}$  values of precipitating sulphides to change from very negative to positive. A  $\delta\text{S}^{34}$  contoured pH-f $\text{O}_2$  diagram for the conditions of the hydrothermal fluid at Echo Bay is in preparation as part of a future publication on the sulphur isotopes and solution geochemistry of the Echo Bay deposit.

Considering the early acanthite to be the first sulphide to be deposited at Echo Bay, then using the  $\delta\text{S}^{34}$  values of these sulphides it is possible to estimate the  $\delta\text{S}^{34}$  value of the hydrothermal fluid at this stage. For a coexisting acanthite and chalcopyrite ( S25 and S67 respectively) then the  $\Delta_{\text{Cp}}^{\text{Ac}}$  is about 7 per mil at 200° C. Assuming that the initial acanthite was deposited at a temperature of somewhere between 150° C. and 200° C., then the  $\Delta_{\text{Cp}}^{\text{Ac}}$  was probably about 8 per mil. The initial acanthites have  $\delta\text{S}^{34}$  values of about 21 per mil and thus a coexisting chalcopyrite would have a  $\delta\text{S}^{34}$  value of -14 per mil. Using the curves in Fig. 28, the fractionation between chalcopyrite and  $\text{SO}_4^{=}$ (aq) at between 150° and 200° C. is about 37 per mil and thus the  $\text{SO}_4^{=}$ (aq) would have a  $\delta\text{S}^{34}$  value of about +23 per mil. Since at this stage the dominant sulphur species in solution was  $\text{SO}_4^{=}$ , then the  $\delta\text{S}^{34}$  value

of the fluid was about +23 per mil. An exact computation can be made by summing all the products of the molalities of the various sulphur species and their corresponding isotopic ratios. For this particular case, the  $\delta S^{34}$  value of the total sulphur in the fluid calculated in this manner is still extremely close to +23 per mil and thus since the temperature uncertainties allow this value to vary from +20 to +27 per mil, then a further refinement of the data was considered to be unjustified.

In the Port Radium deposit which has been described previously, gypsum occurs at an early stage. Assuming a similar temperature and chemical regime for this vein, a sulphur isotope measurement on the gypsum, assuming it to be unaltered, would give the  $\delta S^{34}$  value of the early fluid. A suitable sample of gypsum from Port Radium has not yet been obtained but should be in the near future.

If the initial sulphur in the hydrothermal fluid at Echo Bay had a  $\delta S^{34}$  value of around +23 per mil and if all the sulphur was extracted from the solution to be precipitated as sulphides, the average  $\delta S^{34}$  value of the sulphides would be around +23 per mil. This was not the case at Echo Bay and in fact the average  $\delta S^{34}$  value for the sulphides is around +7 per mil. Thus, the amount of sulphur extracted from solution was probably not greater than one order of magnitude difference in the molalities and therefore the total dissolved sulphur in the fluid was considered in the last chapter to remain around  $10^{-3}$  m.

The second consideration to be discussed as a possible cause of the variation in the  $\delta S^{34}$  values of the vein sulphides is a kinetic isotope effect. Kinetic isotope effects have been found to occur in

nature and in laboratory experiments; they are often caused by inorganic and microbiological reductions. WELLMAN et al. (1968) found that the abundances of  $N^{15}$  and  $N^{14}$  are significantly altered during experiments in which nitrate and nitrite are microbiologically reduced to nitrogen gas. The enrichment of the heavy isotope in the polysulphide and sulphide during the fractional removal of the polysulphidic sulphur where sulphur-sulphur bond rupture takes place was noted by SAKAI (1966) and interpreted as a kinetic isotope effect. A kinetic isotope effect of 1.5% was found in a chemical reduction of selenite ion to elemental selenium (KROUSE and THODE, 1962) and similar effects have been detected with tellurium (SMITHERS and KROUSE, 1968). Experiments have also shown that large kinetic isotope effects occur in the reduction of  $GeO_2$  to  $GeO$  (BROWN and KROUSE, 1964). Similarly, kinetic isotope effects accompanying the oxidation of  $CO$ ,  $H_2$  and  $CH_4$  have been observed (ZIELINSKI, 1966). The kinetic isotope effect, thus, simply implies that different rates of reaction for isotopic atoms or molecules can take place.

If it is assumed that equilibrium was not attained in the hydrothermal fluid at Echo Bay, then a kinetic isotope effect could have taken place. In this model, then, the lighter sulphur isotope reacts faster and consequently the initially-formed sulphides exhibit lighter sulphur than the later ones. A kinetic isotope effect at the source has been used to interpret the spread of sulphur isotope values obtained for the Rammelsberg Ore Deposit, Germany (ANGER et al., 1966). These proposed kinetic effects produce the same effect as the process of diffusion used to explain the sulphur isotope values observed in sulphides in the gold-quartz deposits of the Yellowknife district (WANLESS et al.,

1960) and the lead-zinc-silver-cadmium deposits of the Keno Hill-Galena Hill Area, Yukon (BOYLE et al., 1970). In the latter deposit, sulphur in the sulphides of the sedimentary rocks is isotopically heavier than the sulphides in the lodes. At Yellowknife, the isotopic studies indicate that the primary sulphur isotope distribution of the area was modified by granitisation and metamorphism during which the  $S^{32}$  was preferentially mobilised. Intense chemical activity associated with the formation of the gold-quartz lenses led again to the preferential mobilisation of the  $S^{32}$ .

Although diffusion processes such as the ones suggested by Boyle can be produced in the laboratory, it is difficult to assess whether they would occur in movement through rock media. Calculations for diffusion effects in solutes demonstrate that the lighter isotope will travel fastest, but it is soon caught up by the diffusion front (P. Fritz, pers. comm., 1969). It should be noted here that a diffusion mechanism for sulphur could produce the observed isotope effects at Echo Bay. However, if the sulphur is thought to have moved any great distance for any great amount of time, then it is hard to believe that a diffusion process could be detected on the basis of isotopic differences.

One other process which is known to affect isotopic abundances is the so-called reservoir effect. A reservoir effect created in the last stage of ore deposition, when small areas of mineralising solutions were possibly being sealed off by abundant deposition in the veins, could be postulated. Continued deposition of sulphide under these circumstances would lead to the sulphides becoming isotopically heavier with time. In fact this type of situation could be responsible for



producing some of the very positive  $\delta S^{34}$  values towards the end of the ore deposition at Echo Bay.

To attempt to depict which processes have been responsible in causing the sulphur isotope fractionation at Echo Bay is difficult, if not virtually impossible. On the basis of the evidence given, equilibrium in the ore fluid between the dissolved species themselves and the precipitating minerals appears to be a reasonable assumption, although it cannot be proven. Even accepting this assumption, the chemical changes in the ore fluids may not have been the main fractionating factors, because diffusion and reservoir effects might have been operative. It is felt by the author that the proposed and fairly well substantiated chemical changes in the ore fluids at Echo Bay explain the change of  $\delta S^{34}$  values in the vein sulphides, but it is conceded that other processes, equally capable of producing fractionation, may have been partially or perhaps totally responsible for the observed fractionation.

Only small fractionations are found to occur within the two chalcopyrite and the two galena samples from El Bonanza and no significance can be placed on the small difference observed. The  $\delta S^{34}$  values of the sulphides in the banded ore at Terra Mine are remarkably constant around +5.5 per mil (4 values) except for one galena at +16.5 per mil. Since very few samples have been analysed in this deposit to date and future work is planned within the Geology Department, University of Alberta, then it appears rather inappropriate to comment on the data at the moment.

In a study of the sulphur isotope geology of vein-type and sandstone-type uranium deposits by FIELD (1960), a relatively narrow

range of sulphur isotope ratios near to the meteorite values of  $\delta S^{34} = 0$  per mil was obtained for primary sulphides of vein type deposits. Values varying from +5.4 per mil to -5.8 per mil were observed (not including much lighter values obtained in marcasite which was considered to be secondary). Although several hundred analyses were made, no correlations with the mineralogy or paragenesis of a deposit and the sulphur isotope values was obtained. Thus the results were thought to be indicative of magmatic hydrothermal mineralisation. It does seem feasible, however, that some of the aforementioned processes could have been responsible for the fractionations observed. The small spread in values was probably due to the fact that all the veins studied belong to the silica-iron-lead vein type uranium deposits of EVERHART and WRIGHT (1953) which are thought to be of a higher temperature origin than the Echo Bay veins.

#### Oxygen Isotopes in the Carbonates

When considering the oxygen isotopes it is not possible to use approaches similar to those employed in the sulphur isotope interpretations. The reason is that the large reservoir of water in the ore fluid acts as a 'buffer' and the main controlling factors of the oxygen isotopes of the carbonates are the  $\delta O^{18}$  value of the water and the temperature plus the possibility of later alteration by meteoric water.

Considering firstly the dolomites at Echo Bay, those associated with the Co-Ni-arsenide minerals have a  $\delta O^{18}$  value of about + 20 per mil. Those from the intermediate sulphide stage spread in  $\delta O^{18}$  values from +15 to +12 per mil. This data could be interpreted as reflecting an

increase in the temperature with time, changing  $\delta O^{18}$  values with time, possibly by the mixing of fluids or a combination of all these factors. For the temperature range required, data are not available for the fractionation of oxygen isotopes between water and dolomite. However, the equation obtained by NORTHROP and CLAYTON (1966) for a temperature range of 300-510° C. is used here for comparative purposes. At 150° C., water in equilibrium with the early dolomites would have a  $\delta O^{18}$  value of about +6 per mil. At 200° C., water in equilibrium with the later dolomites would have a  $\delta O^{18}$  value of between 0 per mil and +3 per mil. From this evidence it would appear that the change in  $\delta O^{18}$  values of the dolomites could possibly be explained by an increase in temperature accompanied by a slight decrease in the  $\delta O^{18}$  value of the water itself. However, since the fractionation factors are not well known and the dolomites in actual fact contain significant amounts of  $MnCO_3$  and  $FeCO_3$ , (see the last section of this chapter), fractionation factors for these minerals would be difficult to estimate. If a change in the  $\delta O^{18}$  values of the fluid did occur, then a mixing of two fluids could be postulated. This is, however, entirely speculative and in actual fact difficult to reconcile with other data as having occurred during the main mineralisation periods. The dolomites labelled 'Echo Bay Area' in Fig. 13 were taken from minor veins on the surface and show similar values to the intermediate sulphide stage dolomites at Echo Bay. At El Bonanza, the rhodochrosites and manganese rich carbonates are banded. The samples from oldest to youngest are 030, 029, 028 and 027.

Considering now the  $\delta O^{18}$  values of the calcites, it is apparent that the group with the lowest values comprises the late vein-calcites.

Using the data of O'NEIL et al., water in equilibrium with calcites possessing  $\delta O^{18}$  values of about +8 per mil would have a  $\delta O^{18}$  value of about -1 per mil at 200° C. Data for rhodochrosite at 240° C. demonstrates that it exhibits a slightly smaller fractionation factor for oxygen isotopes than calcite. Thus the manganese contents of the calcites will not affect the  $\delta O^{18}$  values to a significant extent for this discussion (O'NEIL et al., op. cit.). Again the  $\delta O^{18}$  values of the late calcites could be interpreted as representing an increasing temperature after dolomite deposition or an ore fluid becoming increasingly more negative in  $\delta O^{18}$  values. It is unlikely to have increasing temperatures at the late stages of ore deposition. Thus if these  $\delta O^{18}$  values of the late calcites are considered to be those initially attained, considering temperature below 200° C., the ore fluid would have had a very negative  $\delta O^{18}$  value. The early- and intermediate-sulphide stage calcites are difficult to fit precisely into the paragenetic sequence, but they are known to have a spread in time of deposition within the sulphide stages mentioned. Sample 022 is later than 023 and thus the  $\delta O^{18}$  values appear to decrease in a similar manner to the dolomites. The calcite phase 023C is later and thus not coexisting with the dolomite 023D. In spite of the fact that both calcite and dolomite were deposited in the same sulphide stage, it is difficult to estimate if the  $\delta O^{18}$  values do indicate that the two minerals were in equilibrium at the established temperatures for mineral deposition in these stages. Using the values given by SCHWARCZ (1966) and SHEPPARD and SCHWARCZ (1970) for the fractionation of carbon and oxygen isotopes between coexisting calcite and dolomite, the difference in  $\delta O^{18}$  values at

200° C. is 1.6 per mil. Thus considering only the oxygen isotopes, many of the dolomites and calcites could have been in equilibrium between themselves and the ore fluids providing that factors discussed previously would account for the  $\delta O^{18}$  values decreasing with time. The samples of vein carbonate from Common Lake lie within the spread of the Echo Bay samples.

An increasing temperature of the ore-fluid for the later stages of mineral deposition in the veins has been rejected as a feasible hypothesis and if the postulation of an ore-fluid whose  $\delta O^{18}$  value decreases with time is not accepted, then an alternative explanation must be offered for the interpretation of the  $\delta O^{18}$  values of the calcites. This alternative interpretation is in essence a selective recrystallisation and isotopic exchange of the calcites with meteoric ground water. DEGENS and EPSTEIN (1964) have explained large fractionations between dolomite and calcite as being in some cases possibly due to selective alteration of calcite by isotopically light meteoric water. This influx of meteoric water into the system could possibly be a waning phase of the ore fluid.

In a study of the oxygen and carbon isotopes of the carbonates of the Pine Point Lead-Zinc Ore Deposit, FRITZ (1969) postulated that the decrease in  $\delta O^{18}$  values found in late vug calcites was due to the influx of isotopically light surface water and was not a function of increasing temperature. Meteoric waters are considered to have possibly been involved in the late stages of mineralisation of other ore deposits such as those at Providencia, Zacatecas, Mexico (RYE and HAFFTY, 1969). This interpretation would account for the relatively light  $\delta O^{18}$  values

of the late calcites at Echo Bay. A percolating meteoric water could also preferentially recrystallise existing calcites and decrease their  $\delta O^{18}$  values as may have happened with samples 04 and 07, for example. The reader is reminded at this stage that in contrast to the dolomite, the calcites do not contain any fluid inclusions. This could possibly be due to late formation and a recrystallisation of existing calcites. It should also be considered that meteoric water could have caused alteration more than once in the history of the calcites.

The oxygen isotope values of calcites and other carbonates at the El Bonanza and Terra Mines demonstrate similar trends to those observed at Echo Bay. In the Terra Mine samples, the four calcites were arranged from oldest to youngest as 034, 038, 036 and 037 on the basis of crystal form and they demonstrate an increase in  $\delta O^{18}$  values with time. If this correlation is real, then it is open to the same interpretation as applied to the Echo Bay carbonates.

#### Carbon Isotopes in the Carbonates

The dolomites at Echo Bay have relatively constant  $\delta C^{13}$  values of around -3 per mil. There is a suggestion of a trend towards heavier values of -2 per mil towards the end of the dolomite sequence. This could be possibly due to the increase in the  $CH_4$  and CO content of the ore fluid as the conditions became more reducing. Solution chemistry calculations demonstrate that these species became increasingly important towards the later stages of ore deposition. The manganese carbonates of the El Bonanza Mine show the same  $\delta C^{13}$  values as Echo Bay but the dolomites and siderites from Terra Mine are somewhat lighter.

Using the data of both SCHWARCZ (1966) and SHEPPARD and SCHWARCZ (1969), it is found that the fractionation of carbon isotopes between coexisting calcite and dolomites is in the order of 1 per mil at 200° C. It is thus apparent that none of the Echo Bay calcites and dolomites represent an equilibrium of carbon isotopes at this temperature. The El Bonanza calcites are in general about 2 per mil lighter in  $\delta C^{13}$  values than the manganese carbonates and the Terra calcites are quite a bit lighter than the dolomites.

All the Echo Bay calcites in general exhibit very negative  $\delta C^{13}$  values. In particular sample 07 has a  $\delta C^{13}$  value of -31 per mil and 04 a value of -19 per mil. Reruns of these samples showed these results to be reproducible. Since the calcites represent a large time interval in vein deposition, it is not possible to explain their  $\delta C^{13}$  values, which are all consistently very negative, by gradual changes in fluid chemistry. If as suspected, the  $CH_4$  content of the fluid increases with time, then in particular the late calcites would show much more positive values. Organic compounds in the fluids such as those described by KRANZ (1970) could possibly upset the balance of carbon species or carbon isotopes or both within the ore fluid. However, if this was the case, then it is difficult to explain why the dolomites and calcites would assume different isotopic values.

Again the only explanation of the  $\delta C^{13}$  values, which is consistent with other data, is the preferential recrystallisation of the calcites either after ore deposition or during the very last stages of mineral deposition at Echo Bay. Even accepting this as a working hypothesis, it is still difficult to explain some of the very negative

carbon isotope values. These would have had to have been inherited from a fluid in which the carbon species were very reduced, that is, one rich in  $\text{CH}_4$  and/or  $\text{CO}$ . If this fluid was oxidised to give  $\text{HCO}_3^-$  species with negative  $\delta\text{C}^{13}$  values then negative values could be obtained in the calcites. Assuming the same model adopted to explain the oxygen isotopes then one is thinking in terms of meteoric water dilution of the ore fluids as the recrystallising media. Reduced carbon species here could be obtained by meteoric waters from a bacterially reducing environment or by contributions from the remaining reduced ore fluid. It should also be remembered that more than one alteration event may have been operative.

The dolomites and calcites at Terra Mine demonstrate that if they were in equilibrium then this would have been at a low temperature. The apparent increase in  $\delta\text{C}^{13}$  values of the calcites with time may be a function of an evolving ore fluid in which the carbon species change with time.

#### Electron Microprobe Analyses of the Carbonates

In the hope of obtaining some trends in composition of the carbonates with time and a possible index of recrystallisation, the carbonate samples from Echo Bay, El Bonanza and Terra Mines were analysed for Mn, Fe and Mg. Separated fragments of the carbonates were mounted in cold setting plastic, polished and carbon-coated for electron microprobe analysis on an Applied Research Laboratories EMX instrument. Peaks and backgrounds were counted for 100 second periods while randomly traversing the individual carbonates. Standards of



hypersthene, synthetic MgO and Mn were used as shown in Appendix F, and these were measured at the beginning and end of each sample batch. The corrected results, given as mole percentage  $\text{MnCO}_3$ ,  $\text{FeCO}_3$ ,  $\text{MgCO}_3$  and  $\text{CaCO}_3$  (by difference), are shown in Table 14. Stoichiometry of the carbonates was assumed. The dolomite analyses are not reported here, since the results were not consistent with the X-ray diffractometry work on the carbonate phases present. An apparent excess of  $\text{CaCO}_3$  was found and is being investigated further.

The El Bonanza manganese-rich carbonates 027, 028, 029 and 030 are mixtures of carbonate rather than one carbonate with lattice substitution. In these cases the probe analysis gives an average of the zones and domains of different composition which exist in the sample. A correlation between the manganese content and the  $\delta\text{O}^{18}$  values is seen whereby a sample with approximately 72 mole %  $\text{MnCO}_3$  has a  $\delta\text{O}^{18}$  value of +17 per mil and a sample with approximately 50 mole %  $\text{MnCO}_3$  has a  $\delta\text{O}^{18}$  value of +16 per mil. This difference is a function of the different fractionation factors according to the relative metal oxygen bond strengths. The El Bonanza calcites have small amounts of lattice substitution of Mn, Fe and Mg but these show no correlation with either the  $\delta\text{O}^{18}$  or  $\delta\text{C}^{13}$  values. Sample 026 is mainly calcite with some rhodochrosite. For the Terra Mine calcites, the assumed earlier sample 034 has a trace of dolomite, but the other calcites all have substitution of Mn, Fe and Mg in the lattice. The only correlation found with the analyses here is that the manganese content of the calcite appears to increase from about 4% to nearly 8% with time. This is found to be a normal trend in some of the silver veins of this area (JORY, 1964).

TABLE 14

Electron microprobe analyses of carbonates

Sample #	Mole % MnCO <sub>3</sub>	Mole % FeCO <sub>3</sub>	Mole % MgCO <sub>3</sub>	Mole % CaCO <sub>3</sub>
01	6.17	0.23	0.38	93.22
02	2.49	4.36	0.18	92.98
03	3.78	0.03	0.45	95.75
04	6.11	0.00	0.45	93.44
05	10.56	0.05	0.18	89.20
06	11.29	0.05	0.28	88.37
07	1.99	0.01	1.45	96.54
08	11.96	0.03	0.12	87.88
09	9.39	0.27	0.22	90.12
011	0.43	0.97	0.24	98.37
012	0.95	0.83	0.13	98.09
014	8.97	0.14	0.31	90.58
018	2.74	0.11	0.40	96.75
021	2.50	0.00	0.56	96.94
022	7.03	0.75	0.04	92.18
025	2.12	0.02	0.02	97.85
026	13.03	1.56	0.45	84.97
027	46.15	6.82	4.06	42.96
028	45.19	7.44	4.95	42.41
029	72.42	11.40	2.66	13.52
030	55.06	7.70	2.88	34.35
031	1.39	0.56	0.45	97.59
032	1.47	0.04	0.00	98.49
033	0.69	0.95	0.05	98.30
034	3.97	2.79	0.44	92.80
036	4.39	1.92	0.24	93.45
037	7.61	0.67	0.04	91.67
038	4.54	0.73	0.05	94.68
042	6.90	0.12	0.19	92.79
043	6.90	0.12	0.19	92.79
044	6.82	0.14	0.27	92.78

The precision of the analyses is  $\pm 1\%$  for 2  $\sigma$  variations

The analyses of the Echo Bay calcites were compared with the corresponding  $\delta O^{18}$  and  $\delta C^{13}$  values by the use of the correlation coefficient program mentioned in Chapter 5. Only one significant correlation was detected - that between the manganese content of the calcites and the  $\delta O^{18}$  values. The calcites with the highest  $\delta O^{18}$  values also have the largest manganese concentrations. X-ray diffractometry studies of the calcites indicated that rhodochrosite is not present and that the manganese is in the calcite lattice. Microprobe analyses showed these calcites to be fairly homogeneous. Since the difference in manganese contents of the calcites is about 9%  $MnCO_3$  and the difference in  $\delta O^{18}$  values is about 15 per mil, it is not feasible that these differences in  $\delta O^{18}$  values may be explained by the differences in metal-oxygen bond strengths between the calcites with different manganese contents. Only minor variations will occur in relation to compositional variations of this order.

This observed correlation trend could be taken to suggest that the isotopically heavier calcites did not recrystallise and exchange with a late meteoric water to a large extent, thus almost retaining their original isotope values and manganese contents. On the other hand the isotopically lighter calcites must have undergone an increased degree of isotopic exchange and manganese loss. The chemistry of these carbonates does not however correlate with the  $\delta C^{13}$  values which were also thought to be a function of depositional alteration. It is feasible though that if post-depositional alteration of some of the calcites did occur, then the processes affecting the change in the carbon isotope ratios could be more complicated than those affecting the change of

oxygen isotope ratios.

Both the oxygen and carbon isotope values will be investigated further in particular with reference to any result obtained from similar vein carbonates.

## CHAPTER 11 - TRANSPORTATION OF METALS IN SOLUTION

Until recently, the mechanism of transporting metals in an ore solution was as much a problem as the source of the metals themselves. Although this problem is by no means solved, experimental work and data from fluid inclusion studies have led to the formulation of various hypotheses. In this present study, no experimental or fluid inclusion analytical data has been obtained which is pertinent to this problem and therefore the present chapter will constitute a short review of the trends of thought pertaining to the transportation and deposition of metals connected with ore fluids. Notwithstanding the lack of analytical data on the Echo Bay fluid inclusions, some of the data and observations recorded so far are of use in testing the hypotheses which are reviewed below.

The solubilities of ore forming sulphides under hydrothermal conditions have been discussed by ROMBERGER and BARNES (1963), MELENT'YEV et al., (1969) and many other workers. Experimental work has shown that ore sulphides would be sufficiently soluble to be transported in the sulphide form and precipitated to give an ore deposit. The solubilities are often sensitive to changes in pH more than changes in temperature. However, from Figs. 21 and 22, it can be seen that a fluid starting in the hematite field and moving into the pyrite field and eventually into the  $\text{HS}^-$  field would not have abundant  $\text{S}^=$  stable at any stage. Thus, this theory does not appear to be applicable to the Echo Bay deposit.

A great deal of experimental work has also been done with the bisulphide complexing of metals, particularly by BARNES (1962). An

attractive theory has been evolved which matches the zonation sequence seen in many ore deposits. The transport of base metals as bisulphide or sulphide complexes appears in fact to be both geologically and chemically feasible at temperatures up to 250° C. (BARNES and CZAMANSKE, 1967). For the Echo Bay deposit, the transport of the metals as bisulphide complexes does not appear to be geochemically feasible, since the bisulphide species is probably not abundant in the fluid in significant concentrations until the later part of ore deposition.

In the Ni-Co-arsenide-native silver-uranium vein type deposits, a very high Ag/Au ratio is always encountered and this is interpreted by BOYLE (1968b) as being due to the preferential mobility of silver over gold, possibly by selective transportation agents. The close affinity of the silver with antimony and arsenic in these veins suggests that the silver migrated as a mobile Ag-As or Ag-Sb complex. However, this does not explain the absence of gold in these veins. If the silver is considered to be transported as a carbonate, then excess CO<sub>2</sub> in the fluid enhances the solubility of silver carbonate but depresses the solubility of gold. In considering the behaviour of uranium in hydrothermal solutions, NAUMOV (1961) concluded from experimental data that uranium could be transported in the form of complex ions amongst which complex-carbonate and fluoride ions would be the most probable. The uranium is most likely transported in the hexavalent condition as complexes and is deposited when those complexes are destroyed. If in fact the silver and uranium did travel as carbonate complexes, their solubility could be lowered by increasing temperatures or by changing the pH of the solution.

Mainly through the work of HELGESON (1964, 1966 and 1970) and the researches on geothermal brines, laboratory and geological evidence suggest the chloride ion as being the major metal transporter under most circumstances. Experimental work has shown chloride complexes to be stable under the conditions of ore formation. It is interesting to note that BARNES and CZAMANSKE (op. cit.) found that the development of  $H_2S$  and  $HS^-$  in a fluid hindered chloride complexing. If indeed the metals in the fluids did move as chloride complexes at Echo Bay, then a mechanism of precipitation could be involved by the development of  $HS^-$  which would affect the stability of the chloride complexes. Abundant evidence is available that the chloride ion is present in ore forming solutions and can in fact carry appreciable amounts of metal in solution. ROEDDER (1967) has found that  $Cl^-$  is usually 2 to 10 times more abundant than any other species in fluid inclusions. Many fluid inclusions, especially the ones at Echo Bay, indicate that very high salt contents are often present in the ore fluids. The source of the chloride ion could be from that initially present in connate waters, from evaporites or from magmatic fluids. Several metalliferous brines have now been tapped from deep bore holes and it appears quite feasible that these brines are actual- or potential-ore forming fluids. Abundant data on brines such as the Salton Sea brine, California and the Cheleken brine, Caspian Sea area is now available (WHITE, 1967 and ELLIS, 1967) and they are found to contain high concentrations of Na, K, Ca, Mg, Fe, Mn, Cl,  $SO_4$  and other metals. Deuterium and oxygen isotope studies on the Salton Sea and Red Sea brines by CRAIG (1966) and lead and strontium isotope work on the Salton Sea brine by HELGESON (1966)

indicate that the fluids and their contents were essentially derived from the sediments in which they occur.

Using a similar analogy for the Echo Bay deposit, the metals and other species in the ore fluid were probably derived from the sediments and volcanics. It appears feasible that the silver and uranium could have been transported as carbonate complexes which became unstable due to an increase in temperature or to other changes in the conditions of the fluid. The other metals were probably transported as chloride complexes which became unstable, either due to changes in the pH of the fluid or to the increasing concentration of reduced sulphur species in the fluid. Since the temperature and pressure at Echo Bay appear to have undergone no major fluctuations during the main ore deposition, then it is felt that chemical changes alone have been responsible for the deposition of the ore. These chemical changes have been discussed in Chapter 9.



## CHAPTER 12 - GENESIS OF THE DEPOSIT

This following account will constitute a summary of the main conclusions made during the geological and geochemical work of this project. The ore deposit is considered as an integral part of and, in fact, a direct function of the total geological evolution of the area.

Around 1800 m.y. ago, the Echo Bay area was the site of sedimentation and intense volcanic activity. Thousands of feet of argillites, calcareous rocks, tuffs, agglomerates and lavas were laid down. Within the same time span, granites, granodiorites, and some feldspar porphyries intruded the area and probably caused folding and tilting of the sedimentary and volcanic sequence. The close association of all these events in time, together with the fairly deep burial of many of the horizons under a few thousand feet of volcanics, probably created a high geothermal gradient. In fact, the K-Ar dating indicates that some minerals did not become closed systems to argon until around 1650 m.y.

During this period of active burial, the banded sulphide horizons in some of the tuffs are thought to have attained their present form. The formation of pyrite during early diagenesis in euxinic sedimentary environments is now a well known feature (DUNHAM, 1970). The sulphur was probably made available in the Echo Bay area by volcanic exhalations. It is probably a valid assumption that pyrite is the original sulphide of the sediments and volcanics (ROBINSON, 1967). Many of the diagenetic features of sulphides such as banding,

segregations and stringers of pyrite documented by AMSTUTZ et al. (1964) are found at Echo Bay. Remobilisation in such an environment, often by hypersaline brines (DUNHAM, loc. cit.) can result in leaching and concentration of metallic ions to produce ore grades. Often the ores are moved to favourable chemical or structural traps. In actual fact, it is found that the pyrite will act as a scavenger for other base metals (ROBINSON and STRENS, 1968) and concentrate these in the deposit. However, at this early stage at Echo Bay, the physical and chemical conditions were presumably not favourable for a large scale mobilisation of sulphides.

On the other hand, it is considered that the embryo ore fluid must have started to form soon after the burial of the area. The lower, dominantly sedimentary, series of the Echo Bay Group was effectively sealed off by the overlying series of lavas. After the intrusion and tilting, the area probably cooled slowly while some erosion took place in the Upper Echo Bay Group. The Hornby Bay and Cameron Bay Groups were then deposited, presumably effecting further isostatic depression of the area. It seems inevitable that any type of water which was buried in the sediments at Echo Bay would, through the processes of time and elevated temperature, become enriched in certain constituents from the host rocks. This process is easier to envisage if the original water is considered to be seawater. On reacting with rocks, sea water is altered substantially especially with increasing temperature. A series of experiments by KISSIN and PAKHOMOV (1969) demonstrated the type of alteration to be expected and also the importance of the carbonate content of the rocks in these alteration reactions. The main

features of alteration are the reduction in the amounts of sulphate and magnesium ions in the water. In rocks with excess carbonate at elevated temperatures, a sodium chloride water low in sulphate, but rich in calcium carbonate, is produced. It, thus, does not seem difficult to envisage a situation where a geothermal brine could develop as the result of connate water sealed in a sedimentary environment, under elevated temperatures. BERRY (1966, 1967) has suggested that the Salton Sea brines achieved their high salinities as a result of hyperfiltration of dilute pore waters through semipermeable shales in the stratigraphic section. HELGESON (1968), however, for the same system, suggests a circulation, evaporation and boiling mechanism to attain the high salinities involved. It is also known that alkalis become enriched at gas-liquid interfaces and thus bubbles moving through a fluid could eventually increase the sodium and potassium contents of the upper parts of the fluid (G.H. Taylor, pers. comm., 1970). It is also possible that the large scale breakdown of the mineral hornblende, which is witnessed mainly in the volcanic rocks of this area, could add significant amounts of sodium and potassium to circulating fluids.

Whatever the actual mechanism, it seems possible that a geothermal brine formed in the Echo Bay area similar to the present day Red Sea brines. This brine would be forming and circulating within the sediments and tuffs from some time after 1800 m.y. through to about 1450 m.y. ago when the ore deposit was formed. During this time, it is postulated that the brine was sufficiently active to extract and complex metals from the sulphide, oxide and possibly silicate phases of the rocks. Highly saline Na-Ca-Cl brines are evidently very potent solvents for Cu, Pb, Zn, Ag and probably other metals dispersed in rocks and minerals (WHITE,

1968). One can soon find analogies to this postulated model in the geological literature. The most quantitative one is the work done by HELGESON (1966) where an arkose initially containing sea water is considered as a 'source bed' for the genesis of hydrothermal solutions with ore-forming potential. Calculations show that at 200° C. sufficient lead could be extracted from K-feldspar in arkosic sediments to eventually form an ore deposit. WHITE (op. cit.) postulated that a selective concentration of metals into a brine could take place at temperatures as low as 100° C. The brines are often deficient in sulphur.

Fluid inclusion and other studies at Echo Bay suggest that the ore forming fluid was highly saline and sulphur deficient. The K-Na ratios of the fluid inclusions suggest that the elements were not derived directly from igneous rocks. The  $\delta S^{34}$  value of the source would allow the sulphate to be of sea water origin. Thus so far, the available information on geothermal brines is compatible with the data obtained from Echo Bay. By analogy with other models adopted, it appears very feasible that the metals were also extracted from the host rocks. This source of metals has been favoured by BOYLE (1968) for the origin of many silver deposits and, in fact, it has been demonstrated in this study that a sufficient quantity of metals exist in the Echo Bay host rocks. However, according to BOYLE (op. cit.), the key to the formation of a vein-type deposit is the proper timing and intensity of two geological events namely: (i) the mobilisation of the elements in the country rocks (a metamorphic event) and (ii) the dilatency of structures (a tectonic event). This theory is extremely applicable to the Echo Bay situation. Thus far in the discussion, it has been proposed that

the mobilisation of elements from the country rocks has been effected by a brine which is the potential ore-fluid.

About 1450 m.y. ago in the Echo Bay area, a sequence of events occurred which are considered to be critical in the formation of the ore deposits. Fracturing and faulting took place on a large scale and the diabase dykes and giant quartz veins were the first media to intrude these fractures. The geothermal gradient would increase with the diabase activity; in particular with the intrusion of diabase sills. Only one sill was intruded at Echo Bay, just after the ore deposit, but its presence suggests more igneous activity beneath and an increase in the geothermal gradient. Coupled with this thermal event, the fractures carrying quartz veins reopened during several phases of movement, thus creating dilatant structures. These structures would affect the pressure regime in the rocks, such that the hitherto trapped ore fluids would migrate to and through them. The change of conditions experienced by the fluids within the fractures led to the deposition of the vein material. The method of transport and deposition and the changing chemistry of the ore fluid resulted in the paragenetic sequence which is observed in the veins today. A temperature maximum of the fluid was probably attained under the influence of the diabase intrusions.

After reaching the temperature maximum, it appears that the ore-fluids cooled very gradually and eventually to temperatures less than 100° C. The processes which tended to cool the fluid would probably be heat loss to the wallrocks and expansion of the fluid. TOULMIN and CLARK (1967) show that the latter process may closely approximate reversible and irreversible adiabatic expansion, where the fluid expands slowly rising along open stretches of vein and expands rapidly

where the vein system is constricted. It has been shown that meteoric water may enter the system during the waning stages of deposition. This may have been responsible for finally cooling and diluting the ore fluid.

It would be quite feasible that the deposition of other similar vein-type U-Co-Ni-Ag deposits followed a similar history to that postulated for Echo Bay. Certainly the other deposits, which have been mentioned previously, often occur in geologically similar situations and have a similar mineralogy. However, there are often differences in the exact paragenesis and thus different chemical regimes have been effective. More data from fluid inclusions, stable isotopes and mineral assemblages would be needed in the Echo Bay deposit and the other deposits to effect comparisons as far as a geochemical evolution is concerned. As expressed by WHITE (loc. cit.), most ore deposits are formed by complex rather than by simple 'end-member' processes and all the constituents in a deposit may have been derived from two or more sources. Isotopic studies at Echo Bay, however, indicate that no magmatic solutions were added to the ore fluid, that is, certainly not in any noticeable proportions. This is not to say, however, that there may have been minor contributions of material by fluids from the diabase activity.

Most ore forming processes have taken place in a series of steps, in order to obtain the necessary enrichment of material, otherwise the more normal trends of geochemical dispersion would be dominant. Regional differences in the mantle may be reflected in volcanic rocks of certain areas such as the silver province of Great Bear Lake. The processes of formation of volcanic tuff through sedimentation and

diagenesis appear to have acted as an initial concentrator of metals from the rock. The later metamorphic event apparently effected a secondary enrichment, in that mobile constituents became part of the potential ore fluid.

Theories as to the origin of ore deposits have been divided into those of syngenetic and those of an epigenetic nature. Considering the position of the Echo Bay deposit within this classification which appears to be based on extreme cases, all gradations between the two extremes would be expected to occur. On the other hand, it has been noted by AMSTUTZ (1959) that missing transitions do occur between the typically contact or non-congruent deposits and the stratiform and congruent deposits. Due to the relatively rapid developments in ore studies, these theories will be undoubtedly modified and probably put on a more quantitative basis. It has been suggested by AMSTUTZ (1969) that theories developed for the origin of ore deposits have displayed a strong human relativity. In fact, only in the last ten years has there been any trend towards the acceptance of syngenetic theories of ore deposition. Also within the last few years, the discovery and detailed documentation of geothermal brines and the application of intense geochemical and isotopic studies has modified and will modify the trends of though concerning the genesis of ore deposits. The geochemical model derived for the Echo Bay deposit is one which could be used to explain other types of ore deposits. Obviously very special conditions must occur to produce such a mineralogy. More work is required on the conditions of metal transport and deposition before the precise conditions can be obtained.

## CONCLUSIONS

A summary of the main conclusions derived from this study has been interpreted in terms of the geological history of the area and presented in the previous chapter. At this stage it is now interesting to review the uses and applications of this kind of study. In particular, the most important fields of study which might serve as a continuation of this work should be suggested.

The detailed geology of the Great Bear Province is not well known. In particular, the dilemmas concerning the equivalence of the Echo Bay and Snare Groups, the presence or absence of Yellowknife Group rocks, the age-spread of the granitic intrusives and the nature of the different feldspar porphyry bodies are probably the most important, among many. A combination of field geology and geochronology would be required on an intense scale to solve these problems within the province. Detailed mapping and geochronology of small areas such as the Echo Bay Mine area would then be more meaningful. More geochronological data such as the age-dating of the diabase sill and dykes are required at Echo Bay, but although such information is of parochial use, its full value would not be realized until further geochronological studies are carried out in the province as a whole.

Turning now to the silver-uranium deposits of this area, a large number of mines of various sizes have been and are at present in production. It thus seems desirable that a correlative study of all these mineral occurrences could be initiated. Features such as the particular kind of mineralisation, the local rock-types, the structure and the geological



history of events would be required as a basic minimum for this study. Geochemical data on the vein materials would also be useful. Also, one should remember that not only areas which are being or have been mined should be studied. On the contrary, any area of mineralisation is of potential interest in adding to the understanding of the ore deposits in this area. However, considering the logistics pertinent to this remote part of the Canadian Shield, then it is often only feasible to work in areas of immediate economic interest. Unfortunately many data have already been lost from the mines which have been closed down and also with them has gone the unique opportunity of sampling these ore bodies and the associated wall-rocks at known levels underground.

It should be stressed here that the Echo Bay Mine is at the moment under development and in fact was so during the course of this study. Six new levels have now been established since the author was last at the mine. Thus a unique opportunity is in the process of developing whereby in the order of one thousand feet of vein sections may be studied. This permits studies on the differences exhibited by the veins and possible correlations with the host rocks to be made much more easily. In particular, petrographic and geochemical work on drill core samples would be of great value in a wall-rock alteration study with relation to the particular vein types present. Drill core studies would also be useful in detecting any depletion of the metals in the host rocks close to the veins. This type of detailed underground work plus the correlations obtained from other mines should further elucidate the major factors controlling the distribution of veins in the area.

The comparison of the geochemical data obtained from Echo Bay with similar data from other deposits in this area should be of value in determining the factors which have controlled the paragenetic sequence of the minerals observed in the veins. In this way, a full picture of the controls of the individual minerals, particularly those of economic value, within the veins would be obtained. The geochemical studies at Echo Bay have shown that probably only the early and late conditions of the vein fluids were favourable to the formation of native silver. Also silver would not be found contemporaneous with the main sulphide and carbonate minerals. The pitchblende and Co-Ni-arsenide minerals are early minerals in the veins because of the particular circumstances of their mode of transportation and early vein fluid conditions. Thus, determining to what stage a vein has developed might be indicative of the potential for finding copper, silver or uranium for example.

The main ore-vein control at Echo Bay appears to be of a dominantly structural nature. Structural traps in the area appear to have formed by a slight vertical movement within the fracture zones and are most common in the sedimentary and tuffaceous members of the Echo Bay group. One of the most intriguing possibilities of ore potential at the Echo Bay Mine is the intersection of Echo Bay fracture system with the favourable rock types of the Port Radium Mine. The stratified tuffs and sediments of the Port Radium Mine intersect the Echo Bay fracture system at approximately the present depth of the internal shaft development. Also the tuffs of the Echo Bay Mine will intersect at depth those fractures which crop out between the Echo Bay Mine and Glacier Bay. Barren quartz veins and some slight radioactivity

and mineralisation have been observed in the latter fractures where they intersect the lavas of the Upper Echo Bay Group. Thus, theoretically, many more ore-bearing veins may occur in the area, but obviously many of the possibilities will be difficult to test.

For the areas not within the immediate vicinity of the mine, similar rock units and structures should be prospected. Mineralisation can be tested for by both geochemical and geophysical methods. Uranium and its daughter products should serve as an indicator of ore zones both in geochemical and scintillometer surveys. Ni, Co, As and possibly Bi would also be of use in geochemical surveys. The small amounts of Hg detected in the native silver at Echo Bay may result in mercury haloes which could prove to be possible indicators for these veins.

REFERENCES

- ABBEY, S. and MAXWELL, J.A., 1960, Determination of potassium in micas. *Chem. Can.* 12, 37-41.
- ALDRICH, L.T., WETHERILL, G.W., TILTON, G.R. and DAVIS, G.L., 1956, Half life of Rb<sup>87</sup>. *Phys. Rev.* 103, 1045-1047.
- ALDRICH, L.T. and WETHERILL, G.W., 1958, Geochronology and radioactive decay. *Ann. Rev. Nucl. Sci.* 8, 257-298.
- ALLEN, E.T., CRENSHAW, J.L. and MERWIN, M.E., 1914, Effect of temperature and acidity in the formation of marcasite and wurtzite; a contribution to the genesis of unstable forms. *Am. J. Sci.* 38, 393-431.
- AMSTUTZ, G.C., 1959, Syngenetic zoning in ore deposits. *Proc. Geol. Assoc. Can.* 11, 95-102.
- AMSTUTZ, G.C., RAMDOHR, P., ELBAZ, F. and PARK, W.C., 1964, Diagenetic behaviour of sulphides. In *Developments in Sedimentology* Vol. 2, *Sedimentology and ore genesis*. Ed. G.C. Amstutz. Elsevier, p. 65-90.
- AMSTUTZ, G.C., 1969, The logic of some relations in ore genesis. In *Sedimentary ores ancient and modern*. Ed. C.H. James. *Proc. 15th Inter. Univ. Geol. Congr., Leicester, 1967*. Pub. Dept. of Geol., Univ. of Leicester, p. 13-29.
- ANDERSON, G.M., 1967, Specific volumes and fugacities of water. In *Appendix I of Geochemistry of hydrothermal ore deposits*. Ed. H.L. Barnes. Holt, Rinehart and Winston, New York, p. 632-635.

- ANGER, G., NIELSEN, H., PUCHELT, H. and RICKE, W., 1966, Sulfur isotopes in the Rammelsberg ore deposit (Germany). *Econ. Geol.* 61, 511-536.
- BAADSGAARD, H., 1965, Geochronology. *Medds. fra Dansk. Geol. Foren.* 16, 1-48.
- BAADSGAARD, H., FOLINSBEE, R.E. and LIPSON, J., 1961, Caledonian or Acadian granites of the Northern Yukon Territory. In *Geology of the Arctic.* University of Toronto Press, Toronto.
- BACHINSKI, D.J., 1969, Bond strength and sulfur isotope fractionation in coexisting sulfides. *Econ. Geol.* 64, 56-65.
- BARNES, H.L., 1962, Mechanisms of mineral zoning. *Econ. Geol.* 57, 137-141.
- BARNES, H.L. and KULLERUD, G., 1961, Equilibria in sulfur-containing aqueous solutions in the system Fe-S-O and their correlation during ore deposition. *Econ. Geol.* 56, 648-688.
- BARNES, H.L. and CZAMANSKE, G.K., 1967, Solubilities and transport of ore minerals. In *Geochemistry of hydrothermal ore deposits.* Holt, Rinehart and Winston, New York. p. 334-436.
- BARNES, H.L. and SCOTT, S.D., 1969, Geothermometry based on iron-rich patches in sphalerite. Abstract in *Geol. Soc. Am. Ann. Mtg., Atlantic City, 1969.*
- BARTON, P.B., Jr., 1959, The chemical environment of ore deposition and the problem of low-temperature ore transport. In *Researches in geochemistry.* Ed. P.H. Abelson. John Wiley and Son, New York, p. 279-300.

- BARTON, P.B., Jr. and TOULMIN, P. III, 1964, The electrometallurgical method for the determination of the fugacity of sulfur in laboratory sulfide systems. *Geochim. Cosmochim. Acta* 28, 619-640.
- BARTON, P.B., Jr. and TOULMIN, P. III, 1966, Phase relations involving sphalerite in the Fe-Zn-S system. *Econ. Geol.* 61, 815-849.
- BARTON, P.B. and SKINNER, B.J., 1967, Sulfide mineral stabilities. In *Geochemistry of hydrothermal ore deposits*. Ed. H.L. Barnes. Holt, Rinehart and Winston, New York, p. 236-333.
- BASTIN, E.S., 1950, Interpretation of ore textures. *G.S.A. Memoir* 45.
- BERRY, F.A., 1966, Proposed origin of subsurface thermal brines, Imperial Valley, California. *Am. Assoc. Petrol. Geol. Bull.* 50, 644-645.
- BERRY, F.A., 1967, Role of membrane hyperfiltration on origin of thermal brines, Imperial Valley, California. Abstract in *Am. Assoc. Petrol. Geol. Bull.* 51, 454-455.
- BOYLE, R.W., 1951, An occurrence of native gold in an ice lens, Giant Yellowknife Gold Mines, Yellowknife, Northwest Territories. *Econ. Geol.* 46, 223-227.
- BOYLE, R.W., 1960, Occurrence and geochemistry of native silver in the lead-zinc-silver lodes of the Keno Hill-Galena Hill area, Yukon, Canada. *Neues Jahrb. f. Min., Festband Ramdohr, Abhand. Bd.* 94, 280-297.
- BOYLE, R.W., 1961, The geology, geochemistry and origin of the gold deposits of the Yellowknife district, *G.S.C. Memoir* 310.
- BOYLE, R.W., 1965, Discussion at Symposium-Problems of postmagmatic ore deposition, Vol. II, Prague 1965, p. 459-460.

- BOYLE, R.W., 1968a, Fahlbands sulfide schists and ore deposition. Econ. Geol. 63, 835-840.
- BOYLE, R.W., 1968b, The geochemistry of silver and its deposits. G.S.C. Bulletin 160.
- BOYLE, R.W., WANLESS, R.K. and STEVENS, R.D., 1970, Sulfur isotope investigation of the lead-zinc-silver-cadmium deposits of the Keno Hill-Galena Hill area, Yukon, Canada. Econ. Geol. 65, 1-10.
- BROWN, H.M. and KROUSE, H.R., 1964, Fractionation of germanium isotopes in chemical reactions. Can. J. Chem. 42, 1971-1978.
- CAMPBELL, D.D., 1955, Geology of the pitchblende deposit of Port Radium, Great Bear Lake, N.W.T. Unpubl. Ph.D. thesis, C.I.T.
- CAMPBELL, D.D., 1957. Port Radium Mine. In Structural geology of Canadian ore deposits. Can. Inst. Min. Met. 2, 177-189.
- CARD INDEX OF ORE PHOTOMICROGRAPHS, 1960. Umschau Verlag, Frankfurt am Alain, W. Germany.
- CHATTERJEE, 1962. Beitr. Miner. Petrogr. 8, 432-439.
- CLAYTON, R.N. and EPSTEIN, S., 1958, The relationship between  $O^{18}/O^{16}$  ratios in coexisting quartz, carbonate and iron oxides from various geological deposits. J. Geol. 66, 352-373.
- COOMBS, D.S., 1961, Some recent work on the lower grades of metamorphism. Australian J. Sci. 24, 203-215.
- CRAIG, H., 1957, Isotopic standards for carbon and oxygen and correction factors for mass-spectrometric analysis of carbon dioxide. Geochim. Cosmochim. Acta 12, 133.

- CRAIG, H., 1966, Isotopic composition and origin of the Red Sea and Salton Sea geothermal brines. *Science* 154, 1544-1548.
- CUMMING, G.L., 1969, A recalculation of the age of the solar system. *Can. J. Earth Sci.* 6, 719-736.
- CUMMING, G.L., WILSON, J.T., FARQUHAR, R.M. and RUSSELL, R.D., 1955, Some dates and subdivisions of the Canadian Shield. *Proceedings Geol. Assoc. Can.* 7, part 2, 27-79.
- DAMON, P.E., 1967, Potassium-argon dating of igneous and metamorphic rocks with applications to the Basin Ranges of Arizona and Sonora. In *Radiometric dating for geologists*. Eds. E.T. Hamilton and K.M. Farquhar. Interscience, London.
- DEGENS, E.T. and EPSTEIN, S., 1964, Oxygen and carbon isotope ratios in coexisting calcites and dolomites from recent and ancient sediments. *Geochim. Cosmochim. Acta* 28, 23-44.
- DICKINSON, W.R., 1970, Relations of andesitic volcanic chains and granitic batholith belts to the deep structures of orogenic arcs. *Proc. Geol. Soc. London* No. 1662, 27-35.
- DUNHAM, K., 1970, Stratabound sulfide deposits: rock association and genesis. IMA-IAGOD meeting Abstracts, Symposium D-IAGOD, Japan, 1970.
- ECKELMANN, W.R. and KULP, J.L., 1957, Uranium-lead method of age determination: Part II - North American localities. *Geol. Soc. Am. Bull.* 68, 1117-1140.
- ELLIS, A.J., 1967, The chemistry of some explored geothermal systems. In *Geochemistry of hydrothermal ore deposits*. Ed. H.L. Barnes. Holt, Rinehart and Winston, New York, p. 465-514.



- ELLIS, A.J. and GOLDING, R.M., 1963, The solubility of carbon dioxide above 100° C in water and in sodium chloride solutions. *Am. J. Sci.* 261, 47-60.
- EPSTEIN, S., GRAF, D.L. and DEGENS, E.T., 1964, Oxygen isotope studies on the origin of dolomites. In *Isotopic and cosmic chemistry*. Eds. H. Craig, S.L. Miller and G.J. Wasserburg. North-Holland Publishing Company, Amsterdam.
- EVERHART, D.L. and WRIGHT, R.J., 1953, The geologic character of typical pitchblende veins. *Econ. Geol.* 48, 77-96.
- FAHRIG, W.H. and WANLESS, R.K., 1963, Age and significance of diabase dyke swarms in the Canadian Shield. *Nature*, 200, 934-937
- FENIAK, M., 1947, The geology of Dowdell Peninsula, Great Bear Lake, N.W.T. G.S.C. Spec. Rept. 14 pp.
- FIELD, C.W., 1960, Sulfur isotope geology of vein-type and sandstone-type uranium deposits. Unpub. Ph.D. Dissertation, Yale University.
- FLYNN, K.F. and GLENDENIN, L.E., 1959, Half-life and beta spectrum of Rb<sup>87</sup>. *Phys. Rev.* 116, 744-748.
- FRITZ, P., 1969, The oxygen and carbon isotopic composition of carbonates from the Pine Point lead-zinc ore deposit. *Econ. Geol.* 64, 733-742.
- GAMMON, J.B., 1966, Fahlbands in the Precambrian of southern Norway. *Econ. Geol.* 61, 174-188.
- GAMMON, J.B., BORCSIK, M. and HOLLAND, H.D., 1969, Potassium-sodium ratios in aqueous solutions and coexisting silicate melts. *Science* 163, 179-181.

- GARRELS, R.M. and CHRIST, C.L., 1965, Solution, minerals and equilibria. Harper and Row, New York, 450 pp.
- GAUCHER, E., 1964, A possible solution to the paradox of the 'sedimentary' bornite. *Econ. Geol.* 59, 303-308.
- GOLDICH, S.S., NIER, A.O., BAADSGAARD, H., HOFFMAN, J.H. and KRUEGER, H.W., 1961, The Precambrian geology and geochronology of Minnesota. *Minn. Geol. Surv. Bull.* 41, 1-193.
- GOLDSCHMIDT, V.M., 1958, *Geochemistry*. Oxford University Press, 730 pp.
- GOODSPEED, G.E., 1952, Mineralisation related to granitisation. *Econ. Geol.* 47, 146-168.
- GREEN, D.C., 1968, Precambrian geology and geochronology of the Yellowknife area, N.W.T. Unpublished Ph.D. thesis, Univ. of Alberta.
- GROOTENBOER, J. and SCHWARCZ, H.P., 1969, Experimentally determined sulfur isotope fractionations between sulfide minerals. *Earth Planet. Sci. Letters* 7, 162-166.
- GROVES, D.I., SOLOMON, M. and RAFTER, T.A., 1970, Sulfur isotope fractionation and fluid inclusion studies at the Rex Hill Mine, Tasmania. *Econ. Geol.* 65, 459-469.
- HARPER, 1967, On the interpretation of K-Ar ages from Precambrian Shields and Phanerozoic orogens. *Earth Planet. Sci. Letters* 3, 128-132.
- HELGESON, H.C., 1964, *Complexing and hydrothermal ore deposition*. Pergamon Press, 128 pp.

- HELGESON, H.C., 1966, Silicate metamorphism in sediments and the genesis of hydrothermal solutions. In Symposia of the genesis of stratiform lead-zinc-barite-fluorite deposits. Econ. Geol., Monograph 3, 333-342. Econ. Geol. Pub. Co., Lancaster, Penna.
- HELGESON, H.C., 1967, Solution chemistry and metamorphism. In Researches in geochemistry, Vol. 2, Ed. P.H. Abelson. John Wiley and Son, New York, p. 362-404.
- HELGESON, H.C., 1968, Geologic and thermodynamic characterisation of the Salton Sea geothermal system. Am. J. Sci. 266, 129-166.
- HELGESON, H.C., 1969, Thermodynamics of hydrothermal systems at elevated temperatures and pressures. Am. J. Sci. 267, 729-804.
- HELGESON, H.C., 1970, A chemical and thermodynamic model of ore deposition in hydrothermal systems. Mineral. Soc. Amer. Spec. Pap. 3, 155-186.
- HELGESON, H.C., BROWN, T.H. and LEEPER, R.H., 1969, Handbook of theoretical activity diagrams depicting chemical equilibria in geologic systems involving an aqueous phase at one atmosphere and 0° to 300° C. Freeman, Cooper and Co., San Francisco, California, 253 pp.
- HEMLEY, J.J. and JONES, W.R., 1964, Chemical aspects of hydrothermal alteration with emphasis on hydrogen metasomatism. Econ. Geol. 59, 538-569.
- HOFFMAN, P., 1969, Proterozoic paleocurrents and depositional history of the East Arm fold belt, Great Slave Lake, Northwest Territories. Can. J. of Earth Sci. 6, 441-462.

- HOLLAND, H.D., 1959, Some applications of thermochemical data to problems of ore deposits I. Stability relations among the oxides, sulfides, sulfates and carbonates of ore and gangue metals. *Econ. Geol.* 54, 184-233.
- HOLLAND, H.D., 1965, Some applications of thermochemical data to problems of ore deposits II. Mineral assemblages and the composition of ore forming fluids. *Econ. Geol.* 60, 1101-1166.
- HOLMES, H., 1965, Principles of physical geology. Nelson, London, 1288 pp.
- HULSTON, J.R., 1970, Theoretical fractionation calculations on sulfides (unpublished data). Source. GROVES et al. (1970).
- HURLEY, P.M., HUGHES, H., PINSON, W.F. and FAIRBAIRN, H.W., 1962, Radiogenic argon and strontium diffusion parameters in biotite at low temperatures from Alpine fault uplift in New Zealand. *Geochim. Cosmochim. Acta* 26, 67-80.
- JENSEN, M.L., 1967, Sulfur isotopes and mineral genesis. In *Geochemistry of hydrothermal ore deposits*. Ed. H.L. Barnes, Holt, Rinehart, and Winston, New York, p. 143-165.
- JOLLIFFE, A.W., 1948, The northwestern part of the Canadian Shield. *Int. Geol. Congress, 18 Session, Part 8*, p. 141-149.
- JORY, L.T., 1964, Mineralogical and isotopic relations in the Port Radium pitchblende deposit, Great Bear Lake, Canada. Unpublished Ph.D. thesis, C.I.T.
- KAJIWARA, Y., KROUSE, H.R. and SASAKI, A., 1969, Experimental study of sulfur isotope fractionation between coexistent sulfide minerals. *Earth Planet. Sci. Letters* 7, 271-277.

- KAJIWARA, Y. and KROUSE, H.R., 1970, Sulfur isotope geothermometry: Pyrite-pyrrholite-chalcopyrite-galena-sphalerite systems. G.S.A. Abstracts vol. 2, no. 7. Milwaukee, Wisconsin, 1970.
- KANASEWICH, E.R., 1968, The interpretation of lead isotopes and their geological significance. In Radiometric dating for geologists. Eds. E.I. Hamilton and R.M. Farquhar. Interscience, London.
- KEILLER, B.J., 1962, Mineralogy of the no. 2 zone Eldorado Mine, Port Radium, N.W.T. Unpubl. M.Sc. thesis, Univ. of Alberta.
- KELLY, W.C. and TURNEAURE, F.S., 1970, Mineralogy, paragenesis and geothermometry of the tin and tungsten deposits of the eastern Andes, Bolivia. Econ. Geol. 65, 609-680.
- KIDD, D.F., 1931, Great Bear Lake - Coppermine River Area, MacKenzie District, N.W.T. G.S.C. Sum. Rept., Part c, p. 47-69.
- KIDD, D.F., 1933, Great Bear Lake Area, N.W.T., G.S.C. Sum. Rept., Part C, p. 1-36.
- KIDD, D.F. and HAYCOCK, M.H., 1935, Mineragraphy of the ores of Great Bear Lake. Bull. Geol. Soc. Amer., 46, 879-960.
- KISSIN, I.G. and PAKHOMOV, S.I., 1969, Alteration of sea water in reactions with rocks at higher temperature. Doklady, ESS 187, 185.
- KLEMENT, W., JAYARAMAN, A. and KENNEDY, G.C., 1963, Phase diagrams of arsenic, antimony and bismuth at pressures up to 70 Kilobars. Phys. Rev. 131, 632-637.
- KOZINTSEVA, T.N., 1965, Solubility of hydrogen sulfide in water and solutions under high temperature. In Geochemical investigations in the field of higher pressures and temperatures. Ed. N.I. Khitarov. Nauka Pub. Office, Moscow, p. 121-134.

- KRANZ, R., 1970, Organic geochemistry and radioactive disequilibrium in the Ag-Co-U-ore veins of Witticher, Black Forest, Germany. IMA-IAGOD Meeting, Japan, 1970.
- KROUSE, H.R. and THODE, H.G., 1962, Thermodynamic properties and geochemistry of isotopic compounds of selenium. Can. J. Chem. 40, 367-375.
- LAMBERT, I.B. and BUBELA, B., 1970, The experimental production of monomineralic sulphide bands in sediments. Minera. Deposita 5, 97-102.
- LEECH, A.P., 1965, A reconnaissance: Basic intrusive rocks of the Precambrian Shield, Canada. Unpublished M.Sc. thesis, Univ. of Alberta.
- LEECH, G.B., LOWDON, J.A., STOCKWELL, C.H., and WANLESS, R.K., 1963, Age determinations and geological studies (including isotopic studies - report 4). G.S.C. Paper 63-17.
- LEMMLEIN, G.G. and KLEVTSOV, P.V., 1961, Relations among the principal thermodynamic parameters in a part of the system  $H_2O-NaCl$ . Geochem. No. 2, 148-158.
- LONG, J.V.P., 1967, Electron probe microanalysis In Physical methods in determinative mineralogy. Ed. J. Zussman. Academic Press, London, p. 215-260.
- LOWDON, J.A., 1960, Age determinations by the Geological Survey of Canada, Report No. 1 Isotopic Ages. G.S.C. Paper 60-17.
- LOWDON, J.A., 1961, Age determinations by the Geological Survey of Canada, Report No. 2 Isotopic Ages. G.S.C. Paper 61-17.

- LOWDON, J.A., STOCKWELL, C.H., TUPPER, H.W., and WANLESS, R.K., 1963, Age determinations and geological studies (including Report No. 3 Isotopic ages). G.S.C. Paper 62-17.
- MACINTYRE, I., 1970, Why the sea is salt. *Sci. Amer.*, 223, 104-115.
- MALLET, J.W., 1887, On the occurrence of silver in volcanic ash from the eruption of Cotopaxi of July 22nd and 23rd, 1885. *Proc. Roy. Soc.* 42, 1-3.
- MALLET, J.W., 1890, On a second case of the occurrence of silver in volcanic dust, namely in that thrown out on the eruption of Tunguragua in the Andes of Ecuador, January 11th, 1886. *Proc. Roy. Soc.* 47, 277-281.
- MCCULLOUGH, H. and KROUSE, H.R., 1965, Application of digital recording to simultaneous collection in mass spectrometry. *Rev. Scient. Instr.* 36, 1132-1134.
- MCKELVEY, V.E., EVERHART, D.L. and GARRELS, R.M., 1955, Origin of uranium deposits. *Econ. Geol.*, 50, 464-533.
- MELENT'YEV, B.N., IVANENKO, V.V. and PAMFILOVA, L.A., 1969, Solubility of some ore-forming sulfides under hydrothermal conditions. *Geochem. International.* 6, No. 2, 416-460.
- MEYER, C. and HEMLEY, J.J., 1967, Wall rock alteration. In *Geochemistry of hydrothermal ore deposits*. Ed. H.L. Barnes. Holt, Rinehart and Winston, New York, p. 166-235.
- MRNA, F., 1963, Deposit of Ag-Bi-Co-Ni ores in Gachymov. *Symposium-Problems of post magmatic ore deposition - Some ore deposits of the Bohemian Masif-guide to excursion*. Czech. Acad. Sci. Prague, p. 43-54.

- MURSKY, G., 1962, Mineralogy, petrology and geochemistry of Hunter Bay area, N.W.T., Great Bear Lake, Canada. Unpub. Ph.D. thesis, Stanford University.
- NAUMOV, G.B., 1961, Some physicochemical characteristics of the behaviour of uranium in hydrothermal solutions. *Geochem.* No. 2, 127-147.
- NICOLAYSEN, L.O., 1961, Graphic interpretation of discordant age measurements on metamorphic rocks. *Ann. N.Y. Acad. Sci.* 91, 198-206.
- NORTHROP, D.A. and CLAYTON, R.N., 1966, Oxygen-isotope fractionation in systems containing dolomite. *J. Geol.* 74, 174-196.
- OHMOTO, H., 1968, The Bluebell Mine, British Columbia, Canada. Part 2 - Chemistry of the hydrothermal fluids. Unpub. Ph.D. thesis, Princeton University.
- OHMOTO, H., 1970, Influence of pH and  $f_{O_2}$  of hydrothermal fluids on the isotopic composition of sulfur species. *Abstract G.S.A. Ann. Mtg., Vol. 2, No. 7, Milwaukee, Wisconsin, 1970.*
- OHMOTO, H. and RYE, R.O., 1970, The Bluebell Mine, British Columbia: 1. Mineralogy, paragenesis, fluid inclusions and isotopes of hydrogen, oxygen and carbon. *Econ. Geol.* 65, 417-437.
- O'NEIL, J.R. and EPSTEIN, S., 1966, Oxygen isotope fractionation in the system dolomite-calcite- $CO_2$ . *Science* 152, 198-201.
- O'NEIL, J.R., CLAYTON, R.N. and MAYEDA, T.K., 1969, Oxygen isotopic fractionation in divalent metal carbonates. *J. Chem. Physics* 51, No. 2, 5547-5558.



- O'NIONS, R.K., 1969, Geochronology of the Bamble Sector of the Baltic Shield, south Norway. Unpubl. Ph.D. thesis, Geology Dept., Univ. of Alberta.
- PARK, C.F. and MACDIARMID, R.A., 1964, Ore deposits. Freeman and Co., San Francisco, 475 pp.
- PETRUK, W., 1968, Mineralogy and origin of the Silverfields silver deposit in the Cobalt area, Ontario. Econ. Geol. 63, 512-531.
- PETRUK, W. and HARRIS, D.C., 1968, Native silver and silver-antimony minerals in the Cobalt-Gowganda ores, G.S.A. Ann. Mtg., Mexico City, 1968.
- PUCHELT, H. and KULLERUD, G., 1970, Sulfur isotope fractionation in the Pb-S system. Earth Planet. Sci. Letters 7, 301-306.
- RAFAL'SKIY, R.P. and ZARUBIN, A.I., 1969, The behaviour of sulfur in hydrothermal solutions. Doklady Akademii Nauk SSSR E.S.S. 187, No. 3, 658-660.
- RAYMAHASHAY, B.C. and HOLLAND, H.D., 1969, Redox reactions accompanying hydrothermal and rock alteration. Econ. Geol. 64, 291-305.
- ROBINSON, B.W., 1967, High pressure and temperature investigations on pyrite with natural rock systems. Unpub. M.Sc. dissertation, Univ. of Leeds.
- ROBINSON, B.W. and STRENS, R.G.J., 1968, Genesis of concordant deposits of base metal sulfides: an experimental approach. Nature 217, 535-536.
- ROBINSON, B.W. and MORTON, R.D., 1971, Mckinstryite from the Echo Bay Mine, N.W.T., Canada. Econ. Geol. in press.

- ROBINSON, H.S., 1933, Notes on the Echo Bay District, Great Bear Lake, N.W.T. Can. Inst. Mining Metal., 609-629.
- ROEDDER, E., 1962, Studies of fluid inclusions: I. Low temperature applications of a dual purpose freezing and heating stage. Econ. Geol. 57, 1045-1061.
- ROEDDER, E., 1963, Studies of fluid inclusions: II. Freezing data and their interpretation. Econ. Geol. 58, 167-211.
- ROEDDER, E., 1966, The noncolloidal origin of "colloform" textures in sphalerite ores. Econ. Geol. 63, 451-471.
- ROEDDER, E., 1967, Fluid inclusions as samples of ore fluids. In Geochemistry of hydrothermal ore deposits. Ed. H.L. Barnes. Holt, Rinehart and Winston, New York, p. 515-574.
- ROMBERGER, S.B. and BARNES, H.L., 1963, Sulfide solubilities in synthetic ore solutions. Trans. Amer. Geophys. Union 44, N-. 1.
- RYE, R.O. and CZAMANSKE, G.K., 1969, Experimental determination of sphalerite-galena sulfur isotope fractionation and application to the ores at Providencia, Mexico. Abstract G.S.A. Mtg., Atlantic City, 1969.
- RYE, R.O. and HAFFTY, J., 1969, Chemical composition of the hydrothermal fluids responsible for the lead-zinc deposits at Providencia, Zacatecas, Mexico. Econ. Geol. 64, 629-643.
- SAKAI, H., 1966, Sulphur isotope chemistry of poly sulphide solution - kinetic isotope effects in thiocyanidization. J. Inorg. Nucl. Chem. 28, 1567-1573.
- SAKAI, H., 1968, Isotopic properties of sulfur compounds in hydrothermal processes. Geochem. Jour. 2, 29-49.
- SASAKI, A. and KAJIWARA, Y., 1969, Evidence of isotopic equilibrium between seawater sulfate and some syngenetic sulfide ores. Abstracts IMA-IAGOD Meeting, 4 Symposium D-IAGOD, Japan 1970.

- SATO, T., 1970, Physicochemical environments of 'Kuroko' mineralisation at Uchinotai Deposit of Kosaka Mine, Akita Prefecture. Abstracts IMA-IAGOD Meetings, 5 Joint Symposium, Japan, 1970.
- SAWKINS, F.J., 1964, Lead-zinc ore deposition in the light of fluid inclusion studies: Providencia Mine, Zacatecas, Mexico. Econ. Geol. 59, 883-919.
- SAWKINS, F.J., 1966, Ore deposition in the North Pennine orefield in the light of fluid inclusion studies. Econ. Geol. 61, 385-401.
- SAWKINS, F.J., 1968, The significance of Na/K and Cl/SO<sub>4</sub> ratios in fluid inclusions and subsurface waters with respect to the genesis of Mississippi Valley - type ore deposits. Econ. Geol. 63, No. 8, 935-942.
- SAWKINS, F.J. and RYE, R.O., 1970, The Casapalca silver-lead-zinc-copper deposit, Peru: An ore deposit formed by hydrothermal solutions of deep seated origin? Abstract G.S.A. Ann. Mtg., Milwaukee, Wisconsin, 1970.
- SCHNEIDER, A., 1970, The sulphur isotope composition of basaltic rocks. Contr. Mineral. Petrol. 25, 95-124.
- SCHWARCZ, H.P., 1966, Oxygen and carbon isotope fractionation between coexisting metamorphic calcite and dolomite. J. Geol. 74, No. 1, 38-48.
- SHARMA, T. and CLAYTON, R.N., 1965, Measurement of O<sup>18</sup>/O<sup>16</sup> ratios of total oxygen of carbonates. Geochim. Cosmochim. Acta. 29, 1347-1353.

- SHEPPARD, S.M.F. and SCHWARCZ, H.P., 1970, Fractionation of carbon and oxygen isotopes and magnesium between coexisting metamorphic calcite and dolomite. *Contr. Mineral. and Petrol.* 26, 161-198.
- SKINNER, B.J., 1966, The system Cu-Ag-S. *Econ. Geol.* 61, 1-26.
- SKINNER, B.J., JAMBOR, S.L. and ROSS, M., 1966, Mckinstryite a new copper-silver sulphide. *Econ. Geol.* 61, 1383-1389.
- SMITH, D.G.W. and TOMLINSON, M.C., 1970, An APL language computer program for use in electron microprobe analysis. *Computer Contribution 45*, State Geological Survey, Univ. of Kansas, Lawrence, 1970.
- SMITH, F.G., 1962, Geothermometry and geobarometry. In *Physical geochemistry*. Addison Wesley Co. Ltd., Massachusetts, p. 476-524.
- SMITHERS, R.M. and KROUSE, H.R., 1968, Tellurium isotope fractionation study. *Can. J. Chem.* 46, 583-591.
- STEINER, R.L. and RAFTER, T.A., 1966, Sulfur isotopes in pyrite, pyrrotite, alunite and anhydrite from steam wells in the Taupo volcanic zone, New Zealand. *Econ. Geol.* 61, 1115-1129.
- STOCKWELL, C.H., 1964, Age determinations and geological studies. Part II Geological studies. G.S.C. Paper 64-17.
- TAKENOUCHI, S. and KENNEDY, G.C., 1965, The solubility of carbon dioxide in NaCl solutions at high temperatures and pressures. *Am. J. Sci.* 263, 445-454.
- TAYLOR, S.R., 1969, Trace element chemistry of andesite and associated calc-alkaline rocks. *Proc. Symp. on Andesites*, Univ. of Oregon.

- TAYLOR, S.R., CAPP, A.C., GRAHAM, A.L. and BLAKE, D.H., 1969, Trace element abundances in andesites. *Contr. Mineral. and Petrol.* 23, 1-26.
- THOMSON, R., 1957, Cobalt camp. In *Structural geology of Canadian ore deposits II*, 6th Commonwealth Mining and Metal. Congress, p. 377-387.
- TOULMIN, P. III and CLARK, S.P. Jr., 1967, Thermal aspects of ore formation. In *Geochemistry of hydrothermal ore deposits*. Ed. H.L. Barnes. Holt, Rinehart and Winston, New York, p. 437-464.
- TURNER, F.J., 1968, *Metamorphic petrology*. McGraw Hill, New York, 403 pp.
- TURNER, F.J. and VERHOOGEN, J., 1960, *Igneous and metamorphic petrology*. McGraw Hill, New York, 694 pp.
- WALKER, G.P., 1960, Zeolite structures and dike distribution in relation to the structure of the basalts of eastern Greenland. *J. Geol.* 68, 515-528.
- WANLESS, R.K., BOYLE, R.W. and LOWDON, J.A., 1960, Sulfur isotope investigation of the gold-quartz deposits of the Yellowknife district. *Econ. Geol.* 55, 1591-1621.
- WANLESS, R.K., STEVENS, R.D., LACHANCE, G.R. and RIMSAITE, J.Y.H., 1965, Age determinations and geological studies. Part I - Isotopic ages, Report 5, G.S.C. Paper 64-17.
- WANLESS, R.K., STEVENS, R.D., LACHANCE, G.R. and RIMSAITE, J.Y.H., 1966, Age determinations and geological studies. K-Ar isotopic ages, Report 6, G.S.C. Paper 65-17.

- WANLESS, R.K., STEVENS, R.D., LACHANCE, G.R. and EDMONDS, C.M., 1967, Age determinations and geological studies. K-Ar isotopic ages, Report 7, G.S.C. Paper 66-17.
- WANLESS, R.K., STEVENS, R.D., LACHANCE, G.R. and EDMONDS, C.M., 1968, Age determinations and geological studies. K-Ar isotopic ages, Report 8, G.S.C. Paper 67-2, Part A.
- WEBB, A.W. and McDOUGALL, I., 1968, The geochronology of the igneous rocks of eastern Queensland. J. Geol. Soc. Australia 15, Part 2, 313-346.
- WELLMAN, R.B., COOK, F.D. and KROUSE, H.R., 1968, Nitrogen 15: Microbiological alteration of abundance. Science 161, 269.
- WHITE, D.E., 1967, Mercury and base metal deposits with associated thermal and mineral waters. In Geochemistry of hydrothermal ore deposits. Ed. H.L. Barnes. Holt, Rinehart and Winston, New York. p. 575-631.
- WHITE, D.E., 1968, Environments of generation of some base-metal ore deposits. Econ. Geol. 63, 301-335.
- WINKLER, H.G.F., 1967, Petrogenesis of metamorphic rocks. Springer-Verlag, 2nd edition, 237 pp.
- YODER, H.S., 1955, The role of water in metamorphism. G.S.A. Spec. Paper 62, 505-524.
- YUND, R.A., 1961, Phase relationships in the system Ni-As. Econ. Geol. 56, 1273-1296.
- ZIELINSKI, M., 1966, Kinetic isotope effects accompanying oxidation of CO, H<sub>2</sub> and CH<sub>4</sub>. Nucl. Applic. 2, 51-54.

## APPENDIX A

DESCRIPTION OF ANALYSED SPECIMENS.

The locations of all the rock specimens mentioned in the text are given in Figure 2.

EB TUFF: Volcanic tuff. The rock is well crystallised and all original texture has been obliterated. However, in the field this rock exhibits numerous sedimentary structures and banding. Pyrite is common, up to about 5% of the total. Hornblende crystals up to 4 mm in length occur mainly in the dark green coloured bands which are about 3-5 cm wide. Actinolite, often almost indistinguishable from the hornblende, occurs as fibrous crystals. Feldspar is concentrated in the lighter coloured bands; it is fine grained and red in colour due to the presence of hematite. Hornblende plus actinolite and feldspar each constitute about 45% of the rock. Pyrite normally averages about 3%. Pistachite, sphene, apatite, scapolite, zoisite, calcite and magnetite total about 7%.

EBT 1.1: Volcanic tuff. The rock is grey-red in colour, banded and has a very fine grained groundmass with phenoclasts up to 4 mm in length. The clastic grains are composed of quartz (about 35% of the rock) and feldspar (about 20% of the rock). Sericitisation and chloritisation are extensive in the rock. Hematitisation gives the feldspars an overall red colour and prevents complete identification. The original mafics have been altered to chlorite which composes about 30% of the rock. Sericite makes up about 10% and hematite about

5% of the rock. Clinzoisite is also present.

EBT 1.2: Porphyritic andesite. The rock has abundant phenocrysts which are mainly composed of andesine with some hornblende. The original hornblende has mainly been altered to chlorite and some actinolite is present. The groundmass is very fine grained and consists of feldspar with disseminated hematite and magnetite. A small amount of feldspar (as phenocrysts) has been altered to sericite. Chabazite is found to be present in the groundmass of the rock. The approximate percentages of the various minerals are as follows: andesine 35%, K-feldspar 5%, hornblende 10%, magnetite 15%, chabazite 10%, apatite, actinolite, chlorite and sericite total 25%.

EBT 1.3: Recrystallised massive tuff. The rock is composed mainly of hornblende (edenite?) as euhedral, often fibrous, crystals of up to 2 mm in length. Feldspar occurs in the fine grained groundmass and as scattered euhedral laths. It is slightly hematized and is of oligoclase-andesine composition. The main opaque mineral is a trace of pyrite. Hornblende comprises about 70% of the rock with feldspar as 25%. Thompsonite, zoisite, biotite, sphene, apatite, calcite, chlorite and pyrite total about 5%.

EBT 1.4: Amygdaloidal andesite. Large quartz amygdales up to 1 cm in diameter characterise the rock. Euhedral feldspar laths up to 5mm in length and andesine in composition are common. Calcite, chlorite and sericite are present in these grains and also in the feldspar groundmass. Original hornblende phenocrysts up to 4 mm in length are virtually all altered to chlorite. Grains of magnetite (0.1 to 0.5 mm)



are disseminated throughout the whole rock. The approximate percentages of the minerals present are as follows: feldspar 40%, quartz (in amygdales) 30%, magnetite 15%, hornblende 5%, calcite, chlorite, sericite, sphene, zoisite and chabazite? total 10%.

The hornblende separate was about 95% pure. Magnetite, sphene and minor chlorite were the main impurities.

EBT 1.5: Volcanic tuff. This rock has abundant pyrite which often constitutes up to 10% of the rock, usually occurring in bands. Quartz grains in the rock comprise about 30% and appear to be detrital. Feldspar grains also comprise about 30% of the total rock, but they are too altered to distinguish the original form and composition. Alteration products are mainly chlorite and sericite which together total 10% of the rock. Hornblende is present possibly as edenite? and comprises 20% of the total. A few grains of original pyroxene (?) are present together with minor amounts of zircon, apatite and sphene.

EBT 2.1: Amygdaloidal andesite. This rock is very similar to EBT 1.4. The amygdales and also the phenocrysts are about half the size, but the mineralogy is the same.

EBT 2.2: Porphyritic andesite. This rock is from the same lava flow as EBT 1.2 but is separated by about 3,000 feet along strike and is about 250 feet higher in the sequence. The mineralogy is very similar except that this rock has suffered a lesser degree of alteration. Actinolite, chlorite and sericite are only about half as abundant.

The hornblende separate was over 95% pure. Magnetite composites were the main impurity.

EBT 2.4: Recrystallised tuff. The rock is a red-grey medium grained tuff which sometimes exhibits banding on the scale of several cms. It is homogeneous and normally appears recrystallised. The hornblende is quite fresh and contains only about 1% chlorite. Feldspar of oligoclase-andesine composition occurs as larger grains up to 2 mm in length. Pyrite is the main opaque mineral and occurs as well crystallised cubes. The approximate percentages of the minerals present are: hornblende 50%, plagioclase 42%, chlorite 2%, calcite, sphene, zoisite, hematite and chabazite total 1%.

EBT 2.5: Porphyritic andesite. The rock contains andesine laths up to 5 mm in length which have been quite heavily altered. Disseminated hematite has completely stained the very fine grained groundmass to a brick-red colour. The hornblende phenocrysts exhibit corroded margins where the mineral has been altered to chlorite and they contain hematite inclusions. Plagioclase comprises 55% of the rock, hornblende 25% and hematite plus chlorite total 5%.

EBT 3.1: Porphyritic andesite. This is a relatively fresh rock showing only some sericitisation of the feldspar and chloritisation of the hornblende. A few relict grains of pyroxene were observed and these probably represent an original mineral. The high amount of opaque mineral appears to be mainly magnetite plus some ilmenite which occur in a finely disseminated form in the groundmass and impart a dark grey colour to the rock. Plagioclase is 65% of the rock, hornblende 10%, sericite plus chlorite 15%, magnetite plus ilmenite 10% and pyroxene and sphene are also present.

EBT 2.1: Dolerite. The rock was classified on the following mineralogical content: plagioclase 50%, augite 15%, K-feldspar 5%, ilmenite plus magnetite 10%, sericite, calcite and chlorite total 20%. Alteration is not extensive and consists of some sericite in the feldspars and chlorite in the pyroxene. Of note is the high ilmenite plus magnetite content of the rock.

EBT QD: Quartz dolerite. The texture of the rock is sub-ophitic with major constituents augite and ladorite. Pyrite, ilmenite and magnetite form very minor sulphide and oxide phases respectively. Very little alteration is present in any of the minerals. Plagioclase and augite each constitute 40% of the rock, K-feldspar 10%, quartz 5%, pyrite, ilmenite and magnetite 3% and biotite, apatite and sphene total 2%.

EBT 4.1 and 4.2: Granodiorite. The rock is coarse grained with feldspar laths up to 6 mm in length. Some of the feldspar has been sericitised but the hornblende and biotite are relatively fresh. Apatite, aegirine and pyrite are very minor minerals. Plagioclase constitutes 35% of the rock, K-feldspar 20%, quartz 10%, hornblende 15%, biotite 15% and sericite 5%.

Both the biotite separates were 98% pure, the main impurities being quartz and chlorite. The hornblende separates were also 98% pure and contained apatite and other heavy minerals.

EBT 7.1 and 7.2: Granite. The rock is coarse grained with large feldspar laths of up to 8 mm in length. K-feldspar and plagioclase are both present in the rock with a dominance of the former mineral.

Hornblende and biotite occur in about equal amounts; the biotite is quite fresh but the hornblende is occasionally altered to chlorite and hematite. There is only minor sericitisation of the feldspars. Calcite, apatite, pyrite, hematite and chlorite are very minor. Quartz comprises about 45% of the rock, K-feldspar 20%, plagioclase 15%, hornblende 8%, biotite 8%, and sericite 3%. Zircon and sphene also occur but are very minor minerals.

Both the EBT 7.1 biotite and hornblende separates were 97% pure. The biotite separate contained quartz and chlorite and the hornblende separate contained apatite and other heavy minerals. The EBT 7.2 biotite separate was 99% pure and contained quartz and chlorite and the EBT 7.2 hornblende separate was 98% pure and contained apatite and other heavy minerals.

EB M1: Banded tuff. The rock contains laths of plagioclase feldspar (andesine) up to 3 mm in length which are comparatively fresh. Some quartz fragments are present and most of the fragments of quartz and feldspar are quite angular which suggests that the rock was not worked before deposition. Hematite occurs in a finely disseminated form in the groundmass. The hornblende present appears to be recrystallised. Plagioclase constitutes 50% of the rock, hornblende 25%, quartz 10%, pyrite up to 10%, sericite, chlorite and hematite total 5%. Calcite is also present but as micro-veins.

EB H1: Hornblende. This sample is from one of the hornblende-magnetite veins. It is associated with actinolite, magnetite, rhodochrosite, scapolite and pyrite. The hornblende separate was 96% pure, the impurities being scapolite and magnetite.

EB H2 and EB H3: Actinolite. These samples are from similar veins as EB H1 was obtained. EB H2 is 99% pure and EB H3 is 98% pure and in each case the impurities are scapolite and magnetite.

## APPENDIX B

CHEMICAL PROCEDURES FOR K, RB AND SR.Potassium

All the potassium determinations were made gravimetrically by the double Abbey leach method (ABBEY & MAXWELL, 1960) which was then followed by a flame photometer determination and the precipitation of  $\text{KB}(\text{C}_6\text{H}_5)_4$ .

For the micas a 0.25 gm. sample was used and a 1 gm. sample was used for the hornblendes and actinolites. The sample was weighed into a platinum dish which had been cleaned with hot con. nitric acid. 3 mls. of distilled water and 3 mls. of 1:1 sulphuric acid or 6 mls. for the 1 gm. samples were added together with 5 mls. of 48% hydrofluoric acid or 10 mls. for 1 gm. samples. This was evaporated to dryness on the hot plate, the  $\text{SO}_3$  fumed off and the residue ignited for 1 hr. on a Tyrrell burner. The residue was moistened with distilled water and transferred to a 20 ml. beaker where the potassium was leached with water four times on a steam bath. After the fourth leach, the residue was transferred back to the same platinum dish and the whole decomposition and leaching procedures repeated. The leaches were combined and  $\text{NaB}(\text{C}_6\text{H}_5)_4$  added dropwise whilst the solution was kept at  $60^\circ \text{C}$ .  $(\text{K}, \text{Rb}, \text{Cs})\text{B}(\text{C}_6\text{H}_5)_4$  was thus precipitated and allowed to settle out for two hours at room temperature. It was then filtered through a fine fritted glass filter, dried and weighed.

$$\% \text{K}_2\text{O} = \frac{\text{Wt. KB}(\text{C}_6\text{H}_5)_4 \times 0.1314 \times 100}{\text{sample wt.}}$$

The  $\text{Rb}_2\text{O}$  content was taken to be 0.2% for the micas and negligible for the hornblendes and actinolites.

An aliquot of the filtrate from the double leach was made up to 100 ml. for potassium analysis on the Perkin-Elmer flame photometer. Comparison with standard solutions enabled the concentration in ppm to be read directly and this was converted to  $\%K_2O$ .

Good agreement between the two methods was obtained, especially for the lower potassium values. The results from the flame photometer analyses were used in the age calculations.

#### Rubidium

Preliminary XRFS analyses were performed on all the Rb-Sr samples. The rubidium was determined by isotope dilution after a decomposition and leaching procedure similar to that employed for potassium. A certain weight of sample was added to a cleaned platinum dish to give 15 to 20 ug of Rb. The sample was moistened with demineralised water and 5 mls. of hydrofluoric acid plus 5 mls. of 1:1 sulphuric acid were added and the sample evaporated to dryness. 20 ug of enriched  $\text{Rb}^{87}$  isotope diluted in hydrochloric acid were added to the sample. All the Rb spikes were made up individually and stored in parafilm wrapped beakers. The amounts are based on calibrations performed by H. Baadsgaard. After the addition of the spike, the samples were again evaporated to dryness and ignited on a Meker burner. The rubidium was leached with 1 ml. of demineralised water and transferred into a cleaned silica vial where it was stored ready for mass spectrometric analysis.

A blank run was carried through the above procedure and analysed

on the mass spectrometer. The blank for the procedure was found to be 0.007 ug total rubidium.

### Strontium

Preliminary XRF analyses were made on the samples for strontium. Isotope dilution analysis was then employed using an enriched  $\text{Sr}^{84}$  spike. Teflon beakers cleaned in hot 1:1 hydrochloric acid were used for the sample decomposition. The sample was weighed into the beaker to give about 20 ug of strontium. Using 2 ug of  $\text{Sr}^{84}$  enriched spike this gave a 86/84 ratio of 1.0. The spike was added directly to the sample and the spike container rinsed with about 10 ml. of warm 1:1 nitric acid. 10 ml. of 48% hydrofluoric acid were added and the sample evaporated to dryness under a cover which carried a positive pressure of filtered air. When dry, 5 mls. of 1:1 nitric acid were added and the sample again taken to dryness, whence 5 mls. of 2.5 M. hydrochloric acid were added and the sample evaporated to dryness.

The sample was taken up in 1 ml. of 2.5 M hydrochloric acid and added to a prepared Dowex 50W-X8 column. It is washed in with 1 ml. of the acid and then eluted with the same acid. The strontium fraction is collected, evaporated to dryness and stored for mass spectrometric analysis.

The columns used in this work were prepared and calibrated by R.K. O'Nions. The specifications are 18 cms. by 1 cm. (i.d.) of Dowex 50W-X8 (200-400 mesh) cation exchange resin. The strontium fraction was found to be eluted in the 72 to 80 mls. interval. Cleaning of the columns was effected by the use of 6 M hydrochloric acid; they were resettled with demineralised water and then 2.5 M acid, at which



time they were ready for use.

The blank for the whole procedure was found to be less than  
0.02 ug Sr.

## APPENDIX C

COMPUTATIONS FOR K-AR AND RB-SR AGE CALCULATIONS.1. Potassium-Argon

For the calculations the following constants were used:

$$\lambda_K = 0.585 \times 10^{-10} \text{ yr}^{-1}$$

$$\lambda_\beta = 4.72 \times 10^{-10} \text{ yr}^{-1}$$

$$\text{ppm Ar}^{40} = 1.786 \times 10^3 \times \text{cc Ar}^{40}/\text{gm. (S.T.P.)}$$

The spike composition was:

$$\text{Ar}^{36}/\text{Ar}^{38} = 0.000105, \quad \text{Ar}^{40}/\text{Ar}^{38} = 0.00354$$

The sample isotope ratios were calculated from the chart data, the values being extrapolated to the time of inlet into the mass spectrometer.

The measured argon isotopes were corrected as follows:

$$40:38:36 \text{ measured} - 40:38:36 \text{ residual} = 40:38:36 \text{ sample} + \text{air} \\ + \text{spike.}$$

Each value was multiplied by the mass discrimination factors as determined from the measurement of air argon.

The air argon correction was then made:

Assuming all the  $\text{Ar}^{38}$  was from the spike the 36 spike argon was subtracted as follows: from mass 40 subtract  $38 \times 0.00354$ , mass 38 remained uncorrected and from mass 36 subtract  $38 \times 0.000105$ .

The air argon was subtracted by taking  $36 \times 295.5$  from mass 40, 38 was uncorrected and mass 36 was cancelled. Thus the radiogenic argon plus the  $\text{Ar}^{38}$  spike was obtained.

$$\text{Then the Ar}^{40} \text{ ppm} = \frac{\text{Ar}^{40}}{\text{Ar}^{38}} \times \frac{\text{ccAr}^{38} \text{ spike (S.T.P.)} \times 10^3 \times 1.7846}{\text{sample weight}}$$

From the  $\text{Ar}^{40}/\text{K}^{40}$  ratio the age may be calculated or it can be read from prepared tables of the  $\text{Ar}^{40}/\text{K}^{40}$  ratios and their corresponding ages using the decay constants given above. The precision error of the apparent age and the total uncertainty in the apparent age can be obtained by the use of a Fortran IV program (KARG) written by R.K. O'Nions.

## 2. Rubidium-Strontium

The rubidium and strontium were determined by isotope dilution analysis using  $\text{Rb}^{87}$  and  $\text{Sr}^{84}$  spikes. The ratios 87/85, 88/86, 84/86 and 87/86 were determined by mass spectrometry from which the total rubidium, total strontium and radiogenic strontium could be determined. The calculations for these determinations are documented by O'NIONS (1969). In actual fact the computations were performed using an A.P.L. program (RBSRCOMP) written by H. Baadsgaard.

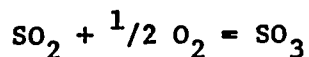
A second A.P.L. program (RBSRISOCRON), also written by H. Baadsgaard, was used for the least-squares fitting of isochrons to the Rb-Sr data. A description of the method is given in O'NIONS (op. cit.). Prior estimates for the precision in both coordinates are incorporated in the program which gives the age and the initial strontium ratio.

## APPENDIX D

STABLE ISOTOPES: ANALYTICAL PROCEDURES AND DATA CORRECTION.1. Sulphur Isotopesa) Preparation of SO<sub>2</sub>

All the samples were crushed in an agate mortar before burning in a glass combustion train. The train consisted of a mullite tube, a quartz tube and a series of pyrex U-tubes and coils which were used in the SO<sub>2</sub> purification process. A large furnace surrounded the quartz tube and was heated electrically to about 1200° C. The temperature was kept constant to within  $\pm 10^\circ$  C. by a temperature regulator and a platinum-rhodium wire thermocouple. The samples were burned to SO<sub>2</sub> within the quartz tubing in a stream of pure tank oxygen.

The oxygen was purified by passing it through Ascarite, a sodium hydrate asbestos absorbent, through concentrated sulphuric acid and then through a heated mullite tube which oxidised any remaining impurities which were removed in a dry ice trap. After these purification processes the oxygen passed into the quartz combustion chamber where samples could be slid in and out on quartz boats. A temperature of 1200° C. was used in the burning process since at this temperature the equilibrium constant for the reaction



is very small and hardly any SO<sub>3</sub> is produced. Good yields were obtained at this temperature but higher burning temperatures were not used, since they would decrease the life of the quartz tube. All the

samples were burned directly and it was not considered necessary to convert them to  $\text{Ag}_2\text{S}$ .

The  $\text{SO}_2$  produced was collected in a liquid oxygen trap along with some excess oxygen and other contaminants. This oxygen could be pumped away while the  $\text{SO}_2$  remains frozen. Water was removed by passing the gas a few times through a dry ice-acetone trap and the  $\text{CO}_2$  removed by trapping the  $\text{SO}_2$  in a liquid nitrogen-ethyl alcohol trap ( $-117.3^\circ \text{C}$ .) and pumping off the  $\text{CO}_2$ . At this temperature the vapour pressure of the  $\text{CO}_2$  was about 800 times that of  $\text{SO}_2$  and the fractionation due to this pumping process was taken to be negligible. The  $\text{SO}_2$  was then transferred into a breakseal ready for analysis.

#### b) Mass Spectrometry

The sulphur isotope ratios were determined on a twelve inch,  $90^\circ$ , magnetic analyser mass spectrometer built by Dr. H.R.Krouse of the Physics Dept., University of Alberta. This machine was equipped for the simultaneous collection of mass 66 and mass 64 which correspond to  $\text{S}^{34}\text{O}^{16}_2$  and  $\text{S}^{32}\text{O}^{16}_2$  respectively. The corrections for other combinations which give mass 66 are discussed later.

On entering the mass spectrometer, the gas was ionised by a stable electron beam at the source end and the individual ions produced were separated according to their masses in the magnetic field. The currents from these masses were collected in a double slit collector assembly and amplified by two vibrating reed electrometers. The ion currents of mass 66 and mass 64 were then fed into an integrating digital voltmeter which integrated the input voltage over a selected period of time and converted it to a proportional frequency. Another

voltage-to-frequency converter was used instead of a standard time base so that the recorded voltage was actually a ratio of the two input voltages. The ratios were displayed visually and could be printed out on a digital recorder for any period of time. The application of the latter equipment described is given in detail by McCULLOUGH & KROUSE (1965). Rapid switching by the use of magnetic valves on the inlet system facilitated the comparison of the 66/64 mass ratio for the unknown sample to the 66/64 mass ratio of a standard. The standard used was YKS-GM1A, whose  $\delta S^{34}$  value was taken to be -1.84 per mil.

For the analysis of each sample a minimum of ten 66/64 mass ratios of the standard were recorded and then a minimum of ten 66/64 mass ratios of the unknown sample were recorded. This procedure was repeated until about five or six sets of ratios for the unknown were recorded. The number of mass ratios recorded and the number of data sets taken depended on the stability of the instrument at the time of running. Both the standard  $SO_2$  and the unknown sample were kept at the same pressure when the readings were being taken. This eliminated the necessity of applying a pressure correction to the data.

The ratios of each set of data obtained were averaged. The ratios for the standard and the unknown sample were then compared and a mean average ratio of the two was calculated. This mean average was then converted to a  $\delta S^{34}$  value.

#### c) Correction Factors

As mentioned previously a contribution to mass 66 is produced from  $S^{32}O^{16}O^{18}$  but the effect of  $S^{33}O^{17}O^{16}$  and  $S^{32}O^{17}O^{17}$  are considered to be negligible. A correction factor for this mass contribution

can be applied as follows:

$$\delta S^{34} = F \times \frac{R_x - R_{std.}}{R_{std.}} \times 10^3$$

where  $F$  = oxygen correction factor and  $R$  = 66/64 mass ratio.

For this study a value of 1.091 was used for  $F$ . During the ratio measurements of unknown sample against the working standard the apparent ratios will tend to become displaced towards each other. This is caused by the low pumping speed of  $SO_2$  gas and thus when standard and unknown gases are being introduced every few minutes the ratios measured are of mixed gases i.e. (residual standard + unknown gas and residual unknown gas + standard gas). Estimates of values for this 'memory' or 'mixing' correction were supplied by H. Ohmoto (pers. comm.). In actual fact a combined oxygen correction factor and memory correction factor was supplied by H.R.Krouse (pers. comm.) and was used in this study. The factor is 1.27 and is applied to the apparent  $\delta S^{34}$  values. The application of this factor agreed well with the correction of the data by the oxygen correction factor and the separate and independently produced memory correction factor mentioned above.

It was also found necessary to apply a time correction factor to all the ratios. This was necessitated by a reservoir effect which develops within the working standard. The working standard was measured against a meteorite standard at the beginning and end of every batch of samples or at the beginning and end of each day. It was found that the working standard fractionated at the rate of 0.1 per mil per hour. Thus the relative times of measurements of all the samples was recorded and the exact fractionation of the standard was found by the

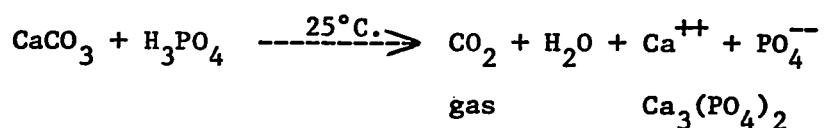
two measurements against the meteorite standard. All the sample values could be thus adjusted accordingly.

The normal precision attained by the instrument used was found to be  $\pm 0.1$  per mil or better but from several replicate samples taken through the whole analytical and preparation procedures the reproducibility was normally found to be about  $\pm 0.2$  per mil.

## 2. Oxygen and Carbon Isotopes

### a) Preparation of CO<sub>2</sub>

All the carbonate samples were ground to a powder in an agate mortar and about 50 ug of each was placed in a vessel for reaction with phosphoric acid. The reaction vessels containing, in separate parts, the carbonate sample and excess 100% phosphoric acid were connected to the vacuum line for complete degassing of the samples and acid. It was sometimes necessary to heat the acid slightly to accelerate degassing. When the acid was outgassed the reaction vessels were transferred into a thermostatically regulated water tank whose temperature was kept constant at 25° C. After an hour the vessel and acid were at 25° C. and the acid could be run into the sample chamber where the reaction to evolve CO<sub>2</sub> took place. Using the example of calcite the following reaction took place:



The normal time for the reaction of the calcite samples was 1 day; the dolomite samples were reacted for about 10 days and the composite siderite and rhodochrosite samples for up to 27 days. No attempt was



made in this study to separate the gases evolved from individual minerals in the siderite, rhodochrosite and dolomite mixtures. However the method of EPSTEIN et al. (1964) was applied to collect the CO<sub>2</sub> developed from calcite and dolomite separately in sample 023. This method uses the marked difference in reaction rates of dolomite and calcite with phosphoric acid. It is established that during the first hour of reaction dolomite will yield only very little CO<sub>2</sub> while calcite will yield more than 90% of its CO<sub>2</sub>. Thus in a mixture where the proportions of dolomite and calcite are roughly equal the calcite CO<sub>2</sub> can be collected after 1 hour, the gas from 1 to about 10 hours is pumped away and the dolomite gas is collected 10 days later.

On the completion of the reactions the vessels were connected to the extraction train for the removal and collection of the CO<sub>2</sub> gas. The CO<sub>2</sub> was first frozen down in a liquid nitrogen trap and any uncondensed contaminant gases were pumped away. An acetone-dry ice trap was set in the line and the CO<sub>2</sub> allowed to pass through this and all water vapour was thus removed. The CO<sub>2</sub> was then finally frozen down in a breakseal with liquid nitrogen. Any residual gases were again pumped away before the breakseal was sealed.

#### b) Mass Spectrometry

The isotope ratios were determined on the same instrument and in the same manner as described in the sulphur isotope section of this Appendix. For the oxygen analysis masses 46 and 44 + 45 were collected simultaneously and for the carbon analysis masses 44 and 45 were collected simultaneously. A precision of +0.1 per mil was obtained for the mass spectrometric analysis and an overall error for the whole procedure was usually about +0.2 per mil.

## c) Correction Factors

Certain correction factors must be applied to the raw data produced from the mass spectrometer and these are discussed by CRAIG (1957). ~~The~~ first correction factor to be applied to the data is a tail correction factor from mass 44. This is applied through the following formula:

$$\delta_{\text{tail}} = \delta_m \times (I + c/146)$$

Where  $\delta_{\text{tail}}$  is the corrected  $\delta$  value,  $\delta_m$  is the  $\delta$  value obtained from the raw mass spectrometer data, I46 is the count on mass 46 and c is equal to the tail plus background and the tail is the average for a tail up and a tail down measurement (P. Fritz, pers. comm.). This is determined for each batch of samples and normally the correction is 1.003 for  $\delta O^{18}$  and 1.01 to 1.02 for  $\delta C^{13}$ . The mass contribution correction is dealt with by CRAIG (1957) and only the formulas are given here. These have been developed for the Fisher Calcite which is used as a working standard by Dr. P. Fritz, University of Alberta, Geology Dept. and are as follows:

$$\delta C^{13} = \delta_{\text{tail}} \times 1.0674 - \delta O^{18} \times 0.0337$$

$$\delta O^{18} = \delta_{\text{tail}} \times 1.00144 - \delta C^{13} \times 0.009$$

No pressure corrections are required since the working standard and the unknown sample are kept at the same pressure during the mass spectrometer run. Memory or mixing effects are not applied to the data since  $CO_2$  has a relatively high pumping speed and the corrections are not critical as they are in the sulphur isotope analyses.

The carbonate analyses have to be corrected for the residual

oxygen not extracted during the phosphoric acid treatment. The values for the kinetic fractionation factors for each type of carbonate mineral have been reported by SHARMA and CLAYTON (1965) and the relevant ones are given below:

Carbonate	Fractionation factor, $\alpha$
Calcite	1.01008
Dolomite	1.01090
Siderite	1.01169
Rhodochoisite	1.00995

The carbonate mixtures were treated as having intermediate fractionation factors. For the pure minerals the values obtained by using the Fisher Calcite as standard can be converted to PDB using the values given below (P. Fritz, pers. comm.):

Calcite	$\delta O^{18} = -13.3$ per mil and $\delta C^{13} = -3.3$ per mil
Dolomite	$\delta O^{18} = -14.2$ per mil and $\delta C^{13} = -3.3$ per mil
Siderite	$\delta O^{18} = -14.7$ per mil and $\delta C^{13} = -3.3$ per mil
Rhodochoisite	$\delta O^{18} = -13.2$ per mil and $\delta C^{13} = -3.3$ per mil

For the  $\delta O^{18}$  values, they can be converted from PDB to SMOW by the following equation:

$$\delta O^{18} \text{ SMOW} = \delta O^{18} \text{ PDB} \times 1.0304 + 30.4$$

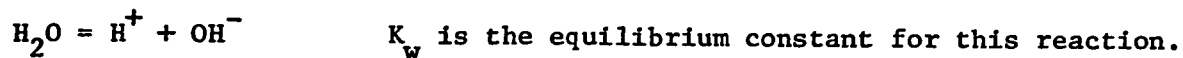
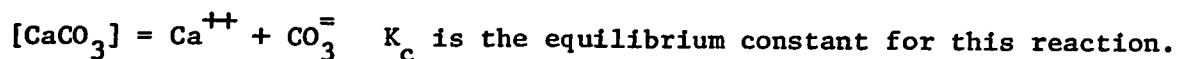
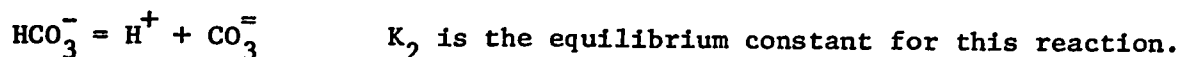
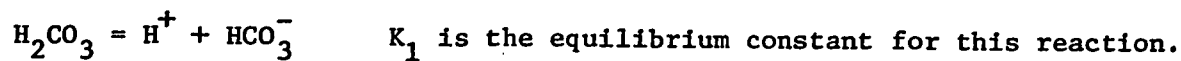
## APPENDIX E

SOLUTION CHEMISTRY COMPUTATIONS

## 1. Sample calculation for a carbonate buffer system.

For the  $\text{H}_2\text{O}-\text{CO}_2-\text{CaCO}_3$  system:

$$a_{\text{H}_2\text{CO}_3} \text{ (app)} = B \cdot f\text{CO}_2$$



From these equations it is possible to obtain the following expression:

$$(a_{\text{H}^+})^3 = \frac{K_1^2 \cdot K_2 \cdot B^2 \cdot f\text{CO}_2^2 \cdot \alpha_{\text{Ca}^{++}}^*}{K_c \cdot 2 \cdot \alpha_{\text{HCO}_3^-}} \quad (\text{H. Ohmoto, pers. comm.})$$

i.e.

$$3\log a_{\text{H}^+} = 2\log K_1 + \log K_2 + 2\log B + 2\log f\text{CO}_2 + \log \alpha_{\text{Ca}^{++}} - \log 2 - \log \alpha_{\text{HCO}_3^-}$$

Thus to calculate the interrelationship between pH and  $f\text{CO}_2$  the above expressions have to be obtained:

$$B = 55.5 / \text{Henry's Law Constant for CO}_2 \quad (\text{HOLLAND, 1965})$$

$$\text{Henry's Law Constant for CO}_2 \text{ with a 5.0 m solution at } 200^\circ \text{ C.} = 13625.$$

This is obtained by extrapolation of the data given by HOLLAND (1965).

\* Note: The activity coefficients are here designated as ' $\alpha$ '

$$B = 55.5/13625 \quad \text{and} \quad \log B = -2.3901$$

$$\log K_1 = -7.08 \quad (\text{HELGESON, 1969})$$

$$\log K_2 = -10.68$$

$$\log K_c = -11.37 \quad (\text{HELGESON, 1969})$$

Temperature = 200° C. or 473° K.

Solution is 30 wt.% NaCl

$$\text{Molality} = (30/58.5) \times 10 = 5.0 \text{ m.}$$

To calculate the activity coefficients:

I, the ionic strength, =  $\frac{1}{2} \sum m_i \cdot z_i^2$ , where  $m_i$  is the molality and  $z_i$  is the charge. With a 5.0 m NaCl solution  $I = 5.0$ .

The activity coefficients can be calculated from the Debye-Huckle theory:

$$-\log \alpha_i = \frac{A \cdot z_i^2 \cdot \sqrt{I}}{1 + a_i^\circ \cdot B \cdot \sqrt{I}}$$

where A and B are constants for a given temperature and  $a_i^\circ$  is the effective radius of the ionic species.

$$\text{For this case } A = 0.8127 \text{ and } B = 0.3659/10^{-8} \quad (\text{HELGESON, 1967})$$

$$a^\circ \text{ for } \text{Ca}^{++} = 6.0 / 10^8 \text{ and for } \text{HCO}_3^- = 4.0 / 10^8 \quad (\text{GARRELS \& CHRIST, 1965})$$

Calculating the activity coefficients from the equation given the following results were obtained:

$$\log \alpha_{\text{Ca}^{++}} = -1.23 \quad \text{and} \quad \log \alpha_{\text{HCO}_3^-} = -0.43$$

From the equation relating pH and  $f\text{CO}_2$  we now have:

$$3\text{pH} = 19.4 - 2 \log f\text{CO}_2$$

Thus for example if  $\log f\text{CO}_2 = -1.5$  then the pH = 7.5

## 2. Sample calculation of the molality of sulphur species in the fluid.

Given conditions:

$$T = 473^\circ \text{ K.}$$

$$\log fS_2 = -12$$

$$\log fO_2 = -39$$

$$\log fCO_2 = +1$$

$$\text{pH} = 6$$

$$\text{Pressure} = 500 \text{ bars}$$

$$f_{H_2O} = \text{fugacity coefficient } H_2O \times p_{H_2O}$$

If  $p_{H_2O} = 500$  bars and  $T = 200^\circ \text{ C.}$  then the fugacity coefficient of  $H_2O = 0.0374$  (ANDERSON, 1967).

$$\text{Thus } f_{H_2O} = .0374 \times 500 = 18.7 \text{ and } \log f_{H_2O} = 1.272$$

$H_2 + \frac{1}{2} O_2 = H_2O$ ,  $\log K = 24.3$  (calculated from data given in HOLLAND, 1965)

$$\text{thus } \log f_{H_2} = -3.6$$

$2CO + O_2 = 2CO_2$ ,  $\log K = 53.28$  (calculated from data given in HOLLAND, 1965)

$$\text{thus } \log f_{CO} = -6.2$$

$2H_2O + CO_2 = CH_4 + 2O_2$ ,  $\log K = -88.27$  (calculated from data given in HOLLAND, 1965).

$$\text{thus } \log f_{CH_4} = -6.91$$

$H_2O + \frac{1}{2}S_2 = H_2S + \frac{1}{2}O_2$ ,  $\log K = -17.00$  (calculated from data given in HOLLAND, 1965).

$$\text{thus } \log f_{H_2S} = -2.3$$

$S_2 + 2O_2 + 2SO_2$ ,  $\log K = 72.44$  (calculated from data given in HOLLAND, 1965).

$$\text{thus } \log f_{SO_2} = -8.78$$

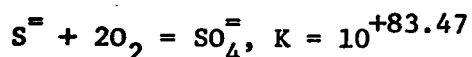
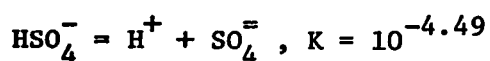
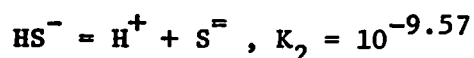
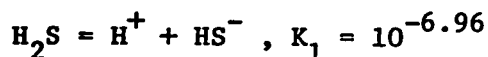
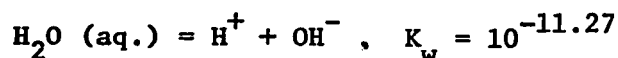
$S_2 + 3O_2 + 2SO_3$ ,  $\log K = 84.06$ , (calculated from data given in HOLLAND, 1965).

$$\text{thus } \log f_{SO_3} = -22.47$$

To convert various fugacities into molalities (of species in solution) Henry's Law Constant is available for  $H_2$  and  $CH_4$  (OHMOTO, 1968) and for  $H_2S$  (KOZINTSEVA, 1965). Values are normally given for up to a 1 or 2 m solution and thus for a 5 m solution the values have to be extrapolated.

Of particular use at the moment is Henry's Law Constant for  $H_2S$ . In a 5 m solution at  $200^\circ C$ . the value is extrapolated to 4,375.

The dissociation constants for the following reactions are taken from HELGESON (1969):



To calculate the activity coefficients for  $H_2S$ ,  $HS^-$ ,  $S^{=}$ ,  $HSO_4^-$  and  $SO_4^{=}$

$I$ , the ionic strength,  $= \frac{1}{2} \sum m_i \cdot z_i^2$ , where  $m_i$  is the molality and  $z_i$  the charge of the species. Then from the Debye-Huckel theory:

$$-\log \alpha_i = \frac{A \cdot z_i^2 \cdot \sqrt{I}}{1 + a_i^{\circ} \cdot B \cdot \sqrt{I}}$$

where  $A$  and  $B$  are constants for a given solution and  $a_i^{\circ}$  is the effective radius of the ionic species.

For 200° C.  $A = 0.8127$  and  $B = 0.3659 / 10^8$  (HELGESON, 1967)

$a^\circ$  values are (GARRELS & CHRIST, 1965):

$$\text{HS}^- = 3.5 / 10^8$$

$$\text{S}^{=} = 5.0 / 10^8$$

$$\text{HSO}_4^- = 4.3 / 10^8$$

$$\text{SO}_4^{=} = 4.3 / 10^8$$

The activity coefficient for  $\text{H}_2\text{S}$  was assumed to be the same as  $\text{H}_2\text{CO}_3$  for which a value of  $\log \alpha_{\text{H}_2\text{S}} = 0.35$  was extrapolated from data given by HELGESON (1967). Thus  $\alpha_{\text{H}_2\text{S}} = 2.239$

The other activity coefficients were calculated to be:

$$\alpha_{\text{HS}^-} = 0.3386$$

$$\alpha_{\text{S}^{=}} = 0.03735$$

$$\alpha_{\text{HSO}_4^-} = 0.3961$$

$$\alpha_{\text{SO}_4^{=}} = 0.02461$$

To calculate the activities and molalities of the various sulphur species:

$m_{\text{H}_2\text{S}} = f_{\text{H}_2\text{S}} \times 55.5 / \text{Henry's Law constant for } \text{H}_2\text{S}$ , thus  $m_{\text{H}_2\text{S}} = 10^{-4.2}$  and using the calculated activity coefficient for  $\text{H}_2\text{S}$  and the relationship that:  $a_i = \alpha_i \times m_i$ , where  $a_i$  is the activity,  $\alpha_i$  is the activity coefficient and  $m_i$  the molality of species  $i$ :

$$a_{\text{H}_2\text{S}} = 10^{-3.8}$$

For  $\text{H}_2\text{S} = \text{H}^+ + \text{HS}^-$ , knowing  $K_1$ , the pH and  $a_{\text{H}_2\text{S}}$  then

$$a_{\text{HS}^-} = 10^{-4.8} \text{ and } m_{\text{HS}^-} = 10^{-4.3}$$

For  $\text{HS}^- = \text{H}^+ + \text{S}^{=}$ , knowing  $K_2$ ,  $a_{\text{HS}^-}$  and the pH then



$$a_{S^=} = 10^{-8.3} \text{ and } m_{S^=} = 10^{-7.8}$$

For  $S^= + 2O_2 (g) = SO_4^=$ , knowing  $K$ ,  $a_{S^=}$  and the  $fO_2$  then

$$a_{SO_4^=} = 10^{-2.6} \text{ and } m_{SO_4^=} = 10^{-1.0}$$

and for:  $HSO_4^- = H^+ + SO_4^=$ , knowing  $K$ , the pH and  $a_{SO_4^=}$  then

$$a_{HSO_4^-} = 10^{-4.1} \text{ and } m_{HSO_4^-} = 10^{-3.7}$$

Thus the following molalities have been obtained:

$$m_{H_2S} = 10^{-4.2}$$

$$m_{HS^-} = 10^{-4.3}$$

$$m_{S^=} = 10^{-7.8}$$

$$m_{HSO_4^-} = 10^{-3.7}$$

$$m_{SO_4^=} = 10^{-1.0}$$

Due to the extrapolations and the uncertainties involved these figures can be rounded off, e.g.  $SO_4^=$  is the dominant species and  $m_{SO_4^=} \approx 10^{-1}$ .

## APPENDIX F

CORRECTIONS OF THE MICROPROBE DATA AND MICROPROBE STANDARDS

Corrections were applied to the apparent element concentrations for the atomic number effect, mass absorption and fluorescence. These corrections are dealt with in a review of electron microprobe analysis (LONG, 1967). All the computations were actually performed by an APL program (PROBEDATA) written by D.G.W. Smith and M.L. Tomlinson (SMITH & TOMLINSON, 1970).

The operating conditions for the microprobe were:

Take off angle = 52.5°

Operating voltage = 15 KV

Emission current = 200 microamps

Beam current = 0.1 microamp.

The standards used during the course of this study were as follows:

1. Mckinstryite analyses

EP/S 4-1                      Cu = 100%

EP/S 9-1                      Ag = 100%

EP/S 3-4 Marcasite              Fe = 46.54%, S = 53.46%

2. Native silver analysis

Co, Ni, Cu, Ag, Cinnabar, As, and Bi were combined into one standard mount made by G. Nordin and used for the analyses.

3. Sphalerite analyses

EP/S 3-4 Marcasite              Fe = 46.54%, S = 53.46%

(Stoichiometry assumed)

4. Carbonate analyses

a) Calcites

EP/S 23-2 Hypersthene. Si = 24.0%, Ti = 0.06%, Al = 1.32%,  
Fe = 18.0%, Mn = 0.39%, Mg = 12.8%,  
Ca = 0.4%, O = 42.53%.

b) Dolomites and others

EP/S 3-12 Synthetic MgO. Mg = 60.32%, O = 39.68%

EP/S 23-2 Hypersthene. Analysis as above.

EP/S 7-10 Mn = 99.879%, Fe = 0.109%, Al = 0.012%.

## APPENDIX G:

## Mckinstryite from the Echo Bay Mine, N.W.T., Canada

B. W. ROBINSON AND R. D. MORTON

## Abstract

Mckinstryite occurs as a late-stage, primary sulfide in the U-Co-Ni-Ag-Bi deposit of the Echo Bay Mine, N.W. Territories, accompanying niccolite, rammelsbergite, chalcopryrite, bornite, covellite and early dolomite. Electron microprobe analyses reveal an average composition of  $Cu_{0.72}Ag_{1.28}S_{0.01}$ . A variable excess of Ag and a S deficiency are probably due to a nonstoichiometric defect structure of the Schottky type. The mineral has an average S.G. of  $6.64 \pm 0.04$ , is light gray, weakly birefractant, strongly anisotropic and biaxial positive. The reflectance at 470 nm = 30.8% (av. min.), 36.7% (av. max.); at 546 nm = 29.0% (av. min.), 32.8% (av. max.); at 589 nm = 23.8% (av. min.), 30.7% (av. max.); at 650 nm = 30.1% (av. min.), 29.1% (av. max.).  $VHN_{20\text{ gm}} = 50.1$  to 67.1 (av. 55.7). Powder diffraction gives  $a = 13.962 \pm 0.001\text{ \AA}$ ,  $b = 15.675 \pm 0.002\text{ \AA}$ ,  $c = 7.755 \pm 0.002\text{ \AA}$ , and  $Z = 32$ .  $\delta S^{34}$  values of +23 to +27‰ exhibited by the mckinstryite are interpreted as being due to the late formation of the mineral at  $<94.4^\circ\text{ C}$ .

## Introduction

MCKINSTRYITE was discovered by Skinner et al. (1966) occurring in a sample from the Foster mine, Cobalt, Ontario. Subsequently mckinstryite has been recorded by Grybeck and Finney, (1968) and Jöhan, (1967).

Situated on the east shore of Great Bear Lake, N.W.T., Canada, the Echo Bay mine, one of Canada's richest silver producers, is adjacent to the old Port Radium mine (lat:  $66^\circ 05'N$ , long:  $118^\circ 02'W$ ). The ores of this area are classified as vein-type U-Co-Ni-Ag-Bi deposits and have a characteristic assemblage of pitchblende, Co-Ni arsenide minerals, sulfide minerals, native silver and bismuth. The Echo Bay veins are lens-shaped and occur within fracture zones which cut the Proterozoic sediments and volcanics. A description of the geology of the area is in the final stages of preparation and will serve to augment the earlier observations of Campbell (1957).

## Occurrence

One sample from the 206A E Drift of the mine (#2 adit level) contained a complex association of carbonate, sulfide (including mckinstryite) and Ni-Co arsenide minerals. The paragenetic sequence of the deposit is shown in Figure 1. Polished section studies have shown rosettes of niccolite rimmed by rammelsbergite (Figs. 2 and 3) occurring within an early granular dolomite matrix (Fig. 2). This dolomite has in many places been replaced by chalcopryrite and bornite. The replacement was apparently followed by the deposition of a later well crystallized calcite, mainly as vug infillings. The mckinstryite has replaced both chalcopryrite (Fig. 3) and also the early granular dolomite (Fig. 2).

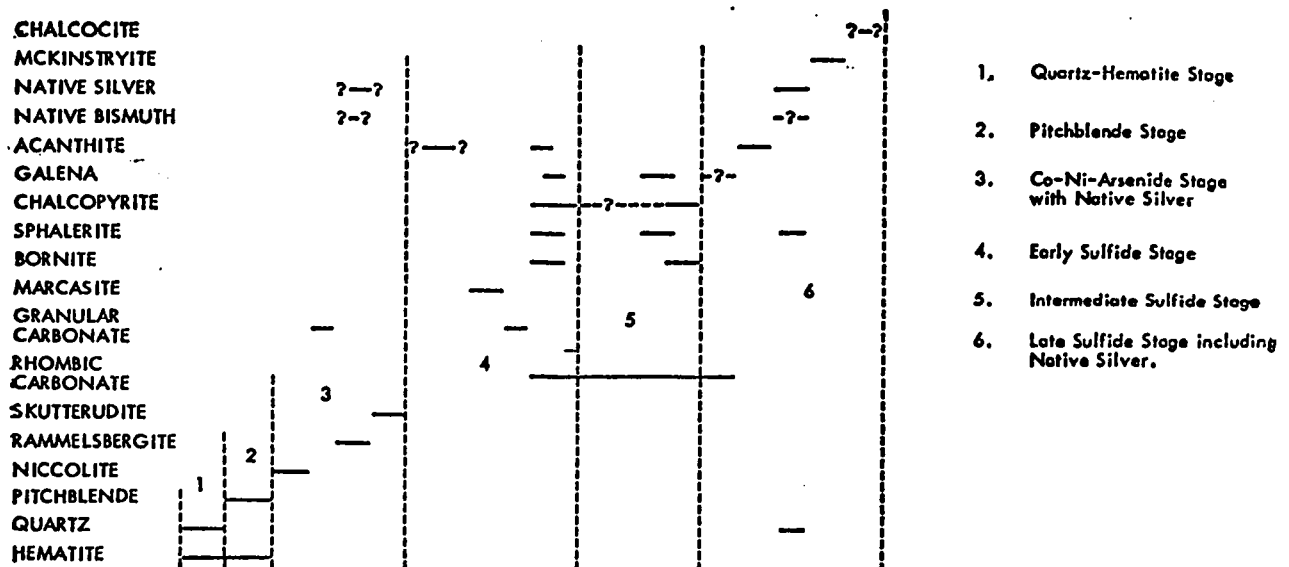


FIG. 1. Paragenetic sequence.



FIG. 2. Rosettes of polycrystalline niccolite (white) with a rim of rammelsbergite (grayish white) occurring within a granular carbonate matrix (dark gray) which is in part replaced by mckinstryite (gray). Echo Bay Mine, 206A E Drift (#2 adit level).

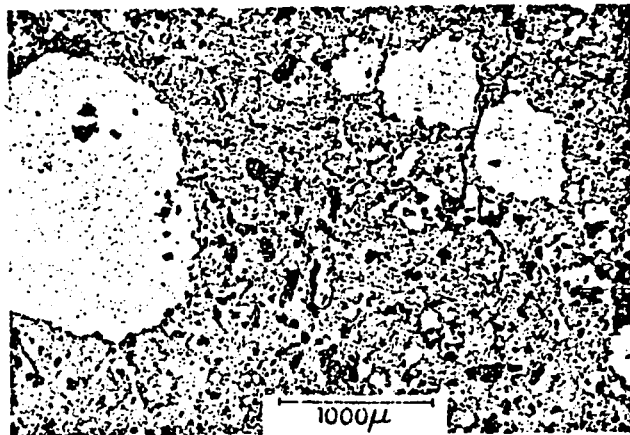


FIG. 3. Rammelsbergite (white) and niccolite (whitish gray) occur within mckinstryite (gray) which has partly replaced chalcopyrite (slightly lighter color and greater relief than mckinstryite). Echo Bay Mine, 206A E Drift (#2 adit level).

### Physical Properties

The physical properties of mckinstryite and etch reactions on the polished surface are given by Skinner et al., (1966). In polished section, the mineral is gray in color and exhibits weak bireflectance and under crossed nicols it is strongly anisotropic with gray interference colors which frequently have a slight blue tinge.

Six separate pycnometric density determinations on three hand-picked samples (from 0.3 to 0.5 gm) gave an average specific gravity of  $6.64 \pm 0.04$ . The higher silver values of the Echo Bay mckinstryite are in accord with a slightly higher specific gravity than that determined by Skinner et al., (1966).

### Reflectance and Microhardness

The apparatus employed for the reflectance measurements consisted of a Vickers M74 Polarizing microscope with a stabilized 100 watt quartz-halogen filament lamp, a running interference-filter monochromator and a EFL Model-165 digital microphotometer. The standard used was a SiC reflectance standard (provided by N. F. M. Henry) whose  $R$  in percent, at 470, 546, 589 and 650 nm, respectively, was 22.1, 21.8, 21.4 and 21.1; the standard being calibrated against the Carborundum National Standard N.2538.26 of the Commission on Ore Microscopy. The results of the reflectance measurements on ten randomly oriented sections of mckinstryite are given in Table 3. The difference in the minimum and maximum average of the reflectance values is due to the weak bireflectance of this mineral and the range of values is due both to the variable orientation of the sections and to the variable chemical composition. The maximum and minimum values obtained at each point usually corresponded to an extinction and a non-extinction position. No statistical data was obtained which might permit cor-

relation of the reflectance values with the silver content of the mineral, but the reflectance values were often found to be higher in areas of proven higher silver content.

From the values obtained, a similar magnitude of range within both the minimum and maximum reflectance values indicates that the mineral is biaxial (Cameron, 1963). For the wavelengths considered it was found that plots of  $R_s$  and  $R_p$  do not cross on a reflectance vs. wavelength diagram. Therefore, the optical sign of the mineral is apparently constant within these wavelengths. Using the method of Cameron (1963), the mineral appears to have a positive optic sign at 546 nm, but the sign could not be determined at the other wavelengths. The reflectance values cannot be used to distinguish mckinstryite from other similar minerals such as stromeyerite.

The microhardness of mckinstryite was determined by the use of a Vickers 136° diamond-indenter objective. Grybeck and Finney (1968) had previously performed six microhardness measurements on mckinstryite from Silver Plume and obtained a VHN of  $60 \pm 2$  (presumably at 100 gram-load) and found that the indentation shape was very characteristic, since it showed a conjugate set of en echelon fractures, often with offsets, at the borders of the indentations. During the present study, it was found that a 100 gram-load produced excessive fracturing and a 20 gram-load was found to be optimum. A similar fracturing pattern was observed. Ten areas in each polished section were measured. One indentation was made in the extinction position and another in the 45° position of the same grain. The former values were very constant over both sections at VHN  $54.8 \pm 2.0$ , but the latter values showed the largest variations since one diagonal of the indentation often lay within the direction of cleavage. Although the values are not statistically distinct, the

Table 1. Electron Microprobe Analyses of Mckinstryite.

	Mean data Specimen 1 Echo Bay N.W.T.	High Ag Specimen 1 Echo Bay N.W.T.	Mean data Specimen 2 Echo Bay N.W.T.	Max. Ag Specimen 2 Echo Bay N.W.T.	Min. Ag Specimen 2 Echo Bay N.W.T.	Average Echo Bay N.W.T.	Foster Mine Cobalt * (Skinner et al. 1966)
Wt. % Cu	20.71	n.d.	22.56	20.69	23.95	21.64	24.9
Wt. % Ag	66.25	70.48	63.86	65.25	61.83	65.06	60.0
Wt. % S	13.22	n.d.	14.15	14.09	14.22	13.69	15.1
TOTAL:	100.18		100.57	100.03	100.00	100.39	100.0

\* X-ray fluorescence Analysis.

value for the "extinction" indentation was higher in Specimen 2 than in Specimen 1 suggesting that the microhardness may be slightly lowered with increasing silver content. The maximum range in VHN and the average of all values are given in Table 3. In most cases, the indentations produced were of a perfect shape.

#### Electron Probe Analyses

The intimate intergrowth of mckinstryite with other minerals in the Echo Bay samples excluded the use of X-ray fluorescence analysis. Quantitative X-ray fluorescence analyses for Cu, Ag and S were carried out on mckinstryite by Skinner et al., (1966) because microprobe results were inconsistent (Skinner, pers. comm., 1968). In the present study, an Applied Research Laboratories' EMX microprobe was used for the analysis of S, Cu and Ag (the only elements detected during preliminary qualitative scans). Standards of native Ag, native Cu and marcasite were used during the analyses and, in order to monitor drift effects, the standards were measured at the beginning and end of each sample analysis.

Corrections for atomic number, absorption and fluorescence effects were employed using an APL program written by Smith and Tomlinson (1970). The results gave consistent totals and are shown in Table 1. The precision on the analyses is  $\pm 1\%$  for  $2\sigma$  variations.

It can be seen that the mckinstryite is not of constant composition. Silver-rich domains exist within the mineral. These domains are not obviously related to zoning or to the proximity of other minerals. The samples were checked for inclusions of native silver both with the microprobe and with a  $600\times$  Normarski differential interference contrast device. For each sample, the whole area of mckinstryite was traversed on the microprobe and this is reported as the mean data. An area of high silver was separately recorded for specimen 1 and areas of maximum and minimum silver are given for specimen 2. Because of these inhomogeneities, the mean data for specimens 1 and 2 is averaged to give what is considered to be a representative analysis of the Echo Bay mckinstryite. This analysis is given in Table 2 to-

Table 3: Reflectance and Microhardness Values.

Microhardness  VHN (20 gm) (in Kg./mm. <sup>2</sup> ) 50.1 - 67.1 Aver. 55.7 p to sf	Reflectance				
	Wavelength  nm	Minimum Reflectance (%)		Maximum Reflectance (%)	
		Range	Average	Range	Average
	470	29.0 - 32.9	30.8	35.5 - 37.6	36.7
	546	27.6 - 31.2	29.0	30.3 - 35.7	32.8
	589	22.0 - 25.0	23.8	28.5 - 32.1	30.7
	650	20.2 - 24.5	22.9	28.5 - 31.3	30.1

TABLE 2. X-ray Powder Diffraction Data for Mckinstryite ( $\text{Cu}_{10}\text{Ag}_{10}\text{S}_{10}$ ), Echo Bay Mine, N.W.T., and Mckinstryite ( $\text{Cu}_{10}\text{Ag}_{10}\text{S}$ ), Foster Mine, Cobalt, Ont. (Skinner et al., 1966).  $I_{\text{est}}$  = intensities by visual estimation. Measurements made in  $\text{FeK}\alpha$  radiation = 1.93728 Å and  $\text{FeK}\alpha 1$  radiation = 1.93597 Å was used for the calculations on back reflections (=B). N.O. = not observed. R = reflections rejected by least squares cell refinement program.  $a = 13.962\text{Å}$ ,  $b = 15.675\text{Å}$ ,  $c = 7.755\text{Å}$ .

hkl	Echo Bay mckinstryite			Foster Mine mckinstryite		
	$d_{\text{calc.}}$	$d_{\text{obs.}}$	$I_{\text{est.}}$	$d_{\text{calc.}}$	$d_{\text{obs.}}$	$I_{\text{est.}}$
011		N.O.		6.985	6.970	0.5
230		N.O.		4.192	4.199	0.5
320		N.O.		4.019	4.017	1
002		N.O.		3.901	3.907	1
231		N.O.		3.693	3.688	0.5
400	3.490 R	3.479	20	3.511	3.508	6
122		N.O.		3.389	3.389	1
150	3.059 R	3.038	30	3.060	3.062	6
312		N.O.		2.944	2.945	0.5
430		N.O.		2.914	2.913	0.5
250	2.860 R	2.844	30	2.863	2.862	6
322	2.785	2.785	10	2.799	2.797	1
042, 510		N.O.		2.765	2.763	0.5
251		N.O.		2.688	2.688	0.5
520		N.O.		2.644	N.O.	
511, 350	2.591	2.591	100	2.606	2.606	10
160, 130	2.568 R	2.555	20	2.566	2.567	4
113	2.509	2.509	20	2.524	2.524	1
521		N.O.		2.504	2.505	1
530, 351		N.O.		2.472	2.472	0.5
161, 203		N.O.		2.439	2.436	0.5
213, 152	2.396	2.396	30	2.408	2.407	4
261, 432		N.O.		2.335	2.333	0.5
252	2.302 R	2.298	20	2.308	2.307	3
313		N.O.		2.250	2.250	1
361, 522	2.177	2.176	15	2.189	2.188	3
352	2.160 R	2.153	15	2.166	2.167	2
350		N.O.		2.136	2.137	0.5
403, 532		N.O.		2.089	2.088	2
333	2.074	2.075	20		N.O.	
413, 243	2.059	2.059	70	2.071	2.070	7
640	2.001	2.001	30	2.009	2.009	1
641, 004		N.O.		1.946	1.948	5
180	1.940	1.940	50		N.O.	
470	1.885	1.885	<10	1.888	1.888	2
650, 632, 730		N.O.		1.874	1.874	0.5
443, 552, 353	1.835 R	1.836	<10	1.844	1.844	1
224, 163		N.O.		1.828	1.827	0.5
044	1.738 R	1.740	10		N.O.	
562	1.712	1.711	<10		N.O.	
652	1.683 R	1.684	<10		N.O.	
572	1.593	1.592	10		N.O.	
064	1.557	1.557	10		N.O.	
283	1.524 R	1.524	10		N.O.	
492	1.446 R	1.446	20		N.O.	
922	1.417	1.417	20 B		N.O.	
871	1.355	1.355	10 B		N.O.	
493	1.335	1.335	10 B		N.O.	
6 10 0	1.300 R	1.300	<10 B		N.O.	
3 10 3	1.288	1.288	<10 B		N.O.	
7 10 0	1.232 R	1.232	15 B		N.O.	
13 3 0	1.052	1.052	70 B		N.O.	
984	1.030 R	1.031	<10 B		N.O.	

gether with the analysis for the original mckinstryite (Skinner et al., 1966). The Echo Bay mckinstryite has less copper, an excess of silver and a deficiency in sulfur compared with the Foster Mine sample.

Existing data does not suggest that mckinstryite may significantly deviate from having a metal to sulfur ratio of 2:1. However, the Echo Bay mckinstryite has an average formula of  $\text{Cu}_{0.72}\text{Ag}_{1.28}\text{S}_{0.91}$  if the metals are computed to total 2 formula units. This formula produces the best agreement with the observed specific gravity and can be generalized as  $\text{Cu}_{0.8-x}\text{Ag}_{1.2+x}\text{S}_{1-y}$  where both  $x$  and  $y$  are relatively large. The silver can attain values of as high as 1.38 formula units for the area of high silver in specimen 1 but, for the area of minimum silver in specimen 2, a formula of  $\text{Cu}_{0.70}\text{Ag}_{1.21}\text{S}_{0.93}$  is obtained.

#### X-Ray Crystallographic Studies

X-ray powder diffraction patterns of mckinstryite produced by Skinner et al. (1966) agreed with those produced from the synthetic  $\beta$ -phase of Djurle (1958) and Skinner (1966). Single-crystal X-ray diffraction studies on mckinstryite (Skinner et al., 1966) showed that the mineral is orthorhombic with space group Pnam or Pna2<sub>1</sub>.

The measured  $d$  Å spacings from the powder camera work done in this study are listed in Table 2 together with those obtained by Skinner et al. (1966). The orthorhombic unit cell parameters  $a$ ,  $b$  and  $c$  were determined using a least-squares unit cell refinement program initially written by Evans et al. (1963) but modified for FORTRAN IV by J. J. Papike. The results of this refinement are:  $a = 13.962 \pm 0.001\text{Å}$ ,  $b = 15.675 \pm 0.002\text{Å}$  and  $c = 7.755 \pm 0.002\text{Å}$ . Comparing these values with those obtained from the Foster mine sample, the  $b$  values are statistically indistinguishable from each other but the  $a$  and  $c$  values are slightly smaller for the Echo Bay sample. This may be a reflection of the sulfur deficiency of this sample.

The volume of the cell is  $1697.2 \pm 0.3\text{Å}^3$ . Using a molecular weight of 212.8 for  $\text{Cu}_{0.722}\text{Ag}_{1.278}\text{S}_{0.906}$  and the observed specific gravity of  $6.64 \pm 0.04$ , the calculated cell occupancy ( $Z$ ) is  $31.9 \pm 0.4$  formula units. This is, therefore, in agreement with Skinner et al. (1966) although the volume of the cell for the Echo Bay sample is significantly lower.

#### The Ag-Cu-S System

Djurle (1958) investigated the phase relations in the system Ag-Cu-S and established phases corresponding to jalpaite, stromeyerite and a so-called  $\beta$ -phase which had a lower transition temperature at about 97° C. Working with the same system, Skinner (1966) found extensive solid solution and reaction rates so rapid as to be unquenchable. Along the  $\text{Cu}_2\text{S-Ag}_2\text{S}$  join, he found the same compounds as Djurle and fixed the lower transition temperature of the  $\beta$ -phase at 94.4° C. Thus the mineral mckinstryite, which has been equated with the  $\beta$ -phase, presumably forms below 94.4° C and should have a metal to sulfur ratio of 2:1. The homogeneity of mckinstryite has not yet been established completely and the Echo Bay analyses suggest that large variations may be involved.

#### Discussion

It was found that the mckinstryite is late in the Echo Bay paragenetic sequence, possibly crystallizing after the late native silver. After the deposition of the native silver, the temperature of the ore-forming solution was presumably less than 94.4° C thus allowing the deposition of mckinstryite. Sulfur isotope measurements on the sulfides demonstrate that the mckinstryite is a part of the primary sulfide sequence and is not a secondary mineral. During its depositional history, the ore forming fluid apparently evolved from one enriched in the  $\text{SO}_4^{2-}$  species to one enriched in  $\text{HS}^-$  due to a postulated increase in pH and a decrease in the fugacity of oxygen (Robinson et al., 1970; Robinson & Ohmoto, in preparation). Because of this change in the chemistry of the fluid, the  $\delta\text{S}^{34}$  values of the sulfides increased with time. The mckinstryite with  $\delta\text{S}^{34}$  values of from +23 to +27‰ (5 measurements) exhibits the heaviest values since it is the last sulfide to form. The spread of values suggests that the mineral may have been deposited over a time interval.

The conditions of formation of this mineral may also reflect its somewhat anomalous composition. At the time of its deposition, the fluid may still have been comparatively rich in silver but was becoming relatively sulfur depleted. The sulfur isotope values suggest that the sulfur was derived from the fluid and not from the replacement of other sulfides.



Sulfur deficiencies in sulfides have been recorded (Deer et al., 1965) especially for pyrite. These are usually very small deficiencies compared to the sulfur deficiency found in the Echo Bay mckinstryite. However, it is noteworthy that Moh (1970) has recorded an analogous situation in the case of the low temperature phase "blue remaining covellite" where a composition of  $Cu_{1.1}S$  is due to a metal excess. No crystal-structure investigation has yet been performed on mckinstryite. The Echo Bay sample presumably has a nonstoichiometric defect which can be considered in two ways: either a deficiency of sulfur or an excess of silver ( $Cu_{0.8}Ag_{1.41}S$ ) is operative. The specific gravity determinations suggest that the former case is most probable. This sulfur deficiency cannot be accompanied by any valency change of the metals to neutralize the excess positive charge. The defect is presumably a type of Schottky defect whereby some of the anion sites in the lattice are vacant. Electrical neutrality must be maintained by a certain amount of metallic bonding probably taking place with the silver. Sufficiently large samples of pure mckinstryite were not available for electrical conductivity tests. The sulfur deficiency exhibited by this mineral will be investigated further.

#### Acknowledgments

The authors wish to thank Dr. D. G. W. Smith and Mr. D. Tomlinson for invaluable assistance with the microprobe analyses and Dr. R. K. O'Nions for helpful discussions of the mineralogy. Special thanks are due to Echo Bay Mines Ltd, particularly to Mr. R. J. Beckett, for assistance at the mine. This work was made possible by finance from grants awarded by the Geological Survey of Canada and by the National Research Council of Canada.

UNIVERSITY OF ALBERTA,  
EDMONTON, ALBERTA, CANADA  
October 1; December 8, 1970

#### REFERENCES

- Cameron, E. N., 1963. Optical symmetry from reflectivity measurements: *Am. Mineralogist*, v. 48, p. 1070-1079.
- Campbell, D. D., 1957. Port Radium Mine. In *Structural Geology of Canadian Ore Deposits*: Can. Inst. Min. Metall. II, p. 177-189.
- Deer, W. A., Howie, R. A., and Zussman, J., 1965. *Rock forming minerals*, Vol. 5: Non-silicates, Longmans, 371 pp.
- Djurle, S., 1958. An X-ray study on the system Ag-Cu-S: *Acta Chem. Scandinavia*, v. 12, p. 1427-1436.
- Evans, H. T., Jr., Appleman, D. E., and Hadwerker, D. S., 1963. The least-squares refinement of crystal unit cells with powder diffraction data by an automatic computer indexing method: *Am. Cryst. Assoc. Meeting*, Cambridge, Mass., p. 42-43 (abs.).
- Grybeck, D., and Finney, J. J., 1968. New occurrences and data for jalpaite: *Amer. Min.*, v. 53, p. 530-542.
- Johan, Z., 1967. Etude de la Jalpaite,  $Ag_{1.25}Cu_{0.15}S$ : *Acta Universitatis Carolinae-Geologica* #2, p. 113-122.
- Moh, G. H., 1970. Phase relations and minerals in the sulfur rich portion of the Cu-S System at low temperatures: *Procs. IMA-IAGOD Meetings, Japan, Open Session IV-1, Abstract 9-11*.
- Robinson, B. W., Fritz, P., Krouse, R. H., and Morton, R. D., 1970. Stable isotopes of the Echo Bay deposit, N.W.T., Canada: Abstract, *Isotopic Geochemistry Section, Geol. Soc. Amer. Mtg. Milwaukee, Wis.*
- Skinner, B. J., Jambor, J. L., and Ross, M., 1966. Mckinstryite a new copper-silver sulfide: *ECON. GEOL.*, v. 61, p. 1383-1389.
- Skinner, B. J., 1966. The system Cu-Ag-S: *ECON. GEOL.*, v. 61, p. 1-26.
- Smith, D. G. W., and Tomlinson, M. C., 1970. An APL language computer program for use in electron microprobe analysis: *Computer Contribution 45, State Geological Survey, The University of Kansas, Lawrence.*
- Suhr, N., 1955. The Ag-S-Cu<sub>2</sub>S system: *ECON. GEOL.*, v. 50, p. 347-350.